Reviews of

120 Physiology Biochemistry and Pharmacology

With 52 Figures and 5 Tables

Springer-Verlag
Berlin Heidelberg New York London Paris
Tokyo Hong Kong Barcelona Budapest

ISBN 3-540-55364-9 Springer-Verlag Berlin Heidelberg New York
ISBN 0-387-55364-9 Springer-Verlag New York Berlin Heidelberg

Library of Congress-Catalog-Card Number 74-3674

Printed in Germany

Typesetting: Best-set Typesetter Ltd., Hong Kong
27/3130 – 5 4 3 2 1 0 – Printed on acid-free paper

Contents

Indexed in Current Contents

Rev. Physiol. Biochem. Pharmacol., Vol. 120

Membrane-Bound Catechol-O-Methyltransferase: A Reevaluation of Its Role in the O-Methylation of the Catecholamine Neurotransmitters

JEROME A. ROTH[1]

Contents

1 Introduction

Ever since the initial work of Axelrod and coworkers (Axelrod and Tomchick 1958; Axelrod et al. 1958), catechol-O-methyltransferase (COMT) has been considered to be one of the major enzymes responsible for inactivation of the catecholamine neurotransmitters. The enzyme catalyzes the transfer of a methyl group from *S*-adenosylmethionine (AdoMet) to acceptor catechol substrates, which include the catecholamine neurotransmitters dopamine, norepinephrine, and epinephrine. Although O-methylation of the catechol-

[1] Department of Pharmacology and Therapeutics, State University of New York at Buffalo, School of Medicine and Biomedical Sciences, Buffalo, New York 14214, USA

amine neurotransmitters results in their inactivation, until recently there has been little clinical interest in COMT because of the lack of any effective pharmacological agents which could inhibit COMT activity in vivo without production of serious side effects. However, the recent development of highly selective, tight binding COMT inhibitors has rekindled interest in the use of COMT inhibitors as a possible treatment for depression and/or as an adjunct therapy along with L-DOPA for treatment of Parkinson's disease (Mannisto and Kaakkola 1990).

Multiple forms of COMT have been identified and characterized in a variety of tissues and animal species (Inscoe et al. 1965; Traiger and Calvert 1969; Assicot and Bohuon 1970, 1971; Verity et al. 1972; McCormick et al. 1972; Aprille and Malamud 1975; Roffman et al. 1976; Huh and Friedhoff 1979; Rivett et al. 1983a,b). Two major classes of COMT have been defined based on their subcellular location and include a soluble cytosolic form and a membrane-bound species (MB-COMT). As will be described in detail below, these transferases possess distinct biochemical and physical properties and appear to be localized within different cell types. The soluble form of COMT is generally regarded as the predominant form in most tissues, whereas the membrane-bound species is assumed to be a minor constituent contributing only a minor fraction to the total COMT activity (Guldberg and Marsden 1975; Kopin 1986). This supposition is primarily based on the observation that, in the majority of tissues examined, the V_{max} for the soluble form of COMT is considerably greater than that observed for the membrane-bound enzyme. In this case, the V_{max} is equated with the presumed functional activity in vivo.

Due to the relatively low COMT activity associated with the membrane fraction, the question has previously been raised as to whether this form of COMT actually represents a distinct molecular entity or is simply an artifact resulting from nonspecific binding of the soluble enzyme to membranes during subcellular fractionation (Broch and Fonnum 1972; Borchardt et al. 1974; Tong and d'Iorio 1977; Borchardt and Cheng 1978; Goldberg and Tipton 1978). However, more recent studies (Grossman et al. 1985; Rivett et al. 1983a; Jeffery and Roth 1984) have established that the membrane-bound species of COMT is a separate and biochemically distinct entity from the soluble enzyme. Although these studies have revealed that MB-COMT actually possesses a higher affinity for the catecholamine substrates, the ramifications of this have not been appropriately investigated and little consideration has been given to

the physiological significance or function of the membrane-bound enzyme. In light of this, there needs to be a reevaluation of the role and capacity of this enzyme regarding the O-methylation of catecholamines and structurally related drugs. Accordingly, this review article will focus attention on the membrane-bound form of COMT and attempt to establish its role and contribution to the O-methylation of the catecholamine neurotransmitters and structurally related drugs.

2 Contribution of Soluble COMT and MB-COMT to O-Methylation of Catecholamines

At least three forms of COMT have been identified in mammalian tissues: two soluble forms, COMT I and II, and one membrane-bound form. The two soluble forms of COMT differ in their molecular weights with COMT I possessing a molecular weight (MW) of approximately 24000 and COMT II of around 48000 (Huh and Friedhoff 1979). Although the large MW species of the soluble transferase has been suggested to be a dimer of the lower MW form, the two enzymes do not appear to be interconvertible upon their isolation and partial purification. Furthermore, these enzymes appear to possess unique biochemical properties including pI value, pH optima, meta to para methylation ratios, and substrate specificity (Marzullo and Friedhoff 1975). The proportion of the two soluble transferases varies with the particular tissue examined, with COMT I being the predominant enzyme in all cases. Several tissues, including brain, apparently lack COMT II. As noted above, it is generally assumed that the O-methylating activity associated with the soluble cell fraction accounts for the majority of the COMT activity observed in essentially all tissues examined.

The relative distributions of the soluble and membrane-bound forms of COMT have been found to vary widely. Except for the catechol estrogens, which possess similar K_m values for both forms of COMT (Reid et al. 1986), all other catechol substrates tested have lower K_m values for MB-COMT. In almost all tissues, the activity associated with the membrane fraction consistently accounted for only a minor fraction of the total transferase activity (Guldberg and Marsden 1975; Kopin 1986), with one notable exception, mouse liver. In the latter case, this enzyme was reported to account for approximately 70% of the total COMT activity (Aprille and Malamud

1975). This can be compared to rat liver which, for example, was estimated to contain only 5% of the total COMT activity in the membrane fraction (Tong and d'Iorio 1977). This and similar data in other tissues have consistently been used to substantiate the preponderance of the soluble transferase responsible for the O-methylation of catecholamines in vivo.

What can account for this difference in the proportion of MB-COMT and soluble COMT between mouse and rat liver? Is this difference simply attributed to species variation or are there other factors or circumstances which might explain these seemingly discrepant observations? Examination of the two studies (Aprille and Malamud 1975; Tong and d'Iorio 1977) reveals that the concentration of the catechol substrate employed to estimate soluble and MB-COMT activities in the two studies was different. The concentration of substrate used to estimate the two rat liver COMT activities was 1000 μmol/l and is representative of that used in the majority of studies in which COMT activity has been and still is assessed. In contrast, the study of COMT activity in mouse liver was performed at a substrate concentration of 12 μmol/l. Can this difference in substrate concentration account for the variation observed in the relative proportion of the activity of membrane-bound and soluble COMT?

The answer to this question is yes. Kinetically, it is known that the measured activities of any two enzymes are directly proportional to the concentration of substrate employed relative to their respective K_m values. For two competing enzymes which possess considerably different K_m values, the relative activities of each will be greatly influenced by the concentration of substrate used in the assay. Accordingly, the low K_m enzyme will exhibit proportionally higher activity when incubations are performed at low substrate concentrations than when a similar experiment is performed at higher substrate concentrations. Obviously, the reverse is true for the high K_m enzyme. This, in fact, is the situation for soluble and membrane-bound forms of COMT. The K_m values differ widely between these enzymes with the K_m value for MB-COMT being approximately 100 times lower than that for the soluble enzyme. Differences in substrate concentration, as employed in the two studies (Aprille and Malamud 1975; Tong and d'Iorio 1977) noted above with rat and mouse liver COMT, may likely result in variation of the relative proportion of the two activities observed in each species. At low concentrations of substrate, the activity associated with the high-affinity form of COMT (MB-COMT) is likely to predominate until the substrate concen-

tration is raised above saturation, at which point the contribution of soluble COMT activity will increase and eventually prevail. Accordingly, differences in substrate concentration may likely account for the disparity in the estimated proportion of the two forms of COMT in mouse and rat liver.

Essentially all of the studies which have attempted to estimate the percentage contribution of MB-COMT activity utilized kinetic conditions which were optimized for the soluble form of the transferase, i.e., high substrate concentrations. Since the soluble form of COMT has both a higher K_m and V_{max} value for the catecholamines, the high nonphysiological concentrations of the substrates employed, such as in the rat liver study noted above, clearly favor the soluble enzyme when comparing relative activities. Under these conditions, the estimated percentages for O-methylation will indicate higher soluble COMT activity relative to the activity associated with the membrane fraction. These estimated activities for soluble COMT and MB-COMT, however, probably do not accurately reflect the functionally relevant activities of these enzymes in vivo since the high substrate concentrations used to determine these values in vitro are not likely representative of catecholamine levels within the cell.

As a consequence of differences in the kinetic constants for soluble and MB-COMT, it can be anticipated that the concentration of catechol substrate will greatly influence the observed metabolic contribution of each species to the overall O-methylation of substrate. As noted above, at low concentrations of catecholamines, O-methylation by the low K_m membrane-bound form of COMT would predominate, and only when this enzyme becomes saturated with substrate does the contribution of the high K_m, soluble form of COMT become significant. This is an important point since this relationship should undoubtedly hold true in vivo as well as in vitro. This correlation, in fact, has been observed experimentally in several intact organelle preparations including rat heart and submaxillary gland and cat nictitating membrane (for review see Trendelenburg 1980, 1988). In each of these systems, a functionally active O-methylating system has been described which rapidly and efficiently metabolizes low concentrations of catecholamines and structurally related drugs such as isoproterenol. As will be described in detail below, the data obtained with these tissue preparations were consistent with a low K_m form of COMT being responsible for O-methylation of these substrates. At low concentrations of the catechols, O-methylation followed a Michaelis-Menten kinetic relationship and only after this low K_m form of COMT was saturated

was there a significant increase in the tissue to medium ratio of the catechols. At still higher concentrations of substrate, the low-affinity, high K_m form of COMT could also be observed experimentally. These studies demonstrate that the high-affinity form of COMT, presumably the membrane-bound species, has the potential of regulating tissue levels of catecholamines.

Most review articles (Guldberg and Marsden 1975; Kopin 1986) have also implied that, in the CNS, the soluble form of COMT is the functionally predominant O-methyltransferase involved in catecholamine metabolism. These conclusions, as noted above, were based on studies which again employed high concentrations of the catechol substrate to assay both soluble COMT and MB-COMT activities and therefore, probably do not accurately reflect conditions within the CNS. The consequence of this is the underestimation of the potential contribution and importance of the membrane-bound form of COMT to the overall inactivation of the catecholamine neurotransmitters. In support of this, studies by Rivett et al. (1982) have suggested that the membrane-bound species in human brain may be the more prevalent and functionally significant form of COMT at concentrations of the catecholamine neurotransmitters that are likely to be physiologically relevant.

3 Biochemical Properties of MB-COMT

Much of the initial literature describing the biochemical properties of MB-COMT was often confusing and misleading because of the lack of knowledge as to the actual existence of this enzyme as a separate and physically distinct entity. As noted above, since MB-COMT had been presumed to contribute a relatively low percentage to the total COMT activity in the majority of tissues examined, it was originally believed that this form of COMT was an artifact caused by the nonspecific binding of the soluble enzyme to the microsomal fraction of cells. In support of this were data demonstrating that many of the biochemical and kinetic properties of the two enzymes were very similar (Borchardt et al. 1974; Rivett et al. 1982; Jeffery and Roth 1984, 1985). These included kinetic mechanism, Ca^{2+} inhibition, pH optimum, Mg^{2+} requirement, and similar K_m values for the methyl donor AdoMet. For example, both enzymes in human brain are inhibited approximately 50% at 1 μmol/l of Ca^{2+} and both enzymes possess a pH optimum between 7.5 and 8.0 (Jeffery and Roth 1984).

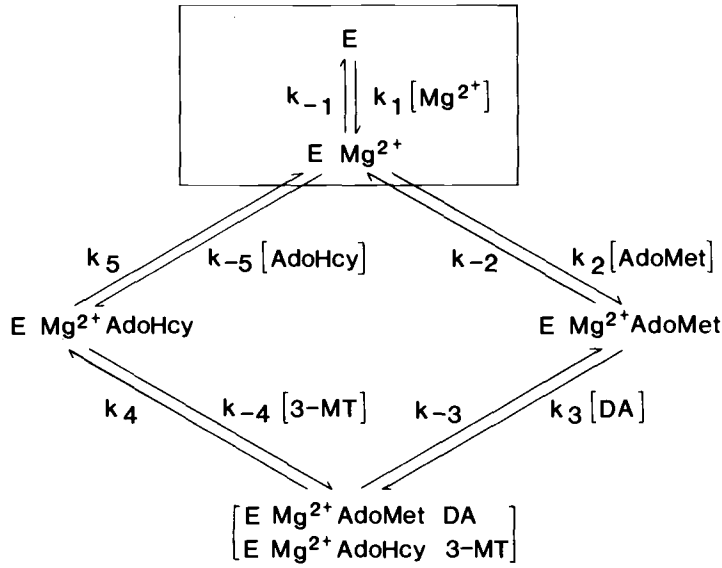

$$\frac{V}{VMAX} = \frac{[A][B][C]}{Kia\ Kib\ Kmc + Kib\ Kmc[A] + Kia\ Kmb[C] + Kmc[A][B] + Kmb[A][C] + [A][B][C]}$$

Fig. 1. Reaction mechanism and rate equation for soluble COMT and MB-COMT O-methylation of dopamine. *AdoMet*, *S*-adenosyl-L-methionine; *AdoHcy*, *S*-adenosyl-L-homocysteine; *DA*, dopamine; *3-MT*, 3-methoxytyramine. The binding of Mg^{2+} to COMT (indicated in the *box*) occurs via a rapid equilibrium mechanism. K_{ia}, dissociation constant for Mg^{2+}; K_{ib}, dissociation constant for AdoMet; K_{m_A}, K_{m_B}, and K_{m_C} K_m for Mg^{2+}, AdoMet, and dopamine, respectively. (Jeffery and Roth 1987)

Similarly, both the membrane-bound and soluble enzymes have been reported (Jeffery and Roth 1987) to proceed via a sequential ordered reaction mechanism with Mg^{2+} binding in a rapid equilibrium sequence prior to addition of AdoMet, as illustrated in Fig. 1 for the O-methylation of dopamine.

Other data supporting the concept that MB-COMT arises from the nonspecific binding of the soluble enzyme to cellular membranes is derived from studies which demonstrated that the K_m values for catecholamine binding to Triton X-100-solubilized MB-COMT were equivalent to those of the cytosolic enzyme (Borchardt et al. 1974). For example, the K_m values for several catechol substrates including norepinephrine increased almost 50-fold and became essentially

identical to those of the cytosolic enzyme when rat liver MB-COMT was solubilized with Triton X-100. These data imply that the low K_m value for substrate binding to MB-COMT is imparted by the interaction of the enzyme within the membrane, and, when solubilized, the properties of the enzyme convert to those of the cytosolic transferase. Consistent with the concept that the membrane-bound and soluble forms of COMT may be identical was the observation that polyclonal antibodies prepared to the soluble enzyme partially cross-reacted with MB-COMT (Creveling et al. 1973; Borchardt et al. 1974; Borchardt and Cheng 1978).

The above data imply that membrane-bound and soluble COMT are most likely structurally very similar and may be identical. This latter conclusion, however, is not adequately justified by the limited results noted above. In fact, a variety of more recent biochemical and physical evidence demonstrates that the two enzymes are structurally distinct. For example, it has been established that MB-COMT is an integral membrane protein since high salt concentrations failed to release the enzyme from the membranes (Jeffery and Roth 1984) and solubilization requires the presence of a detergent. These studies have also revealed that the change in the K_m value for MB-COMT observed upon solubilization with Triton X-100 was simply caused by apparent competitive inhibition of the enzyme by Triton X-100. Thus, the increase in the K_m value upon solubilization of MB-COMT noted previously is not indicative of the two species of COMT being identical. In addition, the fact that the polyclonal antibodies raised against soluble COMT are capable of cross-reacting with MB-COMT is not unexpected, since the two enzymes possess similar biochemical properties and most likely have some antigenic sites in common.

Although it is reasonable to assume that the two forms of COMT have considerable structural similarity, it is also clearly evident that differences exist in the physical structure and biochemical properties of the soluble and membrane-bound species. The data to support this include differences in the MWs of the two species (Grossman et al. 1985; Heydorn et al. 1986), differences in the K_m value for the acceptor substrates (Rivett et al. 1982, 1983a; Jeffery and Roth 1984), differences in the localization of the two enzyme forms (Rivett et al. 1983a,b), and preparation of antibodies to the soluble enzyme which do not cross-react with MB-COMT (Assicot and Bohuon 1969).

From a functional perspective, the major biochemical difference between the membrane-bound and soluble forms of COMT is the fact that K_m values for the catecholamines are consistently 1–2

orders of magnitude lower for the membrane-bound species than for the soluble enzyme (Tong and d'Iorio 1977; Borchardt and Cheng 1978; Rivett et al. 1983a). For example, in human brain the K_m for dopamine with MB-COMT is 3 μmol/l, whereas, at 260 μmol/l, this kinetic constant for the soluble transferase is almost 100 times greater (Rivett et al. 1983a). Similarly, structural analogues, such as tropolone, that act as reversible dead-end inhibitors of COMT, possess a higher affinity for the membrane-bound form of the transferase (Jeffery and Roth 1984). This latter observation is expected since these inhibitors compete with the acceptor substrates for binding to the same site on COMT. For example, the K_i value for tropolone binding to MB-COMT was found to be 5 μmol/l compared to 45 μmol/l for the soluble enzyme. This difference in affinity of inhibitors for the two forms of COMT has considerable clinical relevance, since the new COMT inhibitors that have been developed for treatment of depression and Parkinson's disease are catechol derivatives and likely to compete for substrate binding. The difference in K_m values is not true for all substrates, since the catechol estrogens have been shown (Reid et al. 1986) to possess similar kinetic constants for both soluble and MB-COMT from rabbit thoracic aorta.

Consistent with the observed differences in the kinetic constants for substrate binding between the membrane-bound and soluble enzymes is the observation that the pI values and MWs of the two forms of COMT in rat liver are different (Grossman et al. 1985). The pI value for the membrane-bound species is 6.2, whereas the pI value for the soluble enzyme is approximately 5.2. Using antibodies prepared to the soluble enzyme form of COMT, Grossman et al. (1985) have reported that the subunit MW for the rat membrane-bound form, based on SDS-polyacrylamide gels, is approximately 26 000 whereas the soluble COMT possess a MW of only 23 000. This difference in the MW of the two enzyme species was also confirmed by Heydorn et al. (1986). Several recent studies (Tilgmann and Kalkkinen 1990; Salminen et al. 1990; Lundstrom et al. 1991; Bertocci et al. 1991) with rat and human COMT cDNA suggest that there is a single gene responsible for synthesis of both soluble and MB-COMT and that the MB-COMT contains an additional hydrophobic portion of 21 amino acids on the 5′ NH_2-terminal end which is responsible for insertion of the enzyme into the endoplasmic reticulum. Initiation of transcription can begin at either of two start codons (ATG), which determines whether the 21 hydrophobic amino acid domain will be coded for.

Most studies have assumed that MB-COMT is associated with the endoplasmic reticulum or plasma membrane and therefore have employed the microsomal fraction to assay MB-COMT activity. In contrast to these studies, Grossman et al. (1985) have observed that a major fraction of MB-COMT immunological activity was associated with the mitochondrial outer membrane and not the microsomal fraction. If this is true, then the two major catecholamine degrading enzymes, monoamine oxidase (MAO), an outer mitochondrial membrane marker, and MB-COMT reside on the same membrane surface. Future immunohistochemical studies with specific antibodies towards MB-COMT are required to determine the precise subcellular location of this enzyme.

4 MB-COMT in Human Brain

There are five major enzymes known to be involved in the catabolism of catecholamines in brain. These are the type A and B forms of MAO, membrane-bound and soluble forms of COMT, and the M form of phenol sulfotransferase. Although these enzymes have been extensively studied in a variety of animals and tissues, little is known about their relative contributions to the overall degradation of the catecholamine neurotransmitters. Since abnormal levels of the catecholamines have been implicated in a variety of behavioral and neurological disorders, it would be important to ascertain the relative contribution of each of the enzymes to the overall inactivation of these endogenous agents in the CNS. Animal models for studying the catabolic fate of catecholamines in humans are not totally applicable, since the levels and properties of the five enzymes vary greatly between humans and common laboratory animals (Roth et al. 1982).

In order to determine the contribution of each of the five enzymes to the overall inactivation of catecholamines in human brain, Rivett et al. (1982) developed an in vitro kinetic model for human brain metabolism of dopamine and norepinephrine. This model attempted to evaluate the relative activities of the five enzymes in human frontal cortex at various concentrations of the catecholamines. This was accomplished by insertion of the measured velocities and the known kinetic constants into the appropriate rate equations established for each enzyme. By varying the catecholamine concentration in each of the rate equations, the relative activity of each enzyme was then determined and the percent contribution of each

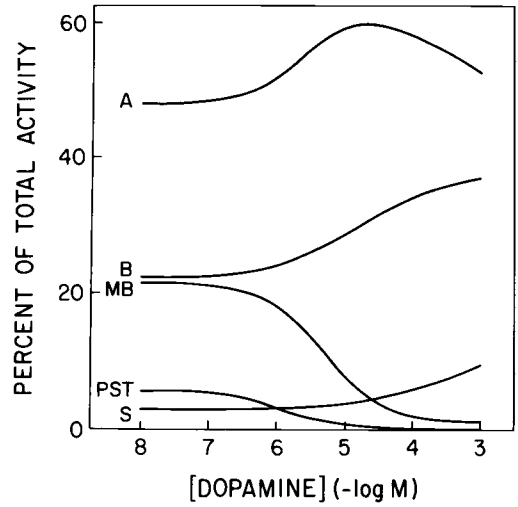

Fig. 2. Results obtained from kinetic modeling studies for dopamine metabolism in human brain. The average percent metabolic contribution of MAO A (*A*), MAO B (*B*), soluble COMT (*S*), MB-COMT (*MB*), and phenol sulfotransferase (*PST*) as determined from homogenates obtained from 3–8 specimens of human frontal cortex. The calculated values at various concentrations of dopamine for soluble and MB-COMT and PST were determined at saturating concentrations of both the methyl donor, AdoMet, and the sulfate doner, 3′-phosphoadenosine-5′-phosphosulphate (PAPS), respectively. The values for dopamine deamination by both MAO A and B were calculated at an oxygen concentration of 218 μmol/l. (Rivett et al. 1982)

was calculated. This model only endeavored to determine the total enzymatic capacity of each reaction and did not attempt to take into account the selective localization of the five enzymes or the preferential transport of catecholamines into specific cells in the CNS.

Results of these modeling studies (Fig. 2) indicated that, at all concentrations of dopamine, deamination by MAO A and B was the predominant reaction. At dopamine concentrations below 1 μmol/l, the relative contribution of O-methylation by the membrane-bound form of COMT to the overall metabolism of dopamine was approximately 20% and essentially equivalent to that of MAO B. Surprisingly, the percent contribution by the soluble form of COMT at dopamine concentrations less than 100 μmol/l was less than 5%, suggesting that its capacity to degrade the catecholamines was considerably less than that of the membrane-bound transferase.

A slightly different picture was observed for norepinephrine metabolism (Fig. 3). In this case, O-methylation by the membrane-bound form of COMT was the predominant pathway at norepine-

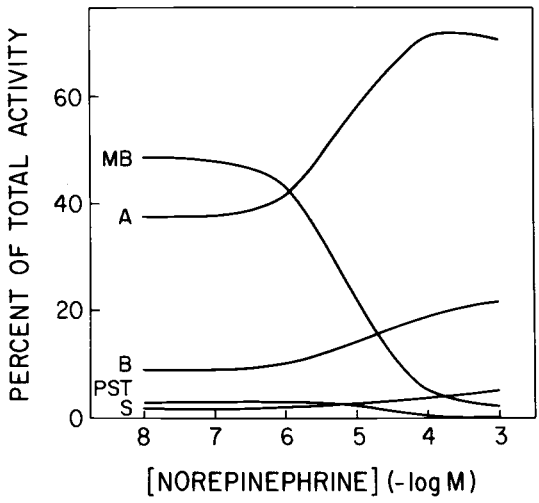

Fig. 3. Results obtained from kinetic modeling studies for norepinephrine metabolism in human brain. The average percent contribution of MAO A (*A*), MAO B (*B*), soluble COMT (*S*), MB-COMT (*MB*), and phenol sulfotransferase (*PST*) as determined from homogenates obtained from 3–8 specimens of human frontal cortex. The concentration of AdoMet and PAPS were considered saturating and the concentration of oxygen was assumed to be 218 μmol/l as described in the legend of Fig. 2. (Rivett et al. 1982)

phrine concentrations less than 1 μmol/l. At higher concentrations of norepinephrine, at which point MB-COMT approaches saturation (K_m = 3.9 μmol/l), deamination by the A form of MAO became the principal degradative pathway. As with dopamine, the soluble form of COMT was estimated to contribute less than 5% to the overall inactivation of norepinephrine.

As illustrated in these figures, O-methylation of both dopamine and norepinephrine by MB-COMT, as compared to that by the soluble enzyme, predominates at concentrations less than 10 μmol/l. For dopamine, the point of intersection at which the soluble enzyme contributes a higher percentage to the overall O-methylation occurs at approximately 20 μmol/l. For norepinephrine, the point of intersection occurs at even a greater concentration, around 300 μmol/l. It can be calculated, based on the kinetic model described above, that at a concentration of dopamine and norepinephrine of 10 μmol/l, the soluble form of COMT would contribute only 34% and 12%, respectively, to the total O-methylating activity. At a substrate concentration of 1000 μmol/l, the soluble transferase would contribute approximately 90% and 70%, respectively. These latter values, obtained at the nonphysiologically high concentrations of the catecholamines, are typical of the percentages reported in the literature for the proportion of soluble enzyme in various tissues. It can further be calculated, for tissues containing the lowest proportion of MB-COMT, such as the liver and kidney, where the ratio of the V_{max} for MB-COMT/soluble COMT is 0.0029 (Rivett et al. 1983b),

that at 1 μmol/l dopamine, MB-COMT would contribute approximately 40% to the total O-methylating activity. These data further illustrate how, in the past, erroneous conclusions have been drawn concerning the potential significance of MB-COMT.

Since the kinetic model described above for catecholamine metabolism was obtained with autopsied human brain specimens, it is reasonable to question whether the calculated values reported actually reflect activities of the various enzymes within the intact living system. In addition, crude homogenates were used to estimate enzyme activities, and access of substrates to the enzymes within different cells of the brain may be limiting. This is true for all the enzymes, since the A form of MAO is known to be present in neurons whereas the B form predominantly resides in astrocytes (Francis et al. 1985), although it may also be present in serotonergic neurons (Levitt et al. 1982). Similarly, the soluble form of COMT is associated with astroglia, whereas MB-COMT predominates in neuronal cells (Rivett et al. 1983a; see discussion below). Recent immunohistochemical studies have further confirmed that phenol sulfotransferase is exclusively present in neuronal cells in human brain (Zou et al. 1990). Thus, it is likely that access of the catecholamines to the different enzymes will influence the extent to which they will contribute to the overall inactivation of the catecholamines.

5 Significance of MB-COMT

In order to lend credence to the kinetic model described above for human brain, it would be advantageous if a prototype whole cell or organ system were available which expresses a similar relationship for soluble and MB-COMT activity, since this may provide a direct approach to evaluating the relative contribution of the two enzymes to the O-methylation of the catecholamine neurotransmitters. Fortunately, a number of systems have been described in the literature which are capable of efficiently O-methylating the catecholamines by both a high- and low-affinity form of COMT. As will be described below, the kinetic properties for the O-methylation of catecholamines in these organ systems are consistent with the reaction proceeding with a form of COMT which possesses a high affinity for catecholamines. These studies further confirm that the concentration of catecholamines within the tissues appears to be regulated by this high-affinity form of COMT.

Within the past two decades, studies by Trendelenburg and coworkers (Trendelenburg et al. 1971; Graefe and Trendelenburg 1974; Bonisch et al. 1974, 1978; Major et al. 1978; Fiebig and Trendelenburg 1978; Henseling 1983; Trendelenburg 1980, 1984a,b, 1988; Grohmann and Trendelenburg 1985, 1988; Grohmann 1987) and others (Paiva and Guimaraes 1978, 1984; Garland and Martin 1984; Magaribuchi et al. 1987) have examined and characterized the extraneuronal uptake and disposition of the catecholamine neurotransmitters and isoproterenol in a variety of tissues, including rat heart and submaxillary gland, cat nictitating membrane, guinea pig trachea, rabbit aortic rings, and dog saphenous vein strips. Extensive kinetic studies have been performed on the transport, deamination, and O-methylation of these substances, and results of these studies have revealed that uptake of the catecholamines into these tissues is characterized by both saturable and nonsaturable processes. The saturable process is distinguished by a low-affinity (high K_m) and high-capacity carrier (high V_{max}). For example, the K_m values for isoproterenol and norepinephrine in rat heart have been estimated to be approximately 100 and 250 μmol/l, respectively, and the V_{max} values for both are in the order of 50–80 nmoles/min/g tissue (Trendelenburg 1980). Similar kinetic constants have also been obtained for the other systems noted above.

The catecholamine taken up into the tissues can be rapidly metabolized by either MAO or COMT. In the presence of an MAO inhibitor, O-methylation of the catecholamines displayed saturation kinetics and obeyed Michaelis-Menten kinetics (Trendelenburg 1980, 1984). In contrast to what might have been expected based on current dogma concerning the functional significance of the two forms of COMT, the apparent K_m value for O-methylation was found to be low compared to that for either uptake or deamination. The estimated K_m values for O-methylation were consistently in the order of 1–5 μmol/l. This can be contrasted to the concentration of catecholamine, 15–40 μmol/l, outside the tissue which apparently half-saturated MAO. The fact that soluble COMT and MAO have similar K_m values in vitro, yet the extracellular concentrations which half-saturated these enzymes were found to be different, implies that O-methylation is not occurring with the soluble form of COMT. In cat nictitating membrane (Graefe and Trendelenburg 1974) and rat submaxillary gland (Major et al. 1978), two apparent K_m values for O-methylation of norepinephrine were observed, one with high affinity with a K_m value approximately 7 μmol/l and the other with a K_m value around 100–300 μmol/l. These data are consistent with the

existence of two forms of COMT, one with high substrate affinity, presumably MB-COMT, and the other with a considerably lower affinity, presumably soluble COMT. Although K_m values estimated for intracellular enzymes based on extracellular substrate concentrations may not be accurate, it appears to be more than coincidence that the kinetic constants determined in the whole organ systems described above are strikingly similar to the reported K_m values for membrane-bound and soluble COMT, respectively (Rivett et al. 1982).

Based on the data obtained with the kinetic model for human brain, the question must be asked as to how important is extraneuronal O-methylation of accumulated catecholamines compared to deamination in the organ systems described above. In rat heart, the rate constants for O-methylation of the catecholamines have been found to exceed those for deamination by MAO (Grohmann 1987). Thus, it can be concluded that, since the K_m value is lower and the rate constant greater for O-methylation than for deamination, the activity of extraneuronal COMT must exceed that of extraneuronal MAO activity, at least in rat heart. This implies that MB-COMT has a greater capacity to inactivate the catecholamine neurotransmitters in these systems. However, the relative contribution and importance of COMT to the overall inactivation of the catecholamines is, of course, dependent on the concentration of substrate outside the tissue. At high extracellular concentrations of catecholamines, the high-affinity form of COMT (MB-COMT) becomes saturated, causing either deamination and/or O-methylation by the low-affinity form of COMT to become the predominant pathway for catecholamine metabolism (Trendelenburg 1984, 1988). At low extracellular concentrations of substrate, at which point MB-COMT is not saturated, the rate of O-methylation is determined by the rate of uptake. Under these conditions, the tissue to medium ratio of the catecholamine is very low, since essentially all the neurotransmitter taken into the cell is rapidly O-methylated. Therefore, O-methylation by presumably MB-COMT can regulate tissue levels of catecholamine. Only after this high-affinity form of COMT is saturated does the tissue to medium ratio increase.

Prior studies have analyzed the relative activities of the two forms of COMT in various rat tissues including rat ventricles (Rivett et al. 1983b). By applying the same method as that used for the kinetic model for catecholamine metabolism in human brain, the percent contribution of each form of COMT can be computed in each of the rat tissues examined. For example, it was reported that the V_{max}

for O-methylation of dopamine by rat heart soluble COMT and MB-COMT was 147 ± 9 and 4.01 ± 0.49 pmol/min/mg protein, respectively (see Table 1). Upon substituting these values into the appropriate rate equation, it can be calculated that, at dopamine concentrations less than 5 μmol/l, greater than 75% of the total O-methylating activity would proceed via MB-COMT. These results are remarkably consistent with those of Trendelenburg and co-workers described above and further establish the predominance of MB-COMT in rat heart.

6 Localization of MB-COMT

The distribution of the membrane-bound and soluble forms of COMT has been examined in a variety of animal tissues, including those of the rat, as indicated by the data in Table 1 (Rivett et al. 1983b). The data are expressed both in terms of V_{max} and as the first order rate constant, $k = V_{max}/K_m$, which approximates the relative turnover of the substrate, dopamine, in the different tissues. As indicated, the V_{max} value for MB-COMT is highest in rat liver but this value represents less than 0.3% of that for the soluble enzyme species. In comparison, the ratio of V_{max}/K_m in rat liver reveals that the rate constant for dopamine O-methylation by MB-COMT is considerably higher, being 80% of that determined for the soluble enzyme. Of the other peripheral tissues examined, striatal muscle and heart displayed the highest ratio of membrane-bound to soluble COMT activity when expressed either as V_{max} or as the rate constant, V_{max}/K_m, and indicate that the rate of dopamine turnover in these tissues is actually greater for MB-COMT. The maximum ratio was found in brain tissue, with the hippocampus, cerebellum, striatum, and cortex exhibiting the greatest MB-COMT activity. Applying a technique similar to that reported above for kinetic modeling of human brain, it can be calculated that at 10 μmol/l dopamine almost 85% of the total O-methylation in the rat striatum would proceed via MB-COMT. Even at 100 μmol/l dopamine approximately 43% of the total O-methylation would occur via the membrane-bound enzyme.

Several studies have also attempted to determine the cellular location of the membrane-bound and soluble forms of COMT. In the early 1970s Jarrott and coworkers (Jarrott and Iversen 1971; Jarrott and Langer 1971; Jarrott 1971, 1973) published a series of papers suggesting that COMT resides in both neuronal and extraneuronal

Table 1. Distribution of soluble COMT and MB-COMT activity in rat tissues

Tissue	V_{max}		MB/Soluble (%)	$V_{max}/K_m \times 10^3$		MB/Soluble
	MB	Soluble		MB	Soluble	
Striatal muscle	2.11 ± 0.18	52.9 ± 9	4.1	0.59	0.053	11.1
Heart (ventricle)	4.01 ± 0.49	147 ± 9	2.7	1.11	0.15	7.4
Vas deferens	14.5 ± 2.4	1068 ± 200	1.4	4.03	1.07	3.8
Spleen	8.51 ± 0.53	1003 ± 69	0.85	2.36	1.00	2.4
Sciatic nerve	2.11 ± 0.17	289 ± 16	0.73	0.59	0.29	2.0
Adrenal	2.21 ± 0.28	329 ± 24	0.67	0.61	0.33	1.8
Kidney	17.0 ± 2.0	5929 ± 453	0.29	4.72	5.93	0.8
Liver	42.1 ± 0.8	14690 ± 496	0.29	11.69	14.69	0.8
Brain						
Hippocampus	11.4 ± 0.9	131 ± 16	8.6	3.17	0.13	24.4
Cortex	9.6 ± 0.2	129 ± 9	7.5	2.67	0.13	20.5
Striatum	9.9 ± 0.5	138 ± 8	7.2	2.75	0.14	19.6
Diencephalon	7.6 ± 0.4	139 ± 9	5.5	2.11	0.14	15.1
Substantia nigra	7.4 ± 0.3	159 ± 11	4.7	2.06	0.16	12.9
Cerebellum	11.1 ± 0.3	240 ± 10	4.6	3.08	0.24	12.8
Brainstem	5.9 ± 0.6	173 ± 2	3.4	1.64	0.17	9.6

Activity is expressed as V_{max} values ±S.E. (pmol/min/mg protein) for soluble and MB-COMT. The K_m of dopamine for membrane-bound and soluble COMT is 0.0036 and 1.0 mmol/l (Rivett et al. 1983b). Units of V_{max}/K_m = ml/min/mg protein

compartments. This was based on the observation that sympathetic denervation of rat and rabbit vas deferens, cat nictitating membrane, and rabbit submaxillary gland resulted in extensive loss of COMT activity. Similarly, Marsden et al. (1971) have observed a decrease in COMT activity in rat sympathectomized submaxillary gland. These studies suggested that the decrease in O-methylating activity upon denervation resulted from selective loss of neuronal COMT. Jarrott (1971) noted that the loss of COMT activity was also associated with selective alterations in the kinetic properties of the enzyme suggesting that different forms of COMT may be present in the neuronal and extraneuronal sites. In contrast to these findings, a more recent study by Branco et al. (1984) implied that the loss of COMT activity observed by Jarrott and coworkers may have occurred at extraneuronal sites and may only have been a secondary response to the sympathetic denervation.

One of the major questions that remains concerning MB-COMT is its subcellular localization. Head et al. (1985) have previously suggested that a small percentage of isoproterenol O-methylation can occur on the extracellular surface of plasma membranes in rabbit intact thoracic aorta. This enzyme was shown to be sensitive to Ca^{2+} since removal of the Ca^{2+} (1 mmol/l) resulted in approximately an eightfold stimulation of the extracellular O-methylation of isoproterenol. The intracellular activity known to be associated with the high-affinity form of COMT, which was 100 times greater than the extracellular O-methylating activity, was not influenced by the Ca^{2+} concentration in the tissue bathing media. Prior studies by Weinshilboum and Raymond (1976) demonstrated that rat liver soluble COMT is inhibited approximately 60% at 1 mmol/l Ca^{2+}. Similarly, Jeffery and Roth (1984) reported that both human membrane-bound and soluble COMT are inhibited approximately 50% at this concentration of Ca^{2+}. Thus, if MB-COMT is exposed to the extracellular surface, its activity would be greatly diminished by the high extracellular Ca^{2+} concentrations, whereas the activity of the intracellular enzyme would be minimally altered due to exposure to relatively low levels of Ca^{2+}.

The presence of COMT in plasma membranes has also previously been suggested by Traiger and Calvert (1969), Raxworthy et al. (1982), and Aprille and Malamud (1975) for rat adipocytes, rat liver, and mouse liver, respectively. In contrast to these findings, Grossman et al. (1985) have suggested that MB-COMT is actually present in the outer mitochondrial membrane. Clearly, future studies are needed to delineate the precise location of MB-COMT.

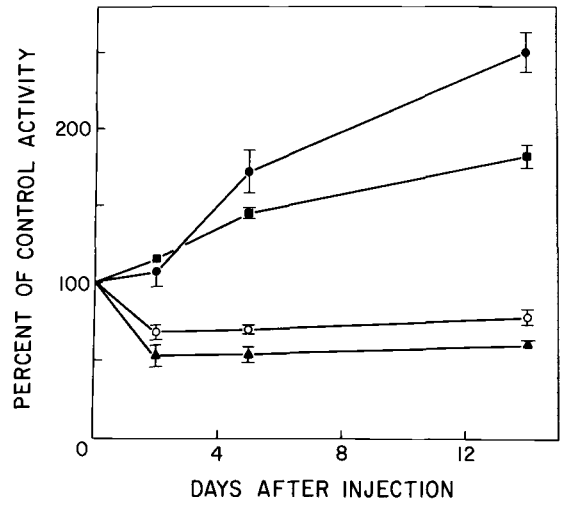

Fig. 4. Time course of changes in COMT activities after kainic acid lesioning of rat striatum. The data represent the mean ± S.E. of the percent of the enzyme activities in lesioned striatum as compared to that in the control contralateral striatum from 5–8 rats. Soluble COMT (●); MB-COMT (○); glutamic acid decarboxylase (▲) (neuronal marker); glutamine synthetase (■) (astroglial marker). (Rivett et al. 1983a)

In regard to the cellular location of COMT in brain, immunohistochemical studies using antibody to the soluble form of COMT have localized the soluble enzyme to nonneuronal elements such as the astroglia (Kaplan et al. 1979). Although MB-COMT activity can be measured in the CNS, these immunohistochemical studies have failed to reveal the presence of this enzyme in brain even though the antibody used in these experiments was reported to cross-react with the membrane-bound species. In order to determine the cellular location of MB-COMT in the CNS, kainic acid lesioning studies of rat striatum were performed by Rivett et al. (1983a). For these studies, membrane-bound and soluble COMT activities were measured up to 7 days after stereotaxic lesioning of rat striatum with 2 μg of the neurotoxin kainic acid. As illustrated in Fig. 4, lesioning of rat striatum with kainic acid occurred within 2 days of treatment and resulted in a loss of MB-COMT activity of approximately 20%. There was a statistically significant correlation between the ratio of lesioned to control activity for MB-COMT and the neuronal marker enzyme glutamate decarboxylase. Since kainic acid selectively destroys neuronal cell bodies at the site of injection but leaves intact the presynaptic nerve endings, these results suggest that the MB-COMT is at least partially localized within the neuronal cells intrinsic to the rat striatum. The decrease in MB-COMT activity observed can be contrasted with that of the soluble enzyme which increased almost 200% at the same time period after kainic acid lesioning. The increase in soluble COMT activity paralleled that of the astroglial

marker enzyme glutamine synthetase. This is consistent with immunohistochemical evidence demonstrating that this form of the enzyme is localized within astroglia, since these cells are known to proliferate after kainic acid lesioning. These results suggest that the low K_m MB-COMT may be localized, in part, within the rat striatal postsynaptic neurons, whereas the high K_m soluble enzyme is almost exclusively associated with the proliferating glial cells.

Previous studies have also demonstrated no change in total COMT activity (measured at high substrate concentration) in rat striatum upon lesioning of the substantia nigra (Marsden et al. 1972). Accordingly, studies involving kainic acid lesioning of rat substantia nigra were performed to determine whether a selective alteration in either membrane-bound or soluble COMT activity occurs in order to demonstrate which form of COMT is present in the dopaminergic nerve terminals that project into the striatum (Francis et al. 1987). These lesioning studies revealed no change in activity in either form of COMT and strongly suggested that neither transferase is present in the dopaminergic presynaptic terminals in the rat striatum. Similar results were reported upon lesioning rat substantia nigra with 6-hydroxydopamine (Kaakkola et al. 1987).

Where in the neuronal cells this membrane-bound form of COMT is located has not been determined, although this is likely to be an important factor in controlling the extent of O-methylation in brain. Both astrocytes, which contain soluble COMT, and neurons intrinsic to the striatum, which contain MB-COMT, possess a low-affinity uptake system for the catecholamine neurotransmitters; thus accessibility of these substrates to either form of COMT may be limiting. If MB-COMT is present on the outer surface of the plasma membrane facing the synaptic cleft, then transport into the postsynaptic neuronal cell would not be required for O-methylation. Since MB-COMT has previously been suggested to be present on the plasma membranes of several tissues, it is tempting to speculate that it may be similarly present on the postsynaptic membranes facing the dopaminergic nerve terminals in the striatum. However, it is important to point out that the activity of this enzyme would be attenuated by extracellular Ca^{2+}. Conceivably this enzyme could be located on the inner surface of the plasma membrane, possibly tightly coupled to the catecholamine transport carrier. In this case, the inwardly facing MB-COMT would be exposed to low intracellular Ca^{2+} concentrations. Future immunohistochemical studies are needed to help determine the precise location of MB-COMT within the neurons in the CNS and in other peripheral organelles.

7 Genetic Regulation of Soluble COMT and MB-COMT

As discussed above, whether soluble COMT and MB-COMT result from posttranslational processing of the same gene product or are the consequence of two separate genes has not been fully resolved. Although extensive studies (for review see Weinshilboum and Raymond 1977a; Weinshilboum 1989) have previously examined the inheritance characteristics of the soluble form of COMT in humans, few studies have attempted to examine the inheritance properties for MB-COMT or whether the two forms of COMT are genetically regulated in a similar manner in vivo.

Studies by Weinshilboum and coworkers (Weinshilboum and Raymond 1977a; Sladek-Chelgren and Weinshilboum 1981) have revealed that soluble COMT is expressed in a bimodal distribution in the human population. About 25% of the population in the U.S. displays either low or high COMT activity and the remaining 50% possess intermediate values of soluble COMT activity. The data demonstrate that a pair of alleles at a specific gene locus is responsible for both high and low COMT activity. Individuals homozygous for the high COMT allele express high COMT activity and individuals possessing the two low COMT alleles exhibit low COMT activity. Heterozygous individuals display intermediate COMT activity.

Weinshilboum and coworkers (Weinshilboum and Raymond 1977b; Weinshilboum et al. 1978; Goldstein et al. 1980) have similarly demonstrated that soluble COMT activity in livers from various rat strains is under genetic control. For example, they reported that COMT activity in the Fischer-344 strain was consistently 60% of the value obtained in livers from Wistar-Furth rats. Upon selective mating of the two strains of rats, it was shown that a pair of alleles was responsible for regulating COMT activity. Based on the inheritance characteristics in the F2 generation, low COMT activity appears to be an autosomal recessive trait.

In contrast to the extensive genetic studies performed with soluble COMT, the inheritance characteristics of MB-COMT, for the most part, have been ignored. It was recently reported (Roth et al. 1990) that the specific activity of MB-COMT in the livers of Fischer-344 rats was 40% lower than in the Wistar-Furth strain. This difference in liver MB-COMT activity was essentially identical to that observed for the soluble enzyme in the two rat strains as noted above (Weinshilboum et al. 1978). There were also small differences observed in the K_m values for dopamine in the two rat strains in-

dicating that the two forms of MB-COMT may be structurally distinct. Since the ratio of activity for MB-COMT in the two animals strains is similar to that of the soluble enzyme, a common genetic factor may regulate the activity of these enzymes.

There are several possible explanations for the similarity in the ratios of the soluble and membrane-bound forms of COMT activity in these rat strains. A single gene may code for both the membrane-bound and soluble enzymes and the differences in the properties of the two enzymes may result from posttranslational modification of the gene product. As noted above, Lundstrom et al. (1991) and Bertocci et al. (1991) have recently suggested that there is a single gene for COMT with a small 2100 MW NH_2-terminal hydrophobic peptide responsible for binding of MB-COMT to the endoplasmic reticulum membranes. Expression of either the soluble COMT or MB-COMT is dependent on transcription initiation from either of two start codons, resulting in the production of a 26000 or 30000 MW polypeptide, respectively.

8 New COMT Inhibitors as Anti-Parkinson's Disease and Antidepressant Agents

Unlike the MAO inhibitors, which have been extensively used for the treatment of depression, the administration of COMT inhibitors for the treatment of behavioral or neurological disorders associated with catecholamine deficiencies has until recently proven unsuccessful. Initial attempts with structural analogues of the methyl donor AdoMet which effectively inhibited COMT were disappointing since these highly charged molecules were unable to get into the cell or cross the blood-brain barrier. Similarly, the catechol analogues that were initially tested were relatively weak inhibitors of COMT. However, in recent years several catechol analogues have been developed and found to be highly potent and selective inhibitors of COMT both in vitro and in vivo. These catechol drugs have been experimentally tested for their potential use in treating Parkinson's disease and depression.

The first of these drugs which will be discussed, OR-462 (nitecapone), has been found to be a tight binding inhibitor of the soluble form of COMT (Mannisto et al. 1988; Nissinen et al. 1988; Linden et al. 1988; Schultz and Nissinen 1989; Mannisto and Kaakkola 1990). The K_i value for binding to rat liver soluble COMT was 0.7 nmol/l;

the affinity of this drug for MB-COMT has not been reported. After an oral dose of 3 mg/kg of OR-462 to rats, duodenal COMT activity was totally inhibited within 15 min, whereas liver COMT was inhibited approximately 40% at this time. Full recovery of activity occurred within 12 h after administration. Importantly, rat striatal COMT activity was shown not to be inhibited by this drug, suggesting that OR-462 is incapable of crossing the blood brain barrier.

When OR-462 was administrated in combination with L-DOPA and carbidopa, serum levels of dopamine increased significantly with a concomitant fall in the formation of the O-methylated product, 3-O-methyldopamine (Nissinen et al. 1988; Linden et al. 1988). In rat striatum, dopamine levels increased along with homovanillic acid and 3-MT, indicating that O-methylation was not inhibited in the brain. In two behavioral Parkinson disease models, OR-462 potentiated the locomotive action in reserpine-pretreated rats and increased contralateral turning behavior in rats unilaterally injected (striatum) with 6-hydroxydopamine over that observed with L-DOPA plus carbidopa treatment alone.

The above data demonstrate that OR-462 may be a useful drug for the treatment of Parkinson's disease when used in conjunction with L-DOPA and the aromatic amino acid decarboxylase inhibitor, carbidopa. The data above suggest that OR-462 is a highly potent and selective peripheral inhibitor of COMT activity and thus has the potential to preferentially prevent formation of the potentially toxic metabolite 3-*O*-methyl-DOPA in the periphery upon administration of L-DOPA. When used in conjunction with carbidopa, this drug may be useful in lowering the dose of L-DOPA required to alleviate the symptoms of Parkinson's disease.

In a similar fashion, DaPrada and coworkers (Zurcher et al. 1989, 1990) have developed a COMT inhibitor, Ro 40-7592, which inhibits both central and peripheral COMT activity. The drug is currently in preclinical trials as a potentially useful agent for treatment of either depression or Parkinson's disease. With rat liver, the IC_{50} value for Ro 40-7592 was approximately ten times lower than that for OR-462 and, similarly, the ED_{50} value for inhibition of rat liver COMT activity after po administration was ten times lower than that for OR-462. However, the effects of the two drugs on increasing dopamine levels after administration of L-DOPA and a DOPA decarboxylase inhibitor are similar. The major functional difference between the two drugs is that Ro 40-7592 is capable of crossing the blood-brain barrier and inhibiting COMT activity in the CNS. Ro 40-7592 has been shown in rat liver homogenates to be a more potent inhibitor of

MB-COMT than of the soluble transferase (da Prada, personal communication).

The two COMT inhibitors described here represent a new class of therapeutic agents for the treatment of Parkinson's disease and depression. As to which form of COMT, membrane-bound or soluble, is being inhibited by these drugs in vivo has not been ascertained. Similarly, whether either or both of these forms of COMT have to be inhibited to produce an adequate therapeutic response is not known. Since catechol substrates and inhibitors of COMT such as tropolone have a higher affinity for MB-COMT (Jeffery and Roth 1984), possibly this form of the transferase is preferentially inhibited by these drugs.

9 Conclusions

This review has attempted to put into proper perspective the potential role of MB-COMT in the O-methylation of the catecholamine neurotransmitters and structurally related drugs. From the studies described here, it can be concluded that the membrane-bound form of COMT is a structural and biochemical entity distinct from the soluble enzyme. Although both the soluble and membrane-bound enzymes are capable of O-methylating the catecholamine neurotransmitters, evidence is presented which suggests that the MB-COMT may be the predominant species at physiologically relevant concentrations of these neurotransmitters in human brain and possibly other tissues. MB-COMT is ubiquitously distributed in almost all tissues and the highest levels are found in the liver. However, the highest ratio of membrane-bound to soluble COMT is found in brain tissue suggesting that MB-COMT may be selectively localized in neuronal cells in the CNS. This was further suggested by kainic acid lesioning studies which demonstrated a loss of MB-COMT activity after neuronal lesioning with this neurotoxin.

The importance of MB-COMT in the degradation of catecholamines is revealed by kinetic model studies with human brain and by metabolic studies using several different organ systems. These data suggest that MB-COMT is responsible for the O-methylation at low and physiologically relevant concentrations of the catecholamine neurotransmitters and that the soluble enzyme activity predominates after saturation of the membrane-bound form.

Many questions still need to be answered in regard to the role

and contribution of MB-COMT to the catabolism of the catecholamines and drugs in the intact animal. Specific questions remain as to the subcellular localization of MB-COMT and whether it is localized on the plasma membrane of cells facing the extracellular space or facing inwardly where it may be coupled to the catecholamine transport system. Answers to these questions are of particular relevance in light of the development of new potent inhibitors of COMT which have the potential to be used for treatment of depression and/or Parkinson's disease.

References

Aprille J, Malamud D (1975) Catechol-O-methyltransferase in mouse liver plasma membranes. Biochem Biophys Res Commun 64:1293–1302

Assicot M, Bohuon C (1969) Production of antibodies to catechol-O-methyltransferase (EC 2.1.1.6) of rat liver. Biochem Pharmacol 18:1893–1898

Assicot M, Bohuon C (1970) Purification and studies of catechol-O-methyltransferase of rat liver. Eur J Biochem 12:490–495

Assicot M, Bohuon C (1971) Presence of two distinct catechol-O-methyltransferase activities in red blood cells. Biochimie 53:871–874

Axelrod J, Tomchick R (1958) Enzymatic O-methylation of epinephrine and other catechols. J Biol Chem 233:702–705

Axelrod J, Senoh S, Witkop B (1958) O-methylation of catechol amines in vivo. J Biol Chem 233:697–701

Bertocci B, Miggiano V, da Prada M, Dembic Z, Lahm H, Malherbe P (1991) Human catechol-O-methyltransferase: cloning and expression of the membrane-bound form. Proc Natl Acad Sci USA 88:1416–1420

Bonisch H, Uhlig W, Trendelenburg U (1974) Analysis of the compartments involved in the extraneuronal storage and metabolism of isoprenaline in the perfused heart. Naunyn Schmiedebergs Arch Pharmacol 283:223–244

Bonisch H, Graefe K-H, Trendelenburg U (1978) The determination of the rate constant for the efflux of an amine from efflux curves for amine and metabolite. Naunyn Schmiedebergs Arch Pharmacol 304:147–155

Borchardt R, Cheng C (1978) Purification and characterization of rat heart and brain catechol methyltransferase. Biochim Biophys Acta 522:49–62

Borchardt R, Cheng C, Cooke P, Creveling C (1974) The purification and kinetic properties of liver microsomal-catechol-O-methyltransferase. Life Sci 14:1089–1100

Branco D, Teixeira A, Azevedo I, Osswald W (1984) Structural and functional alteration caused at the extraneuronal level by sympathetic denervation of blood vessels. Nauny Schmiedebergs Arch Pharmacol 326:302–312

Broch O, Fonnum F (1972) The regional and subcellular distribution of catechol-O-methyltransferase in the rat brain. J Neurochem 19:2049–2055

Creveling C, Borchardt R, Isersky C (1973) Immunological characterization of catechol-O-methyltransferase. In: Usdin E, Snyder S (eds) Frontiers in catecholamine research. Pergamon New York, pp 117–119

Fiebig ER, Trendelenburg U (1978) The kinetic constants for the extraneuronal uptake and metabolism of ^{3}H-(−)-noradrenaline in the perfused rat heart. Naunyn Schmiedebergs Arch Pharmacol 303:37–45

Francis A, Pearce LB, Roth JA (1985) Cellular localization of MAO A and B in brain: evidence from kainic acid lesions in striatum. Brain Res 334:59–64

Francis A, Whittemore R, Jeffery D, Pearce L, Roth J (1987) Catecholamine-metabolizing enzyme activity in the nigrostriatal system. Biochem Pharmacol 36:2229–2231

Garland LG, Martin GR (1984) Extraneuronal metabolism and supersensitivity to catecholamines in Guinea pig trachea. In: Fleming WW, Langer SZ, Graefe KH, Weiner N (eds) Neuronal and extraneuronal events in autonomic pharmacology. Raven, New York, pp 139–155

Goldberg R, Tipton K (1978) The distribution of catechol-O-methyltransferase in pig liver and brain. Biochem Pharmacol 27:2623–2629

Goldstein D, Weinshilboum R, Dunnette J, Creveling C (1980) Developmental patterns of catechol-O-methyltransferase in genetically different rat strains: enzymatic and immunochemical studies. J Neurochem 34:153–162

Graefe K-H, Trendelenburg U (1974) The effect of hydrocortisone on the sensitivity of the isolated nictitating membrane to catecholamines. Relationship to extraneuronal uptake and metabolism. Naunyn Schmiedebergs Arch Pharmacol 286:1–48

Grohmann M (1987) The activity of the neuronal and extraneuronal catecholamine-metabolizing enzymes of the perfused rat heart. Naunyn Schmiedebergs Arch Pharmacol 336:139–147

Grohmann M, Trendelenburg U (1985) The handling of five catecholamines by the extraneuronal O-methylating system of the rat heart. Naunyn Schmiedebergs Arch Pharmacol 329:264–270

Grohmann M, Trendelenburg U (1988) The Handling of five amines by the extraneuronal deaminating system of the rat heart. Naunyn Schmiedebergs Arch Pharmacol 337:159–163

Grossman M, Creveling C, Rybczynski R, Braverman M, Isersky C, Breakefield X (1985) Soluble and particulate forms of rat catechol-O-methyltransferase distinguished by gel electrophoresis and immune fixation. J Neurochem 44:421–432

Guldberg HC, Marsden CA (1975) Catechol-O-methyltransferase: pharmacological aspects. Pharmacol Rev 27:135–206

Head RJ, Irvice RJ, Barone S, Stitzel RE, de la Lande IS (1985) Nonintracellular cell-associated O-methylation of isoproterinol in the isolated rabbit thoracic aorta. J Pharmacol Exp Ther 234:184–189

Henseling M (1983) Kinetic constants for uptake and metabolism of ^{3}H-(−)-noradrenaline in rabbit aorta. Possible falsification of the constants by diffusion barriers within the vessel wall. Naunyn Schmiedebergs Arch Pharmacol 323:12–23

Heydorn WE, Creed GJ, Creveling CR, Jacobowitz DM (1986) Molecular analysis of catechol-O-methyltransferase (COMT) in rat brain. Pharmacologist 28: 232

Huh M, Friedhoff A (1979) Multiple molecular forms of catechol-O-methyltransferase: evidence for two distinct forms, and their purification and physical characterization. J Biol Chem 254:299–308

Inscoe J, Daly J, Axelrod J (1965) Factors affecting the enzymatic formation of O-methylated dihydroxy derivatives. Biochem Pharmacol 14:1257–1263

Jarrott B (1971) Occurrence and properties of catechol-O-methyltransferase in adrenergic neurons. J Neurochem 28:17–27

Jarrott B (1973) The cellular localisation and physiological role of catechol-O-methyltransferase in the body. In: Usdin E, Snyder S (eds) Frontiers in catecholamine research. Pergamon, New York, pp 113–115

Jarrott B, Iversen L (1971) Noradrenaline metabolizing enzymes in normal and sympathetically denervated vas deferens. J Neurochem 18:1–6

Jarrott B, Langer S (1971) Changes in monoamine oxidase and catechol-O-methyltransferase activities after denervation of the nictitating membrane of the cat. J Physiol (Lond) 212:549–559

Jeffery D, Roth J (1984) Characterization of membrane-bound and soluble catechol-O-methyltransferase from human frontal cortex. J Neurochem 42:826–832

Jeffery D, Roth J (1985) Purification and kinetic mechanism of human brain soluble catechol-O-methyltransferase. J Neurochem 44:881–885

Jeffery D, Roth J (1987) Kinetic reaction mechanism for magnesium binding to membrane-bound and soluble catechol-O-methyltransferase. Biochemistry 26:2955–2958

Kaakkola S, Mannisto P, Nissinen E (1987) Striatal membrane-bound and soluble catechol-O-methyltransferase after selective neuronal lesions in the rat. J Neural Transm 69:221–228

Kaplan G, Hartman B, Creveling C (1979) Immunohistochemical demonstration of catechol-O-methyltransferase in mammalian brain. Brain Res 167:241–250

Kopin I (1986) Catecholamine metabolism: basic aspects and clinical significance. Pharmacol Rev 37:334–364

Levitt P, Pintar J, Breakefield X (1982) Immunochemical demonstration of monoamine oxidase B in brain astrocytes and serotonergic neurons. Proc Natl Acad Sci USA 79:6385–6389

Linden I, Nissinen E, Etemadzadeh E, Kaakkola S, Mannisto P, Pohto P (1988) Favorable effect of catechol-O-methyltransferase inhibition by OR-462 in experimental models of Parkinson's disease. J Pharmacol Exp Ther 247:289–293

Lundstrom K, Salminen M, Jalanko A, Savolainen R, Ulmanen I (1991) Cloning and characterization of human placental catechol-O-methyltransferase cDNA. DNA Cell Biol 10:181–189

Magaribuchi T, Hama T, Kurahashi K, Fujiwara M (1987) Effects of extraneuronal uptake inhibitors on the positive chronotropic response to isoprenaline and on the accumulation of isoprenaline in perfused rat heart after inhibition of catechol-O-methyltransferase. Naunyn Schmiedebergs Arch Pharmacol 335: 123–128

Major H, Sauerwein I, Graefe K (1978) Kinetics of the uptake and metabolism of ^{3}H-(±) isoprenaline in the rat submaxillary gland. Naunyn Schmiedebergs Arch Pharmacol 305:51–63

Mannisto P, Kaakkola S (1990) Rationale for selective COMT inhibitors as adjuncts in the drug treatment of Parkinson's disease. Pharmacol Toxicol 66:317–323

Mannisto P, Kaakkola S, Nissinen E, Linden I, Pohto P (1988) Properties of novel effective and highly selective inhibitors of catechol-O-methyltransferase. Life Sci 43:1465–1471

Marsden C, Broch O, Guldberg H (1971) Catechol-O-methyltransferase and monoamine oxidase activities in rat submaxillary gland: effects of ligation, sympathectomy and some drugs. Eur J Pharmacol 15:335–342

Marsden C, Broch O, Guldberg H (1972) Effect of nigral and raphe lesions on the catechol-O-methyltransferase and monoamine oxidase activities in the rat striatum. Eur J Pharmacol 19:35–42

Marzullo G, Friedhoff A (1975) Catechol-O-methyltransferase from rat liver: two forms having different *Meta:Para* methylation ratios. Life Sci 17:933–942

McCormick J, Flanagan R, Lloyd A (1972) A microsomal catechol-O-methyltransferase from rat liver. Biochem J 130:83–84

Nissinen E, Linden I, Schultz E, Kaakkola S, Mannisto P, Pohto P (1988) Inhibition of catechol-O-methyltransferase activity by two novel disubstituted catechols in the rat. Eur J Pharmacol 153:263–269

Paiva MA, Guimaraes S (1978) A comparative study of the uptake and metabolism of noradrenaline and adrenaline by the isolated saphenous vein of the dog. Naunyn Schmiedebergs Arch Pharmacol 303:221–228

Paiva MA, Guimaraes S (1984) The kinetic characteristics of the extraneuronal O-methylating system of the dog saphenous vein and the supersensitivity to catecholamines caused by its inhibition. Naunyn Schmiedebergs Arch Pharmacol 327:48–55

Raxworthy M, Gulliver P, Hughes P (1982) The cellular location of catechol-O-methyltransferase in rat liver. Naunyn Schmiedebergs Arch Pharmacol 320:182–188

Reid J, Stitzel R, Head R (1986) Characterization of the O-methylation of catechol oestrogens by intact rabbit thoracic aorta and subcellular fractions thereof. Naunyn Schmiedebergs Arch Pharmacol 334:17–28

Rivett A, Eddy B, Roth J (1982) Contribution of sulfate conjugation, deamination, and O-methylation to metabolism of dopamine and norepinephrine in human brain. J Neurochem 39:1009–1016

Rivett A, Francis A, Roth J (1983a) Distinct cellular localization of membrane-bound and soluble forms of catechol-O-methyltransferase in brain. J Neurochem 40:215–219

Rivett A, Francis A, Roth J (1983b) Localization of membrane-bound catechol-O-methyltransferase. J Neurochem 40:1494–1496

Roffman M, Reigle T, Orsulak P, Schildkraut J (1976) Properties of catechol-O-methyltransferase in soluble and particulate preparations from rat red blood cells. Biochem Pharmacol 25:208–209

Roth JA, Rivett AJ, Renskers KJ (1982) Properties of human brain phenolsulfotransferase and its role in the inactivatio of catecholamine neurotransmitters. In: Mulder G, Caldwell J, van Kempen G, Vonk R (eds) Sulfate metabolism and sulfate conjugation. Taylor and Francis, London, pp 107–114

Roth J, Grossman M, Adolf M (1990) Variation in hepatic membrane-bound catechol-O-methyltransferase activity in Fischer and Wistar-Furth strains of rat. Biochem Pharmacol 40:1151–1153

Salminen M, Lundstrom K, Tilgmann C, Savolaimen R, Kilkkinen N, Ulmanen I (1990) Molecular cloning and characterization of rat liver catechol-O-methyltransferase. Gene 93:241–247

Schultz E, Nissinen E (1989) Inhibition of rat liver and duodenum soluble catechol-O-methyltransferase by a tight-binding inhibitor OR-462. Biochem Pharmacol 38:3953–3956

Sladek-Chelgren S, Weinshilboum R (1981) Catechol-O-methyltransferase biochemical genetics: human lymphocyte enzyme. Biochem Genet 19:1037–1053

Tilgmann C, Kalkkinen N (1990) Purification and partial characterization of rat liver soluble catechol-O-methyltransferase. FEBS Lett 264:95–99

Tong J, d'Iorio A (1977) Solubilization and partial purification of particulate catechol-O-methyltransferase from rat liver. Can J Biochem 55:1108–1113

Traiger G, Calvert D (1969) O-methylation of ^{3}H-norepinephrine by epididymal adipose tissue. Biochem Pharmacol 18:109–117

Trendelenburg U (1980) A kinetic analysis of the extraneuronal uptake and metabolism of catecholamines. Rev Physiol Biochem Pharmacol 87:35–115

Trendelenburg U (1984a) Metabolizing systems. In: Fleming W, Langer S, Graefe K, Weiner N (eds) Neuronal and extraneuronal events in autonomic pharmacology. Raven, New York, pp 93–109

Trendelenburg U (1984b) The influence of inhibition of catechol-O-methyltransferase or of monoamine oxidase on the extraneuronal metabolism of ^{3}H-(−)-noradrenaline in the rat heart. Naunyn Schmiedebergs Arch Pharmacol 327: 285–292

Trendelenburg U (1988) The extraneuronal uptake and metabolism of catecholamines. In: Trendelenburg U, Weiner (eds) Handbook of experimental pharmacology, vol 90/1. Springer, Berlin Heidelberg New York, pp 279–319

Trendelenburg U, Hohn D, Graefe K, Pluchino S (1971) The influence of block of catechol-O-methyltransferase on the sensitivity of isolated organs to catecholamines. Naunyn Schmiedebergs Arch Pharmacol 271:59–92

Verity M, Su C, Bevan J (1972) Transmural and subcellular localization of monoamine oxidase and catechol-O-methyltransferase in rabbit aorta. Biochem Pharmacol 21:193–201

Weinshilboum R (1989) Methyltransferase pharmacogenetics. Pharmacol Ther 43:77–90

Weinshilboum R, Raymond F (1976) Calcium inhibition of rat liver catechol-O-methyltransferase. Biochem Pharmacol 25:573–579

Weinshilboum R, Raymond F (1977a) Inheritance of low catechol-O-methyltransferase activity in man. Am J Hum Genet 29:125–135

Weinshilboum R, Raymond F (1977b) Variations in catechol-O-methyltransferase activity in inbred strains of rats. Neuropharmacology 16:703–706

Weinshilboum R, Raymond F, Frohnauer M (1978) Monogenic inheritance of catechol-O-methyltransferase activity in the Rat – biochemical and genetic studies. Biochem Pharmacol 28:1239–1247

Zou J, Pentney R, Roth J (1990) Immunohistochemical detection of phenol sulfotransferase containing neurons in human brain. J Neurochem 55:1154–1158

Zurcher G, Keller HH, Borgulya J, da Prada M (1989) Neuropharmacological effects in rats of the new reversible COMT inhibitors Ro 40-7592 and Ro 41-0960. J Neurochem 52:S16

Zurcher G, Keller HH, Kettler R, Borgulya J, Bonetti EP, da Prada M (1990) Ro-40-7592, a novel, very potent and orally active inhibitor of catechol-O-methyltransferase – a pharmacological study in rats. Parkinsons Disease: Anatomy, Pathology and Therapy 53:497–503

Rev. Physiol. Biochem. Pharmacol., Vol. 120

Molecular Characteristics of Amiloride-Sensitive Sodium Channels

DALE J. BENOS, SONIA CUNNINGHAM, R. RANDALL BAKER, K. BETH BEASON, YOUNGSUK OH, and PETER R. SMITH[1]

Contents

[1] Department of Physiology and Biophysics, University of Alabama at Birmingham, Birmingham, AL 35294, USA

1 Introduction

The function of transporting epithelia as selective permeability barriers between the transcellular and interstitial compartments depends upon the establishment and maintenance of functional polarity within the epithelial cell. Net transepithelial Na^+ transport across the epithelium requires spatial localization of the (Na^+/K^+) ATPase to the basolateral plasma membrane (Cala et al. 1978; Farquhar and Palade 1966; Keynes 1969; Mills and Ernst 1975; Stirling 1972), and Na^+-selective ion channels to the apical or luminal plasma membrane (Garty and Benos 1988; Sariban-Sohraby and Benos 1986a). This sodium entry channel is rate limiting for overall transepithelial transport, is inhibited by the diuretic drug amiloride, and is regulated hormonally, specifically by the peptide hormone vasopressin and the steroid hormone aldosterone. The first experimental evidence that this amiloride-sensitive entry pathway may be an ion channel came from blocker-induced current noise experiments in which the deduced single-site turnover number (approximately 10^6 ions per second per site) is consistent with channel-mediated transport (Lindemann and Van Driessche 1977). However, the most compelling evidence for this transport system being an ion channel has come from the direct recording of quantal current jumps generated by the spontaneous opening and closing of individual transport molecules. Single-channel activity has been measured either by the patch clamp technique (Cantiello et al. 1989; Frings et al. 1988; Gogelein and Greger 1986; Hamilton and Eaton 1985, 1986; Light et al. 1988; Ling and Eaton 1989; Palmer and Frindt 1987a; Vigne et al. 1989) or in planar lipid bilayers into which amiloride-sensitive Na^+ channels have been incorporated (Olans et al. 1984; Sariban-Sohraby et al. 1984b). Interestingly, electrophysiological, kinetic, and pharmacological evidence accumulated over the past 3 years indicates that there may not be a unique class of amiloride-sensitive Na^+ channel, but rather a family of epithelial Na^+ channels. This feature would be consistent with the observations made for voltage-gated

Na^+, Ca^{2+}, and K^+ channels (Catterall 1988; Hille 1984; Jan and Jan 1990; Rehm and Tempel 1991).

Amiloride-sensitive Na^+ channels can be broadly classified as having either high or low sensitivity to the drug [i.e., an apparent equilibrium inhibitory dissociation constant (K_i) of less than or greater than 1 μM at >100 mM extracellular Na^+ concentration, respectively]. Na^+ channels with a relatively high affinity for amiloride are typically found in high-resistance epithelia like frog skin, toad urinary bladder, or mammalian collecting tubules. In addition, there are at least two types of high amiloride affinity channels that differ in their Na^+ versus K^+ selectively and their open state conductances. For example, Na^+ channels from renal cortical collecting tubules (CCT) and toad urinary bladder have Na^+/K^+ selectivity ratios greater than 10:1 and a conductance less than 10 pS, while Na^+ channels from renal inner medullary collecting tubule cells and human sweat duct have low Na^+/K^+ selectivity (less than 5:1) and relatively high conductance (greater than 15 pS) (Benos 1989; Smith and Benos 1991), although some low-selective, low-conductance channels have been described (Verrier et al. 1989).

Recently, a second class of amiloride-sensitive Na^+ channel has been reported that displays a low affinity for amiloride (i.e., an inhibition constant greater than 1 μM at high Na^+ concentrations). These low amiloride affinity Na^+ conductive pathways have been found in rabbit blastocyst trophectodermal cells (Robinson et al. 1991), rat and porcine brain endothelia (Vigne et al. 1989), porcine kidney cortex (Barbry et al. 1987, 1990b), rabbit type II pneumocytes (Matalon et al. 1991), rabbit proximal tubules (PT) (Gogelein and Greger 1986), LLC-PK1 cells (Cantiello and Ausiello, personal communication; Moran and Moran 1984), rat colonic enterocytes (Bridges et al. 1988), and in the basolateral membrane of the toad urinary bladder (Moran et al. 1980). This class of channels differs not only in their amiloride affinity but also in their ion selectivity and kinetic properties. Preliminary evidence suggests that the two aforementioned classes of epithelial Na^+ channels differ in their biochemical composition as well (see below). Hence, they may originate from different genes or result from alternative splicing from the same gene. Table 1 summarizes the properties of the known low amiloride affinity epithelial Na^+ channels and their pharmacological profiles for inhibition by various analogs of amiloride. Interestingly, even within this low amiloride affinity category, one can distinguish at least three different types of channels. The Na^+ channels from

Table 1. Order of inhibitory potency of amiloride and analogs for various low amiloride affinity epithelial Na^+ channels

System	Order of potency (K_i)	Reference
Rat and pig brain endothelium	Phenamil > benzamil > amiloride (0.04 μ*M*) (0.4 μ*M*) (2.4 μ*M*)	Vigne et al. (1989)
Pig kidney cortex	Phenamil > benzamil > amiloride, EIPA (0.07 μ*M*) (0.25 μ*M*) (6 μ*M*)	Barbry et al. (1987, 1990a)
LLC-PK1 cells	EIPA > amiloride > phenamil (4.8 μ*M*) (28.4 μ*M*) (65.8 μ*M*)	Cantiello and Ausiello (personal communication), Moran and Moran (1984)
Rabbit blastocysts (7-day)	Phenamil > amiloride > EIPA > benzamil (15 μ*M*) (20 μ*M*) (25 μ*M*) (80 μ*M*)	Robinson et al. (1991)
Toad urinary bladder	EIPA > amiloride > phenamil (2.6 μ*M*) (3.4 μ*M*) (10 μ*M*)	Asher et al. (1987)
Alveolar type II cells	EIPA > amiloride > phenamil (20 μ*M*) (50 μ*M*) (50 μ*M*)	Matalon et al. (1991)
Rat colonic cells	Amiloride > phenamil EIPA > benzamil (4.1 μ*M*) (9.9 μ*M*) (10.6 μ*M*)	Bridges et al. (1988)

endothelium and pig kidney cortex seem to have a relatively high affinity for inhibition by the amiloride analog phenamil, with the lowest affinity for inhibition by amiloride itself and ethylisopropyl amiloride (EIPA). In LLC-PK1 cells the low amiloride affinity channel has a much higher sensitivity to EIPA as compared to amiloride or phenamil. Also, there appears to be a third type of low amiloride affinity channel in rabbit blastocysts, alveolar type II cells, toad urinary bladder cells, and rat colonic cells. These channels barely distinguish between the various analogs of amiloride, that is, all K_i values are within a factor of 5.

Recently, another category of amiloride-sensitive Na^+ channels has also been described. These channels are, again, poorly selective between Na^+ and K^+ and even allow Ca^{2+} to pass. These channels are gated by cGMP and are found in sensory organs, e.g., olfactory epithelium and rod outer segments. They are inhibited with a low affinity by amiloride and have been cloned (Kaupp et al. 1989). Nonselective low amiloride affinity channels have also been described in inner ear hair cells, but the gating of these channels by cGMP has not yet been determined (Jorgensen and Ohmori 1988).

In this review, we will first summarize what is known about the macroscopic and single-channel properties of these different cat-

egories of amiloride-sensitive Na^+ channels, and the use of amiloride as an inhibitor of these ion channels. We will then turn to a consideration of the biochemical properties of these channels and how these properties relate to the physiological function of the various regulatory molecules. We will then discuss the regulation of these channels by various hormones, ions, and ligands. Fourth, we will depict what is known thus far about the molecular biology of these channels. Fifth, we will detail the involvement (or dysfunction) of epithelial Na^+ channels in an important genetic disease of children and young adults, namely cystic fibrosis (CF), and the use of amiloride as a therapeutic agent. We will conclude with a perspective on future experimentation.

2 Characteristics of Epithelial Na^+ Channels

2.1 Macroscopic Measurements

2.1.1 Short-Circuit Current

Koefoed-Johnsen and Ussing first postulated in 1958 that the apical or luminal membrane of sodium-reabsorbing epithelia such as frog skin and toad urinary bladder was Na^+ selective while the basolateral membrane was dominated by a K^+ conductance. Na^+ movement through the basolateral membrane was accomplished by the actions of a ouabain-sensitive Na^+- and K^+-activated adenosine triphosphatase (Na^+/K^+ ATPase) or Na^+ pump. These initial observations formed the paradigm for analyzing Na^+ transport across these epithelia, even up to the present day.

Figure 1 illustrates the transepithelial Na^+ movement that occurs in a wide variety of epithelia. Na^+ ions enter a polarized epithelial cell through specific pathways (channels) in the apical membrane, and are pumped out of the cell across the basolateral membrane by the Na^+/K^+ ATPase. Apical entry of sodium through this Na^+ channel occurs down the ion's electrochemical potential energy gradient. Na^+ entry at the apical membrane is the rate-limiting step for net transport across the epithelial layer (Biber and Curran 1970; Helman and Fisher 1977; MacKnight et al. 1980; Nagel et al. 1981; Rick et al. 1978). Experimental observations consistent with the apical entry step being rate limiting are: (a) apical Na^+ entry as well as transepithelial Na^+ influx is rapidly and completely inhibited by

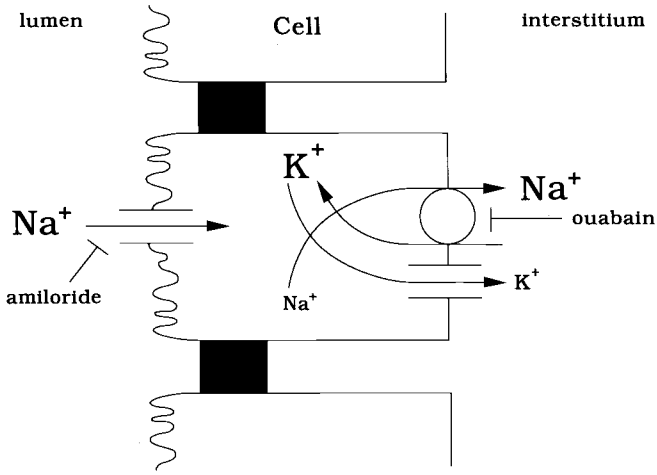

Fig. 1. Schematic model for transepithelial Na^+ reabsorption in a typical epithelium. The ouabain-sensitive Na^+/K^+ ATPase is localized in the basolateral membrane, while amiloride-sensitive Na^+ selective channels are located in the apical or luminal (and often referred to as mucosal) membrane. A relatively low (10 m*M*) intracellular Na^+ activity is maintained by the Na^+/K^+ ATPase. That fact, coupled with the negative electrical potential difference across the apical membrane, creates a large inwardly directed electrochemical gradient from Na^+ movement

the diuretic, K^+-sparing drug amiloride (which has no appreciable effect on Na^+/K^+ ATPase activity at the concentrations used to inhibit high amiloride affinity sodium channels, see below); (b) the resistance of the apical membrane is 75%–90% of the total transepithelial electrical resistance; and (c) the short-circuit current (a measure of net Na^+ transport) across an entire epithelial layer is identical to amiloride-sensitive Na^+ transport across the apical membrane alone. The amiloride-sensitive Na^+ channel is, therefore, a critical regulatory protein involved in the maintenance of systemic Na^+ balance through Na^+ reabsorption in the distal nephron, and serves key functions in the large airways, exocrine sweat ducts, colon, and other epithelia.

The idea that the apical membrane of the frog skin behaves as a Na^+-selective electrode was supported by early microelectrode measurements that demonstrated "correct" polarity of the apical membrane potential for Na^+ reabsorption under in vivo or in vitro conditions (Cereijido and Curran 1965; Ussing and Windhager 1964). The question of the magnitude and direction of the Na^+ electrochemical potential energy gradient was addressed in microelectrode studies (Helman and Fisher 1977; Helman et al. 1979; Nagel 1976;

Nagel et al. 1981) and electron probe studies (Rick et al. 1978) in frog skin epithelia. Under most experimental conditions, the apical membrane potential is negative with respect to the outer bathing solution, and, in addition, when the tissue is bathed with high [Na^+] Ringer solution, a large chemical gradient for Na^+ exists across the apical membrane. Intracellular Na^+ concentration was found to be approximately 10–13 m*M*. The decrease in the steady state intracellular Na^+ concentration and the hyperpolarization of the apical membrane potential when external sodium was reduced suggested that a large electrochemical gradient favoring inward Na^+ movement across the apical membrane was present under most conditions. In addition, Na^+ movement through amiloride-sensitive Na^+ channels was found to be in excellent agreement with that predicted by the flux ratio equation over a wide range of electrochemical potential energy gradients (Benos et al. 1983a; Palmer 1982a). Thus, Na^+ movement across the apical membrane can be entirely accounted for by free diffusion in which the Na^+ ions obey independence (Benos et al. 1983a; Palmer 1982a). Further, surface charge does not appear to influence the rate of Na^+ flow through these apical entry pathways (Benos et al. 1981).

Another major question that arose in early studies concerned the nature of the pathway for apical Na^+ movement. What are the characteristics of the Na^+ ion interaction with the apical membrane and how does Na^+ translocation occur? In early studies, Cereijido et al. (1964) and Biber et al. (1966) concluded that Na^+ could not enter the epithelial cells by electrodiffusion because the permeability coefficient of Na^+ across the apical membrane decreased with an increase in external Na^+ concentration. Likewise, rapid uptake measurements of $^{22}Na^+$ across the apical membrane of frog skin showed that the influx saturated with increasing external Na^+ concentration (Biber and Curran 1970; Mullen and Biber 1978). An apparent explanation for this saturation behavior of Na^+ influx came from two different sets of experiments by Lindemann and colleagues (Fuchs et al. 1977; Lindemann 1984; Lindemann and Voute 1976) on current-voltage relations and step changes in external [Na^+]. In these experiments, the basolateral membranes of frog skin were first depolarized with solutions containing high K^+ concentrations. Under these conditions, the authors reasoned that the transepithelial electrical properties were dominated by the apical membrane because the increase in basolateral membrane conductance resulted in total transepithelial resistance falling almost entirely across the apical membrane. Therefore, the applied transepithelial voltage difference

would essentially be equivalent to the apical membrane potential. These predications were confirmed by several investigators (Benos et al. 1983a; Lindemann 1980; Thompson et al. 1982). This high serosal K^+ treatment obviates the need for measuring intracellular voltages with the more experimentally challenging application of microelectrodes.

In the first set of experiments, instantaneous current-voltage (I-V) curves for the amiloride-sensitive apical entry pathway were determined by recording the current response to a voltage staircase in the absence and presence of 0.1 m*M* amiloride. The I-V curve of the Na^+ entry pathway was determined by subtraction. It was assumed that amiloride did not affect the paracellular shunt pathway, an assumption that may not be strictly true (Helman and Fisher 1977). The I-V curve could be fitted by the Goldman-Hodgkin-Katz (GHK) constant field current equation. The authors estimated the Na^+ permeability (P_{Na}) of this membrane to be approximately 3×10^{-5} cm/s at 5.5 m*M* external Na^+. Further, P_{Na} decreased with increasing Na^+ concentrations. Comparable results were found for toad urinary bladder (Palmer et al. 1980). Thompson et al. (1982) extended these observations and found that the I-V relations of the amiloride-sensitive Na^+ entry system in K^+-depolarized rabbit descending colon likewise conformed to the GHK equation over the voltage range −120 to +50 mV. Thus, all groups concluded that Na^+ entry does occur by electrodiffusion through homogeneous channels. I-V curves well described by the GHK equation were also measured from microelectrode recordings in the frog skin and Necturus urinary bladder (Delong and Civan 1984; Lindemann 1984).

Current transients after an abrupt change in external Na^+ concentration ($[Na^+]_o$) were also measured using K^+-depolarized preparations. These measurements were done with a fast flow chamber so that the halftime for solution replacement was on the order of 10 ms. Upon increasing $[Na^+]_o$, the short-circuit current rose rapidly and within 1 or 2 s, reached a peak value (I_p) followed by relaxation over the next 2–5 s to a lower steady state value (Iss). The declining current was attributed to a slow decrease in P_{Na} in response to an increase in $[Na^+]_o$. In fact, when I_p was plotted against $[Na^+]_o$, no saturation was observed at least up to 100 m*M* Na^+ concentration. On the other hand, when Iss versus $[Na^+]_o$ was plotted, the typical saturation behavior of the macroscopic current was observed with a half maximal Na^+ concentration of 5–20 m*M*. The slow decline in current could be prevented and the increased transport rate maintained by adding a variety of compounds, including *p*-chloromer-

curibenzoate (p-CMB), benzimidazolylguanidine (BIG), mersalyl, and Tween 80 (see Garty and Benos 1988, Benos 1982, Lindemann and Voute 1976 for discussion). These observations have led to a model (called Na^+ self-inhibition) of epithelial Na^+ channel regulatory activity in which the binding of Na^+ to an externally accessible regulatory site induces a relatively slow (over several seconds) conformational closing of the pathway (Lindemann and Voute 1976). Compounds like p-CMB that block this Na^+ self-inhibition would act as antagonists either by binding at the regulatory site or by binding to another site on the channel, leading to stabilization of the open configuration of the pathway. The idea that external Na^+ can down-regulate its own rate of transport into the cell has been proposed as a physiologically important regulatory phenomenon. Furthermore, it has been speculated that endogenous compounds functionally similar to those listed above might release the Na^+ entry pathway from inhibition and act as physiological luminal antidiuretic compounds. An important prediction for this substrate inhibition model was that the entry pathways themselves do not saturate with an increase in $[Na^+]_o$, although this prediction was not borne out by experiment (Olans et al. 1984; Palmer et al. 1990). The saturation behavior of the macroscopic short-circuit current would be due to a reduction in the total number of conducting units as the $[Na^+]_o$ is increased. Thus, it would appear that the phenomenon of self-inhibition results from the direct effects of external Na^+ on the Na^+ entry pathway itself rather than from indirect effects on intracellular Na^+, calcium, or pH. This idea has dominated the interpretation of apical membrane P_{Na} even at the single-channel level (see below).

2.1.2 Noise Analysis

Current fluctuation (noise) analysis has been used extensively to acquire information about channel properties in both biological and artificial membrane preparations. This experimental approach is useful for deducing molecular characteristics of single channels, such as channel conductance, channel density, and the rate constants associated with channel opening and closing, as compared to multi-channel behavior. Detailed explanations of this technique are beyond the scope of this review; the reader is referred to Benos (1983) and Lindemann (1980, 1984) for further information. Because epithelial Na^+ channels display spontaneous current fluctuations that are very slow, i.e., frequencies less than 1 or 2 Hz, current fluctuations can only be measured through these pathways by the addition of sub-

maximal concentrations of reversible blocking agents like amiloride. From these measurements, models can be constructed so that the number of ions flowing through a single conducting site and the total number of conducting sites can be calculated under a given set of experimental conditions. Lindemann and Van Driessche (1977) demonstrated for the first time that the mechanism of apically located amiloride-sensitive Na^+ transport must be via a channel because the rate of ion movement through individual entry sites was too fast for a carrier type of transport mechanism. Later Van Driessche and Lindemann (1979) showed that there was a decrease in the density of conducting ion channels with increasing Na^+ concentrations with no evidence of saturation of individual channels, at least up to 60 mM external Na^+ activity. These results supported earlier evidence of a self-inhibition model of Na^+ entry. However, as indicated, single-channel measurements do not support these model-dependent deductions. One possible explanation for the difference between macroscopic and single-channel saturation effects is that single-channel properties deduced from the noise experiments of Lindemann and Van Driessche may have been influenced by K_i depolarization, e.g., alterations in intracellular adenosine 3′, 5′-cyclic monophosphate (cAMP) levels. We will return to this point later (see Sect. 4.3.2). Nonetheless, the importance of these elegant measurements was that mechanism of Na^+ transport through the apical membrane was determined in a preparation not easily amenable to measurement by patch electrodes.

2.2 Single-Channel Measurements

Although the use of macroscopic techniques such as short-circuit current measurements, noise analysis, and intracellular microelectrodes generated a considerable amount of information concerning the kinetics, inhibition, and regulation of Na^+ movement through amiloride-sensitive channels (Abramcheck et al. 1985; Biber et al. 1966; Palmer et al. 1980; Sariban-Sohraby and Benos 1986a), the elucidation of specific molecular characteristics in an unambiguous fashion was not possible until the development of techniques such as patch clamping and planar lipid bilayer reconstitution. These techniques have permitted individual amiloride-sensitive Na^+ channels to be characterized at the single-channel level in terms of their conductance, cation selectivity, and open state probability in a manner free from constraints imposed by any model.

2.2.1 Single-Channel Characteristics

Single amiloride-sensitive Na^+ channel activity was first demonstrated by Benos and colleagues (Sariban-Sohraby et al. 1984b; Olans et al. 1984). Channel activity was observed after incorporation of apical membrane vesicles from A6 cells (a cell line derived from the toad kidney) into planar lipid bilayers. These Na^+ channels exhibited the following characteristics: the single-channel conductance ranged from 4–80 pS at 200 m*M* NaCl; the channel was perfectly cation selective, with a Na^+/K^+ selectivity ratio of 2:1; amiloride reduced the open time conductance in a dose-dependent manner when in the *cis* (or vesicle-containing) chamber, with a K_i of 0.1 μ*M*, and it induced a flickering-type (slow) inhibition when present in the *trans* chamber. Subsequently, many measurements of single amiloride-sensitive Na^+ channels have been made in a variety of epithelial preparations using the patch clamp technique.

Hamilton and Eaton (1985, 1986) have observed two different types of amiloride-sensitive channel in native intact A6 cells: (a) a channel with a single-channel conductance of 1–3 pS and a Na^+/K^+ selectivity ratio greater than 20:1, and (b) a channel with a single-channel conductance of 7–10 pS and a Na^+/K^+ selectivity ratio of 3–4:1. The highly selective channel was open ~10% of the time, whereas the low cation selective channel was open ~30% of the time. The primary effect of amiloride was to reduce channel mean open time (t_{open}) and increase channel mean closed time as the cell was hyperpolarized. The fact that $1/t_{open}$ was linearly dependent on the amiloride concentration suggests an interaction of one amiloride molecule with one channel to produce the block. However, it is possible that the channel could contain more than one amiloride binding site, and that these additional sites could be located in regions different than the channel pore. Although amiloride produced channel flickering at negative potentials, the single-channel conductance and the Na^+ versus K^+ selectivity were not altered by amiloride. Hamilton and Eaton (1986) argued that their membrane patches contained functionally distinct epithelial Na^+ channels, and that the type of channel observed may depend on the specific transport and/or growth requirements (i.e., cells grown on impermeable versus permeable supports) of the epithelial cells. Likewise, Frings et al. (1988) have measured four kinetically different types of epithelial cation channels in toad urinary bladder with conductances ranging from 5 to 59 pS. These channels vary in their cation selectivity and sensitivity to amiloride. The physiological relevance of the

Table 2. Characteristics of single amiloride-sensitive Na^+ channels in different tissues

	A6 cells[a]	A6 cells[b]	Rat CCT[c]	Rabbit straight PT[d]	Toad urinary bladder[e]	Rat IMCD[f]	Human sweat duct cells[g]	Porcine thyroid follicular cells[h]	Porcine and rat endothelial cells (brain cortex)[i]
Technique	Bilayer reconstitution	Patch clamp	Patch clamp	Patch clamp	Patch clamp	Patch clamp	Patch clamp	Patch clamp	Patch clamp
Open state conductance (pS) ([NaCl] > 100 m*M*)	4–80	7–10/1–3	5–8	12	5	28	15	3	23
I-V relationship (symmetrical NaCl solutions)	Linear (±60 mV)	Linear (±80 mV), nonlinear	Linear (±80 mV)	Linear (±50 mV)	Linear	Linear	Linear	Linear	Linear
P_{Na^+}/P_{K^+} selectivity	2–3	3–4/>20	≥10	≥19	>20	1	2–4	1.2	1.5
Saturation of single-channel conductance	Yes (K_s = 17 m*M*)	Yes K_s = 20 m*M*)	Yes K_s = 75 m*M*)	NT	NT	NT	NT	NT	NT
Mean open time	2–10s	43 ms/20 ms	3–4s	<500 ms	389 ms	~30 ms	~30 ms	ND	ND
Mean closed time	5s	97 ms/86 ms	3–4s	>1s	876 ms	~40 ms	ND	ND	ND
K_i for amiloride (1 μ*m*)	0.1	0.87	0.07	10	0.1	<0.5	<0.5	0.15	10

Amiloride block	Cis: fast; trans: flickering	Flickering	Flickering	Flickering	*	Flickering	Flickering?	*	Flickering
Amiloride effect on mean open time	Cis: increase	Decrease	Decrease	Decrease	Decrease	Decrease	*	*	*
Amiloride effect on mean closed time	Cis: no change	Increase	Decrease	*	Decrease	Increase	*	*	*
Amiloride effect on apparent open state conductance	Cis: decrease; trans: no change	NC	NC	NC	*	NC	*	*	*
Voltage dependence of block	NT	Yes	NT	NT	Yes	Yes	NT	NT	NT

NT, not tested; NO, not determined; NC, no change; *, the authars made no comments on these characteristics K_s, concentration of Na^+ ■ for 50% of maximal transport
[a] Sariban-Sohraby et al. (1984b), Olans et al. (1984); apical membrane vesicles derived from cells grown on permeable supports were used.
[b] Hamilton and Eaton (1985); Eaton and Hamilton (1988); cells in culture on permeable and impermeable supports, respectively, were patched.
[c] Palmer and Frindt (1986); cells from intact tables were patched.
[d] Goegelein and Greger (1986); cells from intact tables were patched.
[e] Frings et al. (1988), Palmer (1984, 1990); cells from intact bladders were patched.
[f] Light et al. (1988); cells in culture on impermeable patch clamp were patched.
[g] Joris et al. (1989); cells in culture on impermeable supports were patched.
[h] Verrier et al. (1989); cells in culture on impermeable supports were patched.
[i] Vigne et al. (1989); cells in culture on impermeable support were patched.

different channels observed by Hamilton and Eaton (1986), Frings et al. (1988), and Sariban-Sohraby et al. (1984b) is not clear, and may be an artifact of the experiment. Perturbation of apical membrane integrity with patch electrodes or reconstitution may induce channel conduction and kinetic states not normally apparent. For example, excising a patch could eliminate important intracellular regulatory elements.

Palmer and Frindt (1986), using the patch clamp technique, have measured single amiloride-sensitive Na^+ channels in the apical membrane of the rat CCT. These channels exhibited several properties associated with Na^+ channels in other tight epithelia. The CCT channels had a single-channel conductance of 5 pS and a P_{Na^+}/P_{K^+} selectivity of ≥ 10. Spontaneous transitions between open and closed states occurred more frequently in the presence of 0.5 μM amiloride. Amiloride reduced channel mean open and closed times and decreased the average open channel probability by ~70%, without affecting single-channel conductance. Subsequently, single-channel activity has been measured in the rabbit straight PT (Gogelein and Greger 1986), toad urinary bladder (Frings et al. 1988), human sweat ducts (Joris et al. 1989), rat inner medullary collecting duct (IMCD) (Light et al. 1988), rat and porcine brain endothelia (Vigne et al. 1989), and porcine thyroid cells (Verrier et al. 1989). The open state conductance of single amiloride-sensitive Na^+ channels in these tissues varied greatly. For example, the conductance was 2.6 pS in porcine thyroid follicular cells and 28 pS in rat IMCD. Channels with a high P_{Na^+}/P_{K^+} selectivity were observed in both rabbit straight PT and toad urinary bladder; however, the toad bladder channel showed high amiloride affinity (apparent K_i of 0.1 μM), whereas the rabbit straight PT channel had a low affinity for amiloride (apparent K_i of 10 μM), although amiloride was added to the cytoplasmic site of the patch. Rat IMCD, human sweat duct, porcine thyroid, and porcine and rat brain endothelia expressed relatively nonselective monovalent cation channels. Although the first three tissues had an apparent K_i for amiloride of <0.5 μM, amiloride blocked brain endothelial channels with an apparent K_i of 10 μM. Amiloride typically exerted a flickering-type block in rabbit straight PT, rat IMCD, human sweat duct, and porcine and rat brain endothelia. One interesting aspect of the amiloride block in rat IMCD was that the channels were inhibited by amiloride only at voltages more negative than +40 mV (Light et al. 1988). Table 2 compares the characteristics of single amiloride-sensitive Na^+ channels in these tissues, and Fig. 2 presents typical patch clamp tracings of single amiloride-sensitive

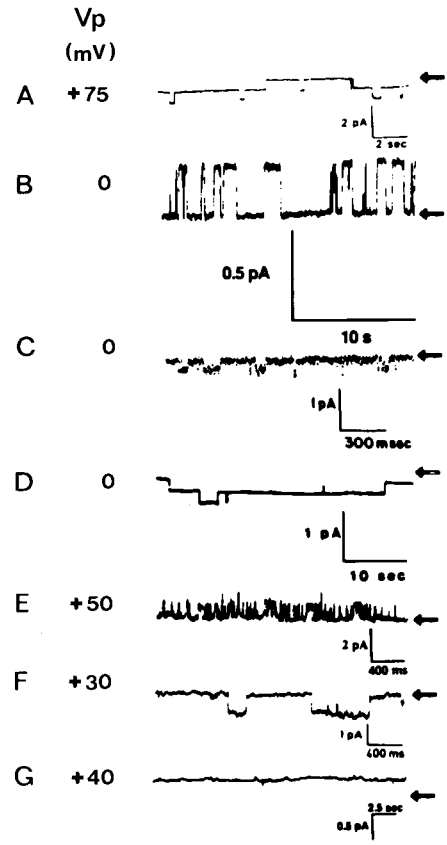

Fig. 2A–G. Patch clamp recordings of single amiloride-sensitive Na^+ channels. **A** Rat CCT (Palmer and Frindt 1986). **B** Toad urinary bladder (Frings et al. 1988). **C** A6 cells grown on impermeable supports (Hamilton and Eaton 1985). **D** A6 cells grown on permeable supports (Eaton and Hamilton 1988). **E** Human sweat duct (Joris et al. 1989). **F** Rabbit straight PT (Gogelein and Greger 1986). **G** Brain endothelial cells (Vigne et al. 1989). The *arrows* represent the baseline current with no channels open. *Vp* is the potential (in mV) applied to the patch. The transmembrane potential (*Vm*) is the potential at the cytoplasmic surface of the patch relative to the potential at the outer surface of the membrane. In this figure, the Vps were chosen so that all of the Vms would be at negative (i.e., physiological) values

Na^+ channels recorded from various epithelia. The channel lifetimes are highly variable. For example, when A6 cells are grown on impermeable supports (Fig. 2C), a fast (millisecond) channel is observed; in contrast, channels of A6 cells grown on permeable supports (Fig. 2D) open and close more slowly (on the order of seconds). The human sweat duct channel (Fig. 2E) undergoes rapid transitions between the open and closed states, while the brain endothelial channel (Fig. 2G) remains open for several seconds at a time. A plot of open state conductance versus P_{Na^+}/P_{K^+} selectivity is presented in Fig. 3. It is apparent that no correlation exists between single-channel conductance and Na^+/K^+ selectivity. However, in the channels examined to date, single-channel conductance is low when the Na^+/K^+ selectivity ratio ≥ 10.

A detailed examination of the kinetic properties of amiloride-blockable cation channels reveals unexplained differences between

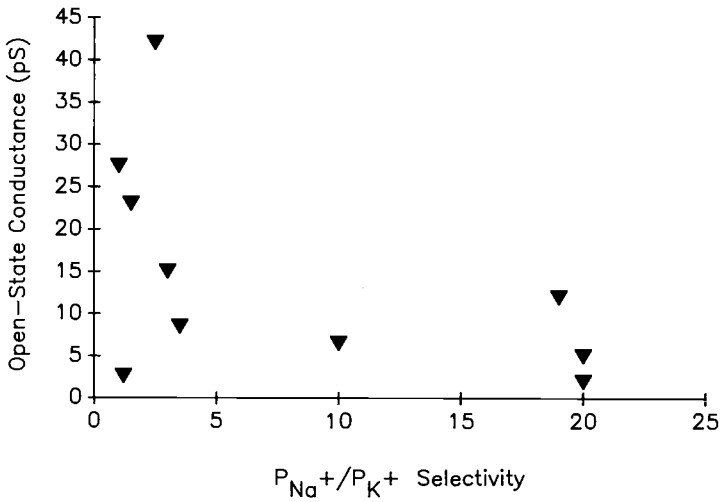

Fig. 3. Relationship between single epithelial Na^+ channel conductance and Na^+ versus K^+ selectivity. Each datum point is an average of the values given in Table 2

the observed behavior of single channels and that predicted from macroscopic short-circuit current measurements and noise analysis (Garty and Benos 1988; Sariban-Sohraby and Benos 1986a). For example, both bilayer and patch clamp studies reveal channels having a much lower Na^+ versus K^+ selectivity than previously described using transepithelial tracer fluxes (Benos et al. 1980) and measurements of apical membrane conductance after basolateral depolarization with high concentrations of K^+ (Palmer 1982b). Na^+ channels observed in bilayer and patch clamp experiments are in an environment different from that in native epithelia. The lipid composition of reconstituted vesicles probably varies from that of the natural membrane and reconstituted Na^+ channels, or channels present in membrane patches may no longer be associated with proteins involved in channel regulation. As indicated earlier, removal of these important control elements could alter channel characteristics.

2.3 Amiloride As an Inhibitor of Epithelial Na^+ Channels

2.3.1 The Chemistry of Amiloride

Amiloride, a K^+-sparing diuretic whose synthesis was first described by Cragoe et al. (1967), is the most commonly used inhibitor of

epithelial Na^+ transport (Benos 1982, 1988; Kleyman and Cragoe 1988). This compound consists of a substituted pyrazine ring with amino groups at ring positions 3 and 5, a chloride at ring position 6, and an acylguanidinium moiety attached to ring position 2 (Fig. 4). Protonation occurs on the guanidinium group, making amiloride a weak base with a pK_a of 8.7 in aqueous solution (Smith et al. 1979). Thus, at physiologial pH (7.35–7.45), amiloride exists primarily as a monovalent cation with the positive charge resonating within the terminal amidinium fragment. These acid-base properties permit amiloride to penetrate biological and artificial membranes (Benos et al. 1983b; Dubinsky and Frizzell 1983; Leffert et al. 1982). Amiloride, in the uncharged form, has a permeability coefficient of 10^{-7} cm/s (Benos et al. 1983b) and can accumulate intracellularly via nonionic diffusion. The charged form of amiloride may possibly also enter cells by substituting for amino acids on Na^+-dependent amino acid transport systems that are present, for example, in hepatocytes, PT, and the small intestine (Benos et al. 1983b). Another possible mechanism for the intracellular accumulation of amiloride involves amiloride substituting for the organic cation on the organic cation/H^+ exchanger, a transporter in the luminal membrane of renal PT that may play a role in organic cation secretion (Wright and Wunz 1989). Using rabbit renal brush-border membrane vesicles

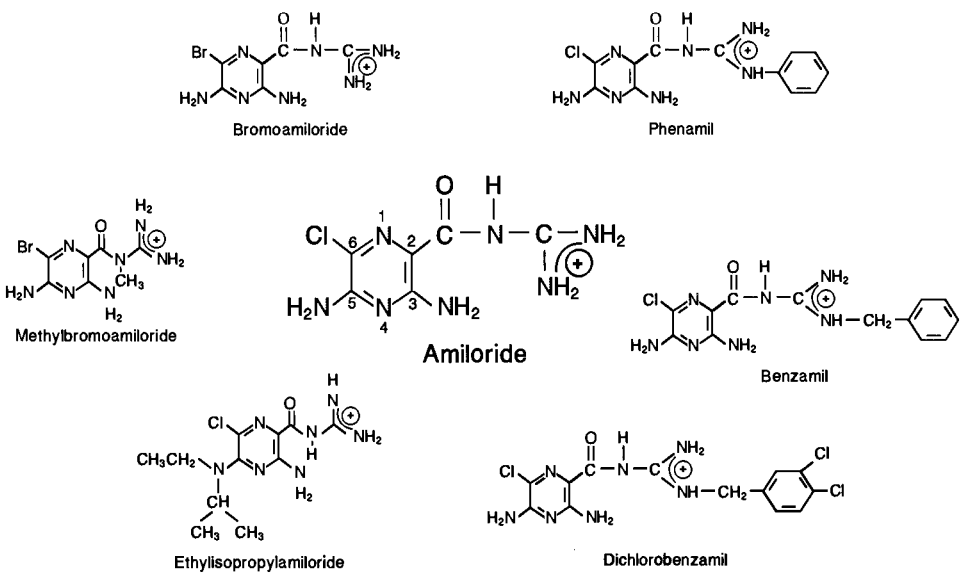

Fig. 4. The structure of amiloride and some of its analogs

(BBMV) to study amiloride transport across the luminal membrane of PT cells, Wright and Wunz (1989) showed that [^{14}C] amiloride uptake was stimulated in the presence of an outwardly directed H^+ gradient; this uptake was inhibited, in the presence or absence of a pH gradient, by unlabeled amiloride or the quaternary amine tetraethylammonium (TEA). Furthermore, Na^+ had no direct effect on proton-driven amiloride transport by BBMV, suggesting that amiloride's interaction with the Na^+/H^+ exchanger is restricted to that of a nontransported inhibitor. Thus, amiloride flux into BBMV appears to involve a carrier-mediated exchange for H^+ that is separate from the Na^+/H^+ exchanger and is shared with other organic cations.

Many analogs of amiloride have been synthesized and proven useful as pharmacological tools to define amiloride-sensitive Na^+ transport pathways. The major classes of amiloride analogs contain modifications at pyrazine ring positions 6 and 5 or at one of the nitrogens on the terminal amidinium group (Benos 1988; Kleyman and Cragoe 1988; Benos et al. 1991). In bromoamiloride, the -Cl moiety at ring position 6 is replaced with -Br; this analog can irreversibly inhibit Na^+ transport after irradiation with ultraviolet light (Benos and Mandel 1978). EIPA contains an alkyl group substitution at ring position 5. Phenamil, benzamil, and dichlorobenzamil possess hydrophobic substitutions of the terminal nitrogen atom of the guanidinium moiety; phenamil and benzamil are the most potent inhibitors of epithelial Na^+ channels, with a K_i of approximately 10 n*M* (Kleyman and Cragoe 1988). Benos et al. (1986, 1987) synthesized [^{3}H]methylbromoamiloride and used it as a molecular probe to purify a 730-kDa protein from bovine renal papillae and cultured A6 cells. Barbry et al. (1987) used [^{3}H]phenamil to purify a 185-kDa protein from pig kidney cortex (see Sect. 3 for details). Figure 4 shows the structures of these amiloride analogs.

Amiloride acts on the entry step of Na^+ across the mucosal (apical) surface of the epithelial cells (Biber 1971). Inhibition of epithelial Na^+ transport by amiloride is generally rapid and reversible. The apparent equilibrium dissociation constant (K_i = the concentration of amiloride required to block 50% of Na^+ transport) varies among amiloride-sensitive Na^+ transport systems and has proven useful in characterizing these systems. For example, Na^+ channels found in high transepithelial electrical resistance epithelia typically have a K_i of $<1\,\mu M$ at physiological Na^+ concentrations, whereas Na^+/H^+ and Na^+/Ca^{2+} exchangers have K_i's in the micromolar and millimolar ranges, respectively (Benos 1988; Benos et al.

1991). Sodium-coupled solute transport systems, such as the Na^+/glucose cotransporter, also tend to have relatively low affinities for amiloride (Cook et al. 1987; Harris et al. 1985; Benos et al. 1991). As indicated earlier, a new class of amiloride-sensitive Na^+ channels has been discovered with a K_i for amiloride of $>1\,\mu M$.

The use of amiloride as a Na^+ transport inhibitor is not without problems. At high concentrations ($>0.1\,mM$), amiloride produces many nonspecific effects including inhibition of protein synthesis (Leffert et al. 1982; Lubin et al. 1982; Yamaguchi et al. 1986) and inhibition of enzymatic functions such as protein kinase C (PKC) (Besterman et al. 1985); the tyrosine kinase activity of the receptors for insulin, epidermal growth factor, and platelet-derived growth factor (Davis and Czech 1985); and the Na^+/K^+-ATPase (Soltoff and Mandel 1983). Additionally, amiloride at concentrations of $10-100\,\mu M$ inhibits cell differentiation (Levenson et al. 1980) and selectively blocks the low-threshold Ca^{2+} channel (Tang et al. 1988). Thus because amiloride, when used at high concentrations for extended periods, can be toxic to intact cells and tissues, caution must be exercised in deducing mechanism of transport based solely on amiloride inhibition.

To inhibit epithelial Na^+ transport (as well as Na^+/H^+ and Na^+/Ca^{2+} exchange), amiloride must carry a positive charge (Benos et al. 1976, 1991; Kaczorowski et al. 1985; L'Allemain et al. 1984). Furthermore, the inhibition patterns of epithelial Na^+ channels and the Na^+/H^+ and Na^+/Ca^{2+} exchangers by amiloride analogs are unique (see Kleyman and Cragoe 1988; Benos 1988 for reviews). For example, replacement of the terminal amidinium fragment with a benzyl group potentiates the ability of the compound to inhibit both the Na^+ channel and the Na^+/Ca^{2+} exchanger, but diminishes blocking effectiveness towards the Na^+/H^+ exchanger. Alternatively, alkyl substitutions on ring position 5 eliminate inhibitory activity towards the epithelial Na^+ channel but magnify inhibitory activity towards both the Na^+/H^+ and Na^+/Ca^{2+} exchangers. The remainder of this section will focus on the use of amiloride as a tool to study epithelial Na^+ channels.

2.3.2 Kinetics and Voltage Dependence of Amiloride Block

Earlier studies on the kinetics of amiloride inhibition have shown the block of the Na^+ channel to be competitive, noncompetitive, or mixed with respect to Na^+ (Benos 1982). On this basis, Benos et al. (1979) hypothesized that the receptor sites for amiloride and the Na^+

translocation site are distinct. The kinetic differences observed between various epithelial tissues may be due to variations in the properties of the binding site for amiloride. Competitive inhibition would be seen if amiloride and Na^+ interacted at this inhibitory site to exclude each other, whereas noncompetitive kinetics would be observed if Na^+ did not affect amiloride binding at this site. Although competition between amiloride and Na^+ can be demonstrated in many cases, both cations may not necessarily interact with the same site. For example, if an interaction of Na^+ with the channel were to produce a conformational change, then amiloride could be prevented from binding to some other site (Garty and Benos 1988).

One major criticism of these earlier experiments is that changes in the apical membrane potential were not considered when apical Na^+ and amiloride concentrations were varied (Sariban-Sohraby and Benos 1986a). Palmer (1984) and Hamilton and Eaton (1985) showed that the magnitude of the apparent amiloride K_i in toad urinary bladder and A6 cells, respectively, appears to depend on the membrane voltage. They estimated that amiloride senses 14%–45% of the total electrical field across the apical membrane. Therefore, alterations of apical Na^+ concentrations that change the apical membrane potential could substantially alter the blocking ability of protonated amiloride, and the results could be confused with a competitive effect of Na^+ on amiloride block (Hamilton and Eaton 1985). Michaelis-Menten kinetic analysis assumes that the Na^+ channel density remains constant while both Na^+ and amiloride concentrations are varied (Li and Lindemann 1983). Using current fluctuation analysis, Warncke and Lindemann (1985), Abramcheck et al. (1985), Helman et al. (1986), Baxendale and Helman (1986), and Helman and Baxendale (1990) have shown that varying the amiloride and the external Na^+ concentrations or changing the transmembrane voltage affects the density of conducting Na^+ channels in the membrane. Thus, two major assumptions used in the determination of macroscopic inhibitory constants, namely, voltage independence of amiloride block and constant channel density, may not be valid.

An examination of the relationship between the K_i value of amiloride and the initial (i.e., in the absence of amiloride) apical membrane voltage in frog skins under different experimental conditions, such as high or low external Na^+ concentrations or hormone treatment, reveals that the absolute magnitude of the K_i depends on voltage (Sariban-Sohraby and Benos 1986a). If a voltage-dependent term for amiloride inhibition and the dependence of apical mem-

brane potential on external Na^+ concentration are incorporated into a purely noncompetitive inhibitory model based upon Michaelis-Menten kinetics, previously observed deviations from simple noncompetitive kinetics, and competitive or mixed inhibition can be accounted for. The competitive inhibitory kinetics between amiloride and Na^+ in a particular species, as compared with the noncompetitive behavior in other species, can thus occur because differences in the magnitude of the change in apical membrane potential or changes in functional channel density when $[Na^+]$ is reduced may result in larger differences in the apparent K_i.

The hypothesis that amiloride and Na^+ interact at separate loci in frog skin epithelium is supported by the following observations:

1. The fractional electrical distance within the electrical field for the amiloride blocking site (0.43) is significantly different from that for Na^+ (0.24) (Sariban-Sohraby and Benos 1986a).
2. By incorporating a voltage-dependent block term and the dependence of apical membrane potential on $[Na^+]_o$ into a purely noncompetitive model, competitive or mixed inhibition curves can be generated (Benos, unpublished observations).
3. A noncompetitive, voltage-dependent amiloride block model is more parsimonious and can account for the observed species and tissue differences in the interaction of amiloride and Na^+.
4. Preliminary experiments measuring amiloride inhibition of single Na^+ channel currents in planar lipid bilayer membranes at constant applied potential but at different Na^+ concentrations indicate that amiloride inhibition of single-channel conductance is independent of $[Na^+]$ in the range of 30–200 m*M* Na^+ (Benos, unpublished results).
5. Models in which the functional Na^+ channel density is allowed to vary as a function of either Na^+ or amiloride concentrations or membrane voltage cannot account for experimentally observed deviations in inhibitory kinetic data (Benos et al. 1979). However, other interpretations exist (see Sect. 2.3.3). In summary, the different kinds of amiloride inhibitory kinetics observed may be due largely to the voltage-dependent block of Na^+ entry channels by amiloride. Another factor that may partially explain the variability in kinetics studies concerns the possibility that there could be more than one amiloride binding site, some within the channel's pore and others located at a distance away from the channel orifice.

2.3.3 Mechanism of Amiloride Block

Although many of the chemical and kinetic aspects of the amiloride-channel interaction have been characterized, the precise mechanism of amiloride block and the exact site of its interaction with the Na^+ channel remains unresolved. Theoretically, amiloride could block Na^+ transport either by physically plugging the channel (Cuthbert 1976) or by binding to some regulatory site and somehow changing the conformation of the channel protein (Benos et al. 1980). The voltage dependence of amiloride inhibition allows an estimation of the depth of the amiloride binding site in the channel (Van Driessche and Erlij 1983; Li and Lindemann 1982). The data suggest that the guanidinium group penetrates the channel from the luminal side to a distance that is 10%–15% of the total electrical distance (Garty and Benos 1988). However, a potential-dependent conformational change in the Na^+ channel protein itself could affect the binding of amiloride to a site outside of the electrical field across the membrane (Smith and Benos 1991).

Li and Lindemann (1982) and Van Driessche and Erlij (1983) have measured the effects of internal Na^+ on the blocking kinetics of amiloride in an attempt to localize the amiloride binding site. If amiloride acts by plugging the Na^+ channel, its inhibitory activity should be relieved by inducing a channel-mediated cell-to-lumen Na^+ flow. This is precisely the result that the aforementioned investigators obtained. These experiments support the idea that the amiloride binding site is within the Na^+ channel itself.

Woodhull (1973) first showed that ions that bind to sites within the pore will exhibit a voltage-dependent block of the channel-mediated current since the blockers must cross part of the trans-membrane electric field to reach their binding sites. Therefore, any impermeant cation that enters and plugs the Na^+ channel's pore will exhibit a voltage-dependent block. Palmer's observations on the voltage dependence of amiloride block (Palmer 1984, 1990; Palmer and Andersen 1989) provide further evidence for an amiloride binding site within the Na^+ channel (Palmer 1991). Another amiloride analog, 6-chloro-3,5-diaminopyrazine-2-carboxamide (CDPC), a pyrazine derivative that lacks a guanidinium moiety and, therefore, lacks a positive charge, also blocks Na^+ channels, but with a much lower inhibitory constant than amiloride. Although the mechanism of the block is similar, the off-rate constant for CDPC block is faster than that for amiloride (Baxendale and Helman 1986; Helman and Baxendale 1990) due to the weak affinity of CDPC (apparent K_i

~100 μ*M*) compared to amiloride (apparent K_i ~100 n*M*). Also, the CDPC block was voltage independent at voltages higher than 60 mV (Palmer 1991), implying that the voltage dependence of the amiloride block arises from an interaction between the charge on the blocker and the electric field. On this basis, Palmer suggests that the amiloride molecule actually penetrates the conduction pathway. Also, the voltage dependence of guanidine block is very similar to that of amiloride, although guanidine blocks epithelial Na^+ channels with a K_i of around 100 m*M* (Palmer 1985a). Other observations consistent with an amiloride binding site within the pore concern the effects of extracellular Na^+ and K^+ on the voltage dependence of amiloride inhibition (Palmer and Andersen 1989). The increase in K_i resulting from competitive interactions of both Na^+ and K^+ with amiloride (Palmer 1984) can be explained by either a cork or allosteric model. The reduction of the voltage dependence of amiloride block in the presence of K^+ is consistent with the idea that both amiloride and K^+ enters the conduction pathway, and are mutually exclusive (Palmer 1992). An increase in voltage simultaneously drives amiloride and K^+ into the pore, thus making K^+ even more effective in competing with amiloride. The fact that changing the mucosal Na^+ concentration did not reduce the voltage dependence of amiloride block can be explained by assuming that amiloride acts as a molecular cork, because the same transmembrane voltage that drives both Na^+ and amiloride into the mucosal site of the pore also forces Na^+ out the cytoplasmic side. If the entry and exit steps were equally voltage dependent, then increasing the voltage would not lead to Na^+ accumulation within the pore. In support of this idea, guanidine, an impermeant channel blocker, reduced the voltage dependence of amiloride block, whereas Li^+, a permeant alkali cation, did not.

Once the interaction between the positively charged guanidinium moiety of amiloride and the channel protein is established, this amiloride-channel complex may be stabilized by additional interactions. By studying the structure-activity relationship of amiloride analogs, Li et al. (1985) concluded that the duration of the block is dependent on an interaction between the halogen at the 6-position and another channel site. The amino group at the 5-position stabilizes the amiloride block by increasing the electron density at the 6-position.

2.3.4 Models of the Na^+-Conducting Pore

Based on the analysis of voltage-dependent block of Na^+ currents by impermeant ions, Palmer (1991) predicted a structural model for the

epithelial Na^+ channel. In this model, the outer mouth of the channel is lined with negative charges and indiscriminately attracts cations. The diameter of this outer portion of the channel must be at least 5 Å wide. The pore of the channel then narrows to exclude all but the smallest cations, and a final narrowing physically and energetically excludes all ions except Na^+, H^+, and Li^+. Because ion movement through channels can be described as a series of energy barriers, with energy wells in between, Palmer (1991) was interested in determining whether the known Na^+ channel properties could be accounted for by Eyring rate theory, (see Palmer and Andersen 1989) which allows calculation of the rate of ion movement through the pore based upon its energy profile. In Palmer's model, two binding sites are specified within the pore that correspond to two putative blocking sites: one for amiloride (at ~15% of the electric field) and the other for K^+ (at ~30% of the electric field). Na^+ is therefore constrained to interact with the amiloride binding site on its passage through the pore. Further, the two binding sites cannot be occupied simultaneously. This assumption is consistent with a Na^+ flux ratio exponent of 1 measured for epithelial Na^+ channels (Benos et al. 1983a; Palmer 1982b). The kinetic scheme for conduction can be written as:

$$Na_0^+ + (0, 0) \underset{k_{-1}}{\overset{k^1}{\rightleftharpoons}} (Na^+, 0) \underset{k_{-2}}{\overset{k^2}{\rightleftharpoons}} (0, Na^+) \underset{k_{-3}}{\overset{k^3}{\rightleftharpoons}} (0, 0) + Na_i^+$$

where Na_0^+, Na_i^+ are Na^+ on the outer and inner sides of the membrane, respectively, and (0, 0), (Na^+, 0), (0, Na^+) are the channel in its unoccupied form, with the outer site occupied by Na^+, and with the inner site occupied by Na^+, respectively.[2]

This model predicts a single-channel conductance at 100 m*M* mucosal [Na^+] and 10 m*M* cytoplasmic [Na^+]; it also predicts an apparent K_m for Na^+ of 50 m*M*. Also, the occupancy of the channel by a Na^+ ion is virtually independent of membrane potential between 0 and 200 mV, thus accounting for the voltage independence of competition between Na^+ and amiloride. Further, the I-V relationship is similar to that predicted by the constant field equation. Thus, this kinetic model of the apical Na^+ channel in tight epithelia is consistent with the known electrophysiological characteristics of Na^+

[2] This conduction scheme is valid as long as external and internal Na^+ concentrations are kept relatively low (i.e., below 150 m*M*); however, raising extracellular Na^+ levels would increase the probability that the outer and inner sites would be occupied by Na^+ simultaneously. The values of the rate constants used are given in Palmer (1991).

movement through these channels. However, Palmer (1991) provides an alternative kinetic model that can also account for the electrophysiological properties of the channel. This model specifies a single energy barrier placed at 15% of the electric field (Palmer and Andersen 1989). It predicts occupancy by Na^+ that also is independent of membrane voltage, and predicts an appropriate I-V relationship. In this model, amiloride and K^+ do not possess distinct blocking sites.[3] There are at present no data extant favoring one model over the other. Further experiments, such as the generation of a complete Na^+ activation curve, must be performed to determine an accurate kinetic model of epithelial Na^+ conduction.

2.3.5 Amiloride-Sensitive Channels in Sensory Systems

Recently, amiloride-sensitive cation channels with a low P_{Na^+}/P_{K^+} selectivity have been characterized electrophysiologically in olfactory, lingual, auditory, and visual epithelia. These channels are believed to play important roles in the signal transduction pathways involved in sensory perception. Further, these channels have been localized to lingual and auditory epithelia in indirect immunofluorescent studies using polyclonal antibodies raised against purified bovine kidney Na^+ channel protein (Simon et al. 1991, Hackney et al. 1991).

Exposure of the cilia of olfactory receptor cells to odorants stimulates adenylate cyclase, thus raising intracellular cAMP levels (Pace et al. 1985; Sklar et al. 1986; Boekhoff et al. 1990). Adenylate cyclase activation, which is GTP dependent, probably involves receptor-coupled GTP binding proteins (Jones and Reed 1989). A cyclic nucleotide-gated, cation-permeable channel is believed to open upon binding of cGMP, thus depolarizing the membrane of the olfactory receptor cell (Nakamura and Gold 1987; Dhallan et al. 1990). An interaction of odorants with the olfactory epithelium elicits an inwardly directed Na^+-dependent short-circuit current (Takagi et al. 1969). Isolated olfactory receptor cells from the nasal mucosa

[3] The question of whether amiloride and K^+ (or for that matter amiloride and Na^+) occupy different binding sites cannot be resolved by considering only the depth to which each molecule penetrates the electric field. For example, it is conceivable that Na^+, K^+, and amiloride interact with the channel at only one site. The voltage dependence of amiloride block would be lower than that of K^+ (or Na^+) because only part of the charge (which is spread over the entire amiloride molecule) can enter the pore.

of the frog have been examined using the patch clamp technique by Frings and Lindemann (1988). Amiloride (50 μM) produced a rapid, complete, and reversible block of the odorant-induced depolarization of olfactory receptor cells by effectively clamping the membrane potential to values near −80 mV. In the absence of odorants (e.g., cineole, amyl acetate, and isobutyl methoxypyrazine), amiloride had no effect on these cells. The authors concluded that amiloride may inhibit chemosensory transduction of olfactory receptor cells by blocking Na^+-dependent pathways that open in the presence of odorants.

An amiloride-blockable Na^+ current has also been observed in isolated taste receptor cells from the frog tongue (Avenet and Lindemann 1988). Under whole-cell patch clamp conditions (held at −80 mV inside the cell), approximately half of the cells had an inward Na^+ current of 10–700 pA. However, this inward Na^+ current was inhibited by amiloride in ony 56% of these cells (K_i = 0.3 μM). The cation selectivity of this current was highly variable, with a P_{Na^+}/P_{K^+} ranging between 1 and 100. Furthermore, while the amiloride-blockable current was weakly voltage dependent, it was not voltage gated. In addition, amiloride inhibited only partially the Na^+-dependent short-circuit current of the intact mucosa and only a fraction of the nerve response to salt intake (DeSimone et al. 1984; Simon and Garvin 1985; DeSimone and Ferrell 1985; Brand et al. 1985), suggesting that taste cells possess more than a single electrogenic Na^+ transport pathway. Depolarization of taste receptor cells, which express amiloride-sensitive Na^+ channels in their apical membranes, may transduce the "salty" taste sensation (Avenet and Lindemann 1988). Interestingly, these same taste cells also express tetrodotoxin-blockable, voltage-gated Na^+ channels, but these do not appear to be involved in taste transduction (Avenet and Lindemann 1988).

Jorgensen and Ohmori (1988) used a whole-cell patch clamp technique to examine the effects of amiloride on mechanoelectrical transduction (MET) currents in dissociated hair cells (sensory receptors in the inner ear) of the chick. The channels in these sensory receptors, which reside in the apical membrane, are mechanically gated and do not discriminate well between monovolent cations (Hudspeth 1982; Ohmori 1985, 1988; Corey and Hudspeth 1979), although the majority of the receptor current is carried by K^+, the dominant cation in the endolymph of the inner ear (Citron et al. 1956). The transduction process also requires a minimal concentration of Ca^{2+} (Sand 1975; Hudspeth and Corey 1977; Jorgensen 1983;

Ohmori 1985). Amiloride (apparent K_i of 50 μM) reversibly blocked the MET channel in a dose- and voltage-dependent manner that was independent of the mechanical gating of the channel (Jorgensen and Ohmori 1988).

Amiloride and its analogs have also been shown to inhibit channels in vertebrate rod photoreceptors. A derivative of amiloride, 3′,4′-dichlorobenzamil (DCPA), completely blocked the light-regulated current (i.e., the current produced by cGMP-activated channels) recorded from frog rod photoreceptors (Nicol et al. 1987). A cGMP-activated current in excised patches of rod plasma membrane and a cGMP-induced Ca^{2+} flux from rod disk membranes were also inhibited by DCPA with apparent K_i of 1 and 10 μM, respectively. In subsequent studies, Pearce et al. (1988) demonstrated that amiloride (apparent K_i of ~30 μM) blocked the 8-bromoguanosine 3′,5′-cyclic monophosphate (8-BrcGMP)-activated Ca^{2+} release from bovine rod outer segment disks. The light-regulated current recorded from the physiologically intact rod photoreceptor was also blocked by DCPA. The DCPA block in intact rod outer segments retaining the mitochondria-rich ellipsoid portion of their inner segments (outer segment–inner segment, OS-IS) differed depending on the Ca^{2+} concentration. At 1 mM Ca^{2+}, the DCPA inhibition of the cGMP-activated current in these intact preparations was similar to that in excised patches of rod membrane, but at 10 nM Ca^{2+}, DCPA reversed that polarity of the photoresponse. Nicol et al. (1987) suggested that the different blocks of DCPA in high and low Ca^{2+} may be due to a Ca^{2+} concentration-dependent modulation of the conformational state of the light-regulated (i.e., cGMP-activated) channel. This channel could possess two different conductance states, one blocked by DCPA, and another induced in low-Ca^{2+} media and modified but not blocked by DCPA. Another interpretation provided by these authors is that two different light-regulated channels may be present in the rod outer segment membrane, one carrying an inward Na^+ current and the other carrying an outward K^+ current.

The channels that conduct the light-regulated current in rod photoreceptors are relatively nonselective ($P_{Na^+}/P_{K^+} \sim 2$) (Yau and Nakatani 1984; Hodgkin et al. 1985) Using the whole-cell patch clamp technique, Gray and Attwell (1985) and Bodoia and Detwiler (1985) estimated the single-channel conductance of the cGMP-activated channel in rod photoreceptors to be ~0.1 pS in 1 mM external Ca^{2+}. However, Ca^{2+} and Mg^{2+} (at physiological concentrations) have been shown to decrease the cGMP-activated conductance in rod photoreceptors (Lamb et al. 1985; Yau and Haynes

1986; Haynes and Yau 1985). Haynes et al. (1986) observed a single-channel conductance of ~25 pS in the absence of divalent cations in excised patches of rod outer segment membrane. With Ca^{2+} or Mg^{2+} present in the cGMP-containing solution, Haynes et al. (1986) observed a flickering block of the open channel. These authors suggested that this block by divalent cations may explain the peculiarly small apparent single-channel conductance previously deduced from noise measurements on intact cells (Gray and Attwell 1985; Bodoia and Detwiler 1985).

In summary, amiloride and its analogs continue to serve as useful probes for characterizing epithelial Na^+ channels. Although the blocking mechanism(s) and amiloride interaction site(s) are beginning to be deciphered, the great apparent diversity of amiloride-sensitive Na^+ channels guarantees the unmasking of further complexities. The recent discoveries of amiloride-blockable channels in sensory organs and low amiloride affinity epithelial Na^+ channels (see Sect. 3) add yet another enigma to the intricacies of epithelial Na^+ transport.

3 Biochemistry of Epithelial Na^+ Channels

When compared to voltage-sensitive Na^+ channels, which were purified as early as 1978 (Agnew et al. 1978) and cloned in 1984 (Noda et al. 1984), our knowledge of epithelial Na^+ channel biochemistry and molecular biology is still rudimentary. One of the main reasons for this slow biochemical achievement is that, while there are rich sources of voltage-sensitive Na^+ channels, such as eel electroplax and brain synaptosomes, there is no convenient source of amiloride-sensitive Na^+ channel protein. Furthermore, excitable membrane Na^+ channels can be studied using a number of high-affinity molecular probes that specifically bind to at least four distinct regions of Na^+ channels producing different physiological effects (Catterall 1986). In contrast, molecular probes of epithelial Na^+ channels have been limited to amiloride analogs. It was only in 1986 that the first report of the isolation and purification of an amiloride-sensitive Na^+ channel appeared (Benos et al. 1986). This channel was purified from bovine renal papillary collecting tubules and A6 cells, an amphibian kidney cell line. It is important to point out the limited quantities of epithelial Na^+ channel protein that can be obtained from these isolation procedures, especially in comparison to the amount of voltage-

sensitive Na^+ channel protein isolated from excitable membranes. In a standard preparation for the isolation of voltage-sensitive Na^+ channel protein from a single eel electroplax (Agnew et al. 1978), approximately 0.5–1 mg of homogeneous channel protein can be obtained. To isolate a comparable amount of epithelial Na^+ channel protein, approximately 50000 12-cm diameter A6 cell filters or 7140 bovine kidneys are required. Approximately 0.4 μg purified protein from forty 12-cm diameter filter dishes of A6 cells, and ~0.07 μg protein per bovine kidney are routinely recovered.

As discussed earlier, epithelial Na^+ channels can be broadly classified as having high or low sensitivity to amiloride (i.e., K_i of less than or greater than 1 μ*M* at physiological Na^+ concentrations, respectively). Therefore, it is more informative and easier to discuss epithelial Na^+ channels by dividing them into two main groups based upon their sensitivity to amiloride. The first group includes the so-called classic epithelial sodium channels present in the apical membranes of high electrical resistance epithelia, such as frog skin, toad urinary bladder, mammalian colon, bovine renal papillary collecting duct, and amphibian renal A6 cells (Smith and Benos 1991). These channels have a high affinity for amiloride with a $K_i <$ 0.5 μ*M* at high external Na^+ concentrations. As recently proposed by Oh and Benos (1992), these channels will be referred to as the H-type channel ("H" denotes high amiloride affinity). The second group has a low affinity to amiloride with a $K_i > 1$ μ*M* and will be referred to as the L-type channel ("L" denotes low amiloride affinity). These L-type Na^+ conductive pathways have been found in a variety of sources over the past few years, including blastocyst trophectodermal cells, brain endothelia, rat colonic enterocytes, porcine kidney, porcine kidney LLC-PK1 cells, lung alveolar type II cells, and the basolateral membrane of the toad urinary bladder (Smith and Benos 1991).

3.1 The H-type Na^+ Channel

Benos et al. (1986, 1987) have described the biochemical characteristics of the H-type Na^+ channel isolated from bovine kidney papillae and amphibian A6 cells. They found that the native H-type Na^+ channel protein has a molecular mass averaging 730 kDa and is comprised of at least six nonidentical subunits held together by disulfide bonds with apparent molecular masses of 315, 150, 95, 70, 55, and 40 kDa. Amiloride-sensitive Na^+ uptake was noted after

Table 3. Amiloride binding proteins

Probe	Source	M_r	Reference
[^{3}H]Methylbromo-amiloride	Purified sodium channels from bovine kidney and A6 cells	130–180, 55–60	Benos et al. (1987)
Anti-idiotypic antibody (RA 6.3)	Purified sodium channels from A6 cells	140, 50	Kleyman et al. (1990)
[^{3}H]Bromobenzamil	Crude membranes from bovine kidney cortex	176, 77, 47	Kleyman et al. (1986)
NMBA	Crude membranes from bovine kidney cortex and A6 cells	130, 75–80, 50	Kleyman et al. (1989)
[^{3}H]Phenamil and [^{3}H]Bromobenzamil	Purified proteins from porcine kidney	105	Barbry et al. (1990b)
RA 6.3 and NMBA	Crude membranes from rat lung	135	Oh et al. (1991)

NMBA, 2′-methoxy-5′-nitrobenzamil

reconstitution of the purified Na^+ channels into liposomes, indicating preservation of transport function (Sariban-Sohraby and Benos 1986b).

The identification of the amiloride binding subunit of the H-type channel has been made possible by using three different approaches (Table 3): (a) the development of irreversible photosensitive amiloride analogs with subsequent radioactive synthesis (Benos et al. 1987; Kleyman et al. 1986; Barbry et al. 1990b); (b) the combination of photosensitive amiloride analogs with anti-amiloride antibodies (Kleyman et al. 1989); and (c) anti-idiotypic antibodies raised against anti-amiloride antibodies (Kleyman et al. 1991). Benos et al. (1987) found that one of the H-type Na^+ channel subunits isolated from bovine kidney papilla, namely, the 150 kDa polypeptide, bound a photoreactive amiloride analog, [^{3}H]-methylbromoamiloride ($K_i < 0.5\,\mu M$), exclusively. It should be emphasized that, for unknown reasons but possibly related to the degree of glycosylation, the apparent molecular mass of this subunit varied between 130 and 180 kDa from preparation to preparation, even under identical gel separation conditions. They also noted, although infrequently, specific labeling of a second lower molecular mass component at 55–60 kDa. The H-type Na^+ channel, present in membrane vesicles isolated from bovine kidney cortex, was also photoaffinity labeled using another photoreactive amiloride analog, [^{3}H]-bromobenzamil (Kleyman et al. 1986). This analog ($K_i = 5\,nM$) was specifically

photoincorporated into three polypeptides with molecular masses of 176, 77, and 47 kDa. Its photoincorporation into all three polypeptides was blocked by addition of excess benzamil or amiloride in a dose-dependent manner.

Kleyman et al. (1986, 1989) developed anti-amiloride antibodies and used the photoreactive amiloride analog 2′-methoxy-5′-nitrobenzamil (NMBA; K_i = 80 n*M*) in combination with these antibodies to identify the amiloride binding subunit(s) of the H-type amiloride-sensitive Na^+ channel from A6 cells. They found that NMBA strongly labeled a polypeptide with an apparent molecular mass of 130 kDa in membrane vesicles from bovine kidney cortex and A6 cells. In addition, polypeptides with an apparent molecular mass of 75–80 kDa and 50 kDa were specifically, but weakly, labeled with NMBA. Kleyman et al. (1991) have also developed monoclonal anti-idiotypic antibodies against polyclonal anti-amiloride antibodies and found that one of the anti-idiotypic antibodies, called RA 6.3, mimicked the effect of amiloride in inhibiting sodium transport across A6 cell monolayers. RA 6.3 specifically reacted strongly with a polypeptide having an apparent molecular mass of about 140 kDa, and reacted weakly and variably with a 50 kDa polypeptide on immunoblots of purified H-type Na^+ channels from A6 cells. These results suggest either the existence of multiple amiloride binding sites in the channel complexes, or that the lower molecular mass polypeptides may be degradation products of the larger ones. This issue is unclear at present. Kinetic studies concerning the stoichiometry of the interaction between amiloride and the Na^+ channel are also controversial, i.e., values range between a 1:1 binding stoichiometry to multiple (>2) amiloride molecules binding per channel (Garty and Benos 1988). Nevertheless, there is no doubt that the 150 kDa subunit of H-type Na^+ channels contains an amiloride binding site. Recently, it was reported that ankyrin and fodrin copurified with the H-type Na^+ channel isolated from bovine kidney (see Sect. 4.5), and ankyrin bound directly to the 150 kDa channel subunit, the same subunit that bound amiloride (Smith et al. 1991).

The monoclonal anti-idiotypic antibody, RA 6.3, has also been used to characterize biochemically the H-type Na^+ channel (Kleyman et al. 1991). Under nonreducing conditions, RA 6.3 specifically immunoprecipitated a 725 kDa protein from metabolically labeled A6 cells. Under reducing conditions, four major nonidentical polypeptides with apparent molecular masses of 260–230, 180, 140–110, and 70 kDa were evident. Essentially the same results were obtained if the apical membrane proteins were radiolabeled in the intact

Table 4. Structure-function relationship of a H-type Na^+ channel

Subunit	M_r (kDa)	Speculative function	Reference
α	315	Effector site of vasopressin; cAMP mediated phosphorylation	Sariban-Sohraby et al. (1988)
β	150	Amiloride and ankyrin binding site; may form a conductive channel	Benos et al. (1987), Smith et al. (1991), Sariban-Sohraby and Fisher (1990)
γ	95	Site of aldosterone-induced methylation	Sariban-Sohraby et al. (1984a), Kemendy and Eaton (1990)
δ	70	Aldosterone-inducible protein	Palvesky et al. (1990), Cox (1991)
ε	55	May be another amiloride binding site	Benos et al. (1987), Kleyman et al. (1991)
ζ	40	Effector site of atrial natriuretic peptide (ANP); α_{i-3}-subunit of G_i protein	Mohrmann et al. (1987) Ausiello et al. (1992)

cell using an impermeant reagent, and then immunoprecipitated. Following this procedure, an additional 50 kDa polypeptide, perhaps corresponding to the 55 kDa subunit described by Benos et al. (1987), was also immunoprecipitated although this polypeptide was not detected consistently. Benos et al. (1987), on the other hand, reported that the 55 kDa subunit was consistently present in the purified channel complex. This discrepancy might be explained by the different composition of reducing sample buffers between the two studies; Benos et al. (1987) used strong reducing sample buffers containing 13 m*M* dithiothreitol (DTT) and 6 *M* urea, whereas Kleyman et al. (1991) used a mild disulfide reducing buffer containing 1 m*M* DTT without urea. The 55 kDa subunit thus seems to be bound tightly to the channel complex and may require relatively strong reduction as well as vigorous noncovalent bond disruption in order to be dissociated.

In summary, the biochemical characterization studies on the H-type Na^+ channels by two groups, Benos and Kleyman, are in close agreement, especially in view of the size of the native Na^+ channel (about 730 kDa), the number of subunits and their sizes (multimeric—possibly hexameric—structure), and location of the amiloride binding subunit (the 150 kDa subunit). Interestingly, Edwardson et al. (1981), using radiation inactivation analysis, measured a target size of 650 kDa for the native benzamil binding site

in bovine kidney cortex. The 150 kDa subunit of the H-type Na^+ channel is very likely to be a membrane spanning protein, having an amiloride binding site on its extracellular surface and an ankyrin binding site on the cytoplasmic side. It may also form a conductive Na^+ channel by itself, as single-channel activity by the amiloride binding subunit (i.e., the 150 kDa polypeptide) of the H-type Na^+ channel from A6 cells was recently measured by Sariban-Sohraby and Fisher (1990) by patch clamping liposomes containing the reconstituted subunit. Table 4 summarizes our current understanding of the structure-function relationship of a H-type sodium channel.

3.2 The L-type Na^+ Channel

Compared to the H-type Na^+ channel, little is known about the biochemistry of L-type Na^+ channels. A candidate for L-type Na^+ channel has been isolated by Barbry and collaborators. They have purified and characterized an amiloride binding protein from the pig kidney outer medulla and cortex (Barbry et al. 1987, 1990b). Pharmacological inhibitory profiles of amiloride and its analogs on Na^+ uptake into native pig kidney membrane vesicles are different from those of classic H-type Na^+ channels in that a low amiloride affinity (K_i = 6 μM) and equal inhibitory potency of EIPA and amiloride were found, (Barbry et al. 1986). This protein was further purified and reconstituted into lipid vesicles to show electrogenic amiloride-sensitive Na^+ transport, suggesting that the amiloride binding protein by itself may function as a Na^+ channel in pig kidney (Barbry et al. 1990b). Barbry et al. (1989) further demonstrated that both crude pig kidney membrane preparations and amiloride binding proteins purified from pig kidney membranes have both high and low amiloride binding sites, although there is a 14-fold larger number of low amiloride affinity binding sites (K_d = 4 μM) than high amiloride affinity binding sites (K_d = 0.1 μM). However, there is only one detectable size of purified protein, namely, a protein with a total molecular mass of 185 kDa. This protein consists of two nearly identical 105 kDa polypeptides crosslinked by disulfide bonds (Barbry et al. 1990b).

At present, it is not known whether these two amiloride interaction sites are located on two different isoforms of this Na^+ channel with a similar structure not resolvable by gel electrophoresis, or on a single type of Na^+ channel protein where the amiloride affinity changes under different physiological conditions. Recently, Barbry

et al. (1990a) cloned this human amiloride binding protein from a human kidney cDNA library by using an oligonucleotide probe synthesized against the purified 105 kDa subunit from pig kidney. Transfection into eukaryotic cell lines showed that the cloned cDNA coded for an amiloride binding protein with high amiloride affinity (K_d = 0.1 μM), suggesting that this protein may be a part of a H-type Na^+ channel in the pig kidney. This protein is glycosylated, but does not contain any consensus phosphorylation sites, and its hydropathy plot is not similar to that of most membrane spanning proteins in that there are no hydrophobic helices.

Because the amiloride binding subunit of the classic H-type Na^+ channel is likely to be an integral membrane protein as previously discussed, the protein with high amiloride binding affinity purified and cloned by Barbry and collaborators does not seem to have any structural homology with the H-type Na^+ channel. Further, polyclonal antibodies raised against the amiloride binding protein isolated by Barbry's group do not cross-react on Western blots with the H-type Na^+ channel from bovine kidney (unpublished observations). Barbry et al. (1990a) also failed to detect amiloride-sensitive Na^+ channel activity in transfected mammalian cells or in a Xenopus oocyte expression system. Therefore, they suggested that either (a) the amiloride binding subunit and the channel subunit might be distinct, and the observation of electrogenic sodium transport in reconstituted purified amiloride binding proteins might be due to contaminating channel subunits, or (b) alternative splicing in transfected cells might remove a protein segment which is short but essential for channel activity. This latter suggestion is unlikely because the cloned protein is not a membrane spanning protein. Because of these uncertainties in the nature of the amiloride binding protein cloned by Barbry et al. (1990a), further work on the purification and characterization of L-type Na^+ channels from pig kidney as well as other sources is necessary to understand more completely the biochemistry and molecular biology of the L-type Na^+ channel.

Recently, the existence of low amiloride-sensitive Na^+ conductive pathways in freshly isolated alveolar type II cells of rabbit lungs has been demonstrated by Matalon et al. (1991). They found that 50% of the electrogenic Na^+ uptake into lung alveolar type II membrane vesicles was inhibited by 10 μM amiloride. In addition, at concentrations of 0.1 and 1 μM, amiloride and its analogs, benzamil and EIPA, all inhibited Na^+ transport similarly. At concentrations higher than 10 μM, EIPA blocked a significantly higher fraction of the electrogenic Na^+ transport than the other two inhibitors. Therefore,

they proposed that alveolar type II cells may have a type of Na^+ channel distinct from the classic H-type Na^+ channel.

Polyclonal antibodies against purified H-type Na^+ channels from bovine kidney have been used on Western blots of membrane proteins from rat alveolar type II cells (Oh et al. 1991). The specificity of these antibodies against epithelial sodium channels has been well characterized through immunocytochemical studies (Brown et al. 1989; Tousson et al. 1989), and recently used to immunolocalize L-type Na^+ channels in rat lung alveolar type II cells (Hu et al. 1991), canine lingual epithelial cells (Simon et al. 1992), and guinea pig cochlear hair cells (Hackney et al. 1992). The antibodies cross-reacted with 135 kDa polypeptides of the lung cell membranes. Anti-idiotypic antibodies against anti-amiloride antibodies, RA 6.3 (Kleyman et al. 1991), and NMBA photolabeling studies consistently recognized the same molecular mass protein, suggesting that the 135 kDa polypeptide in lung alveolar type II cells could be an amiloride binding subunit of the L-type Na^+ channel (Oh et al. 1991). Because the anti-Na^+ channel antibodies reacted with at least four different subunits of the H-type Na^+ channels from bovine kidney and A6 cells (Sorscher et al. 1988; Tousson et al. 1989), but with only one presumed subunit of the L-type Na^+ channel, the hypothesis of a single type of Na^+ channel with two different amiloride affinity stages is unlikely to be true. Instead, it would be more reasonable to suspect the existence of different amiloride-sensitive Na^+ channels with distinct biochemical structures, consistent with the findings of widely variable kinetic and pharmacological characteristics of amiloride-sensitive Na^+ channels. However, because the size of the actual amiloride binding protein is comparable in both H- and L-type Na^+ channels, we cannot as of yet exclude the possiblity of a conservation of this subunit.

4 Regulation of Epithelial Na^+ Channels

4.1 Hormonal Regulation

4.1.1 Aldosterone

The adrenal steroid hormone aldosterone is a regulator of Na^+ reabsorption in tight epithelia. Aldosterone enters the cell and binds to a receptor, which in turn elicits an increase in protein synthesis

and a concomitant two- to fourfold increase in Na^+ transport. Although the mineralocorticoid receptor is commonly viewed as being situated within the nucleus, recent immunocytochemical studies using antibodies directed against the receptor suggest that the receptor is also distributed throughout the cytoplasm (Gasc et al. 1991). The increase in Na^+ transport subsequent to aldosterone treatment is primarily due to an increase in apical Na^+ permeability; however aldosterone also induces the Na^+/K^+ ATPase pump (Garty 1986; Garty and Benos 1988). The response of an epithelium to aldosterone consists of three phases: (1) a latent period of 20–90 min in which intracellular "priming" events occur; (2) an early response in which there is a two- to fourfold increase in Na^+ transport, due entirely to an increase in apical membrane P_{Na}; and (3) a longer response (>6 h) in which there is de novo synthesis of Na^+/K^+ ATPase and an increase in certain enzymes important in energy metabolism. During this later period there is a continued increase in short-circuit current (I_{sc}) resulting from new pump synthesis (Garty 1986).

The first major insight into how aldosterone may augment apical P_{Na} was provided by Palmer et al. (1982). Using amiloride-induced current fluctuation analysis, these authors observed that a 4- to 6-h treatment of the toad bladder with aldosterone evoked an increase in both I_{sc} and the density of Na^+ channels situated within the apical membrane without affecting single-channel current. Thus, aldosterone appeared to regulate the number of apical Na^+ channels rather than the single-channel conductance. Based upon these data, it was proposed that aldosterone either (a) induces the synthesis and/or insertion of new channels or a regulatory protein into the apical membrane; or (b) activates preexisting quiescent channels situated within the apical membrane. Because one of the effects of this hormone is induction of protein synthesis, the first mechanism was favored by a number of investigators; however, recent electrophysiological and biochemical studies have provided evidence in support of the latter mechanism.

Palmer and Edelman (1981) observed that treatment of the toad urinary bladder with diazosulfonic acid (DSA), a protein modifying agent, reduces Na^+ transport to 60%–70% of the control values. Exposure of DSA-treated bladders to aldosterone resulted in an increase in I_{sc}; however, the increase was less than in non-DSA-treated bladders. The DSA-induced inhibition of Na^+ transport was the same for basal and aldosterone-stimulated tissues. These investigators interpreted these results to mean that conductive and non-

conductive channels were equally affected by DSA. Thus, aldosterone activated channels that preexisted in the apical membrane. A similar conclusion was reached by Garty and Edelman (1983), who demonstrated that trypsinization of the apical membrane of the toad bladder resulted in an irreversible decrease in both basal and aldosterone-stimulated I_{sc}. The fact that trypsin affected the aldosterone-activated channels suggested that they were already present within the apical membrane in a nonconductive but trypsin-sensitive form. More recently, the effects of aldosterone on individual Na^+ channel activity was examined in A6 cells using the patch clamp technique. Ling et al. (1990) reported that exposure of A6 cells to aldosterone increased the density of functional channels detectable in the apical membrane with a time course similar to that for the increases in I_{sc} observed in intact epithelia. Aldosterone also increased the mean open time and open probability of the single channels. These authors likewise concluded that aldosterone activates preexisting quiescent channels.

At the biochemical level, Kleyman et al. (1989) used NMBA photolabeling, in combination with anti-amiloride antibodies, to determine if aldosterone alters the cellular pool and apical expression of Na^+ channels in A6 cells. A6 cell monolayers were exposed to aldosterone for 16 h, subsequently photoaffinity labeled with NMBA, and solubilized for gel electrophoresis and immunoblotting. NMBA that bound to channel protein was detected by anti-amiloride antibodies. Densitometric scans of the immunoblots revealed no detectable differences between control or aldosterone-treated cells, thereby demonstrating that the cellular pool and apical expression of Na^+ channels in A6 cells is not altered in response to aldosterone stimulation. Immunoprecipitation of surface radiolabeled Na^+ channels with antiamiloride anti-idiotypic antibodies also failed to detect a difference between control and aldosterone-treated A6 cell monolayers (Kleyman et al. 1990), further corroborating the idea that the apical expression of epithelial Na^+ channels is not altered by aldosterone. Additional evidence supporting aldosterone-induced activation of quiescent channels comes from the work of Tousson et al. (1989), who have shown immunocytochemically, using polyclonal antibodies directed against the channel, that aldosterone treatment does not stimulate fusion of Na^+ channel-containing vesicles with the apical membrane.

The mechanism by which aldosterone activates Na^+ channels remains unclear. However, two alternative mechanisms have been proposed to explain the aldosterone-induced increase in transepithelial Na^+ transport; these are summarized in Fig. 5. Sariban-

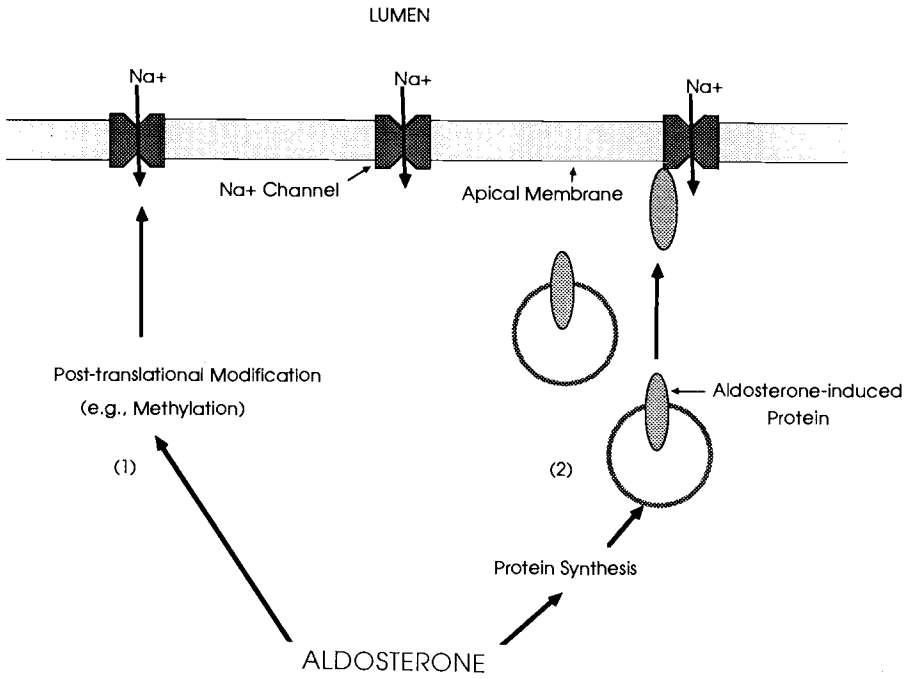

Fig. 5. Schematic diagram summarizing two possible explanations for the aldosterone-induced activation of epithelial Na^+ channels. One explanation is that aldosterone induces a post-translational modification which activates quiescent channels situated within the apical membrane (*1*). Sariban-Sohraby et al. (1984a) have presented evidence that aldosterone may activate Na^+ channels through the methylation of a channel subunit(s) or surrounding lipids. An alternative explanation is that one of the aldosterone induced proteins, namely the 70-kDa protein (Palvesky et al. 1990; Cox 1991), is a channel subunit or a regulatory protein that complexes with the channel, thereby activating inactive Na^+ channels preexisting within the apical membrane (*2*)

Sohraby et al. (1984a) observed that incubating apical membrane vesicles derived from A6 cells with the methyl donor *S*-adenosyl-L-methionine leads to a twofold increase in amiloride-blockable P_{Na}. Vesicles prepared from aldosterone-treated cells had a twofold higher rate of $^{22}Na^+$ uptake than controls, and this flux could not be further stimulated by *S*-adenosyl-L-methionine. In addition, aldosterone was observed to increase the amount of methylated proteins and lipids within the membrane. Based upon these data the authors suggested that aldosterone stimulates transmethylation of the channel or surrounding lipids, through the induction of a specific methyltransferase or through elevation of the cellular concentration

of *S*-adenosyl-L-methionine by acting upon other cytoplasmic enzymes (Sariban-Sohraby et al. 1984a). While such observations are strongly suggestive of a role of transmethylation of apical Na^+ channels or regulatory components by aldosterone, much work remains to be done. In this regard, Kemendy and Eaton (1990) determined the effect of 3-deazaadenosine on aldosterone-induced sodium transport at the single-channel level in A6 cells. They found that incubating control cells with this methylation inhibitor for 4–5 h decreased the single-channel open probability (P_o) from 0.26 to 0.02 and decreased the number of apparent open channels per patch from 2.1 to 0.4. In addition, they found that by depriving cells of serum and aldosterone for 3 days, P_o was decreased to 0.04. Subsequent addition of aldosterone returned P_o to 0.26, and also increased the apparent number of channels per patch from one to four. No channel activity could be detected in aldosterone-deprived cells incubated with both aldosterone and deazaadenosine. However, further work is necessary to see if a direct methylation of these channels can increase P_o.

In addition to Na^+/K^+ ATPase, other proteins are induced by aldosterone (Garty 1986; Szerlip and Cox 1989; Szerlip et al. 1989). There is also evidence from several studies that the aldosterone-induced proteins may act as regulatory proteins which activate preexisting apical channels. Interestingly, one of these aldosterone-induced proteins is a 70 kDa glycoprotein (Szerlip et al. 1989) that shows cross-reactivity with the 70 kDa subunit of a purified bovine Na^+ channel in immunoblots (Palvesky et al. 1990; Cox 1991). This suggests that the 70 kDa protein may either be a subunit of the channel or a regulatory protein that complexes with the channel. Ling et al. (1990), based upon single-channel data from A6 cells, suggest that because the single-channel kinetics are dramatically different depending upon whether aldosterone is present or not, at least one of the aldosterone-induced proteins must act as a regulatory protein. However, they suggest that the major action of aldosterone is the activation of channels via post-translational modifications of the channel or the surrounding membrane components, presumably mediated through an aldosterone-induced regulatory protein. Kleyman et al. (1990) have observed that although a 70 kDa subunit of the channel is present in aldosterone-treated A6 cells, a 70 to 80 kDa doublet is present in the Na^+ channel in cells treated with spironolactone, an antagonist of aldosterone. They suggest that post-translational modification of the 70 kDa subunit may be the

mechanism by which aldosterone regulates the Na^+ channel. G proteins have also recently been suggested to be involved in the aldosterone-induced activation of Na^+ channels (see below).

4.1.2 Vasopressin

The peptide hormone vasopressin (antidiuretic hormone, ADH) is known to increase Na^+ transport in electrically high resistance epithelia. Vasopressin interacts with V_2 receptors on the basolateral membrane and promotes the interaction of the receptor with a stimulatory G protein (G_s). This interaction leads to stimulation of adenylate cyclase activity and an increase in intracellular cAMP levels (Orloff and Handler 1967). Cyclic AMP presumably activates protein kinase A, which in turn phosphorylates various proteins, ultimately leading to increases in apical Na^+ transport. The addition of ADH to an epithelium leads to a two- to fourfold increase in I_{sc} within 10–20 min of application (Garty and Benos 1988).

Li et al. (1982), using the technique of blocker-induced noise analysis, demonstrated in the toad urinary bladder that vasopressin-induced Na^+ transport results from an increased density of open channels situated within the apical membrane with no change in single-channel conductance. These observations were confirmed by Helman et al. (1983) using frog skin. As summarized in Fig. 6, the increase in density of open channels may be explained either through the recruitment of new channels and/or a regulatory subunit of the channel, or through the vasopressin-mediated opening of inactive channels preexisting within the apical membrane.

Because both vasopressin and aldosterone increase channel density without affecting single-channel conductance, it is conceivable that both hormones activate the same pool of channels. The available data, however, argues against this possibility: (a) the antinatriuretic effect of both hormones is additive and synergistic (Handler et al. 1969; Fanestil et al. 1967; Sharp and Leaf 1966); and (b) trypsinization of the apical surface of the toad bladder inhibits the

Fig. 6A,B. Schematic diagram summarizing the two alternative mechanisms which have been proposed to explain the vasopressin-induced increase in transepithelial Na^+ transport. One explanation is that vasopressin causes the insertion of new functional channels into the apical membrane from an intracellular pool of channel-containing vesicles (**A**). The other explanation is that inactive channels situated within the apical membrane are activated by vasopressin through a cAMP-dependent kinase (*PKA*)-induced phosphorylation of the 315-kDa subunit of the channel (Sariban-Sohraby et al. 1988) (**B**)

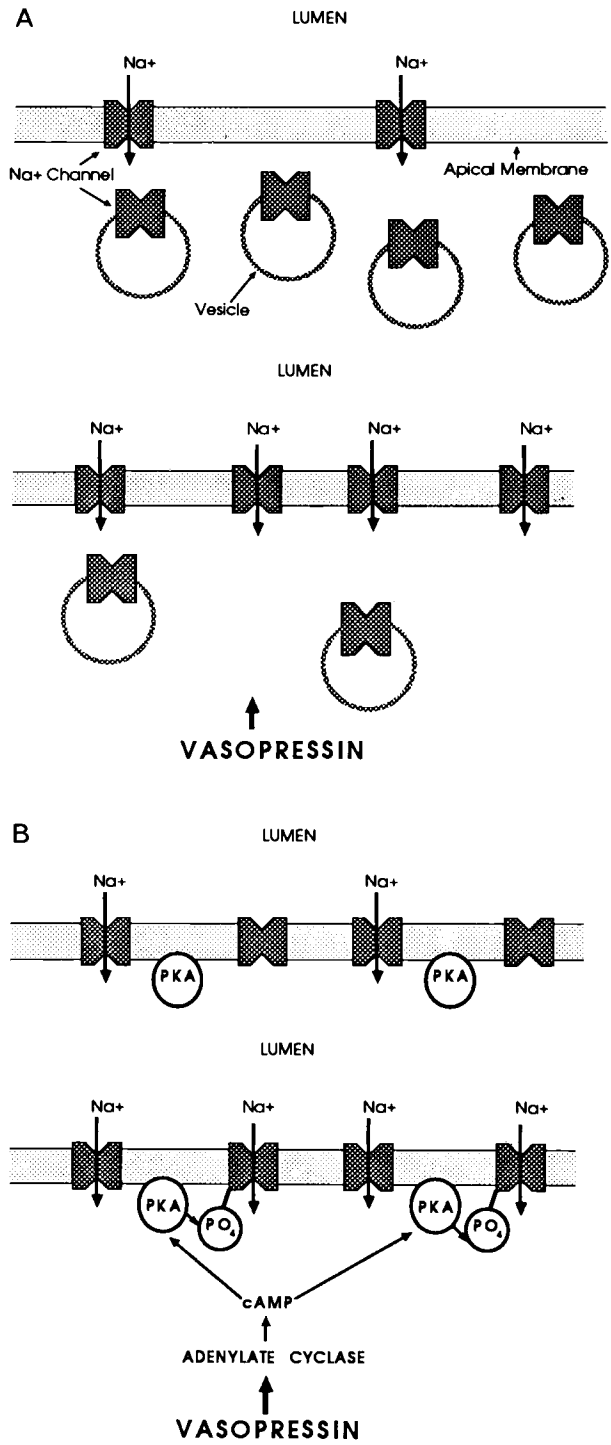
A
LUMEN
Na+
Na+
Na+ Channel
Apical Membrane
Vesicle
LUMEN
Na+
Na+
Na+
Na+
VASOPRESSIN
B
LUMEN
Na+
Na+
PKA
PKA
LUMEN
Na+
Na+
Na+
Na+
PKA
PKA
cAMP
ADENYLATE CYCLASE
VASOPRESSIN

response to aldosterone but not to vasopressin (Garty and Edelman 1983). This latter observation suggests that vasopressin stimulates Na^+ transport by recruiting channels from a subapical pool. One caveat in the interpretation of these trypsin experiments is that pretreating the apical membrane of the toad bladder epithelium with tyrosine-specific reagents inhibited both the baseline and vasopressin-stimulated Na^+ currents to the same extent (Park and Fanestil 1980; Palmer and Edelman 1981). One explanation for this finding is that the channels may be continuously present in the apical membrane in a conformational state that is resistent to trypsin proteolysis, but still susceptible to other protein-modifying reagents (Garty and Edelman 1983; Garty and Benos 1988). It is still possible, of course, that these protein reagents indirectly inhibit channel insertion by altering other apical proteins involved in an insertional process.

A recent study by Marunaka and Eaton (1991) attempted to further clarify whether or not the vasopressin-induced increase in I_{sc} is due to channel insertion. Using the patch clamp technique, these authors showed that vasopressin, when compared to controls, increased the number of conductive channels in isolated patches from A6 cells with little or no change in the open probability of individual Na^+ channels. A similar phenomenon was observed when cells were pretreated with N^6, 2′-*O*-dibutyryladenosine 3′,5′-cyclic monophosphate (db-cAMP) or cholera toxin. These authors concluded that vasopressin and its second messenger, cAMP, increases Na^+ transport by recruiting new channels into the apical membrane.

Vasopressin activates a cAMP-dependent protein kinase (protein kinase A), which suggests that protein kinase A may directly phosphorylate a regulatory subunit(s) of the channel. Alternatively, protein kinase A may phosphorylate other proteins that regulate the channel or induce insertion of new channels into the apical membrane. Lester et al. (1988) have shown that toad bladder apical membrane vesicles, into which purified cAMP-dependent kinase A, cAMP, and ATP were incorporated, failed to exhibit a stimulated Na^+ conductance. Their data favor the explantation that the vasopressin-stimulated increase in Na^+ conductance arises through the phosphorylation of a regulatory protein. The data of Marunaka and Eaton (1991) suggest that protein kinase A either phosphorylates a regulatory protein or a subunit of the channel that is not related to the kinetics of channel opening or closing.

In contrast to the observations of Lester et al. (1988), Sariban-Sohraby et al. (1988) have demonstrated that protein kinase A directly phosphorylates the 315 kDa subunit of the channel both in

vitro and in vivo in A6 cells. Furthermore, addition of the catalytic subunit of protein kinase A to isolated patches of A6 cell membranes activates quiescent channels (Cantiello et al., unpublished). These data argue in favor of a direct activation of quiescent channels by protein kinase A. Further evidence corroborating a direct phosphorylation of the Na^+ channel comes from Frings et al. (1988). Using the patch clamp technique, they demonstrated that addition of protein kinase A, cAMP, and ATP to isolated patches of toad urinary bladder apical membrane activated quiescent channels. Despite the numerous investigations of vasopressin action, the molecular mechanism underlying the increase in P_{Na} remains enigmatic, although some insight into this interesting problem is now being achieved.

4.1.3 Atrial Natriuretic Peptide and G Proteins

Atrial natriuretic peptide (ANP), a hormone released from the atrium of the mammalian heart in response to volume expansion, inhibits Na^+ reabsorption by the IMCD of the kidney. ANP-induced inhibition of Na^+ reabsorption was first suggested to be mediated through cGMP by Cantiello and Ausiello (1986). Using LLC-PK1 cells, they demonstrated that ANP stimulates cGMP production and that both ANP and cGMP reduce the amiloride-inhibitable $^{22}Na^+$ uptake by 40%–60%. Subsequently, Light et al. (1989) directly demonstrated at the single-channel level that ANP acts through the second messenger cGMP to inhibit Na^+ reabsorption through a low amiloride affinity, nonselective cation channel of the IMCD. Cyclic GMP inhibits this channel by two mechanisms: (a) a phosphorylation-independent mechanism which presumably acts through cGMP interacting with an allosteric modifier site on the channel; and (b) a phosphorylation-dependent mechanism involving cGMP kinase and the G protein, $G\alpha_{i-3}$ (Light et al. 1989, 1990b). The latter mechanism was hypothesized to be a sequential pathway with cGMP kinase modulating the ability of $G\alpha_{i-3}$ to activate the cation channel. This inhibition of the channel by two cGMP-dependent mechanisms, cGMP and cGMP kinase, may produce both a short-lived and a sustained reduction in Na^+ reabsorption by the IMCD in response to ANP (Light et al. 1990b).

In addition to mediating the effect of ANP on Na^+ resorption by the mammalian collecting duct, cGMP has been postulated to have an effect on Na^+ transport by the toad urinary bladder. Transepithelial Na^+ transport by the toad bladder is inhibited by muscarinic

agents and an increase in intracellular cGMP levels has been observed to occur (Sahib et al. 1978), thereby suggesting that cAMP and cGMP have opposite effects on Na^+ transport. However, addition of cGMP to the bathing medium had either no effect on Na^+ transport or only a small stimulatory effect. One caveat of these experiments is that the cGMP may not have penetrated the cells. Therefore, Palmer and associates (Das et al. 1991) have recently reinvestigated the action of cGMP on Na^+ transport in the toad bladder using 8-BrcGMP, a permeable analog of cGMP. Addition of 8-BrcGMP to the serosal bathing medium resulted in almost a twofold increase in I_{sc} and the effect of cGMP was not additive to those of cAMP or ADH. Based upon these observations, Das et al. (1991) concluded that cGMP modulates the same pathway or one closely related to that involving cAMP in channel activation. However, the physiological significance of this response is unknown.

4.1.4 Other Hormones

The peptide hormones insulin and insulin-like growth factor 1(IGF-1) stimulate a marked increase in I_{sc}. In A6 renal epithelial cells, for example, insulin produces a sixfold increase in steady state I_{sc} (Fidelman and Watlington 1984). It has been demonstrated using the toad bladder that the natriuretic response of insulin and IGF-1 is triggered by the binding of the hormone to basolateral membrane receptors, with stimulation of transport occurring at hormone concentrations of 0.1 n*M* (Blazer-Yost et al. 1989). Neither insulin nor IGF-1 saturated the maximal Na^+ transporting capacity because either ADH or aldosterone plus insulin stimulated a further increase in Na^+ transporting capacity (Blazer-Yost et al. 1989). This phenomenon is similar to the additive and synergistic effects of aldosterone and ADH on apical Na^+ transport in tight epithelia. The insulin-induced increase in Na^+ transport is now known to be mediated through the activation of PKC (Civan et al. 1988). However, the nature of the interaction between PKC and the channel remains unclear. Additionally, catecholamines (MacKnight et al. 1980) and prolactin (Snart and Dalton 1973) stimulate an increase in I_{sc} in toad bladder. However, their mechanisms of action are also unclear.

4.2 Intracellular Ions

4.2.1 Sodium

The regulation of apical Na^+ permeability by intracellular Na^+ ions is referred to as either feedback inhibition or homocellular regulation (Schultz 1981). MacRobbie and Ussing (1961), using the frog skin, were the first to observe that inhibition of basolateral Na^+/K^+ ATPase by ouabain also decreases apical Na^+ permeability. They suggested that the extrusion of Na^+ ions by the basolateral pump is coupled to the passive uptake of Na^+ ions. Subsequently, Lewis et al. (1976) and Turnheim et al. (1978), studying the rabbit bladder and colon, respectively, observed that blocking the basolateral Na^+/K^+ ATPase by ouabain elevates intracellular Ca^{2+} levels and also inhibits apically located amiloride-sensitive Na^+ channels. This led both groups to propose that elevated intracellular Ca^{2+} has a negative feedback effect on apical P_{Na}. Additional studies of this effect revealed that blocking of the basolateral pump by ouabain decreases apical P_{Na} only if the serosal medium contains a high Ca^{2+} concentration (Chase 1984; Garty and Lindemann 1984; Palmer 1985b). Furthermore, channel-mediated Na^+ influx into apical membrane vesicles showed little or no dependence upon the internal Na^+ ion concentrations (Chase and Al-Awqati 1983; Garty et al. 1987; Bridges et al. 1988). This result suggests that although the level of intracellular Na^+ is involved in the regulation of apical P_{Na}, it does not directly inhibit channel activity. Rather, as discussed below, it is probable that intracellular Na^+ influences apical Na^+ channels through modulation of intracellular Ca^{2+} concentrations.

4.2.2 Calcium

Increases in intracellular Ca^{2+} levels, which are associated with increases in cytoplasmic Na^+ concentrations, are correlated with the downregulation of apical Na^+ channels. A role for intracellular Ca^{2+} in the downregulation of Na^+ channels was first proposed by Grinstein and Erlij (1978) and Taylor and Windhager (1979). These authors suggested that an increase in intracellular Ca^{2+} in the toad urinary bladder decreases P_{Na} with the Ca^{2+} levels being regulated by a basolateral Na^+-Ca^{2+} exchanger. Under physiological conditions the exchanger is poised to catalyze Na^+ influx and Ca^{2+} efflux. Increasing intracellular Na^+ concentrations lead to an increase in intracellular Ca^{2+} levels, resulting from a decrease in Ca^{2+} exchange

across the basolateral membrane. The concomitant decline in basolateral Ca^{2+} exchange was due to a reduction in the Na^+ gradient across the basolateral membrane. It is also likely that Na^+ discharges Ca^{2+} from mitochondria via an exchange mechanism, as occurs in cardiac tissue (Carafoli 1987), thereby providing another way to increase intracellular Ca^{2+}. This mechanism for Ca^{2+}-induced downregulation of apical Na^+ channels has received support from additional studies. $^{22}Na^+$ uptake into apical membrane vesicles derived from the toad urinary bladder is inhibited by submicromolar concentrations of Ca^{2+} (Chase and Al-Awqati 1983; Garty et al. 1987; Garty and Asher 1985, 1986) and channel conductance in intact bladders is dependent upon the basolateral Na^+ gradient in the presence of a high serosal Ca^{2+}, but not in its absence (Chase and Al-Awqati 1981; Garty and Lindemann 1984; Palmer 1985b). Furthermore, basolateral flux studies using intact epithelia (Grinstein and Erlij 1978) and membrane vesicles (Chase and Al-Awqati 1981) have documented a Na^+-Ca^{2+} coupling.

The measurement of channel-mediated Na^+ fluxes in membrane vesicles derived from the toad bladder has led to the identification of two different Ca^{2+}-dependent processes that directly regulate apical Na^+ channels. The first process is a direct, reversible Ca^{2+}-Na^+ channel interaction mediated by cation binding to a site on the cytoplasmic face of the channel protein (Garty et al. 1987; Chase and Al-Awqati 1983). In the second process, protonation of the binding site through changes in intracellular pH prevents the Ca^{2+}-dependent blocking of the channel, whereas deprotonation renders the channel conductive (Garty et al. 1987).

The Ca^{2+}-induced downregulation of apical Na^+ channels has also been examined at the single-channel level. Using the patch clamp technique, Palmer and Frindt (1987a) have shown that the open time probability of Na^+ channels in excised patches from rat CCT shows no Ca^{2+} dependence. Nevertheless, in the cell-attached mode, addition of the Ca^{2+} ionophore ionomycin to the bath decreases channel activity, and omission of Ca^{2+} from the bath abolishes the effect of ionomycin. Ling and Eaton (1989), using the cell-attached patch clamp configuration, have demonstrated that the single-channel activity induced in A6 cells by low Na^+ is eliminated by exposure of the cells to the calcium ionophore A23187. The patch clamp data suggest that intracellular Ca^{2+} may also regulate epithelial Na^+ channels via an indirect mechanism. As presented in Fig. 7, one possible mechanism is through the Ca^{2+}/phospholipid-activated protein kinase, PKC. A role for PKC in channel regulation by the

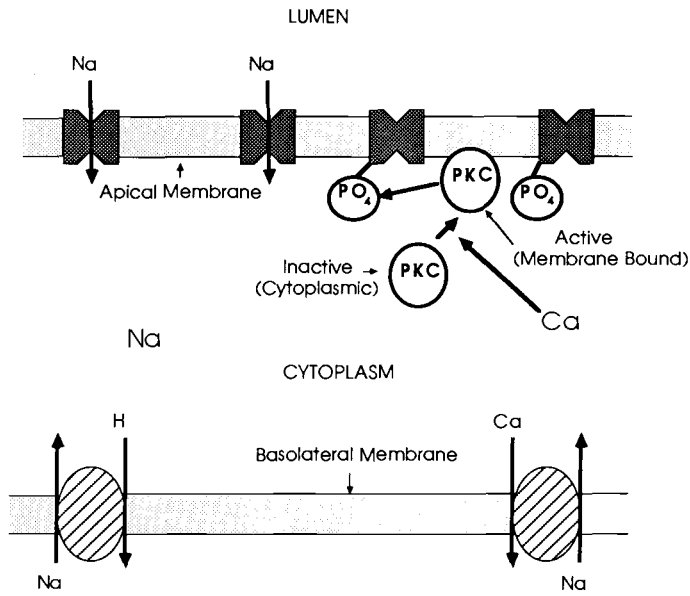

Fig. 7. Diagram illustrating the model for Na^+ self-inhibition proposed by Ling and Eaton (1989). Raising luminal Na^+ concentration increases the apical Na^+ entry through the amiloride-sensitive Na^+ channels and thereby raises the intracellular Na creating a Na^+ gradient which favors H and Ca entry by the basolateral Na-H antiporter and Na-Ca exchanger, respectively. This results in intracellular acidification which decreases apical Na^+ entry and also raises intracellular Ca levels. This would in turn induce translocation of the inactive cytoplasmic form of PKC to the membrane where it would undergo activation. The activated form of PKC would subsequently induce phosphorylation of the Na^+ channel, thereby downregulating the channel. (Modified from Ling and Eaton 1989)

action of phorbol esters, activators of PKC, has been suggested. Phorbol esters inhibit I_{sc} in A6 cells (Yanase and Handler 1986), $^{22}Na^+$ uptake into LLC-PK1 cells (Mohrmann et al. 1987), and net Na^+ reabsorption in isolated rat (Palmer and Frindt 1987b) and rabbit (Hayes et al. 1987) renal collecting tubules. Using the cell-attached patch configuration, it has been documented that phorbol esters decrease the mean number of open channels in isolated rat CCT (Palmer and Frindt 1987b) and A6 cells (Ling and Eaton 1989). The inactivation by PKC is presumably due to a phosphorylation of the channel or a regulatory protein (Ling and Eaton 1989). This is corroborated by the fact that PKC phosphorylates the 150- and 95-kDa subunits of the channel in vitro (Benos 1991). Alternatively, increases in intracellular Ca^{2+} may inactivate Na^+ channels by activating a phospholipase which modifies the phospholipid com-

position of the apical membrane (Garty and Asher 1985) through Ca^{2+}-dependent cytoskeletal-channel interactions (Garty and Asher 1985), or by altering cAMP levels by the stimulation of prostaglandin synthesis (Omachi et al. 1974). Thus, it is not yet clear if Ca^{2+} itself can directly modulate individual Na^+ channel activity, or if its effects are secondary.

4.2.3 Hydrogen

Palmer and Frindt (1987a) used the patch clamp technique to examine the effects of cytoplasmic pH on Na^+ channels from rat CCT. When the pH of the solution bathing the cytoplasmic side of the patch was decreased from 7.4 to 6.9 or 6.4 at constant Ca^{2+} ($0.1\,\mu M$), the P_o of single channels was reduced from 0.41 to 0.19 and 0.05, respectively. A decrease in the mean open time and an increase in the mean closed time of the channel at more acidic pH values resulted in the decrease in P_o. At pH 6.4, the channels were mostly closed, with occasional brief openings. The single-channel conductance was not affected by changes in pH.

Two possible, nonmutually exclusive hypotheses have been proposed by Palmer and Frindt (1987a) to explain the gating of epithelial Na^+ channels by protons. According to the first hypothesis, H^+ binds to sites either in the mouth of the channel or at a more distant site. This binding induces a conformational change converting the functional channel into a nonconducting state. In contrast, the second hypothesis is that protonation of a site on the channel protein shifts the equilibrium between the spontaneously open and closed states of the channel, such that the mean lifetime of the channel in the proton-blocked state (many seconds) would be longer than the spontaneously closed state. This latter hypothesis is supported by the observation that acidification increased the mean closed time of the channel. However, these closed times were shorter (4 s) than those predicted by the first hypothesis. Palmer and Frindt (1987a) therefore proposed a kinetic model in which the closed state has a higher affinity for H^+ than the open state, and an increased H^+ concentration shifts the equilibrium toward the closed state. In summary, the decrease in single Na^+ channel activity that is observed with cytoplasmic acidification is consistent with earlier measurements of transepithelial Na^+ transport in amphibian epithelia (Ussing and Zerahn 1951; Palmer 1985b) and suggests that cytoplasmic pH can directly influence channel activity.

4.3 Luminal Factors

4.3.1 Osmotic Effects

Tight epithelia exhibit a volume-related regulation of transepithelial Na^+ transport when exposed to an anisosmotic medium. Ussing (1965), using isolated frog skin, was the first to demonstrate that a decrease in the osmolarity of the bathing medium increased I_{sc}, whereas an increase in osmolarity decreased I_{sc}. The effects of a hyperosmotic mucosal solution on apical Na^+ channels in frog skin was subsequently examined by Zeiske and Van Driessche (1984) using current noise analysis. These authors observed that an increase in mucosal osmolarity decreases I_{sc} by decreasing both the density of functional apical Na^+ channels and the single-channel current. The effects of solution osmolarity on Na^+ channel activity was recently examined in A6 renal epithelial cells by Wills et al. (1991). In contrast, they reported that changes in mucosal osmolarity did not affect I_{sc}; however decreases in serosal osmolarity resulted in a threefold stimulation of I_{sc}. Current fluctuation analysis indicated that single-channel currents were similar for isosmotic and hyposmotic conditions, but the number of conducting channels were threefold higher for epithelia bathed in hyposmotic solutions. The reasons for the differences in the observations of Zeiske and Van Driessche (1984) and Wills et al. (1991) are not apparent.

These cell volume-related changes in apical Na^+ permeability may be related to (a) direct modulation of channels by stretching or compressing the apical membrane; (b) changes in intracellular concentration of a second messenger involved in regulation, thereby activating nonconductive channels; or (c) insertion of new channels into the apical membrane from an intracellular pool (Wills et al. 1991). The lack of detectable changes in membrane capacitance and the similarities in single-channel characteristics in anisosmotic and isosmotic conditions, together with the slow time course of the osmolarity effects on channel activation, led Wills and associates (Wills et al. 1991) to suggest that in A6 cells an intracellular messenger system, such as cAMP, Ca^{2+}, or leukotrienes, activates quiescent channels through a phosphorylation or methylation of the channels or their regulatory polypeptides. Nevertheless, it is possible that the number of vesicle fusion events needed to insert new channels into the apical membrane, thereby increasing the apical Na^+ permeability, are so small that they cannot be detected by transepithelial

capacitance measurements. Indeed, there is evidence from the rabbit urinary bladder that a reduction in mucosal osmolarity does lead to an increase in the epithelial capacitance concomitant with an increase in apical Na^+ channel density (Lewis and de Moura 1982). Lewis and de Moura (1982) propose that these events are due to the fusion of channel-containing vesicles with the apical membrane. However, Na^+ channel-containing vesicles have not, as of yet, been demonstrated within rabbit urinary bladder cells.

4.3.2 Extracellular Na^+

There is a reduction in apical P_{Na} in response to increasing mucosal Na^+ concentrations. This phenomenon is termed Na^+ self-inhibition and is distinct from the homocellular ("feedback") mechanism mediated by intracellular Na^+ activity. Self-inhibition has recently been reviewed by Turnheim (1991). Biber and colleagues (Biber et al. 1966; Biber and Curran 1970; Biber 1971) first observed this phenomenon in frog skin. Using short-circuit current measurements and $^{22}Na^+$ fluxes, they demonstrated that P_{Na} saturated with increasing external Na^+ concentrations. Subsequently, Fuchs et al. (1977) reported that an increase in mucosal Na^+ concentration resulted in a rapid increase in I_{sc} to a maximum value, followed by a slow decline to a lower steady state value over a time course of seconds. This delayed decline in I_{sc} was interpreted as being due to a decrease in apical P_{Na} induced by the increase in luminal Na^+. These authors postulated a direct interaction between apical Na^+ ions and an allosteric site on the channel, resulting in the modification of the channel protein and inhibition of conductance. Van Driessche and Lindemann (1979), using amiloride-induced current fluctuation analysis, revealed that although the I_{sc} across frog skin increases, the deduced single-channel current shows no saturation in response to increases in mucosal Na^+. This observation led them to conclude that increasing external Na^+ exerts its inhibitory effect by decreasing the density of open channels within the apical membrane, rather than by direct saturation of individual channels. Similar observations have been made for the chicken coprodeum (Christensen and Bindslev 1982) and the rabbit urinary bladder (Lewis et al. 1984).

Although noise analysis has suggested that self-inhibition is not due to the saturation of individual channels, amiloride-sensitive Na^+ channels that have been examined at the single-channel level by reconstitution into lipid bilayers (Olans et al. 1984) and by the patch clamp technique (Palmer and Frindt 1986; Ling and Eaton 1989;

Palmer et al. 1990) exhibit saturation with increasing Na^+ concentration. The apparent K_m (i.e., the $[Na^+]$ where channel conductance is 50% of the value at which the single-channel conductance saturates) varies between 17 and 50 m*M*. Garty and Benos (1988) have suggested that the lack of single-channel current saturation observed in frog skin by Van Driessche and Lindemann (1979) resulted from the fact that the experiments were performed in tissues depolarized by a high K^+ solution on the serosal side. Support for this idea comes from experiments performed in nondepolarized frog skin where saturation of single-channel Na^+ current has been detected using noise analysis (Helman et al. 1983). However, in nondepolarized rabbit urinary bladder (Lewis et al. 1984) and hen coprodeum (Christensen and Bindslev 1982), no saturation was observed. In any case, the fact that single Na^+ channels saturate with increasing Na^+ activity, even in oocyte expression studies (Palmer et al. 1990), suggests that unknown regulatory factors in the intact epithelium may shift the extracellular Na^+ affinity to higher values.

Ling and Eaton (1989) applied the cell-attached patch clamp methodology to A6 renal epithelial cells. These authors were able to demonstrate that a reduction in external Na^+ increased P_o and increased the number of channels in a single patch. They found that unit channel conductance and amplitude were not different when the luminal surface of the patch was bathed with high (129 m*M*) or low (3 m*M*) Na^+, consistent with saturation of individual channels. This increase in channel activity was prevented by the Ca^{2+} ionophore, A23187, and the PKC activators, phorbol myristate (PMA) and oleyl-acetyl-glycerol (OAG). The protein kinase inhibitor, sphingosine, increased the P_o and the number of channels within a patch. Ling and Eaton (1989) concluded that the regulation of apical Na^+ permeability by luminal Na^+ does not require direct interaction of Na^+ with channel protein; rather it involves intracellular regulatory mechanisms. The increase in luminal Na^+ results in an increase in intracellular Na^+, thereby activating the homocellular regulatory pathway. Downregulation of the channels occurs through an increase in cytosolic Ca^{2+} which in turn activates PKC (see discussion above and Fig. 7). Presumably it is through the activation of PKC that the channel is ultimately inactivated. Thus, the downregulation of apical Na^+ channels by Na^+ self-inhibition is directly linked to the homocellular regulatory mechanism and intracellular Ca^{2+}.

4.3.3 Luminal Proteases

The serine proteases, urokinase and kallikrein are known to block amiloride-sensitive Na^+ channels. These two enzymes are secreted into the urine of mammals and amphibians by the distal tubules and alter the channels through proteolysis (Lewis and Alles 1986; Garty and Benos 1988). The presence of amiloride protects the channels from inhibition by these enzymes. It has been proposed by Lewis and colleagues (Lewis and Alles 1986; Zweifach and Lewis 1988) that urinary kallikrein may be involved in the physiological regulation of Na^+ transport by the mammalian urinary bladder. The kallikrein-induced degradation involves two steps – conversion of the channels first to an amiloride-insensitive, nonselective cationic channel, followed sometime thereafter by actual physical loss of the channels into the urine. Interestingly, noise analysis and more recently bilayer and single-channel recordings have shown that kallikrein-induced proteolysis of the channel does not affect the single-channel current in spite of drastic changes in selectivity and amiloride sensitivity (Lewis et al. 1984; Zweifach and Lewis 1988). The degradation of Na^+ channels is dependent upon the concentration of urinary kallikrein, which is increased by corticoid hormones such as aldosterone. It has been hypothesized that channel density in the distal tubule and urinary bladder can be regulated by this mechanism (Lewis and Alles 1986). Aldosterone can directly increase the number of active channels in the apical membrane by mechanisms discussed earlier, and can indirectly downregulate the natriuretic response of the epithelium by increasing the release of kallikrein into the urine. The physiological significance of this dual regulation of channel activity is obscure.

Luminal proteolysis and loss of channels into the urine are viewed as the final stage of Na^+ channel turnover in the urinary bladder. Lewis and de Moura (1982) have suggested, based upon capacitance measurements of rabbit urinary bladder following exposure to reduced mucosal osmolarity, that there are short-lived contacts between the apical membrane and subapical cytoplasmic channel-containing vesicles that lead to transfer of Na^+ channels to the apical membrane or, alternatively, actual fusion of these vesicles with the apical membrane. Apical membrane channels are subsequently degraded by urinary kallikrein into amiloride-insensitive leak pathways that may be internalized into the cell (Lewis and de Moura 1982). The amiloride-insensitive channels remaining within the apical membrane are further destabilized by kallikrein and are lost into the urine.

However, Bridges (unpublished observations) has found that high concentrations of kallikrein or urokinase have no effect on amiloride-sensitive $^{22}Na^+$ uptake into membrane vesicles isolated from dexamethasone-treated rat colon.

4.4 G Proteins

The guanine nucleotide-binding protein (G protein) family is composed of three subunits (α, β, and γ) that couple membrane receptors to a variety of ion channels (Brown and Birnbaumer 1988). Typically, their mechanism of action is as follows: agonist binding to a membrane receptor induces a conformational change in the G protein, thereby facilitating GTP replacement of GDP on the α-subunit. The GTP-α complex subsequently dissociates from the β-and γ-subunits and interacts with the effector, such as an ion channel, which produces a physiologic response. The intrinsic GTPase activity of the subunit then hydrolyses GTP to GDP and the α-GDP complex reassociates with the β- and γ-subunits, thereby terminating the response (Brown and Birnbaumer 1988).

A role for G proteins in the regulation of epithelial Na^+ channels was first suggested by Ausiello and collaborators (Mohrmann et al. 1987). Pertussis toxin (PTX), a compound that prevents receptor-dependent activation of the G proteins G_i and G_o, reduced electrogenic Na^+ transport across LLC-PK1 cells to the same extent as did ANP, cGMP, or PKC. PTX treatment also abolished completely amiloride-sensitive Na^+ transport in A6 renal epithelial cells. Subsequently, Garty et al. (1989), using membrane vesicles derived from toad urinary bladder cells, demonstrated that the nonhydrolyzable GTP analog, GTPγS, can stimulate amiloride-blockable Na^+ transport across the vesicles, and that GDPβS can reverse this effect, thereby providing further evidence for the role of G proteins in regulating the activity of amiloride-sensitive Na^+ channels.

Recently the patch clamp technique has been used to examine the effects of PTX and GTP and its analogs on the single-channel activity of an amiloride-sensitive, nonselective cation channel in renal medullary collecting duct cells (Light et al. 1989), and on an amiloride-sensitive Na^+-selective channel in A6 cells (Cantiello et al. 1989, 1990). Using excised inside out patches, it was shown that GTPγS increases the open probability of the channels, whereas both GDPβS and PTX inhibit the channels. Furthermore, the addition of the $\alpha_{i\text{-}3}$-subunit of G_i to the cytoplasmic surface of the patches increases the

P_o in both preparations, thereby directly demonstrating that the α-subunit of G_i activates amiloride-sensitive Na^+ channels.

Ausiello et al. (1991) provided further evidence for the role of G proteins in the regulation of epithelial Na^+ channels. They demonstrated that the epithelial Na^+ channel complex purified from A6 cells contains a 41 kDa polypeptide that is ADP ribosylated by PTX, and that cross-reacts with anti-$G\alpha_{i-3}$ antibodies on immunoblots. Confocal imaging of A6 cells with specific antibodies revealed that both $G\alpha_{i-3}$ and the Na^+ channel localize to distinct but adjacent domains of the apical surface. These data led to the suggestion that G-protein coupling to the Na^+ channel may not be direct; rather, its ion transport stimulatory capacity may be enhanced by further signal transduction pathways, such as phospholipase and lipoxygenase pathways, or by cytoskeletal rearrangements (the proteins ankyrin and fodrin are linked to the Na^+ channel complex, see below). It is therefore probable that the purified channel complex consists of regulatory proteins, such as $G\alpha_{i-3}$, sequestered through noncovalent linkages with cytoskeletal proteins. G proteins are known to be linked to the cytoskeleton in other systems. Interestingly, an additional polypeptide of the channel complex, the 95 kDa subunit, is ADP ribosylated by PTX; however, as it does not crossreact with anti-G protein antibodies on immunoblots and cannot be ADP ribosylated when the experiment is performed on the purified channel complex, its functional significance is unknown (Ausiello et al. 1991).

The apical G-protein channel complex is geographically separated from the receptor-coupled G_s and G_i proteins which are situated within the basolateral membrane where they are responsible for the generation of second messengers. Three hypotheses are currently extant to explain how G proteins may regulate apical Na^+ channels. First, although an apically situated receptor coupled to the G protein has yet to be identified, phospholipase A2 and lipoxygenase pathways, both of which are distinct from the signal transduction pathways present in the basolateral membrane, have been implicated in mediating G protein regulation of apical Na^+ channels (Light et al. 1989). The proposed model for G protein-mediated regulation of the epithelial Na^+ channel by phospholipase A_2 and lipoxygenase pathways is presented in Fig. 8. Using the patch clamp technique, Cantiello et al. (1990) have shown that activation of phospholipase by G_i induces both an increase in the number and percent open time of Na^+ channels in apical patches excised from A6 cells. Interestingly, this response is similar to that reported for the aldosterone-induced

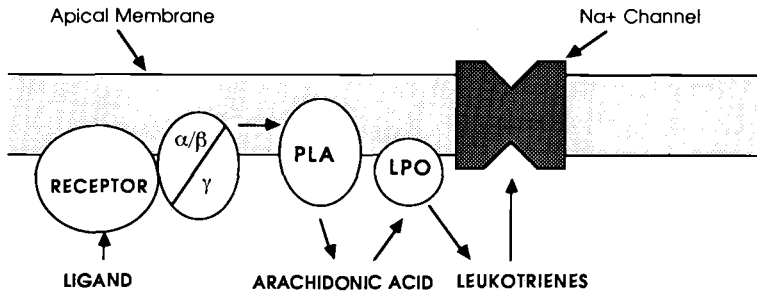

Fig. 8. Diagram summarizing the proposed model for G protein-mediated regulation of the epithelial Na^+ channel via phospholipase A_2 and lipoxygenase pathways. The apically situated G protein is activated by ligand binding to a receptor which is also apically situated. The G protein in turn activates phospholipase A_2 (*PLA*) leading to the production of arachidonic acid and lipoxygenase (*LPO*). Lipoxygenase products, such as leukotrienes, either directly, or through additional pathways, activate the epithelial Na^+ channel. (Modified from Cantiello et al. 1990)

activation of Na^+ channels in toad urinary bladder (Yorio and Bentley 1978). Both basal and aldosterone-stimulated Na^+ channel activities in the toad bladder epithelium are inhibited by mepacrine, a phospholipase inhibitor, indicating that G protein-induced phospholipase A_2 activity may play a role in the aldosterone-induced activation of Na^+ channels. A second possible mechanism is that the apical G protein–phospholipase pathway may be coupled to a basolateral receptor–G protein complex through a second messenger pathway, thereby offering a potential explanation for the role of G proteins in the hormonal regulation of apical Na^+ channels (Light et al. 1989). A third possible mechanism has been suggested by Ling et al. (1990) to explain Na^+ self-inhibition. They propose that there may be a nonreceptor-mediated modulation of the G protein/Na^+ channel complex by intracellular messengers, such as PKC. PKC has been documented in other systems to phosphorylate G proteins and to modulate the function of the G protein effector. Further experiments are required to unravel the intricacies of these regulatory mechanisms.

4.5 Cytoskeletal Interactions

Tousson et al. (1989) have demonstrated, with immunoelectron-microscopy, that amiloride-sensitive Na^+ channels are polarized to the microvillar domain of the apical membrane in Na^+-reabsorbing

epithelia. This polarized distribution of the Na^+ channels to the apical membrane is essential for electrogenic Na^+ transport. It is becoming increasingly apparent that ion channels and transporters maintain their distribution within specific membrane domains through direct association with the underlying cortical cytoskeleton. For example, Na^+/K^+ ATPase (Morrow et al. 1989; Nelson and Veshnock 1987), band 3 analog of renal cells (Drenckhahn et al. 1985), cGMP cation channel of photoreceptors (Molday et al. 1990), and the voltage-dependent Na^+ channel of neurons (Srinivasan et al. 1988) are all linked to the cytoskeleton, predominantly through ankyrin and fodrin.

Recently Smith et al. (1991) demonstrated that the epithelial Na^+ channel is also linked to the cortical cytoskeleton by the proteins ankyrin and fodrin. Ankyrin, fodrin, and actin were observed to colocalize with the Na^+ channel to microvilli in A6 cells. Immunoblot analysis of partially purified bovine Na^+ channel complex revealed that actin, fodrin, and ankyrin copurified with the channel complex. A direct interaction between the cytoskeleton and the channel was demonstrated by ^{125}I-labeled ankyrin binding to the 150-kDa amiloride binding subunit of the channel. Further evidence corroborating a linkage of the channel to the cytoskeleton was obtained by measurements of lateral diffusion of fluorescently labeled Na^+ channels on the apical membranes of A6 cells using the technique of fluorescence recovery after photobleaching [FRAP]. These measurements revealed that the Na^+ channels are immobile or have a very limited mobility (lateral diffusion coefficient $= 4 \times 10^{-11}$ cm/s; Smith et al. 1991).

In addition to maintaining the polarized distribution of Na^+ channels to the microvillar domain of the apical membrane, there is increasing evidence that the cytoskeleton may play a role in the regulation of Na^+ channel activity. Ausiello and collaborators (Cantiello et al. 1991; Pratt et al. 1991), using patch clamp methodology, demonstrated that the actin filament disrupter, cytochalasin D, induced Na^+ channel activity in excised patches as well as in quiescent cell-attached patches. Addition of purified polymeric G actin to excised patches induced an increase in the average channel number, and the subsequent addition of ATP further increased the number of G actin-induced channels per patch as well as the percent open time. The addition of DNase 1, a G actin binding protein, was found to reverse the effect of actin on both channel activity and percent open time. Furthermore, the addition of the actin binding protein filamin to the patches had the same effect as DNase 1. Based

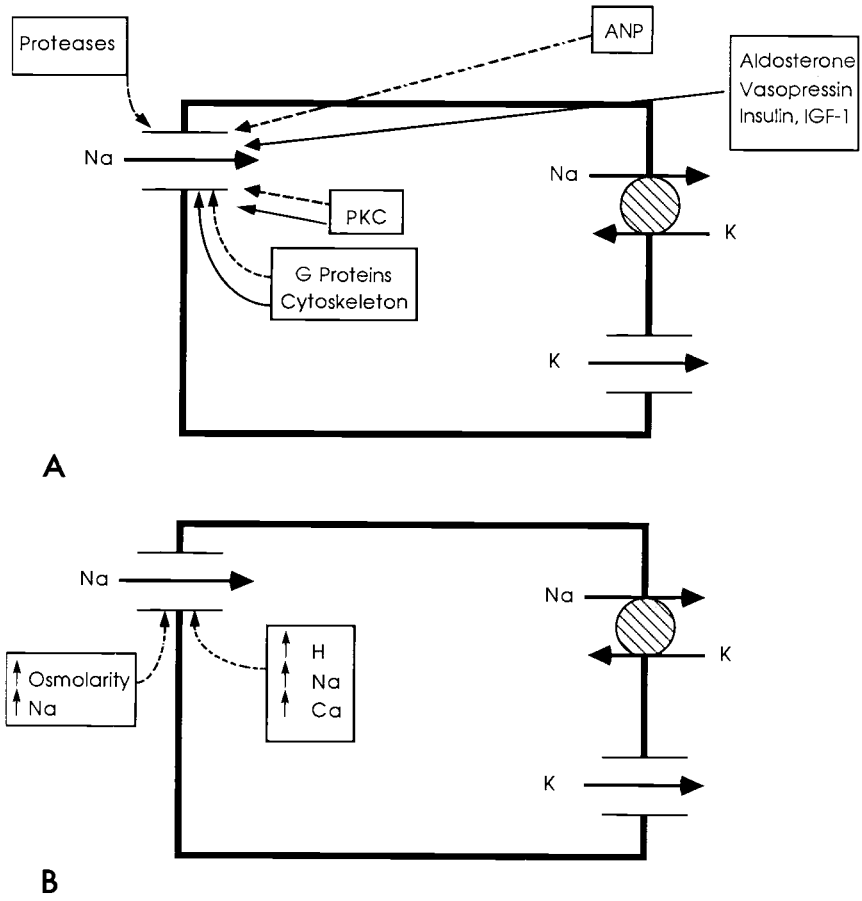

Fig. 9A,B. Schematic diagrams summarizing the regulation of the epithelial Na^+ channel by the various hormones, ions, and ligands discussed Sect. 4. **A** The hormones aldosterone, vasopressin, insulin, and insulin-like growth factor (*IGF-1*) activate the Na^+ channel, whereas atrial natruretic peptide (*ANP*) downregulates the channel. Protein kinase C (*PKC*), G proteins, and the cytoskeleton have been documented to be involved both in the activation and downregulation of the Na^+ channel. The luminal proteases kallikrein and urokinase downregulate the channel via proteolysis. **B** Increases in the concentration of intracellular H^+, Na^+, or Ca^{2+} ions or increases in either the osmolarity or Na^+ ion concentration of the luminal fluid downregulate the channel. *Solid lines*, activation of the channel; *dashed lines*, downregulation of the channel

upon these data, it was proposed that the short polymeric form of actin may be involved in regulating Na^+ channel activity.

Alternatively, the cytoskeleton may indirectly mediate channel activity through a cytoskeletally linked G protein. It has been proposed that the $G\alpha_{i-3}$ which copurifies with the channel is linked to

the cytoskeleton (Ausiello et al. 1991). These data suggest that the linkage between the cytoskeleton and the channel may be a site for hormonal modulation of epithelial Na^+ transport. Figure 9 presents a composite model summarizing all the positive and negative regulating effectors of epithelial Na^+ channels.

4.6 Biosynthetic Studies

The recent development of antibodies that recognize the amiloride-sensitive Na^+ channel facilitates the examination of channel biosynthesis. Kleyman et al. (1991) have provided a preliminary examination of channel biosynthesis in A6 epithelial cells using an antibody directed against the amiloride binding site of the epithelial Na^+ channel (anti-idiotypic). Filter-grown cells were metabolically labeled for 15 min with [^{35}S]methionine, chased with excess free methionine, and labeled channels were subsequently immunoprecipitated from solubilized membranes using antibodies generated against the amiloride binding domain of the channel. Following a 2-h chase period, channel subunits with apparent molecular masses of 230–260 kDa, 180 kDa, 140 kDa, and 70 kDa were observed. However, when the chase period was reduced to 15 min, neither the channel complex nor a precursor of the amiloride binding subunit were observed. These authors suggest that at least 15–75 min is needed for assembly of the epithelial Na^+ channel complex and/or development of an epitope which is recognized by the anti-idiotypic antibody. Furthermore, they propose that post-translational modification or assembly of the channel complex is a prerequisite for antibody binding.

One such post-translational modification is glycosylation. At least three subunits of the Na^+ channel are glycosylated, namely the 315, 150, and 95 kDa subunits (Garty and Benos 1988; Benos 1989). There is evidence from TMB cells, a cell line derived from the toad urinary bladder, that glycosylation is necessary for channel function. When TMB cells are cultured in the presence of tunicamycin, an inhibitor of N-linked glycoslyation, there is a marked decrease in apical Na^+ entry (Zamofing et al. 1989).

Barbry et al. (1990a), using a molecular biological approach, have determined the rate of biosynthesis of a 97-kDa amiloride binding protein (ABP) isolated from the human kidney. Human 293S cells were transfected with the cDNA encoding the ABP, and metabolically labeled with [^{35}S]methionine. Following varying chase periods with excess unlabeled methionine, the labeled ABP was immuno-

precipitated from solubilized membranes using a monoclonal antibody directed against the ABP isolated from pig kidney cortex (Barbry et al. 1990a). The half-life of synthesis for the human kidney ABP was found to be approximately 30 min. Incubation of transfected cells in tunicamycin led to the disappearance of the 97 kDa polypeptide and replacement with a 70 kDa polypeptide. As indicated earlier, although this protein is presumably a subunit of the epithelial Na^+ channel, its functional role is unknown as it fails to conduct Na^+ when expressed in a transfection system (Barbry et al. 1990a).

5 Molecular Biology of Epithelial Na^+ Channels

An insight into the molecular biology of the amiloride-sensitive Na^+ channel was obtained using the Xenopus oocyte expression system. This technique relies on the ability of prophase-arrested oocytes to faithfully express exogenous mRNA isolated from heterologous sources. The main advantage of this technique is that it allows advances in gene cloning when protein sequence information or antibodies to the protein of interest are unavailable. Because oocytes do not express an endogenous amiloride-sensitive Na^+ channel, this system is ideal for attempting the expression cloning of this protein.

Successful translation of the amiloride-sensitive Na^+ channel in the oocyte has been documented for RNA isolated from the toad kidney A6 cell line (Hinton and Eaton 1989; George et al. 1989; Palmer et al. 1990), human nasal polyps (Kroll et al. 1989), and the chicken intestine (Garty and Asher 1991) using voltage clamping or $^{22}Na^+$ influx methodologies to assay for the expressed channel. A6 cells grown on impermeable supports require aldosterone pretreatment prior to RNA isolation in order to record channel activity by dual electrode voltage clamp (Hinton and Eaton 1989; Palmer et al. 1990). When the cells are grown on collagen-coated Millipore filters, the extracted mRNA is capable of expressing tenfold more Na^+ current than that prepared from cells grown on collagen-coated Millipore filters, the extracted mRNA is capable of expressing tenfold more Na^+ current than that prepared from cells grown on plastic dishes. In addition, aldosterone treatment is unable to further enhance the magnitude of the expressed Na^+ current (Palmer et al. 1990). The results of George et al. (1989), using a radioisotopic $^{22}Na^+$ influx assay to monitor translation of the channel, are in

agreement with these voltage clamp studies. These data demonstrate that the largely undifferentiated plastic-grown A6 cells require aldosterone, itself an inducer of differentiation, to express an active amiloride-sensitive Na^+ channel in the oocytes. These data directly correlate with the short-circuit current measurements made across the monolayer. Aldosterone may perturb the transcription of an inhibitory protein or induce an activator of the already transcribed and/or translated channel protein. Alternatively, aldosterone may directly activate the transcription of the amiloride-sensitive Na^+ channel. In order to address these possibilities, Garty and Asher (1991) injected chicken intestine poly(A+) mRNA into oocytes maintained in a medium containing actinomycin D. The mRNA was prepared from chickens fed on either a normal sodium (NS) or sodium-free (LS) diet (to enhance aldosterone levels chronically in vivo) for 10 days. Injection of mRNA isolated from NS hens did not result in any amiloride-sensitive Na^+ currents as measured by $^{22}Na^+$ influx. However, the LS preparation did enhance Na^+ uptake and this was unaffected by either actinomycin D or coinjection of NS mRNA. Thus, under their experimental conditions in the chicken intestine, it appears unlikely that the inability of the NS mRNA to express active amiloride-sensitive Na^+ channels in the oocyte is due to the translation of an inhibitory protein.

In all studies so far reported, expression of channel activity was always monitored as a tonically active conductance or influx: i.e., stimulation of the channel by second messengers was not required. Replacement of extracellular Na^+ with the impermeant cation NMDG showed the amiloride-inhibitable current to reverse at +60 mV (Hinton and Eaton 1989; Palmer et al. 1990). This reversal potential provided proof for the expression of a highly Na^+-selective current from A6 cell-derived mRNA. Palmer et al. (1990) reported an enhancement of amiloride-sensitive conductance when the oocytes were preincubated at 25°C for 6 h prior to recording. This temperature-dependent conductance was not diminished by a 15-min preincubation of the oocyte with trypsin at 19°C prior to temperature elevation.[4] The authors thus concluded that in the oocyte maintained at 19°C the channel was synthesized. However, the protein either remained at an intracellular location or was inserted into the mem-

[4] Trypsinization of the intact toad urinary bladder has previously been shown to attenuate the amiloride-sensitive Na^+ current, presumably by cleaving part of the channel at the plasma membrane (Garty and Edelman 1983).

brane in a different conformational form which rendered it inactive and unsusceptible to trypsin.

At −90 to −100 mV the K_i for amiloride inhibition of the Na^+ channel expressed from A6 cells lies between 48–110 n*M* (Hinton and Eaton 1989; Palmer et al. 1990). Sodium influx measurements demonstrated that benzamil at 0.1 μ*M* was just as effective as 1 μ*M* amiloride while 1 μ*M* EIPA decreased the Na^+-selective current by only 16% (George et al. 1989). These results are consistent with the synthesis of a high amiloride affinity Na^+ channel. Thus, translation of A6 cell mRNA in Xenopus oocytes results in the expression of a Na^+ channel with high affinity for amiloride and high selectivity for Na^+. These characteristics are identical to those of the channel found in tight epithelia.

Fractionation of the A6 poly(A+) mRNA by nondenaturing sucrose gradient centrifugation prior to injection has been accomplished by two groups. George et al. (1989) found that a fraction containing mRNAs ranging from 1.4 to 4.4 kb resulted in maximum Na^+ influx. Palmer et al. (1990) were able to record maximum amiloride-sensitive conductance from mRNAs of approximately 2–2.4 kb. Both results taken together suggest that a protein of approximately 70–75 kDa is sufficient for the expression of amiloride-sensitive Na^+ channels in the *Xenopus* oocyte.

Epithelial Na^+ channels have also been expressed from poly(A+) mRNA isolated from human nasal tissue (Kroll et al. 1989). Using dual electrode voltage clamp, maximum expression was measured 2 days following injection of 25 ng mRNA. The amiloride-inhibitable current correlated with the amount of injected mRNA when 12.5 ng or less was used. These dose-response values are similar to those found by George et al. (1989) for A6-derived poly(A+) mRNA. The K_i values of amiloride inhibition on the membrane potential and resistance of the oocyte were 95 n*M* and 130 n*M*, respectively. However, because this measurement was not made under a holding clamp potential these results cannot be directly compared to the those derived from the A6 cell mRNA.

The more classical approach to molecular cloning has most recently been utilized in order to clone a phenamil binding protein from the pig kidney cortex (Barbry et al. 1990a). Initial work involved the purification of a 105-kDa phenamil binding protein from this tissue. Reconstitution of this protein into liposomes resulted in a phenamil-sensitive Na^+ influx which was inhibited by phenamil and amiloride with a K_i of 10 μ*M*. This low amiloride affinity binding protein was subject to partial amino acid sequence analysis following

trypsin digestion. An oligonucleotide 66 bases in length was designed from these data and used to screen a human kidney cDNA library. A full length cDNA clone was isolated which contained an open reading frame of 713 amino acids. The predicted molecular weight of this protein is 78886 Da. It contains a signal peptide sequence and three potential N-linked glycosylation sites. Hydrophobicity plots do not show any potential membrane spanning helices which is surprising in light of the previous reconstitution studies. Expression of the clone in 293S and NIH 3T3 cells resulted in the synthesis of a 97 kDa protein as demonstrated by immunoprecipitation with monoclonal antibodies raised against the purified protein. Overnight incubation of the transfected cells with the N-linked glycosylation inhibitor tunicamycin caused a reduction in the apparent molecular weight of the protein by 27 kDa. Scatchard analysis of [^{3}H]phenamil binding to membranes of transfected 293S cells showed that the cloned protein bound phenamil with a K_d of 2.5 nM. A K_d of either 1 or 60 nM was previously reported for phenamil binding in intact pig kidney membranes. Thus, when expressed in a heterologous system, the protein retains pharmacological characteristics similar to those in its native environment (see Sect. 3.1). However, although phenamil binding was retained the protein did not display conductive properties. Neither patch clamp analysis nor cRNA injection into Xenopus oocytes revealed Na^+ channel activity. These results may imply that a multi-protein channel complex is responsible for Na^+ transport in the kidney cortex similar to that operative in the papillae (Garty and Benos 1988).

The cloning of a kidney apical membrane protein has recently been reported and implicated as a putative subunit of the amiloride-sensitive sodium channel (Staub et al. 1990). The protein was identified by its cross-reactivity with a polyclonal antibody prepared against the Na^+/K^+ ATPase (Rossier et al. 1989). Its cloning was achieved by initially screening an A6 cell expression cDNA library and subsequently a Xenopus ovary cDNA library. The cDNA contained an open reading frame of 1420 amino acids and Northern analysis revealed a 5.2 kb message in both A6 cells and stage VI occytes. The length of the open reading frame suggests that the clone could potentially encode the 150 kDa amiloride binding subunit of the Na^+ channel. However, the amiloride binding potential of this protein has not yet been reported. It should be realized that although the protein is expressed in stage VI Xenopus oocytes there is no evidence for an amiloride-sensitive Na^+ current in this system.

Progress in our laboratory has been made with cloning one of the subunits of the bovine papilla sodium channel. Polyclonal antibodies directed against the complex were used to screen a bovine kidney expression cDNA library. A positive clone containing a 6.5 kb insert was purified. On northern blots of bovine papilla mRNA, the clone reacted with two messages of 7 kb and >9.5 kb, respectively. Western blotting of proteins prepared from bovine kidney membranes using an antibody preabsorbed against the expressed clone revealed a 55 kDa protein. The sequencing of this clone is in progress (Cunningham et al. 1990).

Quite recently two nonselective cation channels have been cloned: one from the bovine rod photoreceptor (Kaupp et al. 1989) and the other from bovine and rat olfactory epithelium (Ludwig et al. 1990; Dhallan et al. 1990). These channels, which are regulated physiologically by cGMP and cAMP, respectively, share extensive homology. Both proteins are similar in molecular mass (79.6 kDa for the rod and 76 kDa for the olfactory), have six putative transmembrane regions and a highly conserved cyclic nucleotide-binding domain. Expression of the rod channel in *Xenopus* oocytes resulted in a cGMP-activated single-channel conductance of 20 pS that did not discriminate between Na^+ and K^+ (Kaupp et al. 1989). Similarly, electrophysiological studies of the olfactory channel in human embryonic kidney cells revealed a K^+-to-Na^+ permeability ratio of 0.82. In addition, this channel could be activated equally well by cAMP, cGMP, and cCMP (Dhallan et al. 1990). Southern genomic blots carried out by these latter authors demonstrated that the rod and olfactory channel are derived from separate genes.

cGMP-regulated cation channels have been described in A6 cells (Ohara et al. 1991) and in the IMCD of the rat kidney (Light et al. 1989). However, while cGMP activates the 1 pS A6 cell channel, it inhibits the 20 to 30 pS conductance in the latter cells. In addition, amiloride is capable of inhibiting the nonselective cation channel of the rat IMCD, while $G_{\alpha i\text{-}3}$ activates the conductance (Light et al. 1989).

Thus, at the physiological level, there appear to be many similarities between the different cyclic-nucleotide gated nonselective cation channels and the amiloride-sensitive Na^+ channel. If the rod and olfactory channels share some sequence homology with the epithelial channels, oligonucleotide probes derived from the cDNA sequence of these channels would be very useful for screening epithelial cDNA libraries.

6 Amiloride-Sensitive Na^+ Channels and Cystic Fibrosis

Cystic fibrosis (CF), the most common hereditary disease among Caucasians (Stern et al. 1976), involves multiple organ systems and is characterized by abnormalities in epithelial water and ion transport (Wood et al. 1976; Dearborn 1976; Knowles et al. 1986) that reduce the water content of epithelial secretions (Chernick and Barbero 1959; Potter et al. 1967). Although the most common cause of death in CF is from viscous airway secretions and recurrent pulmonary infections which lead to decreases in gas exchange (Wood et al. 1976; Kohler et al. 1986), the pathology of CF is also manifested by increased Cl^- content in sweat (>80 mEq/l), malabsorption of foodstuffs secondary to pancreatic enzyme insufficiency, and intestinal obstruction due to thickened meconium (Wood et al. 1976; Orlando et al. 1989; Newhouse et al. 1976; Wanner 1976). The chronic airway and bowel obstruction observed in CF is due, at least in part, to abnormalities in epithelial electrolyte transport, principally ascribed to a defect in Cl^- ion transport (Frizzell 1987; Knowles et al. 1983b; Quinton 1986). However, a growing body of in vitro and in vivo data suggests that epithelial Na^+ transport is also abnormal (Knowles et al. 1981, 1986; Gowen et al. 1986; Boucher et al. 1985, 1986). Much of the evidence for abnormalities in the Na^+ transport in CF comes from cellular or tissue responses to the diuretic amiloride.

It was first hypothesized that an abnormality in Na^+ transport played a role in the pathology of CF in 1981, when in vivo measurements across intact nasal, tracheal, and bronchial respiratory epithelia demonstrated greater transepithelial electrical potential differences (PD) in CF patients than in non-CF or diseased controls (Knowles et al. 1981). This hypothesis was supported by greater reductions in CF nasal and airway epithelial PD as compared to controls following treatment with amiloride (Knowles et al. 1981). As in adults and children, the transepithelial PD in the respiratory epithelia of neonates with CF (32–42 weeks gestation) was twice that of controls (Fig. 10), while exposure to amiloride caused significantly greater PD decreases in CF epithelia than in epithelia from normals or diseased controls (Gowen et al. 1986). These data were recorded prior to infection (Knowles et al. 1981; Gowen et al. 1986) and the results suggested that Na^+ transport abnormalities in CF are inherent to the epithelia rather than the result of chronic infections or lung disease. In addition, neither differences in aldosterone levels (Knowles et al. 1981), nasal polyp morphology (Oppenheimer and

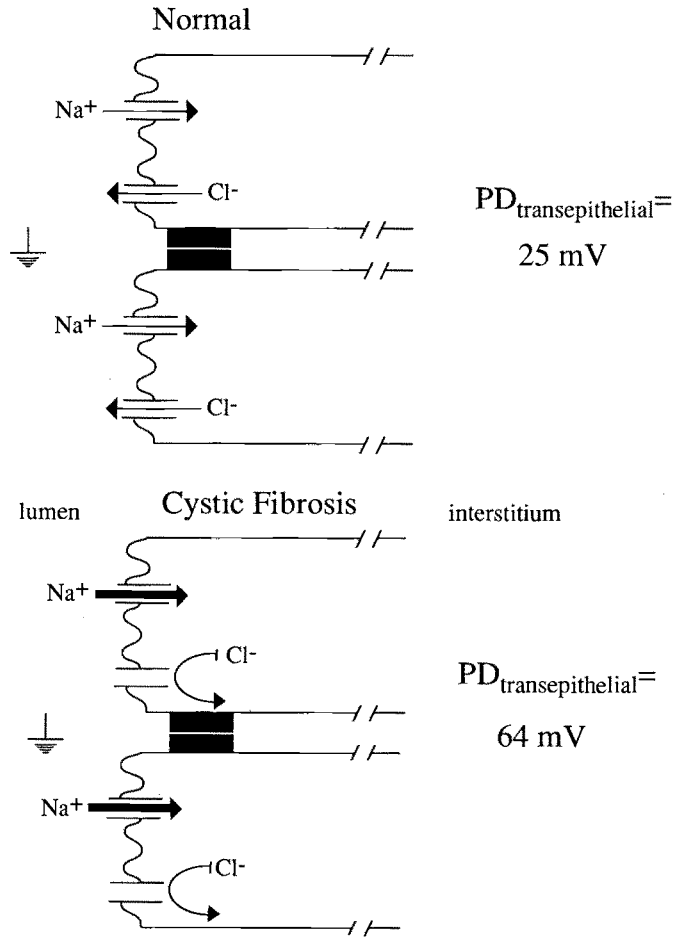

Fig. 10. Schematic model for Na^+ transport across the apical membrane of nasal epithelia from normal and CF patients. Compared to normal nasal epithelia, apical Na^+ transport in tissue from patients with CF shows relative impermeability to Cl^- flux, while Na^+ flux is increased. These epithelial transport abnormalities in CF tissue result in a twofold increase in the electrical potential difference across the epithelium ($P_{D\ transepithelial}$); 70% of $P_{D\ transepithelial}$ was sensitive to amiloride while $P_{D\ transepithelial}$ in normal tissues decreased only 30% in response to amiloride treatment. (Data from Knowles et al. 1981, 1983a; Gowen et al. 1986)

Rosenstein 1979), nor age-related changes in cell density (Stutts et al. 1986) could account for differences in the electrical properties of the nasal epithelial tissue. In vitro studies have further characterized electrolyte transport abnormalities across CF respiratory epithelia. These tissues demonstrated excess Na^+ absorption and relatively low

Cl^- permeability (Boucher et al. 1986; Widcombe et al. 1985; Knowles et al. 1983a,b).

Net Na^+ absorption accounts for 90% of the measured short-circuit current in epithelium excised from nasal polyps and mounted in Ussing chambers (Boucher et al. 1986). In CF tissues, net Na^+ absorption occurred at a greater rate, principally due to increased unidirectional Na^+ flux from the mucosa to serosa (Boucher et al. 1986). While there was no difference in basal net Cl^- flux between normal and CF respiratory epithelia, unidirectional Cl^- fluxes in CF tissue were significantly less than those measured in normal and diseased controls (Boucher et al. 1986). Differences in ion flux in these tissues were not linked to defects in β-adrenergic receptor function of cAMP levels as previously proposed (Davis et al. 1980; Galant et al. 1981) because CF tissues responded to isoproterenol treatment. In control tissues isoproterenol increased unidirectional Cl^- flux (serosa to mucosa) and net Cl^- secretion without altering Na^+ movement across the tissue. In contrast, isoproterenol treatment of CF tissues resulted in increased Na^+ absorption with no change in Cl^- flux (Boucher et al. 1986). The amiloride response of CF tissues also differed from that of control tissues. In contrast to epithelia excised from normals, the entire short-circuit current in CF nasal epithelia was sensitive to amiloride. Furthermore, pretreatment of CF epithelia with amiloride prevented any increase in short-circuit current (Boucher et al. 1986). The increase in cAMP levels in CF tissues following exposure to either isoproterenol or forskolin was similar to that measured in non-CF tissue (Boucher et al. 1986).

Further evidence that the CF defect includes increased Na^+ transport was demonstrated by increases in O_2 consumption and Na^+ pump sites. Excised nasal epithelia from CF patients consumed O_2 at two to three times the rate of normal tissue and had 60% more ouabain binding sites (Stutts et al. 1986). In addition, the absolute inhibition of O_2 consumption in CF tissue by amiloride was three to four times that of non-CF tissue (Stutts et al. 1986). As in other studies, these effects could not be accounted for by increases in endogenous aldosterone or chronic inflammation (Stutts et al. 1986; Knowles et al. 1981; Gowen et al. 1986).

Although much has been learned about the transport properties of CF epithelia, the basic defect, or defects, remain(s) unknown and, thus, treatment is symptomatic (Wood et al. 1976). Because the excessive Na^+ flux associated with CF epithelia is decreased by amiloride treatment, intrapulmonary amiloride has been used in both animal and human studies to investigate its ability to ameliorate the

symptoms associated with CF (Mentz et al. 1986; Kohler et al. 1986; Knowles et al. 1990; App et al. 1990; Boucher et al. 1987). Direct application of amiloride on the trachea of sheep increased the water content of airway mucus (Mentz et al. 1986). To date there have been only limited clinical trials testing the effectiveness of amiloride in treating CF patients (Kohler et al. 1986; Knowles et al. 1990; App et al. 1990). Thus far, the results from these limited clinical trials with amiloride have been encouraging, with respect to increasing both mucociliary and cough clearance of airway secretions (Kohler et al. 1986; Knowles et al. 1990; App et al. 1990), and maintaining adequate lung function (Knowles et al. 1990). Clinical improvements were observed with no signs of pulmonary or systemic toxicity (Kohler et al. 1986; Knowles et al. 1990; App et al. 1990), confirming findings in animal models (Mentz et al. 1986; Boucher et al. 1987).

The mechanism by which amiloride improves lung function is unknown. It could work by decreasing the viscous nature of the airway secretions, improving ciliary function, or both (Wood et al. 1976; Newhouse et al. 1976; Chernick and Barbero 1959; App et al. 1990). Water content in CF sputum is less than in normal sputum (Lutz et al. 1973; Reasor et al. 1978; Matthews et al. 1963). Following amiloride inhalation, sputum from CF patients was less viscous (Knowles et al. 1990; App et al. 1990) and the Na^+ content was higher than in sputum following inhalation of a placebo (App et al. 1990). Although sputum Na^+ content was still significantly less in CF patients treated with amiloride than in the secretions of non-CF disease control patients (122/vs 160 mmol/l; App et al. 1990), there was a trend toward normalizing Na^+ content. It is unlikely that amiloride improves mucociliary transport by increasing ciliary beat frequency because its effect is weak and transient (di Benedetto et al. 1990).

Regardless of the mode of action, therapeutic levels of amiloride were deposited in the airways by aerosolization and inhalation of the drug (Knowles et al. 1990; App et al. 1990). Maximal improvement in mucociliary clearance occurred 30 min after amiloride inhalation and lasted for 60–80 min (Kohler et al. 1986; App et al. 1990). Chronic administration of amiloride (four times daily for 25 weeks) improved cough clearance to a greater extent than mucociliary clearance (Knowles et al. 1990; App et al. 1990). Although lung function did not improve following chronic inhalation of amiloride, the forced vital capacity decreased at a significantly slower rate than during a similar period in which vehicle alone was breathed (Knowles et al. 1990). Airway obstruction was not lessened, however, as

indicated by similar FEV_1 values during inhalation of either amiloride or vehicle alone (Knowles et al. 1990). Although amiloride inhalation appears to have some acute and chronic benefits in CF patients, these trials have been conducted in only a few patients over relatively short periods of time. The pulmonary disease process in CF takes place over many years, and amiloride trials of similar duration in a larger group of patients is required to confirm its therapeutic effect and lack of toxicity.

The most recent advances in the study of CF have been in the molecular biological aspects of the disease. The defect in CF has been associated with a single gene defect, located on the long arm of chromosome 7 (Knowlton et al. 1985; Wainwright et al. 1985; White et al. 1985; Rommens et al. 1989; Riorden et al. 1989). The recent mapping of a human cDNA encoding for a human amiloride binding protein (hABP) on chromosome 7 in a region adjacent to the area implicated in CF (Barbry et al. 1990c) may indicate that abnormalities in Cl^- and Na^+ transport are linked. Although the gene for hABP was not directly modified by mutations causing CF, The possible link between hABP and CF is an area which demands further investigation. Electrophysiological data from patients who did not express the CF defect, yet were heterozygotes for the disease, make this area of study even more important. When the nasal epithelium of patients heterozygous for CF were studied, the transepithelial PD and amiloride responses were not intermediate between those of healthy subjects and those of homozygotes (Knowles et al. 1981). Thus, the Na^+ defect appeared to be linked with the clinical expression of CF (Knowles et al. 1981).

In conclusion, changes in luminal secretions in CF are compatible with both decreased Cl^- secretion and increased Na^+ reabsorption and, hence, water absorption (Knowles et al. 1981). However, there are many issues in regard to abnormal electrolyte transport that are yet to be resolved. Aerosolized amiloride may have therapeutic implications if excessive epithelial Na^+ absorption is important in the pathogenesis of pulmonary disease in CF (Knowles et al. 1981). However, clinical abnormalities in lung function characteristic of CF are often not evident for years, and, thus, evaluation of amiloride's effectiveness may take an equally long time (Knowles et al. 1981). In addition, the lungs of infants with CF develop normally in utero (Wood et al. 1976). Because there appears to be a normal driving force for prenatal liquid secretion into the lumen of CF fetal airways (Gowen et al. 1986), abnormal transition or regulation of perinatal ion transport processes is suggested (Boucher et al. 1981). Finally,

increased airway Na^+ influx can contribute to transepithelial PD, but it is not known whether the number of channels is increased or if the characteristics of the Na^+ channel are altered (Cuthbert et al. 1990). These issues may be addressed as the family of channels identified by their amiloride-inhibitable Na^+ transport are isolated and characterized.

7 Coda

Amiloride-sensitive ion channels exist in most of the Na^+ reabsorbing epithelia of vertebrates. Historically, these channels have been studied in frog skin, toad urinary bladder, and renal distal and collecting tubules. Thus, their prime physiological function involves the regulation of extracellular Na^+ homeostasis. Recent applications of the patch electrode technique and the development of immunological probes of epithelial Na^+ channels have revealed that these channels may subserve other functions, for example, lung fluid clearance and sensory transduction. These techniques have also opened up new possibilities for understanding amiloride-inhibitable channels at the molecular biological level.

Thus, a new era of research is commencing with the promise of elucidating regulatory pathways of transport, structural correlates of conduction, and genetic control of expression. The knowledge derived from these studies will undoubtedly be useful in the design and use of specific drugs for therapy.

Acknowledgements. The authors gratefully thank LaCon Crocker and Cathy Guy for their patience and painstaking care in the preparation of this manuscript. This work was supported by funds from the National Institutes of Health (DK37206), the U. S. Department of the Navy, the Cystic Fibrosis Foundation, and the American Lung Association.

References

Abramcheck FJ, Van Driessche W, Helman SI (1985) Autoregulation of apical membrane Na^+ permeability of tight epithelia. J Gen Physiol 85:555–582

Agnew WS, Levinson SR, Brabson JS, Raftery MA (1978) Purification of the tetrodotoxin-binding component associated with the voltage-sensitive sodium channel from *Electrophorus electricus* electroplax membranes. Proc Natl Acad Sci USA 75:2606–2610

App EM, King M, Helfesrieder R, Kohler D, Matthys H (1990) Acute and long-term amiloride inhalation in cystic fibrosis lung disease: a rational approach to cystic fibrosis therapy (Abstr). Am Rev Respir Dis 141:605–612

Asher C, Cragoe EJ Jr, Garty H (1987) Effects of amiloride analogs on Na^+ transport in toad bladder membrane vesicles: evidence for two electrogenic transporters with different affinities towards pyrazinecarboxamides. J Biol Chem 262:8566–8573

Ausiello DA, Stow JL, Cantiello HF, Benos DJ (1992) Purified epithelial Na^+ channel complex contains the pertussis toxin-sensitive $G_{\alpha i-3}$ protein. J Biol Chem 267:4759–4765

Avenet P, Lindemann B (1988) Amiloride-blockable sodium currents in isolated taste receptor cells. J Membr Biol 105:245–255

Barbry P, Frelin C, Vigne P, Cragoe EJ Jr, Lazdunski M (1986) [^{3}H]phenamil, a radiolabelled diuretic for the analysis of the amiloride-sensitive Na^+ channels in kidney membranes. Biochem Biophys Res Commun 135:25–32

Barbry P, Chassande O, Vigne P, Frelin C, Ellory C, Cragoe EJ Jr, Lazdunski M (1987) Purification and subunit structure of the [^{3}H] phenamil receptor associated with the renal apical Na^+ channel. Proc Natl Acad Sci USA 84:4836–4840

Barbry P, Chassande O, Duval C, Rousseau B, Frelin C, Lazdunski M (1989) Biochemical identification of two types of phenamil binding sites associated with amiloride-sensitive Na^+ channels. Biochemistry 28:3744–3749

Barbry P, Champe M, Chassande O, Munemitsu S, Champigny G, Lingueglia E, Maes P, Frelin C, Tartar A, Ullrich A, Lazdunski M (1990a) Human kidney amiloride-binding protein: cDNA structure and functional expression. Proc Natl Acad Sci USA 87:7347–7351

Barbry P, Chassande O, Marsault R, Lazdunski M, Frelin C (1990b) [^{3}H] phenamil binding protein of the renal epithelium sodium channel. Purification, affinity labeling and functional reconstitution. Biochemistry 29:1039–1045

Barbry P, Simon-Bouy B, Mattei M-G, Le Guern E, Jaume-Roig B, Chassande O, Ullrich A, Lazdunski M (1990c) Localization of the gene for amiloride binding protein on chromosome 7 and RFLP analysis in cystic fibrosis families. Hum Genet 85:587–589

Baxendale LM, Helman SI (1986) Sodium concentration dependence of apical membrane single channel Na^+ current and density of nondepolarized frog skin (three state model). Biophys J 49:106a

Benos DJ (1982) Amiloride: a molecular probe of sodium transport in tissues and cells. Am J Physiol 242:C131–C145

Benos DJ (1983) Ionic channels in epithelia. Commun Mol Cell Biophys 2:111–128

Benos DJ (1988) Amiloride: chemistry, kinetics, and structure-activity relationships, In: Grinstein S (ed) Na^+/H^+ exchange. CRC Uniscience, Boca Raton, pp 121–136

Benos DJ (1989) The biology of amiloride-sensitive sodium channels. Hosp Pract [off] 24:149–164

Benos DJ (1991) Purification of an epithelial sodium channel: vasopressin-dependent subunit phosphorylation, Jard S, Jamison R (eds) Vasopressin. Libbey Eurotext, Paris, pp 125–134 (Colloque INSERM, vol 208)

Benos DJ, Mandel LJ (1978) Irreversible inhibition of sodium entry sites in frog skin by a photosensitive amiloride analog. Science 199:1205–1206

Benos DJ, Simon SA, Mandel LJ, Cala PM (1976) Effect of amiloride and some of its analogues on cation transport in isolated frog skin and thin lipid membranes. J Gen Physiol 68:43–63

Benos DJ, Mandel LJ, Balaban RS (1979) On the mechanism of the amiloride-sodium entry site interaction in anuran skin epithelia. J Gen Physiol 73:307–326

Benos DJ, Mandel LJ, Simon SA (1980) Cationic selectivity and competition at the sodium entry site in frog skin. J Gen Physiol 76:233–247

Benos D, Latorre R, Reyes J (1981) Surface potentials and sodium entry in frog skin epithelium. J Physiol (Lond) 321:163–174

Benos DJ, Hyde BA, Latorre R (1983a) Sodium flux ratio through the amiloride-sensitive entry pathway in frog skin. J Gen Physiol 81:667–685

Benos DJ, Reyes J, Shoemaker DG (1983b) Amiloride fluxes across erythrocyte membranes. Biochim Biophys Acta 734:99–104

Benos DJ, Saccomani G, Brenner BM, Sariban-Sohraby S (1986) Purification and characterization of the amiloride-sensitive sodium channel from A6 cultured cells and bovine renal papilla. Proc Natl Acad Sci USA 83:8525–8529

Benos DJ, Saccomani G, Sariban-Sohraby S (1987) The epithelial sodium channel: subunit number and location of amiloride binding site. J Biol Chem 262:10613–10618

Benos DJ, Warnock DG, Smith JB (1991) Amiloride-sensitive transport mechanism. In: Giebisch G, Ussing HH, Kristensen P, Schafer JA (eds) Membrane transport in biology, vol 5. Academic, New York (in press)

Besterman JM, May WS Jr, Le Vine H III, Cragoe EJ Jr, Cuatrecasas P (1985) Amiloride inhibits phorbol ester-stimulated Na^+/H^+ exchange and protein kinase C. J Biol Chem 260:1155–1159

Biber TUL (1971) Effect of changes in transepithelial transport on the uptake of sodium across the outer surface of the frog skin. J Gen Physiol 58:131–144

Biber TUL, Curran PF (1970) Direct measurement of uptake of sodium at the outer surface of the frog skin. J Gen Physiol 56:83–99

Biber TUL, Chez RA, Curran PF (1966) Na transport across frog skin at low external Na concentration. J Gen Physiol 49:1161–1176

Blazer-Yost B, Cox M, Furlanetto R (1989) Insulin and IGF1 receptor mediated sodium transport in toad urinary bladders. Am J Physiol 257:C612–C620

Bodoia RD, Detwiler PB (1985) Patch-clamp recordings of the light-sensitive dark noise in retinal rods from the lizard and frog. J Physiol (Lond) 367:183–216

Boekhoff I, Tareilus E, Strotmann J, Breer H (1990) Rapid activation of alternative second messenger pathways in olfactory cilia from rats by different odorants. EMBO J 9:2453–2458

Boucher RC, Stutts MJ, Gatzy JT (1981) Regional differences in canine airway epithelial ion transport. J Appl Physiol 54:706–714

Boucher RC, Stutts MJ, Knowles MR, Cantley L, Gatzy JT (1985) Na^+ transport in cystic fibrosis nasal epithelia: abnormal basal rate and response to adenylate cyclase activation (Abstr). Clin Res 33:467

Boucher RC, Stutts MJ, Knowles MR, Cantley L, Gatzy JT (1986) Na^+ transport in cystic fibrosis (CF) respiratory epithelia. J Clin Invest 78:1245–1252

Boucher RC, James MK, Friedman M, Fulton J, Pimmel R, Gatzy JT (1987) Acute cardiovascular and pulmonary effects of intravenous and aerosolized amiloride in the dog (abstract). Toxicol Appl Pharmacol 87:264–275

Brand JG, Teeter JH, Silver WL (1985) Inhibition by chorda tympani responses evoked by monovalent salts. Brain Res 334:207–214

Bridges RJ, Garty H, Benos DJ, Rummel W (1988) Sodium uptake into colonic enterocyte membrane vesicles. Am J Physiol 254:C484–C490

Brown A, Birnbaumer L (1988) Signal transduction by G proteins. Am J Physiol 254:H401–H410

Brown D, Sorscher EJ, Ausiello D, Benos D (1989) Immunocytochemical localization of sodium channels in rat kidney medulla. Am J Physiol 256:F366–F369

Cala PM, Cogswell N, Mandel LJ (1978) Binding of [^{3}H]ouabain to split frog skin: the role of the Na, K-ATPase in the generation of the short circuit current. J Gen Physiol 71:347–367

Cantiello HF, Ausiello DA (1986) Atrial natriuretic factor and cGMP inhibit amiloride sensitive Na^+ transport in the cultured renal epithelial cell line, LLC-PK1. Biochem Biophys Res Commun 134:852–860

Cantiello HF, Patenaude CR, Ausiello DA (1989) G protein subunit, α_{i-3}, activates a pertussis toxin-sensitive Na^+ channel from the epithelial cell line, A6. J Biol Chem 264:20867–20870

Cantiello HF, Patenaude CR, Codina J, Birnbaumer L, Ausiello DA (1990) $G\alpha_{i-3}$ regulates epithelial Na^+ channels by activation of phospholipase A_2 and lipoxygenase pathways. J Biol Chem 265:21624–21628

Cantiello HF, Stow JL, Ausiello DA (1991) Cortical actin filaments co-localize with and regulate apical epithelial Na^+ channels in A6 cells (Abstr). FASEB J 5:A690

Carafoli E (1987) Intracellular calcium homeostasis. Annu Rev Biochem 56:395–433

Catterall WA (1986) Molecular properties of voltage-sensitive sodium channels. Annu Rev Biochem 55:953–985

Catterall WA (1988) Structure and function of voltage-sensitive ion channels. Science 245:50–61

Cereijido M, Curran PF (1965) Intracellular electrical potentials in frog skin. J Gen Physiol 48:543–557

Cereijido M, Herrera FC, Flanigan WJ, Curran PF (1964) The influence of Na concentration on the Na transport across frog skin. J Gen Physiol 47:879–893

Chase HS Jr (1984) Does calcium couple the apical and basolateral membrane permeabilities in epithelia? Am J Physiol 247:F869–F876

Chase HS Jr, Al-Awqati Q (1981) Regulation of sodium permeability of the luminal border of the toad bladder by intracellular sodium and calcium. Role of sodium-calcium exchange in the basolateral membrane. J Gen Physiol 77:693–712

Chase HS Jr, Al-Awqati Q (1983) Calcium reduces the sodium permeability of luminal membrane vesicles from toad bladder. Studies using a fast-reaction apparatus. J Gen Physiol 81:643–665

Chernick WS, Barbero GJ (1959) Composition of tracheobronchial secretions in cystic fibrosis of the pancreas and bronchiectasis. Pediatrics 24:739–745

Christensen O, Bindslev N (1982) Fluctuation analysis of short-circuited current in a warm-blooded sodium-retaining epithelium: site current, density and interaction with triamterene. J Membr Biol 65:19–30

Citron L, Exley D, Hallpike CS (1956) Formation, circulation and chemical properties of the labyrinthine fluids. Br Med Bull 12:101–104

Civan MM, Peterson-Yantorno K, O'Brien TG (1988) Insulin and phorbol ester stimulate conductive Na^+ transport through a common pathway. Proc Natl Acad Sci USA 85:963–967

Cook JS, Shaffer C, Cragoe EJ Jr (1987) Inhibition by amiloride analogues of Na^+–dependent hexose uptake in LLC-PK1/C14 cells. Am J Physiol 53:C199–C204

Corey DP, Hudspeth AJ (1979) Ionic basis of the receptor potential in a vertebrate hair cell. Nature 281:675–677

Cox M (1991) Relationship of the aldosterone-induced protein GP 70 to the renal epithelial conductive Na^+ channel. In: Bonvalet JP, Farman N, Refestin-Oblin ME (eds) Aldosterone: functional aspects. Libbey Eurotext, Paris, pp 249–257 (Collogue INSERM, vol 215)

Cragoe EJ Jr, Woltersdorf OW Jr, Bicking JB, Kwong SF, Jones JH (1967) Pryazine diuretics. II. N-amidino-3-amino-5-substituted-6-halo-pyrazinecarboxamides. J Med Chem 10:66–75

Cunningham SA, Clements ML, Arrate MP, Frizzell RA, Benos DJ (1990) Cloning and expression of the 55 kDa subunit of the epithelial amiloride-sensitive sodium channel (Abstr). J Cell Biol 111:63a

Cuthbert AW (1976) Importance of guanidinium groups for blocking sodium channels in epithelia. Mol Pharmacol 12:945–957
Cuthbert AW, Brayden DJ, Dunne A, Smyth RL, Wallwork J (1990) Altered sensitivity to amiloride in cystic fibrosis. Observations using cultured sweat glands. Br J Clin Pharmacol 29:227–234
Das S, Garepapaghi M, Palmer LG (1991) Stimulation by cGMP of apical Na channels in toad urinary bladder. Am J Physiol 260:C234–C241
Davis PB, Shelhammer JR, Kaliner M (1980) Abnormal adrenergic and cholinergic sensitivity in cystic fibrosis. N Engl J Med 302:1453–1456
Davis RJ, Czech MP (1985) Amiloride directly inhibits growth factor receptor tyrosine kinase activity. J Biol Chem 260:2543–2551
Dearborn DB (1976) Water and electrolytes of exocrine secretions. In: Mangos JA, Talamo RC (eds) Cystic fibrosis: projections into the future. Symposia Specialists, New York, pp 179–191
Delong J, Civan MM (1984) Apical sodium entry in split frog skin, current-voltage relationship. J Membr Biol 82:25–40
DeSimone JA, Ferrell F (1985) Analysis of amiloride inhibition of chorda tympani taste response of rat to NaCl. Am J Physiol 249:R52–R61
DeSimone JA, Heck GL, Mierson S, DeSimone SK (1984) The active ion transport properties of canine lingual epithelia in vitro. Implications for gustatory transduction. J Gen Physiol 83:633–656
Dhallan RS, Yau K-W, Schrader KA, Reed RR (1990) Primary structure and functional expression of a cyclic nucleotide-activated channel from olfactory neurons. Nature 347:184–187
Di Benedetto G, Lopez-Vidriero MT, Carratu L, Clarke SW (1990) Effect of amiloride on human bronchial ciliary activity in vitro. Respiration 57:37–39
Drenckhahn D, Schluter K, Allen DP, Bennett V (1985) Colocalization of band 3 with ankyrin and spectrin at the basal membrane of intercalated cells in the rat kidney. Science 230:1287–1289
Dubinsky WP Jr, Frizzell RA (1983) A novel effect of amiloride on H^+-dependent Na^+ transport. Am J Physiol 245:C157–C159
Eaton DC, Hamilton KL (1988) The amiloride-blockable sodium channel of epithelial tissue. In: Narahashi T (ed) Ionic channels, vol 1. Plenum, New York, pp 251–282
Edwardson JM, Fanestil DD, Ellory JC, Cuthbert AW (1981) Extraction of a [^{3}H]benzamil binding component from kidney cell membranes. Biochem Pharmacol 30:1185–1189
Fanestil DD, Porter GA, Edelman IS (1967) Aldosterone stimulation of sodium transport. Biochim Biophys Acta 135:74–88
Farquhar MG, Palade GE (1966) Adenosine triphosphatase localization in amphibian epidermis. J Cell Biol 30:359–379
Fidelman FL, Watlington CO (1984) Insulin and aldosterone interaction on Na^+ and K^+ transport in cultured kidney cells (A6). Endocrinology 115:1171–1178
Frings S, Lindemann B (1988) Odorant response of isolated olfactory receptor cells is blocked by amiloride. J Membr Biol 105:233–243
Frings S, Purves RD, MacKnight ADC (1988) Single channel recordings from the apical membrane of the toad urinary bladder epithelial cell. J Membr Biol 106:157–172
Frizzell RA (1987) Cystic fibrosis: a disease of ion channels? Trends Neurosci 10:190–193
Fuchs W, Hviid Larsen E, Lindemann B (1977) Current-voltage curve of sodium channels and concentration dependence of sodium permeability in frog skin. J Physiol (Lond) 267:137–166
Galant SP, Norton L, Herbst J, Wood C (1981) Impaired beta adrenergic receptor binding and function in cystic fibrosis neutrophils. J Clin Invest 68:253–258

Garty H (1986) Mechanisms of aldosterone action in tight epithelia. J Membr Biol 90:193–205

Garty H, Asher C (1985) Ca^{2+}-dependent, temperature-sensitive regulation of Na^+ channels in tight epithelia. A study using membrane vesicles. J Biol Chem 260:8330–8335

Garty H, Asher C (1986) Calcium induced down regulation of Na channels in toad bladder epithelium. J Biol Chem 261:7400–7406

Garty H, Asher C (1991) Does aldosterone induce de novo synthesis of Na^+ channels? In: Bonvalet JP, Farman N, Lambda M, Rafectin-Oblin ME (eds) Aldosterone: fundamental aspects. Libbey Eurotext, Paris, pp 273–283 (Colloque INSERM, vol 215)

Garty H, Benos DJ (1988) Characteristics and regulatory mechanisms of the amiloride-blockable Na^+ channel. Physiol Rev 68:309–373

Garty H, Edelman S (1983) Amiloride-sensitive trypsinization of apical sodium channels. Analysis of hormonal regulation of sodium transport in toad bladder. J Gen Physiol 81:785–803

Garty H, Lindemann B (1984) Feedback inhibition of sodium uptake in K^+-depolarized toad urinary bladders. Biochim Biophys Acta 771:89–98

Garty H, Asher C, Yeger O (1987) Direct inhibition of epithelial Na^+ channels by a pH-dependent interaction with calcium, and by other divalent ions. J Membr Biol 95:151–162

Garty H, Yeger O, Yanovsky A, Asher C (1989) Guanosine nucleotide dependent activation of the amiloride blockable Na^+ channel. Am J Physiol 256:C965–C969

Gasc J-M, Lombes M, Oblin M-E, Bonvalet J-P, Farman N (1991) Localization of renal mineralocorticoid and glycocorticoid receptors: an immunohistochemical study. In: Bonvalet JP, Farman N, Lambda M, Rafectin-Obelin ME (eds) Aldosterone: fundamental aspects. Libbey Eurotext, Paris, pp 45–53 (Colloque INSERM, vol 215)

George AL Jr, Staub O, Geering K, Rossier BC, Kleyman TR, Kraehenbuhl J-P (1989) Functional expression of the amiloride-sensitive sodium channel in *Xenopus* oocytes. Proc Natl Acad Sci USA 86:7295–7298

Gogelein H, Greger R (1986) Na^+ selective channels in the apical membrane of rabbit late proximal tubules (pars recta). Pflugers Arch 406:198–203

Gowen CW, Lawson EE, Gingras-Leatherman J, Gatzy JT, Boucher RC, Knowles MR (1986) Increased nasal potential difference and amiloride sensitivity in neonates with cystic fibrosis. J Pediatr 108:517–521

Gray P, Attwell D (1985) Kinetics of light-sensitive channels in vertebrate photoreceptors. Proc R Soc Lond [Biol] 223:379–388

Grinstein S, Erlij D (1978) Intracellular calcium and the regulation of sodium transport in the frog skin. Proc R Soc Lond [Biol] 202:353–360

Hackney CM, Furness DN, Benos DJ (1992) Localization of putative mechanoelectrical transducer channels in cochlear hair cells by immunoelectron microscopy. Scanning Microsc (in press)

Hamilton KL, Eaton DC (1985) Single-channel recordings from amiloride-sensitive epithelial sodium channel. Am J Physiol 249:C200–C207

Hamilton KL, Eaton DC (1986) Single channel recordings from two types of amiloride-sensitive epithelial Na channels. Membr Biochem 6:149–171

Handler JS, Preston AS, Orloff J (1969) Effect of adrenal steroid hormones on the response of the toad's urinary bladder to vasopressin. J Clin Invest 48:823–833

Harris RC, Lufburrow RA III, Cragoe EJ Jr, Seifter JL (1985) Amiloride analogs inhibit Na-glucose and alanine cotransport in renal brush border membrane vesicles (BBMV) (Abstr). Kidney Int 27:310

Haynes LW, Yau K-W (1985) Cyclic GMP-sensitive conductance in outer segment membrane of catfish cones. Nature 317:61–64

Haynes LW, Kay AR, Yau K-W (1986) Single cyclic GMP-activated channel activity in excised patches of rod outer segment membrane. Nature 321:66–70

Hayes SR, Baum M, Kokko JP (1987) Effects of protein kinase C activation on sodium, potassium chloride, and total CO_2 transport in the rabbit cortical collecting tubule. J Clin Invest 80:1561–1570

Helman SI, Baxendale LM (1990) Blocker-related changes of channel density. Analysis of a three-state model for apical Na channels of frog skin. J Gen Physiol 95:647–678

Helman SI, Fisher RS (1977) Microelectrode studies of the active sodium transport pathway of frog skin. J Gen Physiol 69:571–604

Helman SI, Nagel W, Fisher R (1979) Ouabain on active transepithelial sodium transport in frog skin. Studies with microelectrodes. J Gen Physiol 74:105–127

Helman SI, Cox TC, Van Driessche W (1983) Hormonal control of apical membrane Na transport in epithelia studies with fluctuation analysis. J Gen Physiol 82:201–220

Helman SI, Baxendale LM, Sariban-Sohraby S, Benos DJ (1986) Blocker-induced noise of Na^+ channels in cultured A6 epithelia (Abstr). Fed Proc 45:516

Hille B (1984) Ionic channels in excitable membranes. Sinauer, Sunderland

Hinton CF, Eaton DC (1989) Expression of amiloride-blockable sodium channels in Xenopus oocytes. Am J Physiol 257:C825–C829

Hodgkin AL, Huxley AF (1952) The components of membrane conductance in the giant axon of Loligo. J Physiol (Lond) 116:473–496

Hodgkin AL, McNaughton PA, Nunn BJ (1985) The ionic selectivity and calcium dependence of the light-sensitive pathways in toad rods. J Physiol (Lond) 358:447–468

Hu P, Oh Y, Jilling T, Benos DJ, Matalon S (1991) Immunofluorescent localization of sodium conductance in culture rat alveolar type II pneumocytes (ATII) (Abstr). Am Rev Respir Dis

Hudspeth AJ (1982) Extracellular current flow and the site of transduction by vertebrate hair cells. J Neurosci 2:1–10

Hudspeth AJ, Corey DP (1977) Sensitivity, polarity and conductance change in the response of vertebrate hair cells to controlled mechanical stimuli. Proc Natl Acad Sci USA 74:2407–2411

Jan LY, Jan YN (1990) A superfamily of ion channels. Nature 345:672

Jones DT, Reed RR (1989) G_{olf}: an olfactory neuron-specific G-protein involved in odorant signal transduction. Science 244:790–795

Jorgensen FO (1983) Influence of Ca^{2+} on the mechano-sensitivity of the hair cells in the lateral line organs of Necturus maculosus. Acta Physiol Scand 118:423–431

Jorgensen F, Ohmori H (1988) Amiloride blocks the mechano-electrical transduction channel of hair cells of the chick. J Physiol (Lond) 403:577–588

Joris L, Krouse ME, Hagiwara G, Bell CL, Wine JJ (1989) Patch-clamp study of cultured human sweat duct cells: amiloride-blockable Na^+ channel. Pflugers Arch 414:369–372

Kaczorowski GJ, Barros F, Dethmers JK, Trumble MJ, Cragoe EJ Jr (1985) Inhibition of Na^+/Ca^{2+} exchange in pituitary plasma membrane vesicles by analogues of amiloride. Biochemistry 24:1394–1403

Kaupp UB, Niidome T, Tanabe T, Terada S, Bonigk W, Stuhmer W, Cook NJ, Kangawa K, Matsuo H, Hirose T, Miyata T, Numa S (1989) Primary structure and functional expression from complementary DNA of the rod photoreceptor cyclic GMP-gated channel. Nature 342:762–766

Kemendy AE, Eaton DC (1990) Aldosterone-induced Na^+ transport in A6 epithelia is blocked by 3-deazaadenosine, a methylation blocker (Abstr). FASEB J 4:A445

Keynes RD (1969) From frog skin to sheep rumen: a survey of transport of salts and water across multicellular structures. Q Rev Biophys 2:177–281

Kleyman TR, Cragoe EJ Jr (1988) Amiloride and its analogs as tools in the study of ion transport. J Membr Biol 105:1–21

Kleyman TR, Yulo T, Ashbaugh C, Landry D, Cragoe EJ Jr, Al-Awqati Q (1986) Photoaffinity labeling of the epithelial sodium channel. J Biol Chem 261:2839–2843

Kleyman TR, Cragoe E, Kraehenbuhl JP (1989) The cellular pool of Na^+ channels in the amphibian cell line A6 is not altered by mineralocorticoid. J Biol Chem 264:11995–12000

Kleyman TR, Ernst S, Rossier B, Kraehenbuhl JP (1990) Aldosterone does not alter cell surface expression of the epithelial Na^+ channel in A6 cells (Abstr). Kidney Int 37:564A

Kleyman TR, Kraehenbuhl J-P, Ernst SA (1991) Characterization and cellular localization of the epithelial Na^+ channel. Studies using an anti-Na^+ channel antibody raised by an anti-idiotypic route. J Biol Chem 266:3907–3915

Knowles MR, Gatzy JT, Boucher RC (1981) Increased bioelectric potential difference across respiratory epithelia in cystic fibrosis. N Engl J Med 305(25):1489–1495

Knowles MR, Gatzy J, Boucher RC (1983a) Relative ion permeability of normal and cystic fibrosis nasal epithelium. J Clin Invest 71:1410–1417

Knowles MR, Stutts MJ, Spock A, Fischer N, Gatzy JT, Boucher RC (1983b) Abnormal ion permeation through cystic fibrosis respiratory epithelium. Science 221:1067–1070

Knowles MR, Stutts MJ, Yankaskas JR, Gatzy JT, Boucher RC (1986) Abnormal respiratory epithelial ion transport in cystic fibrosis. Clin Chest Med 7:285–297

Knowles MR, Church NL, Waltner WE, Yankaskas JR, Gilligan P, King M, Edwards LJ, Helms RW, Boucher RC (1990) A pilot study of aerosolized amiloride for the treatment of lung diseases in cystic fibrosis. N Engl J Med 22(17):1189–1194

Knowlton RG, Cohen-Haguenauer O, Van Cong N, Fre'zal J, Brown VA, Barker D, Bramen JC, Schumm JW, Tsui LC, Buchwald M, Donis-Keller H (1985) A polymorphic DNA marker linked to cystic fibrosis is located on chromosome 7. Nature 318:380–382

Koefoed-Johnsen V, Ussing HH (1958) The nature of the frog skin potential. Acta Physiol Scand 42:298–308

Kohler D, App E, Schmitz-Schumann M, Wurtemberger G, Mattys H (1986) Inhalation of amiloride improves the mucociliary and the cough clearance in patients with cystic fibrosis. Eur J Respir Dis 69(146):319–326

Kroll B, Bautsch W, Bremer S, Wilke M, Tummler B, Fromter E (1989) Selective expression of an amiloride-inhibitable Na^+ conductance from mRNA of respiratory epithelium in Xenopus laevis oocytes. Am J Physiol 257:C284–C288

L'Allemain G, Franchi A, Cragoe EJ Jr, Pouyssegur J (1984) Blockade of the Na^+/H^+ antiport abolishes growth factor-induced DNA synthesis in fibroblasts. Structure-activity relationships in the amiloride series. J Biol Chem 259:4313–4319

Lamb TD, Matthews HR, Torre VJ (1985) Rapid and delayed components in the response of salamander retinal rods to reduced external calcium. J Physiol (Lond) 369:34P

Leffert HL, Koch KS, Fehlmann M, Heiser W, Lad PJ, Sdelly H (1982) Amiloride blocks cell-free protein synthesis at levels attained inside cultured rat hepatocytes. Biochem Biophys Res Commun 108:738–745

Lester DS, Asher C, Garty H (1988) Characterization of cAMP-induced activation of epithelial sodium channels. Am J Physiol 254:C802–C808

Levenson R, Housman D, Cantley L (1980) Amiloride inhibits murine erythroleukemia cell differentiation: evidence for a Ca^{2+} requirement for commitment. Proc Natl Acad Sci USA 77:5948–5952

Lewis SA, Alles W (1986) Urinary kallikrein: a physiological regulator of epithelial sodium transport. Proc Natl Acad Sci USA 83:5345–5348

Lewis SA, de Moura J (1982) Incorporation of cytoplasmic vesicles into apical membrane of mammalian urinary bladder epithelium. Nature 297:685–688

Lewis SA, Hanrahan JW (1985) Apical and basolateral membrane ionic channels in rabbit urinary bladder. Pflugers Arch 405:S83–S88

Lewis SA, Eaton DC, Diamond JM (1976) The mechanism of Na^+ transport by the rabbit urinary bladder. J Membr Biol 28:41–70

Lewis SA, Ifshin M, Loo D, Diamond J (1984) Studies of sodium channels in rabbit urinary bladder by noise analysis. J Membr Biol 80:135–151

Li, JH-Y, Lindemann BJ (1982) Movement of Na^+ and Li^+ across the apical membrane of frog skin. In: Emrich HM, Aldenhoff JB, Lux HD (eds) Basic mechanisms in the action of lithium. Excerpta Medica, Amsterdam, pp 23–35

Li JH-Y, Lindemann BJ (1983) Competitive blocking of epithelial sodium channels by organic cations: the relationship between macroscopic and microscopic inhibition constants. J Membr Biol 76:235–251

Li JH-Y, Palmer LG, Edelman IS, Lindemann B (1982) The role of sodium channel density in the natriferic response of the toad urinary bladder to an antidiuretic hormone. J Membr Biol 64:77–89

Li JH-Y, Cragoe EJ, Lindemann BJ (1985) Structure-activity relationship of amiloride analogs as blockers of epithelial Na channels. I. Pyrazine-ring modifications. J Membr Biol 83:45–56

Light DB, McCann FV, Keller TM, Stanton BA (1988) Amiloride-sensitive cation channel in apical membrane of inner medullary collecting duct. Am J Physiol 255:F278–F286

Light DB, Schwiebert EM, Karlson KH, Stanton BA (1989) Atrial natriuretic peptide inhibits a cation channel in renal inner medullary collecting duct cells. Science 243:383–385

Light DB, Ausiello DA, Stanton BA (1989) Guanine nucleotide-binding protein. α_{i-3}, directly activates a cation channel in rat renal inner medullary collecting duct cells. J Clin Invest 84:352–356

Light DB, Corbin JD, Stanton BA (1990) Dual ion-channel regulation by cyclic CMP and cyclic GMP-dependent protein kinase. Nature 344:336–339

Lindemann B (1980) The beginning of fluctuation analysis of epithelial ion transport. J Membr Biol 54:1–11

Lindemann B (1984) Fluctuation analysis of sodium channels in epithelia. Annu Rev Physiol 46:497–515

Lindemann B, Van Driessche W (1977) Sodium-specific membrane channels of frog skin are pores: current fluctuations reveal high turnover. Science 195:292–294

Lindemann B, Voute C (1976) Structure and function of the epidermis. In: Llinas R, Precht W (eds) Frog neurobiology. Springer, Berlin Heidelberg New York, pp 169–210

Ling BN, Eaton DC (1989) Effects of luminal Na^+ on single Na^+ channels in A6 cells, a regulatory role for protein kinase C. Am J Physiol 256:F1094–F1103

Ling BN, Kemendy AE, Kokko KE, Hinton CF, Marunaka Y, Eaton DC (1990) Regulation of the amiloride-blockable sodium channel from epithelial tissue. Mol Cell Biochem 99:141–150

Lubin M, Cahn F, Coutermarsh BA (1982) Amiloride, protein synthesis, and activation of quiescent cells. J Cell Physiol 113:247–251

Ludwig J, Margalit T, Eismann E, Lancet D, Kaupp B (1990) Primary structure of cAMP-gated channel from bovine olfactory epithelium. FEBS Lett 270: 24–29

Lutz RJ, Litt M, Chakrin LW (1973) Physical-chemical factors in mucus rheology. In: Gabelnick HL, Litt M (eds) Rheology of biological systems. Thomas, Springfield, pp 119–157

MacKnight ADC, DiBona DR, Leaf A (1980) Sodium transport across toad urinary bladder: a model "tight" epithelium. Physiol Rev 60:615–715

MacRobbie EAC, Ussing HH (1961) Osmotic behavior of the epithelial cells of frog skin. Acta Physiol Scand 53:348–365

Marunaka Y, Eaton DC (1991) Effects of vasopressin and cAMP on single amiloride-blockable Na channels. Am J Physiol 260:C1071–C1084

Matalon S, Bridges RJ, Benos DJ (1991) Amiloride-inhibitable Na^+ conductive pathways in alveolar type II pneumocytes. Am J Physiol 260:L90–L96

Matthews LW, Spector S, Lemm J, Potter J (1963) Studies on pulmonary secretions. I. The overall composition of pulmonary secretions from patients with cystic fibrosis, bronchiectasis, and laryngectomy. Am Rev Respir Dis 88:199–204

Mentz WM, Brown JB, Friedman M, Stutts MJ, Gatzy JT, Boucher RC (1986) Deposition, clearance, and effects of aerosolized amiloride in sheep airways (Abstr). Am Rev Respir Dis 134:938–943

Mills JW, Ernst SA (1975) Localization of sodium pump sites in frog urinary bladder. Biochim Biophys Acta 375:268–273

Mohrmann M, Cantiello HF, Ausiello DA (1987) Inhibition of epithelial Na^+ transport by atriopeptin, protein kinase C, and pertussin toxin. Am J Physiol 253:F372–F376

Molday L, Cook NJ, Kaupp UB, Molday RS (1990) The cGMP-gated cation channel of bovine rod photoreceptor cells is associated with a 240-kDa protein exhibiting immunochemical cross-reactivity with spectrin. J Biol Chem 265:18690–18695

Moran A, Moran N (1984) Amiloride-sensitive channels in LLC-PK_1 apical membranes (Abstr). Fed Proc 43:44a

Moran A, Asher C, Cragoe EJ Jr, Garty H (1980) Conductive sodium pathway with low affinity to amiloride in LLC-PK1 cells and other epithelia. J Biol Chem 263:19586–19591

Morrow JS, Cianci CD, Ardito T, Mann AS, Kashgarian M (1989) Ankyrin links fodrin to the alpha subunit of Na^+,K^+ATPase in Madin-Darby canine kidney cells and in intact renal tubule cells. J Cell Biol 108:455–465

Mullen TL, Biber TUL (1978) Sodium uptake across the outer surface of the frog skin. In: Hoffman JF (ed) Membrane transport processes. vol 1. Raven, New York, pp 199–212

Nagel W (1976) The intracellular electrical potential profile of the frog skin epithelium. Pflugers Arch 365:135–143

Nagel W, Garcia-Diaz JF, Armstrong WM (1981) Intracellular ionic activities in frog skin. J Membr Biol 61:127–134

Nakamura T, Gold G (1987) A cyclic nucleotide-gated conductance in olfactory receptor cilia. Nature 325:442–444

Nelson WJ, Veshnock PJ (1987) Ankyrin binding to (Na^+ + K^+) ATPase and implications for the organization of membrane domains in polarized cells. Nature 328:533–536

Newhouse MT, Rossman CM, Dolovich J, Dolovich MB, Wilson WM (1976) Impairment of mucociliary transport in cystic fibrosis. Mod Probl Pediatr 19:190–198

Nicol GD, Schnetkamp PPM, Saimi Y, Cragoe EJ Jr, Bownds MD (1987) A derivative of amiloride blocks both the light-regulated and cyclic GMP-regulated conductances in rod photoreceptors. J Gen Physiol 90:651–669

Noda M, Shimizu S, Tanabe T, Takai T, Kayano T, Ikeda T, Takahashi T, Nakayama H, Kanaoka Y, Minamino A, Kangawa K, Matsuo H, Rafferty MA, Hirose T, Inayama S, Hayashida H, Miyata T, Numa S (1984) Primary structure of Electrophorus electricus sodium channel deduced from cDNA sequence. Nature 312:121–127

Oh Y, Benos DJ (1992) Amiloride-sensitive sodium channels. In: Kleyman TR, Cragoe E, Simchowitz L (eds) Amiloride and its analogs: unique transport inhibitors. VCH, New York (in press)
Oh Y, Hu P, Kleyman TR, Saccomani G, Matalon S, Benos DJ (1991) Evidence for the presence of an amiloride binding protein in adult alveolar type II (ATII) pneumocytes (Abstr). FASEB J 5:A690
Ohara A, Matsumoto P, Eaton DC, Marunaka Y (1991) A non-selective cation channel induced by cyclic GMP and nitroprusside in a distal nephron cell line (A6) (Abstr). FASEB J 5(4):A689
Ohmori H (1985) Mechano-electrical transduction currents in isolated vestibular hair cells of the chick. J Physiol (Lond) 359:189–217
Ohmori H (1988) Mechanical stimulation and Fura-2 fluorescence in the hair bundle of dissociated hair cells of the chick. J Physiol 399:115–137
Olans L, Sariban-Sohraby S, Benos D (1984) Saturation behavior of single amiloride sensitive sodium channels in planar lipid bilayers. Biophys J 46:831–835
Omachi RS, Robbie DE, Handler JS, Orloff J (1974) Effects of ADH and other agents on cyclic AMP accumulation in the toad bladder epithelium. Am J Physiol 226:1152–1157
Oppenheimer EHJ, Rosenstein BJ (1979) Differential pathology of nasal polyps in cystic fibrosis and atopy. Lab Invest 40:445–449
Orlando RC, Powell DW, Croom RD, Berschneider HM, Boucher RC, Knowles MR (1989) Colonic and esophageal transepithelial potential difference in cystic fibrosis. Gastroenterology 96:1041–1048
Orloff J, Handler JS (1967) The role of adenosine 3′,5′-phosphate in the action of antidiuretic hormone. Am J Med 42:757–768
Pace U, Hanski E, Salomon Y, Lancet D (1985) Odorant-sensitive adenylatecyclase may mediate olfactory reception. Nature 316:255–258
Palmer LG (1982a) Na^+ transport and flux ratio through apical Na^+ channels in toad bladder. Nature 297:688–690
Palmer LG (1982b) Ion selectivity of the apical membrane Na channels in the toad urinary bladder. J Membr Biol 67:91–98
Palmer LG (1984) Voltage-dependent block by amiloride and other monovalent cations of apical sodium channels in the toad urinary bladder. J Membr Biol 80:153–165
Palmer LG (1985a) Interactions of amiloride and other blocking cations with the apical sodium channel in the toad urinary bladder. J Membr Biol 87:191–199
Palmer LG (1985b) Modulation of apical sodium permeability of the toad urinary bladder by intracellular Na^+, Ca^{2+}, and H^+. J Membr Biol 83:57–69
Palmer LG (1991) The epithelial Na^+ Channel: Inferences about the nature of the conducting pore. Comm Mol Cell Biophys 7:259–283
Palmer LG, Andersen OS (1989) Interactions of amiloride and small monovalent cations with the epithelial sodium channel. Inferences about the nature of the channel pore. Biophys J 55(4):779–787
Palmer LG, Edelman IS (1981) Control of apical sodium permeability in the toad urinary bladder by aldosterone. Ann NY Acad Sci 372:1–14
Palmer LG, Frindt G (1986) Amiloride sensitive Na channels from the apical membrane of the rat cortical collecting tubules. Proc Natl Acad Sci USA 83:2767–2770
Palmer LG, Frindt G (1987a) Effects of cell Ca and pH on Na channels from rat cortical collecting tubule. Am J Physiol 253:F333–F339
Palmer LG, Frindt G (1987b) Ca ionophore and phorbol ester inhibit Na channels in rat cortical collecting tubules (Abstr). Fed Proc 46:495

Palmer LG, Edelman IS, Lindemann B (1980) Current-voltage analysis of apical sodium transport in toad urinary bladder: effects of inhibitors of transport and metabolism. J Membr Biol 57:59–71

Palmer LG, Li JH, Lindemann B, Edelman IS (1982) Aldosterone control of the density of sodium channels in the toad urinary bladder. J Membr Biol 64:91–102

Palmer LG, Corthesy-Theulaz I, Gaeggeler H-P, Kraehenbuhl J-P, Rossier B (1990) Expression of epithelial Na channels in *Xenopus* oocytes. J Gen Physiol 96:23–46

Palvesky P, Blazer-Yost B, Cox M, Szerlip H (1990) Aldosterone induces a subunit of the epithelial Na^+ channel (Abstr). Kidney Int 37:233A

Park CS, Fanestil DD (1980) Covalent modification and inhibition of an epithelial sodium channel by tyrosine-reactive reagent. Am J Physiol 239:F299–F306

Pearce LB, Calhoon RD, Burns PR, Vincent A, Goldin SM (1988) Two functionally distinct forms of guanosine cyclic 3′,5′-phosphate stimulated cation channels in a bovine rod photoreceptor disk preparation. Biochemistry 27:4396–4406

Potter JL, Matthews LW, Spector S, Lemm J (1967) Studies on pulmonary secretions. II. Osmolality and the ionic environment of pulmonary secretions from patients with cystic fibrosis, bronchiectasis, and laryngectomy. Am Rev Respir Dis 96:83–87

Pratt AG, Ausiello DA, Cantiello HF (1991) Actin filament organization controls Na^+ channel activity in A6 epithelial cells (Abstr). FASEB J 5:A690

Quinton PM (1986) Missing Cl conductance in cystic fibrosis. Am J Physiol 221:C649–C652

Reasor MJ, Cohen D, Proctor DF, Rubin RJ (1978) Tracheobronchial secretions collected from intact dogs. II. Effects of cholinomimetic stimulation. J Appl Physiol 45:190–194

Rehm H, Tempel BL (1991) Voltage-gated K^+ channels of the mammalian brain. FASEB J 5:164–170

Rick R, Dorge A, Van Arnim E, Thurau K (1978) Electron microprobe analysis of frog skin epithelium: evidence for a syncytial Na^+ transport compartment. J Membr Biol 39:257–271

Riorden JR, Rommens JM, Kerem B, Alon N, Rozmahel R, Grzelczak Z, Lok S, Plavsic N, Chou JL, Drumm ML, Ianuzzi MC, Collins FS, Tsui LC (1989) Identification of the cystic fibrosis gene: cloning and characterization of complementary DNA. Science 245:1066–1073

Robinson DH, Bubien JK, Smith PR, Benos DJ (1991) Epithelial sodium conductance in rabbit preimplantation trophectodermal cells. Dev Biol 147:313–321

Rommens JM, Ianuzzi MC, Kerem B, Drumm ML, Melmer G, Dean M, Rozmahel R, Cole JL, Kennedy D, Hidaka N, Zsiga M, Buchwald M, Riordan JR, Tsui LC, Collins FS (1989) Identification of the cystic fibrosis gene: chromosome walking and jumping. Science 245:1059–1065

Rossier BC, Verrey F, Kraehenbuhl J-P (1989) Transepithelial sodium transport and its control by aldosterone: a molecular approach. In: Schultz S (ed) Current topics in membranes and transport, vol 34. Academic, San Diego, pp 167–183

Sahib MK, Schwartz JH, Handler JS (1978) Inhibition of toad urinary bladder sodium transport by carbamylcholine: possible role for cGMP. Am J Physiol 250:F586–F591

Sand O (1975) Effects of different ionic environments on the mechanosensitivity of lateralline organs in the mudpuppy. J Comp Physiol 102:27–42

Sariban-Sohraby S, Benos D (1986a) The amiloride-sensitive sodium channel. Am J Physiol 250:C175–C190

Sariban-Sohraby S, Benos DJ (1986b) Detergent solubilization, functional reconstitution, and partial purification of epithelial amiloride-binding protein. Biochemistry 25:4639–4646

Sariban-Sohraby S, Fisher RS (1990) Single channel activity by the amiloride binding subunit of the epithelial Na^+ channel (Abstr). Biophys J 57:87a

Sariban-Sohraby S, Burg M, Wiesmann WP, Chiang PK, Johnson JP (1984a) Methylation increases sodium transport into A6 apical membrane vesicles: possible mode of aldosterone action. Science 225:745–746

Sariban-Sohraby S, Latorre R, Burg M, Olans L, Benos D (1984b) Amiloride-sensitive epithelial Na^+ channels reconstituted in planar lipid bilayer membranes. Nature 308:80–82

Sariban-Sohraby S, Sorscher EJ, Brenner BM, Benos DJ (1988) Phosphorylation of a single subunit of the epithelial Na^+ channel protein following vasopressin treatment of A6 cells. J Biol Chem 263:13875–13879

Schultz SG (1981) Homocellular regulatory mechanisms in sodium transporting epithelia: avoidance of extinction by "flush-through". Am J Physiol 241:F579–F590

Sharp GWG, Leaf A (1966) Mechanism of action of aldosterone. Physiol Rev 46:593–633

Simon SA, Garvin JL (1985) Salt and acid studies on canine lingual epithelium. Am J Physiol 249:C398–C408

Simon SA, Holland VF, Benos DJ, Zampigh GA (1992) Transcellular and paracellular pathways in lingual epithelia and their influence in taste transduction. J Electron Microsc Methods (in press)

Sklar PB, Anholt RRH, Snyder SH (1986) The odorant-sensitive adenylate cyclase of olfactory receptor cells: differential stimulation by distinct classes of odorants. J Biol Chem 261:15538–15543

Smith PR, Benos DJ (1991) Epithelial Na^+ channels. Annu Rev Physiol 53:509–530

Smith PR, Saccomani G, Joe E-H, Angelides KJ, Benos DJ (1991) Amiloride-sensitive sodium channel is linked to the cytoskeleton in renal A6 epithelial cells. Proc Natl Acad Sci USA 88:6971–6975

Smith RL, Cochran DW, Gund P, Cragoe EJ Jr (1979) Proton, carbon-13, and nitrogen-15 nuclear magnetic resonance and CNDO/2 studies on the tautomerism and configuration of amiloride, a novel acylguanidine. J Am Chem Soc 101:191–201

Snart RS, Dalton T (1973) Response of toad bladder to prolactin. Comp Biochem Physiol [A] 45:307–311

Soltoff SP, Mandel LJ (1983) Amiloride directly inhibits the Na,K-ATPase activity of rabbit kidney proximal tubules. Science 220:957–958

Sorscher EJ, Accavitti MA, Keeton D, Steadman E, Frizzell RA, Benos DJ (1988) Antibodies against purified epithelial sodium channel protein from bovine renal papilla. Am J Physiol 24:C835–C843

Srinivasan Y, Elmer L, Davis J, Bennett V, Angelides K (1988) Ankyrin and spectrin associate with voltage-dependent sodium channels in brain. Nature 333:177–180

Staub O, Verrey F, Rossier BC, Kraehenbuhl J-P (1990) Gene expression of a kidney apical protein (AP) in Xenopus laevis oocyte and during early development (Abstr). J Cell Biol 111:310a

Stern RC, Boat TF, Doershuk CF, Tucker AS, Primiano FP, Matthews LW (1976) Course of cystic fibrosis in 95 patients. J Pediatr 89:406–411

Stirling CE (1972) Radioautographic localization of sodium pump sites in rabbit intestine. J Cell Biol 53:704–714

Stutts MJ, Knowles MR, Gatzy JT, Boucher RC (1986) Oxygen consumption and ouabain binding sites in cystic fibrosis nasal epithelium. Pediatr Res 20(12):1316–1320

Szerlip H, Cox M (1989) Aldosterone induced glycoproteins: further characterization. J Steroid Biochem 32:815–822

Szerlip H, Weisberg L, Clayman M, Neilson E, Wade J, Cox M (1989) Aldosterone induced proteins: purification and localization of GP65,70. Am J Physiol 256:C865–C872

Takagi SF, Kitamura H, Imai K, Takeuchi H (1969) Further studies on the roles of sodium and potassium in the generation of the electro-olfactogram. Effects of mono-, di- and trivalent cations. J Gen Physiol 53:115–130

Tang C-M, Preser F, Morad M (1988) Amiloride selectively blocks the low threshold (T) calcium channel. Science 240:213–215

Taylor A, Windhager EE (1979) Possible role of cytosolic calcium and Na-Ca exchange in regulation of transepithelial sodium transport. Am J Physiol 236:F505–F512

Thompson SM, Suzuki Y, Schultz SG (1982) The electrophysiology of rabbit descending colon. I. Instantaneous transepithelial current-voltage relations of the Na-entry mechanism. J Membr Biol 66:41–54

Tousson A, Alley C, Sorscher E, Brinkley B, Benos D (1989) Immunocytochemical localization of amiloride-sensitive sodium channels in sodium-transporting epithelia. J Cell Sci 93:349–362

Turnheim KR (1991) Intrinsic regulation of apical sodium entry in epithelia. Physiol Rev 71:429–445

Turnheim KR, Frizzell RA, Schultz SC (1978) Interaction between cell sodium and the amiloride-sensitive sodium entry step in rabbit colon. J Membr Biol 39:233–256

Ussing HH (1965) Relationship between osmotic reactions and active sodium transport in the frog skin epithelium. Acta Physiol Scand 63:141–155

Ussing HH, Windhager EE (1964) Nature of shunt path and active sodium transport path through frog skin epithelium. Acta Physiol Scand 61:484–504

Ussing HH, Zerahn K (1951) Active transport of sodium as the source of electric current in short-circuited isolated frog skin. Acta Physiol Scand 23:110–127

Van Driessche W, Erlij D (1983) Noise analysis of inward and outward Na^+ currents across the apical barrier of ouabain-treated frog skin. Pflugers Arch 398:179–188

Van Driessche W, Lindemann B (1979) Concentration-dependence of currents through single sodium-selective pores in frog skin. Nature 282:519–520

Verrier B, Champigny G, Barbry P, Gerard C, Mauchamp J, Lazdunski M (1989) Identification and properties of a novel type of Na^+-permeable amiloride-sensitive channel in thyroid cells. Eur J Biochem 183:499–505

Vigne P, Champigny G, Marsault R, Barbry P, Frelin C, Lazdunski M (1989) A new type of amiloride-sensitive cationic channel in endothelial cells of brain microvessels. J Biol Chem 264:7663–7668

Wainwright BJ, Scambler PJ, Schmidke J, Watson EA, Law HY, Farral M, Cooke HJ, Eiberg H, Williamson R (1985) Localization of cystic fibrosis locus to human chromosome 7 cen-q22. Nature 318:384–388

Wanner A (1976) Clinical aspects of mucociliary transport. Am Rev Respir Dis 113:833–878

Warncke J, Lindemann B (1985) Voltage dependence of Na^+ channel blockade by amiloride: relaxation effect in admittance spectra. J Membr Biol 86:255–265

White R, Woodward S, Leppert M, O'Connell P, Hoff M, Herbst J, Lalouel JM, Dean M, Vande Woude G (1985) A closely linked genetic marker for cystic fibrosis. Nature 318:382–384

Widdecombe JH, Welsh MJ, Finkbeiner WE (1985) Cystic fibrosis decreases the apical membrane chloride permeability of monolayers cultured from cells of tracheal epithelium. Proc Natl Acad Sci USA 82:6167–6171

Wills NK, Millinoff LP, Crowe WE (1991) Na^+ channel activity in cultured renal (A6) epithelium: regulation by solution osmolarity. J Membr Biol 1221:79–90

Wood RE, Boat TF, Doershuk CF (1976) State of the art: cystic fibrosis. Am Rev Respir Dis 113:833–878

Woodhull AM (1973) Ionic blockage of sodium channels in nerve. J Gen Physiol 61:687–708

Wright SH, Wunz TM (1989) Amiloride transport in rabbit renal brush-border membrane vesicles. Am J Physiol 256:F462–F468

Yamaguchi DT, Sakai R, Bahn L, Cragoe EJ Jr, Jordan SC (1986) Amiloride inhibition of DNA synthesis and immunoglobulin production by activated human peripheral blood mononuclear cells is independent of sodium/hydrogen antiport. J Immunol 137:1300–1304

Yanase M, Handler JS (1986) Activators of protein kinase C inhibit sodium transport in A6 epithelia. Am J Physiol 250:C517–C522

Yau K-W, Haynes LW (1986) Effect of divalent cations on the macroscopic cGMP-activated current in excised rod membrane patches (Abstr). Biophys J 49:33a

Yau K-W, Nakatani K (1984) Cation selectivity of light-sensitive conductance in retinal rods. Nature 309:352–354

Yorio T, Bentley PJ (1978) Phospholipase A and the mechanisms of action of aldosterone. Nature 271:79–81

Zamofing D, Rossier BC, Geering K (1989) Inhibition of N-glycosylation affects transepithelial Na^+ but not Na^+-K^+-ATPase transport. Am J Physiol 256:C958–C996

Zeiske W, van Driessche W (1984) The sensitivity of apical Na^+ permeability in frog skin to hypertonic stress. Pflugers Arch 400:130–139

Zweifach A, Lewis S (1988) Characterization of a partially degraded sodium channel from urinary tract epithelium. J Membr Biol 101:49–56

Rev. Physiol. Biochem. Pharmacol., Vol. 120

Adaptation of Mammalian Skeletal Muscle Fibers to Chronic Electrical Stimulation

DIRK PETTE[1] and GERTA VRBOVÁ[2]

Contents

[1] Fakultät für Biologie, Universität Konstanz, Postfach 5560 W-7750 Konstanz, FRG
[2] Department of Anatomy and Developmental Biology, University College London, London WC1E 6BT, UK

1 Introduction

Chronic low-frequency stimulation is by now a well-established method for inducing specific changes in muscle properties. Over the past decade several reviews have been published which summarized the major effects of chronic stimulation (Jolesz and Sréter 1981; Salmons and Henriksson 1981; Pette 1984, 1985, 1991; Pette and Vrbová 1985; Lieber 1986; Pette and Düsterhöft 1992). The increased use of this model has led to an expansion of knowledge in this field and a large body of information has accumulated on the numerous phenomena of the activity-induced transformation of muscle fiber phenotype. These data emphasize that fully differentiated muscle fibers retain the potential to respond to altered functional demands with specific adaptive changes.

Chronic low-frequency stimulation represents an approach that allows researchers to relate functional changes to specific molecular events in the stimulated muscle. Unlike exercise, the activity is restricted to the stimulated muscle and, thus, the muscle is less influenced by other changes that can occur in the body during training. Artificial stimulation bypasses the central nervous system and activates all motor units equally, whereas during exercise individual motor units are activated in a graded and hierarchical manner. Therefore, chronic stimulation can provide information as to the extent of the muscle plasticity. It has also become clear that chronic electrical stimulation of a skeletal muscle may evoke changes which exceed those induced by any other form of increased contractile activity. It has, thus, provided information as to the limits of muscle adaptation. In addition, the effects of chronic stimulation on skeletal muscle have inspired clinical investigators to use this method for medical purposes.

The chronic stimulation model enables researchers to correlate functional changes with alterations at the molecular level. Moreover, it offers the possibility of investigating the influence of activity on the expression of specific genes. By following the time course of changes it is possible to deduce coordinations in gene expression of different

functional elements of the muscle fiber. Finally, this model offers a unique opportunity to study the regulatory mechanisms involved in the control of gene expression in excitable cells.

The use of chronic electrical stimulation in different experimental models has produced numerous interesting results which pose several new questions. These include the problem of whether stimulation-induced changes occur as a result of an increased amount of activity or a specific impulse pattern. Also, the observation that the same muscles in different animal species respond in a variable manner to a similar activity pattern raises the question as to the existence of species-specific ranges of adaptation. This suggests that additional factors may modulate the outcome of chronic low-frequency stimulation. Such factors may include internal environment, i.e., hormonal factors, or mechanical conditions, e.g., locomotor patterns or load.

The present review will cover only material related to the contractile apparatus and its energy-supplying machinery. The effect of activity on other muscle-specific proteins, such as the acetylcholine receptor and cholinesterase, has recently been reviewed (Laufer and Changeux 1989; Sketelj et al. 1991).

2 Fast-to-Slow Transitions by Chronic Low-Frequency Stimulation

Chronic stimulation of extensor digitorum longus (EDL) and tibialis anterior (TA) muscles of the rabbit and flexor digitorum longus (FDL) muscle of the cat at 10 Hz converts these fast-twitch muscles into slower contracting ones (Salmons and Vrbová 1969). Concomitant with these changes, various elements of the muscle fiber are also modified. Nevertheless, the relationship between alterations in structural and molecular properties of the muscle fiber and changes of physiological characteristics has not been entirely explained.

2.1 Methods of Stimulation

In animal experiments with long-term stimulation it is desirable to use either fully or partially implantable devices, for it is difficult to habituate the animal to externally applied electrodes. The development of implantable electrodes required materials that can be tolerated by the organism. The method was first developed in rabbits (Vrbová 1966; Salmons and Vrbová 1969) using bipolar platinum or

stainless steel electrodes insulated except for the tip. The electrodes were placed on either side of the nerve to be stimulated and secured to the surrounding tissue so as not to mechanically disturb the nerve. The positioning of the electrodes in relation to the nerve is extremely important for achieving adequate stimulation of all the nerve fibers. This may be more difficult to achieve if the electrodes are perpendicular to the nerve (Chachques et al. 1988). The electrodes can be externalized and connected either to a conventional stimulator (Pette et al. 1973) or to a miniaturized portable stimulator (Tyler and Wright 1980). One improvement has been the use of a miniaturized receiver carried by the animal for transmitting the desired stimulus pattern by telestimulation (Schwarz et al. 1983; Eerbeek et al. 1984). Implantable stimulators with fixed parameters of stimulation were initially used in animal experiments (Salmons and Vrbová 1969), but these have been improved so as to provide a facility to vary the stimulus parameters by a remote transcutaneous optical link (Brown and Salmons 1981). More elaborate implantable devices are used in muscle pacing for cardiac assist where the muscle stimulation must be linked to the cardiac function (Chachques et al. 1988; Grandjean et al. 1990). For stimulating human muscles both invasive and noninvasive techniques can be used. Occasionally, noninvasive, transcutaneous stimulation has also been used in experiments on rabbits (Mabuchi et al. 1982). This method is fraught with several disadvantages, e.g., the animals must be restrained to prevent them from removing the stimulating electrodes. In addition, currents used to produce effective stimulation have to be so great that the sensation caused by the stimulation is not easily tolerated by the animal. Therefore, the currents used will probably stimulate only the lowest threshold motor axons which supply selected muscle fiber populations. The situation may be different when the stimulated limb is denervated and the sensory innervation is also interrupted (Mokrusch et al. 1990). However, for transcutaneous, direct stimulation of denervated muscle excessively high currents are necessary in order to achieve contraction of the whole muscle.

2.2 Physiological Characteristics

The effects first noted in chronically stimulated TA and EDL muscles of the rabbit and FDL muscle of the cat were increases in the time to peak twitch tension and half-relaxation time (Fig. 1) (Vrbová 1966; Salmons and Vrbová 1969; Pette et al. 1973). Consistent with this,

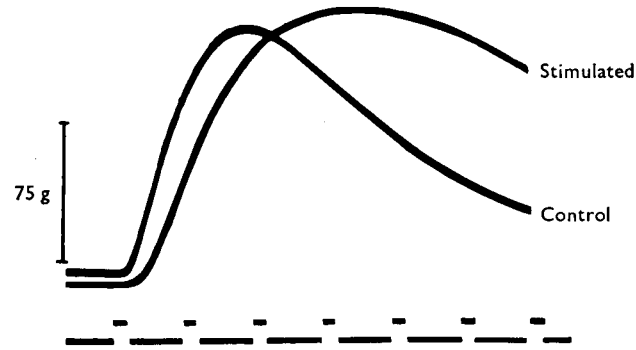

Fig. 1. Isometric twitch contractions of chronically stimulated (10 Hz, 24 h daily, 41 days) and contralateral (*control*) tibialis anterior muscles of the rabbit. The *marker* represents 10-ms intervals. (From Salmons and Vrbová 1969)

decreases in the maximum rate of tetanic tension development were also observed (Salmons and Sréter 1976; Sweeney et al. 1988; J.M.C. Brown et al. 1989). To exclude reflexively elicited movements, which could be produced by stimulation of the peripheral nerve, Buller and colleagues stimulated ventral roots in the cat. They observed the expected slowing of the time course of twitch contraction and, in addition, a change in the force–velocity relationship (Al-Amood et al. 1973; Buller and Pope 1977). Experiments on rabbits (Pette et al. 1973, 1976; Salmons and Sréter 1976; Hudlická et al. 1982a; Klug et al. 1988; Simoneau et al. 1989) and cats (Eerbeek et al. 1984) have also shown increases in the twitch to tetanus ratio in low-frequency stimulated muscle, indicating that the duration of the active state was prolonged.

A consistent finding with chronic low-frequency stimulation has been an increased resistance to fatigue (Fig. 2). This was first described for the stimulated TA muscle of the cat (Peckham et al. 1973) and rabbit (M.D. Brown et al. 1973) and later confirmed for rabbit (Pette et al. 1975; Salmons and Sréter 1976; Hudlická et al. 1977, 1982a; J.M.C. Brown et al. 1989), the rat (Kwong and Vrbová 1981; Pette and Simoneau 1990), the cat (Eerbeek et al. 1984; Kernell et al. 1987a,b; Kernell and Eerbeek 1989), the dog (Ciesielski et al. 1983; Mannion et al. 1986; Acker et al. 1987a,b; Clark et al. 1988), the goat (Chachques et al. 1988), and the human (Edwards et al. 1982; Scott et al. 1985).

The increase in resistance to fatigue may be associated with the increased capillarization and marked elevation in aerobic-oxidative capacity (see Sect. 2.6) induced by chronic low-frequency stimula-

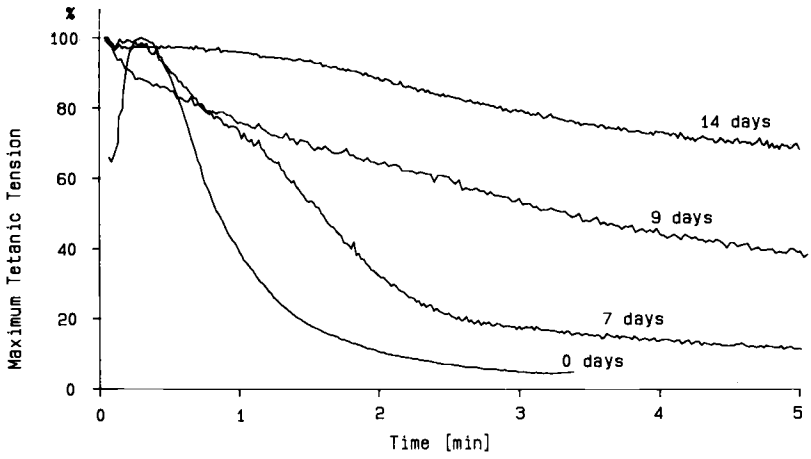

Fig. 2. Time-dependent increase in resistance to fatigue as induced by chronic low-frequency stimulation (10 Hz, 12 h daily). Resistance to fatigue was assessed using the protocol of Burke et al. (1971, 1973). Measurements on the same animal were performed noninvasively on the foot levers of the stimulated leg at different time points after the onset of stimulation

tion. Gross inspection of chronically stimulated fast-twitch TA and EDL muscles of the rabbit reveals a deep red color as compared to the pale, unstimulated contralateral muscle. This change in color is a consequence of stimulation-induced increases in capillary density (Cotter et al. 1972, 1973; M.D. Brown et al. 1976; Myrhage and Hudlická 1978; Hudlická and Tyler 1984; Hudlická et al. 1980, 1982b, 1984; Eisenberg and Salmons 1981; J.M.C. Brown et al. 1989) and myoglobin content (Pette et al. 1973; Kaufmann et al. 1989). Increases in capillary density (Fig. 3) following chronic stimulation have also been noticed in other species and other muscles, e.g., in cat gracilis muscle (Hoppeler et al. 1987; Hudlická et al. 1987), EDL and TA muscles of the rat (Myrhage and Hudlická 1978; Hudlická et al. 1984; Ciske and Faulkner 1985; Dawson and Hudlická 1989; Hudlická and Price 1990), and latissimus dorsi of the goat (Chachques et al. 1988). However, other factors may contribute to the improved resistance to fatigue, e.g., increases in substrate supply (see Sect. 2.6).

Evidence has been accumulating indicating that increases in enzyme activities related to aerobic-oxidative metabolism represent only one factor responsible for the increased fatigue resistance (Hudlická et al. 1986; Kernell et al. 1987b; Pette and Simoneau 1990; Simoneau et al. 1992). Thus, a linear correlation seems to exist between the increase in citrate synthase activity, a commonly

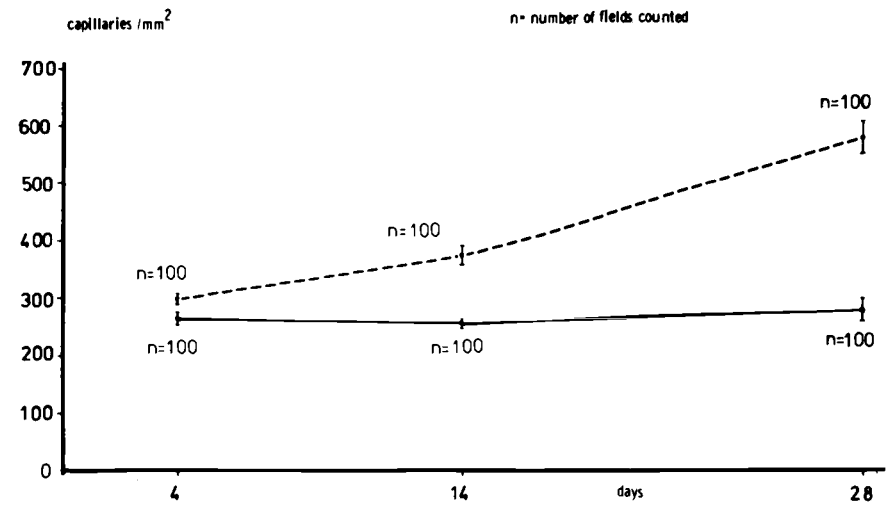

Fig. 3. Increase in capillary density of chronically stimulated (10 Hz, 8 h daily) rabbit extensor digitorum longus muscle. *n*, number of fields counted. (From Hudlická 1984)

accepted marker of mitochondrial content and aerobic-oxidative capacity (Reichmann et al. 1985; J.M.C. Brown et al. 1989; Hoppeler 1990), and the enhanced resistance to fatigue in low-frequency stimulated fast-twitch muscles of both the rat and rabbit. However, this correlation exists only within a certain range of citrate synthase activity (Fig. 4). Citrate synthase activities of chronically stimulated muscle, which exceed the very high values of heart muscle in rat and rabbit, are not accompanied by further improvements in resistance to fatigue (Pette and Simoneau 1990; Pette and Düsterhöft 1992; Simoneau et al. 1992).

The reported increase in capillary density, i.e., number of capillaries per area, is a combination of a true increase in the number of capillaries and a decrease in muscle fiber diameter (Fig. 5) both of which occur after chronic stimulation (Pette et al. 1975, 1976; M.D. Brown et al. 1976; Salmons and Henriksson 1981; Ciesielski et al. 1983; Hudlická et al. 1982b; Hudlická and Tyler 1984; Eisenberg et al. 1984; Reichmann et al. 1985; Maier et al. 1986; Mannion et al. 1986; Acker et al. 1987c; Donselaar et al. 1987; Kernell et al. 1987a; Staron et al. 1987). The stimulation-induced decrease in fiber size is less in old than in young rats because the initial size of muscle fibers in old rats is relatively small (Cotter and Hudlická 1977). Nevertheless, there is also an increase in capillary density in old rats. Taken

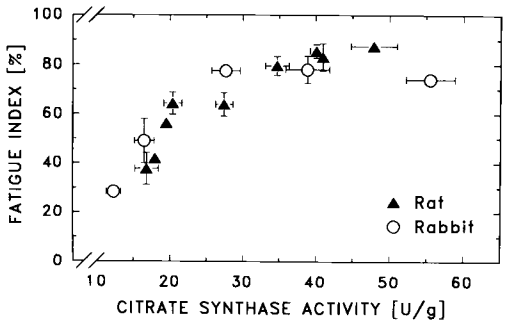

Fig. 4. Relation between increases in citrate synthase activity and increases in resistance to fatigue (expressed as fatigue index) of chronically (10 Hz) stimulated tibialis anterior muscles of rat and rabbit. Values represent means ± SE (n = 3–6 animals for each point). (Modified from Simoneau et al. 1992)

together, the changes in fiber size and number of capillaries improve the oxygen supply to the working muscle fibers. In addition, an increase in oxygen uptake of chronically stimulated muscle has been demonstrated (Hudlická et al. 1977, 1980, 1984; Hoppeler et al. 1987).

2.3 Stimulation-Induced Changes in Muscle Fibers

Many of the overall functional changes described so far are a consequence of stimulation-induced changes in the muscle fiber phenotype. A conspicuous finding in low-frequency stimulated rabbit EDL and TA muscles is that the normally broad distribution of fiber cross-sectional areas in these muscles changes into a more homogeneous population of fibers with a smaller cross-sectional area (Fig. 5; Pette et al. 1975). Total fiber counts show that long-term stimulated rabbit TA muscles contain approximately the same number of fibers as the unstimulated contralateral TA muscles (Pette et al. 1976). Therefore, the reduction in muscle weight commonly observed after long-term low-frequency stimulation results from the decrease in fiber caliber, but not from a loss of fibers (Pette et al. 1976).

Chronic low-frequency stimulation affects the major functional elements of the muscle fiber, i.e., the myofibrillar apparatus, the Ca^{2+}-regulatory system, and energy metabolism. Taking into account the extreme heterogeneity of the fiber population in most skeletal muscles (for review see Pette and Staron 1990), stimulation-induced changes can only be properly evaluated at the single fiber level. A commonly used approach is the combination of whole muscle biochemistry with histochemical or immunocytochemical analyses of the fiber population. A more precise analysis utilizes single fiber preparations for quantitative biochemical studies.

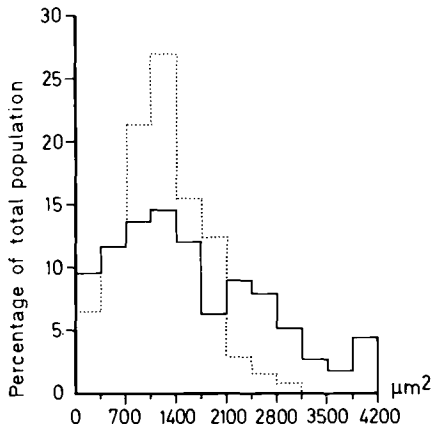

Fig. 5. Distribution of mean fiber area in control and in 21-day stimulated (10 Hz, 8 h daily) rabbit tibialis anterior muscles. Values are means from five animals. *Full line*, control muscles; *dotted line*, stimulated muscles. (From Pette et al. 1975)

2.3.1 Histochemistry and Immunocytochemistry of Transforming Muscle Fibers

The classification of muscle fiber types is based on two different approaches. One classifies fiber types according to differences in the histochemically assessed stability of the myofibrillar actomyosin adenosine triphosphatase (mATPase) activity (Guth and Samaha 1969; Brooke and Kaiser 1970; Samaha et al. 1970). The differences in the mATPase activity relate to specific myosin heavy chain (MHC) complements (Staron and Pette 1986; Pette and Staron 1990; Staron 1991) and make it possible to distinguish specific muscle fiber types. This classification distinguishes muscle fibers solely on the basis of differences with regard to the myosin molecule. The use of antibodies raised against various myosin isoforms, therefore, leads to a similar classification. Another scheme is based primarily on histochemically identified differences in metabolic properties using selected key enzymes of anaerobic or aerobic-oxidative metabolism. In combination with a simplified mATPase method, which distinguishes only between fast and slow fibers, it leads to the following classification: fast-twitch glycolytic (FG), fast-twitch oxidative (FOG), and slow-twitch oxidative (SO) fiber types (Barnard et al. 1971; Peter et al. 1972).

Increases in the fraction of oxidative fibers in rabbit (Pette et al. 1972, 1973; Romanul et al. 1974) and cat (Peckham et al. 1973) EDL and TA muscles were the first indication of a profound metabolic effect of chronic low-frequency stimulation on fast-twitch muscles (Fig. 6). These observations have been substantiated by quantitative measurements of the extent of the changes. These

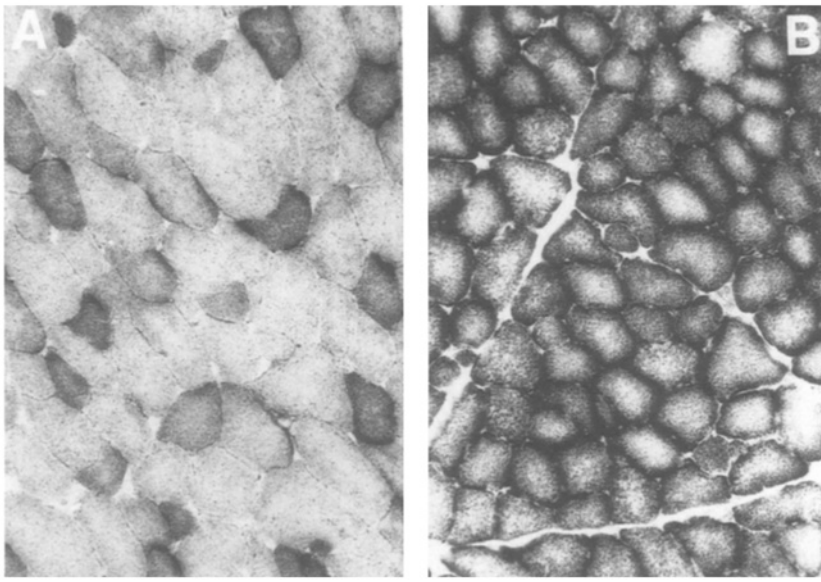

Fig. 6A,B. Histochemical staining for succinate dehydrogenase in cross sections of **A** contralateral and **B** chronically stimulated (10 Hz, 8 h daily, 28 days) rabbit TA muscles (×190). (From Pette et al. 1972)

studies found several-fold increases in enzyme activities related to aerobic substrate oxidation concomitant with marked decreases in glycolytic enzyme activities (Pette et al. 1972, 1973; see also Sect. 2.6.2). Increases in the proportion of oxidative fibers have been reported in many successive studies on chronically stimulated muscles in different species (Pette et al. 1975; M.D. Brown et al. 1976; Hudlická et al. 1977, 1982b, 1984; Rubinstein et al. 1978; Kwong and Vrbová 1981; Pette and Tyler 1983; Buchegger et al. 1984; Ciske and Faulkner 1985; Frey et al. 1986; Maier et al. 1986; Mannion et al. 1986, 1990; Donselaar et al. 1987; Kernell et al. 1987b; J.M.C. Brown et al. 1989; Magovern et al. 1990). The increases in enzyme activities representative of the aerobic-oxidative metabolism correlate well with electron microscopically demonstrated augmentations in mitochondrial volume density (Fig. 7; Salmons et al. 1978; Heilig and Pette 1980; Eisenberg and Salmons 1981; Ciesielski et al. 1983; Reichmann et al. 1985; Hoppeler et al. 1987; Chachques et al. 1988).

Myofibrillar ATPase histochemistry has revealed a stimulation-induced increase in the number of slow-twitch (type I) fibers in several animal species. These include the rabbit (Romanul et al.

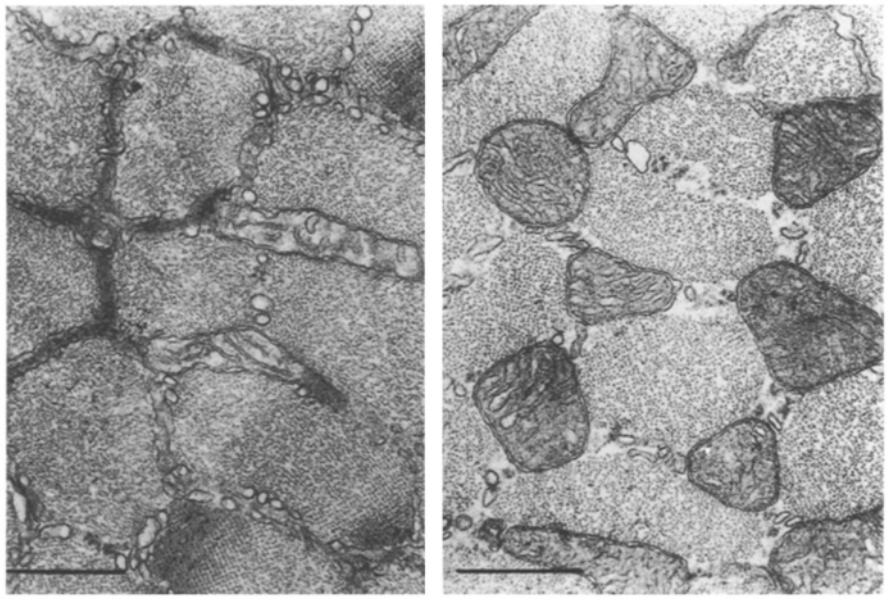

Fig. 7. Electron micrographs of cross sections from contralateral (*left*) and 23-day continuously (10 Hz, 24 h daily) stimulated (*right*) rabbit tibialis anterior muscles. (From Heilig and Pette 1980)

1974; Pette et al. 1976; Rubinstein et al. 1978; Roy et al. 1979; Pette 1984; Maier et al. 1986, 1988; Cotter and Phillips 1986; P. Williams et al. 1986; Staron and Pette 1987a; Staron et al. 1987), the cat (Donselaar et al. 1987; Ferguson et al. 1989), the dog (Ciesielski et al. 1983; Hoffman et al. 1985; Mannion et al. 1986; Acker et al. 1987b,c; Clark et al. 1988; Havenith et al. 1990; Ianuzzo et al. 1990a,b; Marzocchi et al. 1990), the sheep (Frey et al. 1984, 1986), the goat (Chachques et al. 1988), and the human (Magovern et al. 1988). An increase in fibers containing slow-type myosin has also been demonstrated immunocytochemically in the rabbit (Franchi et al. 1990; Mabuchi et al. 1990) and in the dog (Havenith et al. 1990), using monoclonal antibodies against MHC, and in the rabbit using polyclonal antibodies against slow type myosin light chains (Rubinstein et al. 1978). The higher proportion of type I fibers in long-term stimulated rabbit muscle correlates with the finding of a large proportion of fibers containing a thicker Z disc, a characteristic of slow-twitch fibers (Salmons et al. 1978; Eisenberg and Salmons 1981).

Detailed analyses on chronically stimulated rabbit EDL and TA muscles revealed that the fast-to-slow transition of muscle fibers is a

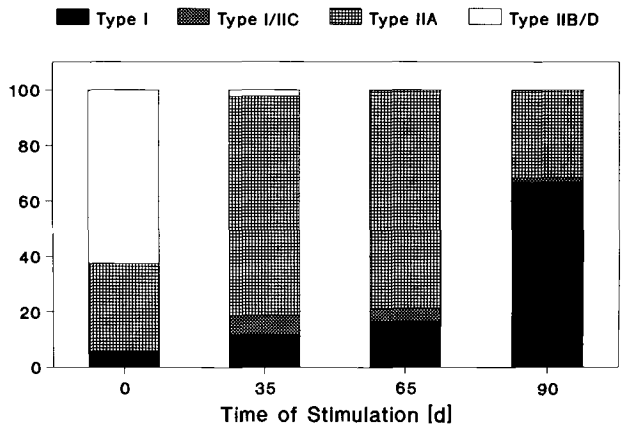

Fig. 8. Time-dependent changes in the percentage distribution of fiber types in low-frequency stimulated (10 Hz, 12 h daily) rabbit extensor digitorum longus muscle. Fiber types were classified according to their histochemically assessed myofibrillar actomyosin ATPase activity. No distinction was made between fiber types IIB and IID. (Modified from Pette 1992)

graded event during which the number of type IIB fibers decreases rapidly after the onset of stimulation and the percentage of type I fibers increases with transient elevations in type IID, type IIA and type C fibers (Staron et al. 1987; Maier et al. 1988; Termin et al. 1989b; Pette 1990). The improvement of electrophoretic separation of MHC isoforms from single fibers has led to the detection in rat muscle of an additional MHC, named HCIId, in specific fast-twitch fibers, designated type IID (Bär and Pette 1988; Termin et al. 1989a,b). These fibers are probably identical with the type 2x fiber described by Schiaffino and collaborators in muscles of mouse, rat, and guinea pig (Schiaffino et al. 1988, 1989; Gorza 1990). Recent findings (D. Pette et al., unpublished) indicate that type IID fibers and the respective MHC isoform are also present in rabbit muscle. Because of the great similarity of the type IID mATPase histochemistry with that of type IIB fibers, it could be that in previous studies type IID fibers have been erroneously taken as type IIB. The stimulation-induced changes in the muscle fiber population may, therefore, proceed in the following order: type IIB → type IID → type IIA → type IIC → type IC → type I (Fig. 8). Fiber types IIB, IID, and IIA are fast-twitch fibers expressing the MHC isoforms HCIIb, HCIId and HCIIa, respectively. Type I represents the slow-twitch fiber type which expresses the slow MHC isoform, HCI. Fiber types IIC and IC are hybrid fibers, containing HCIIa and HCI in

variable proportions (type IIC, HCIIa > HCI; type IC, HCI > HCIIa).

An unexpected finding was that in the rat chronic low-frequency stimulation of fast-twitch muscles (EDL and TA) did not lead to an increase in slow-twitch (type I) fibers (Kwong and Vrbová 1981; Ciske and Faulkner 1985; Termin et al. 1989a,b), even after prolonged stimulation. Further investigations have shown that the stimulation-induced changes in the fiber population of rat muscle remain restricted to a rearrangement of the fast fiber subtypes, leading ultimately to a type IIB → type IID → type IIA transition with only slight increases in type I fibers. In the course of this transition the appearance of hybrid fibers containing more than one MHC isoform is quite common. According to their MHC composition, these fibers were termed type IIBD (HCIIb + HCIId) and type IIDA (HCIId + HCIIa) (Termin et al. 1989a,b). The finding that chronic low-frequency stimulation does not lead in rat fast-twitch muscle to significant increases in type I fibers has also been shown in denervated rat EDL stimulated at low frequency (Schiaffino et al. 1990).

Interestingly, the same stimulation protocol that leads to an increase in type I fibers in the rabbit or to an increase in type IIA fibers in the rat, does not cause conspicuous changes in the mATPase-based fast fiber types in mouse fast-twitch muscle (TA). The only histochemical change is an increase in the aerobic-oxidative capacity as revealed by elevations in succinate dehydrogenase and NADH tetrazolium reductase activities (A. Termin, N. Hämäläinen, D. Pette 1990, unpublished). Thus, chronic low-frequency stimulation of mouse fast-twitch muscle seems to induce a FG to FOG fiber transition. These observations further support species-specific differences in response to low-frequency stimulation (Simoneau and Pette 1989a,b).

2.4 Myofibrillar Proteins

The stimulation-induced changes in contractile properties are associated with alterations in the composition of myofibrillar proteins. Studies of myofibrillar proteins in chronically stimulated muscles were initially performed on whole muscle extracts and later on single fibers. Particular attention has been given to changes in the isoform patterns of the major protein of the thick filament, myosin, and the regulatory proteins of the thin filament, tropomyosin (TM) and troponin (TN).

2.4.1 Proteins of the Thick Filament

As would be expected from the changes in contractile speed, as well as by the mATPase-based histochemistry, chronic low-frequency stimulation leads to alterations in myosin composition. This was first shown by Sréter et al. (1973, 1974, 1975) who observed a partial exchange of the fast myosin light chains (LC) with their slow counterparts in rabbit EDL and TA muscles stimulated for 2–4 weeks. These observations were confirmed in subsequent studies (Pette et al. 1976; Salmons and Sréter 1976; Pette and Schnez 1977; Rubinstein et al. 1978; Roy et al. 1979; Hudlická et al. 1982a; Mabuchi et al. 1982; W.E. Brown et al. 1983, 1985; Pluskal and Sréter 1983; K. Seedorf et al. 1983; Heilig and Pette 1983; Heilig et al. 1984; Staron et al. 1987; Staron and Pette 1987a; Sweeney et al. 1988; Kirschbaum et al. 1989a). The complete fast-to-slow transition of the LC isoforms appears to take a long time, i.e., several months. Considerable amounts of the fast alkali LC1f are present in long-term stimulated EDL and TA muscles of the rabbit (Pette et al. 1976; Pette and Schnez 1977; Roy et al. 1979; W.E. Brown et al. 1983, 1985; Pluskal and Sréter 1983; K. Seedorf et al. 1983; Staron et al. 1987). The relatively long-term persistence of the fast alkali LC1f suggests that it may coexist within the same fiber together with slow myosin light and heavy chains.

Stimulation-induced fast-to-slow transitions of the myosin light chains were observed in other muscles and animal species, e.g., the cat (Ferguson et al. 1989), the dog (Hoffman et al. 1985; Acker et al. 1987c), the goat (Mannion et al. 1990), and the sheep (Carraro et al. 1988; Cumming et al. 1991). Interestingly, only a limited fast-to-slow exchange has been observed in chronically stimulated fast-twitch muscle of the rat. Long-term low-frequency stimulation leads to an increase in the fast alkali LC1f and a decrease in the fast alkali LC3f. Only slight increases in the alkali LC1sb and an even smaller increase in the regulatory LC2s are observed in rat muscle (Bär et al. 1989; Kirschbaum et al. 1989b, 1990a; Termin and Pette 1990, 1991). The increase in the slow LC1sb does not necessarily indicate the expression also of the slow MHC. It has been shown that the fast HCIIa may be associated with both the fast and slow alkali light chains (Fitzsimons and Hoh 1983; Staron and Pette 1987b,c; Maréchal et al. 1989; Termin and Pette 1990, 1991).

An interesting observation, related to the changes in the myosin LC pattern in stimulated rabbit muscle, concerns the activity of the myosin light chain kinase. In rabbit TA muscle stimulated 24 h/day at

10 Hz, there is a rapid decrease in the activity of this enzyme. After 5 days, myosin light chain kinase decays to approximately 50% of its original activity and stays at this level for up to 35 days of stimulation (Klug et al. 1986).

In view of the fact that both ATPase activity and actin binding are associated with the MHC, the investigation of this part of the myosin molecule during fast-to-slow transition of skeletal muscle is of primary importance. Comparative studies have indicated that there is a relationship between contraction speed and actin-activated mATPase activity (Bárány 1967; Bárány and Close 1971). The first indication that fast myosin was replaced by slow myosin in chronically stimulated fast-twitch muscle came from the observation of a decrease in *N*-methylhistidine content, an amino acid abundant in fast-type myosin, but deficient in slow-type myosin (Sréter et al. 1975). Chymotryptic peptide cleavage studies on myosin from low-frequency stimulated rabbit EDL and TA muscles (W.E. Brown et al. 1983) and dog diaphragm (Hoffman et al. 1985) have shown increases in slow myosin with a concomitant decrease in fast myosin. The resolution of the peptide cleavage method used precluded more detailed analyses, especially with regard to changes in the proportions of the various fast MHC isoforms. Stimulation-induced expression of the slow myosin HCI as demonstrated by electrophoresis under denaturing conditions, has been described in various muscles of different species, i.e., the rabbit (Staron et al. 1987; Staron and Pette 1987a), sheep (Carraro et al. 1991; Cumming et al. 1991; I. Christlieb, B. Gohlsch, D. Pette 1991, unpublished), and the calf (N. Guldner, B. Gohlsch, D. Pette 1990, unpublished).

Using electrophoresis under denaturing conditions, Staron et al. (1987) were able to show a gradual replacement of MHC isoforms in rabbit EDL and TA muscles stimulated for different time periods: HCIIb → HCIIa → HCI. This pattern of HC isoform transitions was also shown in single fibers (Staron and Pette 1987a).

Additional information has emerged from single fiber studies showing the coexistence of more than one MHC isoform in individual fibers. The coexistence of fast and slow myosins had been previously suggested by the presence of fast and slow myosin light chain isoforms in fibers microdissected from stimulated rabbit muscles (Pette and Schnez 1977), a finding corroborated by immunocytochemistry (Rubinstein et al. 1978). Also, mATPase histochemistry detected numerous hybrid fibers in transforming muscles (Staron and Pette 1987a; Staron et al. 1987; Termin et al. 1989). The coexistence of HCIIb and HCIIa, as well as of HCIIa and HCI, has been demon-

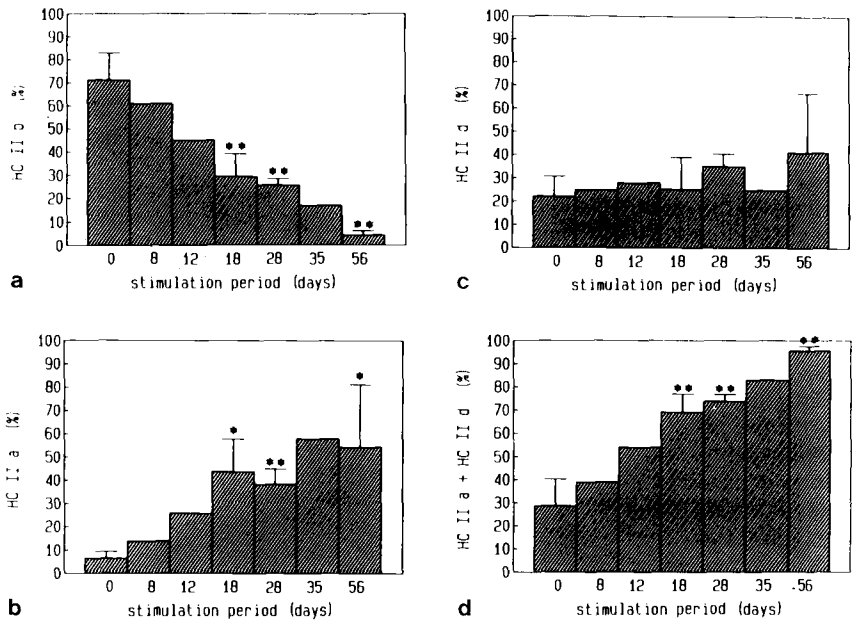

Fig. 9a–d. Changes in the percentage distribution of myosin heavy chain isoforms in tibialis anterior muscles of the rat subjected to low-frequency stimulation (10 Hz, 10 h daily) for different time periods (8–56 days): **a** HCIIb, **b** HCIIa, **c** HCIId, and **d** HCIIa + HCIId. Values are given as means ± SD (n = 2–4 for each time point). *, $p < 0.05$, **, $p < 0.01$. HCIIb, HCIId, HCIIa, fast myosin heavy chain isoforms. (From Termin et al. 1989b)

strated electrophoretically in single fibers isolated from low-frequency stimulated rabbit fast-twitch muscles (Staron et al. 1987; Staron and Pette 1987a). In addition, histochemically assessed mATPase activity, as well as electrophoretic analyses on single fiber fragments, indicated that fast and slow myosins are unevenly distributed along the length of transforming fibers in these muscles (Staron and Pette 1987a).

A clear picture of the sequence of the transitions has emerged from the analysis of chronically stimulated rat fast-twitch muscles. In spite of the fact that stimulation does not induce measurable increases in type I fibers or the slow HCI isoform, the MHC composition is altered (Termin et al. 1989b). The predominant HC isoform of normal rat EDL and TA, HCIIb, decreases to minute amounts, HCIIa increasing concomitantly. The HCIId isoform, which is thought to be functionally intermediate (Schiaffino et al. 1988; Termin et al. 1989b) between HCIIb and HCIIa, increases only moderately in whole muscle extracts (Fig. 9). Single fiber analyses on

chronically stimulated rat muscle show that many fibers express more than one MHC isoform. Some fibers may contain up to four different HC isoforms, i.e., HCIIb, HCIId, HCIIa, and HCI. As a result of this, the distinction of the normal mATPase-based fiber types is no longer possible (Termin et al. 1989b). A large fraction of fibers in 28-day stimulated muscle contains HCIIb and HCIId, whereas fibers from muscles stimulated for longer time periods frequently display the combination of HCIId with HCIIa (Termin et al. 1989b).

These changes in MHC suggest the following sequence: HCIIb → HCIId → HCIIa. This is different from the rabbit where the fiber transformation ultimately includes the HCIIa → HCI transition (Staron et al. 1987; Pette 1990). This sequential exchange of the various MHC isoforms suggests different thresholds of the respective genes (see also Sect. 2.7).

The pronounced alterations of the isomyosin pattern in chronically stimulated muscles result from the changes in myosin light and HC composition. Increases in slow isomyosins have been described in long-term stimulated fast-twitch muscles of the rabbit (Pluskal and Sréter 1983; Klug et al. 1986; Sréter et al. 1987), the dog (Hoffman et al. 1985; Acker et al. 1987c; Ianuzzo et al. 1990a,b; Marzocchi et al. 1990), the goat (Chachques et al. 1988; Mannion et al. 1990), and sheep (Carraro et al. 1991). In the rabbit, during stimulation under conditions which do not lead to a complete fast-to-slow transition, the rearrangement of the isomyosin pattern is restricted to the fast isomyosins and consists of a decrease in fast-twitch muscle isomyosins FM1 and FM2, with an increase in FM3 (Mabuchi et al. 1982; Sweeney et al. 1988). This is similar to what occurs in the rat even with vigorous prolonged stimulation. Therefore, in this species the changes in the fast isomyosins can be investigated in more detail. Recent methodical improvements have made it possible to separate myosin HCIIb-, HCIId- and HCIIa-based isomyosin triplets (Termin and Pette 1990, 1991). In chronically stimulated rat muscle, the proportions of these different fast HC-based isomyosins change so that HCIIb-based isomyosins decrease and HCIIa-based isomyosins increase. In addition, there is a shift from FM1 (LC3f homodimer) to FM3 (LC1f homodimer) isomyosins which is concomitant with the decrease in LC3f and the increase in LC1f (Termin and Pette 1991, 1992).

The altered expression of myosin light and heavy chains that have been described so far relate to corresponding alterations at the mRNA level. With the use of specific cDNA probes, S1-nuclease mapping assays have revealed changes of particular MHC mRNA

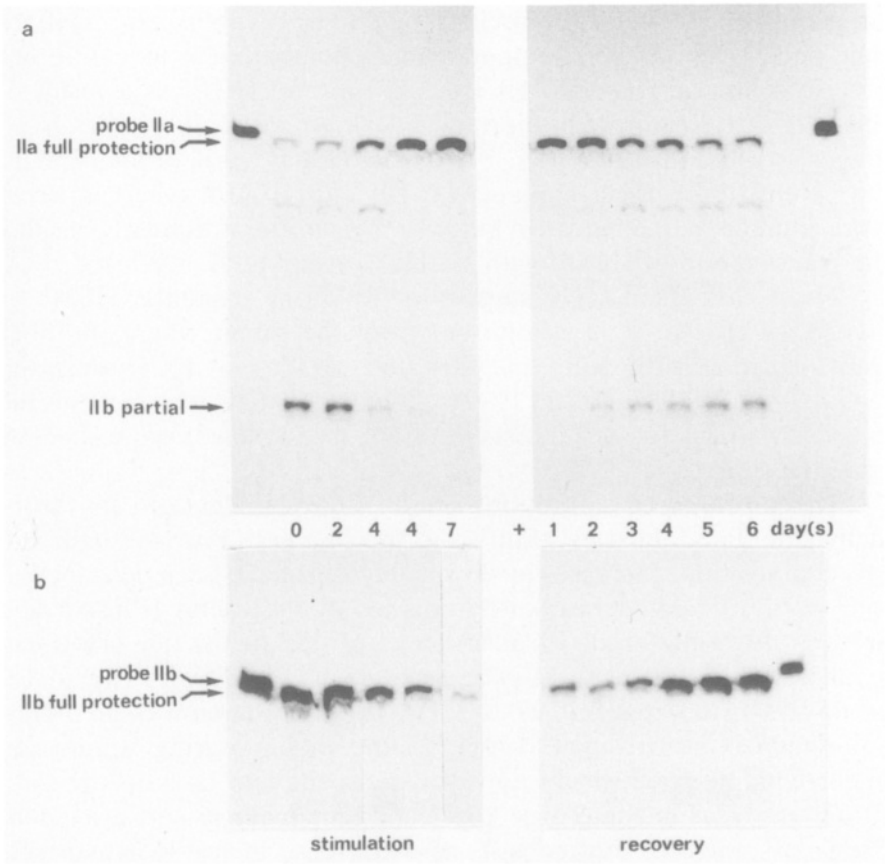

Fig. 10a,b. Changes in myosin HCIIa and HCIIb mRNA levels in rat tibialis anterior muscle with low-frequency (10 Hz, 10 h daily) stimulation and recovery. Total RNA was extracted from muscles stimulated for different time periods (*left panels*) and from 14-day stimulated muscles which were allowed to recover for different time periods after stimulation had been interrupted (*right panels*). The amounts of the two mRNAs were assessed by S1-nuclease mapping with the use of the myosin HCIIa probe pMHC40 (**a**) and the myosin HCIIb probe pMHC62 (**b**). The pMHC probe for HCIIa mRNA yields, in addition to the fully protected fragment, a partially protected fragment (170 nt) specific of HCIIb mRNA. Therefore, the use of this probe makes it possible to compare the ratio of these two mRNA isoforms. (Data from Kirschbaum and Pette 1988; Kirschbaum et al. 1989c, 1990b)

isoforms (Kirschbaum and Pette 1988; Kirschbaum et al. 1989c, 1990b). In the stimulated rat EDL and TA muscles there is a rapid decrease in HCIIb mRNA which is noticeable after only 2 days of stimulation, and the HCIIb mRNA becomes almost undetectable after 7 days. A reciprocal change of the mRNA encoding HCIIa is found (Fig. 10); it progressively increases during the same time

period (Kirschbaum and Pette 1988; Kirschbaum et al. 1989c, 1990b). Because specific cDNA probes for HCIId are not yet available, no data exist for changes of HCIId at the mRNA level.

In rabbit fast-twitch muscle, chronic low-frequency stimulation leads to progressive decreases in fast MHC mRNAs and induces the expression of the slow myosin HCI mRNA (Brownson et al. 1988, 1992; Kirschbaum et al. 1989a). In animals stimulated 12 h/day, HCI mRNA becomes detectable after stimulation periods exceeding 20 days (Kirschbaum et al. 1989a). Continuous stimulation (24 h/day) leads to an earlier appearance, i.e., HCI mRNA is first detected in 9-day stimulated rabbit EDL and TA muscles (Brownson et al. 1992). The difference between the time course of changes in these two studies (Kirschbaum et al. 1989a; Brownson et al. 1992) is most likely due to the different stimulation regimes, i.e., 12 h/day and 24 h/day stimulation. Nevertheless, these results support the notion that changes in the amount of contractile activity, as induced by chronic low-frequency stimulation, lead to rapid changes in the amounts of specific MHC mRNA isoforms and occur much earlier than the corresponding changes at the protein level. Similarly, cessation of chronic low-frequency stimulation has pronounced effects on the mRNA pattern leading to a rapid reversal of the stimulation-induced repression of HCIIb mRNA, as well as of the induction of HCIIa mRNA (Fig. 10).

A progressive increase in the amount of HCI mRNA has also been demonstrated by in situ hybridization in rabbit TA and EDL muscles subjected to different stimulation periods (Fig. 11; Aigner and Pette 1990, 1992). The number of fibers reacting positively with the specific cRNA probe correlated with the fraction of HCI protein determined electrophoretically in homogenates from the same EDL and TA muscles (Fig. 12; Aigner and Pette 1992). The appearance of mRNA encoding HCI in low-frequency stimulated rabbit muscle strongly suggests alterations in gene transcription within the fast-twitch fibers since these normally do not contain this isoform.

In vitro translation assays and hybridization assays with specific cDNA probes demonstrate that the rearrangement of the myosin light chain pattern is also preceded by changes at the mRNA level. However, as follows from time course studies, qualitative changes in the amounts myosin light chain mRNAs occur later than those of the MHC mRNAs (Kirschbaum et al. 1989a,b). In the rat, where the stimulation-induced changes are restricted to a rearrangement of the fast MHC isoforms (Kirschbaum et al. 1989b,c; Termin et al. 1989b),

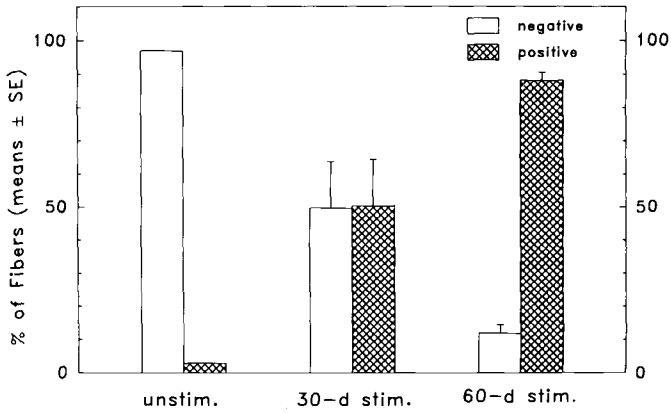

Fig. 11. Increases in myosin HCI mRNA-positive fibers as induced by chronic low-frequency stimulation (10 Hz, 24 h daily) in rabbit extensor digitorum longus muscle. HCI mRNA was assessed by in situ hybridization. (Data from Aigner and Pette 1992)

the alterations are restricted to the fast alkali light chains and consist of increases in the LC1f/LC3f ratio (Bär et al. 1989), with corresponding changes in the amounts of the LC1f and LC3f mRNAs (Kirschbaum et al. 1989b). Most likely, these alterations relate to decreasing affinities of LC3f to the fast MHC isoforms in the order HCIIb, HCIId, HCIIa (Termin and Pette 1991). Thus, the exchange of HCIIb with HCIIa in chronically stimulated rat muscle is followed by a decrease in the relative concentration of LC3f. The finding that the synthesis of LC3f continues in long-term stimulated muscles seems to disagree with its reduced protein amount. However, this discrepancy is explained by the observation that LC3f displays an enhanced turnover under these conditions. Obviously, LC3f is bound to a lesser degree to HCIIa and, therefore, accessible to degradation (Bär et al. 1989). Chronic low-frequency stimulation induces only small amounts of the slow alkali light chain isoforms LC1sa and LC1sb in rat muscle (Bär et al. 1989; Kirschbaum et al. 1989b). The appearance of these slow alkali light chain isoforms agrees with the suggestion that HCIIa combines, in addition to the fast LC1f, also with the slow LC1s (Termin and Pette 1991). The slow isoform of the regulatory light chain LC2 does not appear in chronically stimulated rat muscle (Bär et al. 1989), and in addition, there is no exchange of the fast LC2f with the slow LC2s at the mRNA level (Kirschbaum et al. 1989b). However, LC2s may be induced at both the mRNA and protein level in chronically stimulated fast-twitch muscle of the

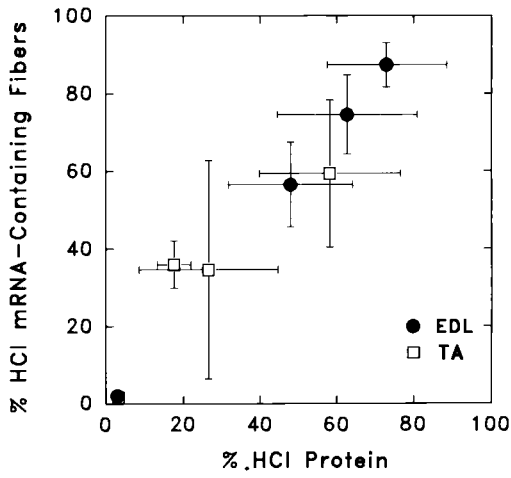

Fig. 12. Correlation between the percentage of myosin HCI mRNA-positive fibers and the percentage of myosin HCI protein in rabbit extensor digitorum longus (*EDL*) and tibialis anterior (*TA*) muscles stimulated (10 Hz, 24 h daily) for different time periods. (Modified from Aigner and Pette 1992)

hypothyroid rat (Kirschbaum et al. 1990a). Under these conditions, its appearance follows the expression of the slow myosin HCI. In the rabbit, where long-term low-frequency stimulation always leads to the expression of the slow myosin HCI, the changes at the mRNA and protein level include the induction of the slow isoforms of both the alkali and regulatory light chains, i.e., LC1sa, LC1sb, and LC2s (Heilig and Pette 1983; Pluskal and Sréter 1983; Heilig et al. 1984; Kirschbaum et al. 1989a).

2.4.2 Proteins of the Thin Filament

To date, studies on stimulation-induced changes in proteins of the thin filament have been focused on the regulatory proteins troponin and tropomyosin. Troponin is composed of three different subunits, troponin-T (TnT), troponin-I (TnI), and troponin-C (TnC). TnI and TnC exist as fast (TnI_f, TnC_f) and slow (TnI_s, TnC_s) isoforms. As a result of alternative RNA splicing (Breitbart and Nadal-Ginard 1986, 1987), TnT is found in several fast and slow isoforms (for review see Pette and Staron 1990). Among these, the major fast isoforms are TnT_{1f}, TnT_{2f}, TnT_{3f} and TnT_{4f} (M.M. Briggs et al. 1987; Briggs and Schachat 1989; Härtner et al. 1989; Schachat et al. 1990).

Chronically stimulated rabbit muscle displays fast-to-slow transitions of all the three troponin subunits. Studies on whole muscle extracts show that TnT changes first and to the greatest extent (Schachat et al. 1988, 1990; Härtner et al. 1989). The four major fast TnT isoforms decay sequentially in the order of TnT_{2f}, TnT_{4f}, TnT_{1f},

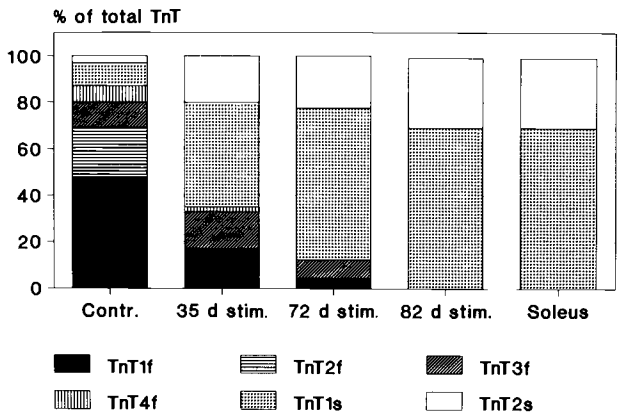

Fig. 13. Time-dependent changes in the percentage distribution of fast and slow troponin-T (*TnT*) isoforms in chronically stimulated (10 Hz, 12 h daily) extensor digitorum longus (EDL) muscle of the rabbit. For comparison, values are given for normal EDL (*Contr.*) and soleus muscles. (Data from Härtner et al. 1989)

TnT_{3f}, leading to a transient increase in the percentage of TnT_{3f} (Fig. 13). Subsequently, there is a progressive increase in the slow TnT isoforms TnT_{1s} and TnT_{2s} with a concomitant decrease in the fast TnT isoforms (Härtner et al. 1989). Single fiber analyses on chronically stimulated rabbit muscles have revealed that the alterations of the TnT isoform pattern follow a similar time course to that of the MHC isoforms (Schmitt and Pette 1990). Thus, the decline in the fast MHC isoforms is accompanied by that of the fast TnT isoforms, and the increase of the slow TnT_{1s} and TnT_{2s} isoforms coincides with the appearance of the slow myosin HCI. These results suggest that the coexpression patterns of MHC and TnT isoforms existing in normal muscle fibers are maintained during the induced fast-to-slow transition.

The exchange of fast with slow isoforms of TnI and TnC, especially of TnI, in chronically stimulated rabbit muscle appears to be less complete than that of TnT during the time period studied. Considerable amounts of fast TnI are still present in long-term stimulated rabbit muscles with complete or nearly complete fast-to-slow transition of TnT and TnC, respectively (Fig. 14; Härtner and Pette 1990). The different time courses in troponin subunit isoform transitions may be the result of the highly conserved nature of TnI (Wilkinson and Grand 1978a,b) which may adequately function with both fast and slow TnT and TnC isoforms. The finding that in long-term stimulated rabbit muscle fast TnT is completely replaced by

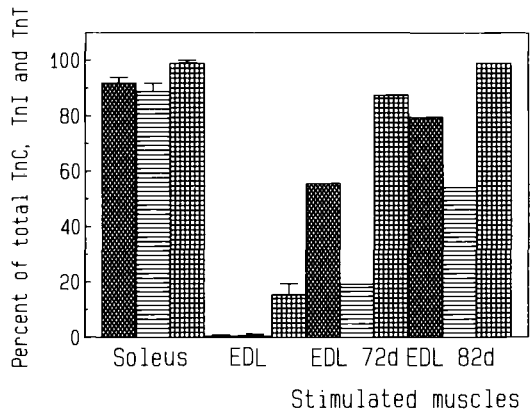

Fig. 14. Effects of long-term low-frequency stimulation (10 Hz, 12 h daily) on the immunochemically assessed isoform pattern of troponin subunits TnC (*dark*), TnI (*striped*), and TnT (*cross-hatched*) in rabbit extensor digitorum longus (*EDL*) muscle. Values are expressed as relative amounts of the slow isoforms, i.e., as percentages of fast and slow TnC, TnI, and TnT isoforms. For comparison, values (means ± SD, $n = 4–5$) are given for normal EDL and slow soleus muscles. (Values are from Härtner and Pette 1990)

slow TnT, while it still contains considerable amounts of fast TnI and some fast TnC, indicates the existence of hybrid troponin molecules composed of slow TnT and fast TnI and TnC (Härtner and Pette 1990).

The increase in slow troponin subunit isoforms in low-frequency stimulated rabbit fast-twitch muscles has also been demonstrated at the mRNA level. In vitro translation assays show progressive increases in the amounts of mRNAs coding for the slow TnI and TnC isoforms (Härtner and Pette 1990). Interestingly, the expression of the slow isoform of the Ca^{2+}-binding subunit TnC seems to coincide with the fast-to-slow isoform transition of the sarcoplasmic reticulum Ca^{2+}-ATPase and the induction of phospholamban, a protein normally present only in slow-twitch fibers and cardiac muscle (Leberer et al. 1989) (see Sect. 2.5.1). The appearance of slow troponin subunits mRNAs in low-frequency stimulated fast-twitch muscle, together with that of other proteins characteristic of slow-twitch muscles, may be taken as additional evidence that chronic low-frequency stimulation qualitatively alters gene transcription.

Changes have also been reported for tropomyosin in chronically stimulated rabbit muscle. According to Roy et al. (1979), 21-day low-frequency stimulated (24 h/day) rabbit TA muscles exhibit a markedly reduced αTM to βTM ratio which approaches that of slow-

twitch soleus muscle. Similar results were obtained by Schachat et al. (1988).

A protein closely associated with the thin filament, α-actinin which is a major constituent of the Z disc, has also been studied. An increase in the slow isoform, $\alpha\text{-actinin}_{1f/s}$ and a decrease in the fast $\alpha\text{-actinin}_{2f}$ have been reported in low-frequency stimulated rabbit EDL and TA muscles (Schachat et al. 1988). These changes may be related to the observed thickening of the Z discs (Salmons et al. 1978; Eisenberg and Salmons 1981).

2.5 Ca^{2+}-Regulatory System

Changes in total and free Ca^{2+} have been reported to occur in low-frequency stimulated rabbit EDL and TA muscles. Measurements with a Ca^{2+}-sensitive microelectrode have indicated an approximately five fold increase in free $[Ca^{2+}]$ in the resting muscle during the first 14 days of stimulation and a decline thereafter to values only slightly higher than normal. This variation in $[Ca^{2+}]$ is preceded by a transient increase in total calcium (Sréter et al. 1980, 1987). Measurements of either free $[Ca^{2+}]$ or total $[Ca^{2+}]$ are difficult and often subject to error. The study of Ca^{2+}-regulatory systems may, therefore, be more informative. The Ca^{2+}-sequestering system of chronically stimulated fast-twitch muscle is profoundly altered. Early changes modify the Ca^{2+}-uptake characteristics of the sarcoplasmic reticulum, as well as the amount of the cytosolic Ca^{2+}-binding protein parvalbumin. Later changes of the sarcoplasmic reticulum concern a fast-to-slow isoform transition of the sarcoplasmic reticulum Ca^{2+}-ATPase.

2.5.1 Sarcoplasmic Reticulum

Structural changes of the sarcoplasmic reticulum in rabbit fast-twitch muscle are observed as early as 6 h after the onset of stimulation and consist of swelling of the longitudinal sarcoplasmic reticulum in many fibers (Eisenberg and Salmons 1981). A change in the distribution of the intramembranous 7–9-nm particles of freeze-fractured membranes of the sarcoplasmic reticulum was observed 2 days after the onset of stimulation (Heilmann et al. 1981). An additional change related to the Ca^{2+}-regulatory system of rabbit muscle consists of a progressive decrease in the T-tubule profile per unit fiber area. This reduction becomes apparent within the first few days of stimulation

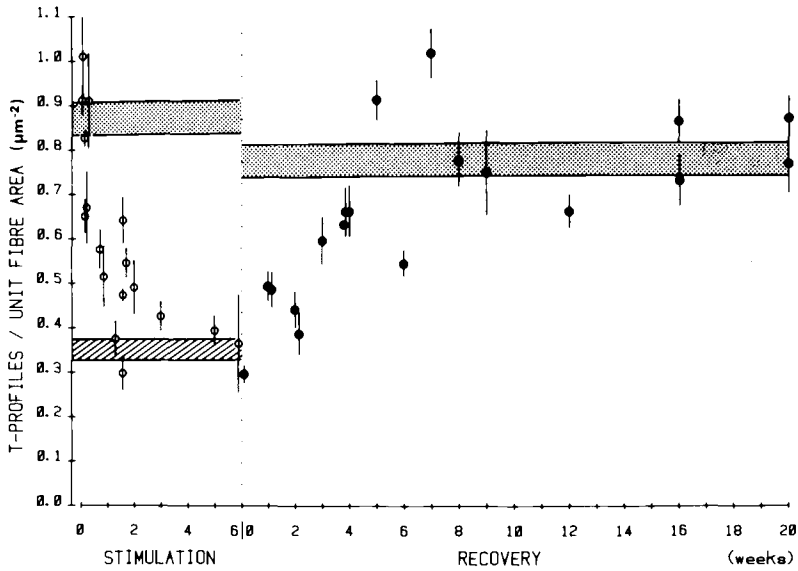

Fig. 15. Time course of changes in extent of T system during chronic low-frequency (10 Hz, 24 h daily) stimulation (*open circles*) and recovery after cessation of stimulation (*filled circles*). Each plot represents mean ± SE of measurements from approximately ten fibers in the left tibialis anterior muscle of one rabbit. Shaded areas, mean ± SE of control data from contralateral fast (*stippled*) or slow (*cross-hatched*) muscles. (From Eisenberg et al. 1984)

and peaks by 2–3 weeks (Fig. 15). At this time, the T-tubule profile becomes similar to that seen in fibers of the slow-twitch soleus muscle (Eisenberg and Salmons 1981; Eisenberg et al. 1984).

As shown by measurements on isolated microsomal fractions, the early structural changes coincide with a progressive reduction in Ca^{2+} uptake by the sarcoplasmic reticulum and a decrease in the activity of Ca^{2+}-ATPase (Ramirez and Pette 1974; Salmons and Sréter 1976; Pette and Heilmann 1977; Heilmann and Pette 1979, 1980; Heilmann et al. 1981; Mabuchi et al. 1982; Wiehrer and Pette 1983; Klug et al. 1983b). A reduction of both Ca^{2+} uptake and Ca^{2+}-ATPase was also revealed by measurements on whole muscle homogenates (Fig. 16; Leberer et al. 1987a; Simoneau et al. 1989; Dux et al. 1990).

The initial rate and maximum capacity of Ca^{2+} uptake by the sarcoplasmic reticulum is reduced by approximately 50% in both rabbit and rat fast-twitch muscles after 1–2 days of low-frequency stimulation (Leberer et al. 1987a; Simoneau et al. 1989). This change is reversed a few days after cessation of stimulation (Leberer et al. 1987a). Quantitative immunochemical measurements show that at

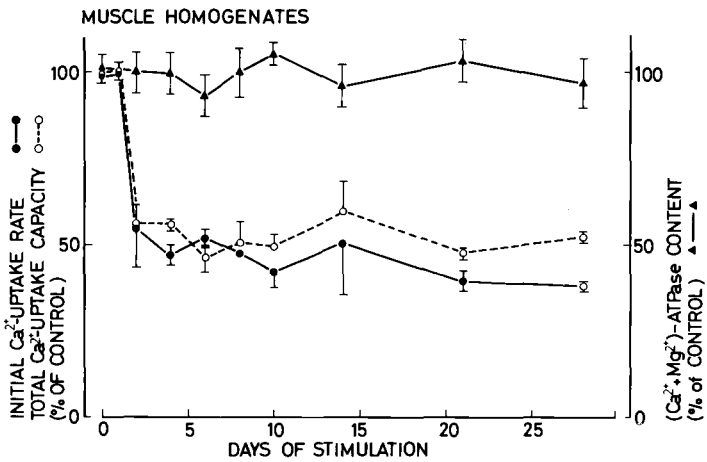

Fig. 16. Time course of changes in initial rate (*filled circles*) and total capacity of Ca^{2+} uptake (*open circles*) of the sarcoplasmic reticulum and of Ca^{2+}-ATPase content (*triangles*) as determined in homogenates of low-frequency stimulated (10 Hz, 12 h daily) extensor digitorum longus muscle of the rabbit. Ca^{2+} uptake was measured with a Ca^{2+}-sensitive electrode. The Ca^{2+}-ATPase content was determined by sandwich enzyme-linked immunosorbent assay. Each time point represents means ± SD from 3–5 independent experiments (animals). The results in the stimulated muscles are given as percentages of the unstimulated contralateral muscles. (From Leberer et al. 1987a)

the time when Ca^{2+} uptake and Ca^{2+}-ATPase activity are reduced the total amount of the Ca^{2+}-ATPase protein is unaltered (Fig. 16; Leberer et al. 1986, 1987a). Taken together, these results indicate that the rapid reduction in Ca^{2+} uptake can be accounted for by a decrease in the specific activity of the sarcoplasmic reticulum Ca^{2+}-ATPase.

The reason for the reduced Ca^{2+}-ATPase activity is not clear, but the inactivation of the enzyme in the stimulated muscle appears to be related to a structural modification in the region close to the first tryptic cleavage site T1 at Arg-505 and the neighbouring binding site for fluorescein isothiocyanate (FITC) at Lys-515 (Leberer et al. 1987a; Dux et al. 1990; Matsushita et al. 1991; Matsushita and Pette 1992). An inactive fraction of Ca^{2+}-ATPase can be separated by density gradient centrifugation from microcrosomal preparations of stimulated muscle. This fraction is characterized not only by its low specific Ca^{2+}-ATPase activity and reduced Ca^{2+} uptake, but by a diminished formation of the phosphorylated intermediate of the enzyme. These data indicate that the inactivation process does not equally affect all Ca^{2+}-ATPase molecules, but is confined to a selected

population of microsomal vesicles. These may originate from the fast-twitch glycolytic fibers that are rapidly fatigued by low-frequency stimulation (Maier and Pette 1987) (see Sect. 2.9).

In long-term (>4 weeks) stimulated rabbit muscles, the total amount of Ca^{2+}-ATPase and its activity may ultimately decrease to values similar to those found for slow-twitch muscle (Pette and Heilmann 1977; Heilmann and Pette 1979, 1980; Heilmann et al. 1981). Accurate estimates of these changes were performed by immunochemical determination of the enzyme protein in whole muscle homogenates with a polyclonal antibody reactive with both fast and slow Ca^{2+}-ATPase isoforms (Leberer and Pette 1986a; Leberer et al. 1986, 1987a).

Data from immunochemically assessed total protein amounts of the sarcoplasmic reticulum Ca^{2+}-ATPase are in apparent contrast with previous findings derived from electrophoretic estimates of total amounts of Ca^{2+}-ATPase in isolated microsomal fractions (Ramirez and Pette 1974; Pette and Heilmann 1977; Heilmann and Pette 1979, 1980; Heilmann et al. 1981; Sarzala et al. 1982; Wiehrer and Pette 1983; Klug et al. 1983b). This discrepancy results from incomplete yields in measurements on microsomal preparations. In addition, microsomal fractions may be contaminated with nonsarcoplasmic membranes. Contamination with nonsarcoplasmic reticulum membranes may also explain to some extent the observed changes in the phospholipid composition of microsomal preparations from low-frequency stimulated rabbit EDL and TA muscles (Sarzala et al. 1982).

In vitro translation assays have indicated that the decrease in Ca^{2+}-ATPase protein in long-term stimulated rabbit muscles is preceded by a reduction in mRNA coding for Ca^{2+}-ATPase (Leberer et al. 1986). In addition, using specific cDNA probes for fast- and slow-type Ca^{2+}-ATPase isoforms, Leberer et al. (1989) showed that chronic stimulation for time periods longer than 4 weeks leads to a progressive exchange of the fast with the slow isoform (Fig. 17). Recently, a fast-to-slow transition of the sarcoplasmic reticulum Ca^{2+}-ATPase has been demonstrated immunochemically in 6–8 weeks' low-frequency stimulated (2 Hz, 24 h/day) latissimus dorsi muscle of the dog (F.N. Briggs et al. 1990; Ohlendieck et al. 1991).

Low-frequency stimulation also induces changes in the composition, and most probably the function, of the sarcoplasmic reticulum related to calsequestrin and phospholamban. Calsequestrin, the major Ca^{2+}-binding protein of the sarcoplasmic reticulum, decreases after prolonged low-frequency stimulation, reaching values charac-

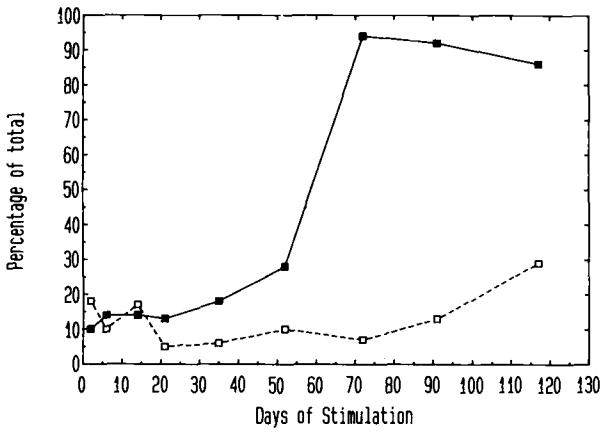

Fig. 17. Time-dependent changes in the levels of mRNA encoding slow/cardiac Ca^{2+}-ATPase in low-frequency stimulated (10 Hz, 12 h daily) and contralateral rabbit extensor digitorum longus muscles. Data are expressed as percentage of the slow/cardiac Ca^{2+}-ATPase mRNA content in normal slow-twitch soleus muscle. *Filled symbols*, stimulated muscle; *open symbols*, contralateral muscle. (From Leberer et al. 1989)

teristic of slow-twitch muscle (Leberer et al. 1986; Leberer and Pette 1986a). In addition, long-term stimulation induces the expression of phospholamban in fast-twitch rabbit muscle (Heilmann and Pette 1980; Leberer et al. 1989). Phospholamban is a regulatory protein of the sarcoplasmic reticulum Ca^{2+}-ATPase in cardiac (Tada and Inui 1983) and slow-twitch muscle (Heilmann and Pette 1980; Jorgensen and Jones 1986). Its expression in rabbit fast-twitch muscle coincides with the appearance of the slow Ca^{2+}-ATPase isoform. Finally, studies conducted by Ohlendieck et al. (1991) on canine skeletal muscle provided evidence that chronic low-frequency stimulation also induces marked changes in the major proteins related to Ca^{2+}-release. Thus, the expression of the ryanodine receptor/Ca^{2+}-release channel from junctional sarcoplasmic reticulum and the transverse tubular dihydropyridine-sensitive Ca^{2+}-channel was greatly suppressed in long-term stimulated muscle. Taken together, the sarcoplasmic reticulum of long-term stimulated fast-twitch rabbit muscle ultimately resembles that of a slow-twitch muscle.

2.5.2 Parvalbumin

Parvalbumin is an acidic, cytosolic Ca^{2+}-binding protein thought to act as a Ca^{2+} buffer and a link in the exchange of Ca^{2+} between TnC and the sarcoplasmic reticulum Ca^{2+}-ATPase (Gillis 1985). It is

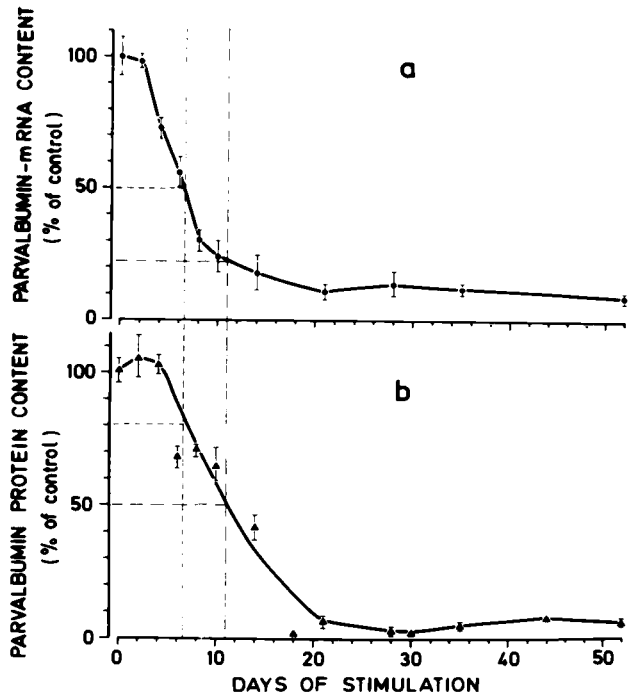

Fig. 18a,b. Time-dependent effects of chronic low-frequency stimulation (10 Hz, 12 h daily) on tissue contents of parvalbumin mRNA (**a**) and parvalbumin protein (**b**) in extensor digitorum longus muscles of the rabbit. Parvalbumin mRNA was quantified in stimulated and contralateral muscles by in vitro translation and immunoprecipitation of the [^{35}S]methionine-labeled translation product. Parvalbumin concentrations were measured in extracts of the same muscles by sandwich enzyme-linked immunosorbent assay. Values represent means ± SE (n = 3–11) or means from two animals and are given as percentages of the contents in the unstimulated contralateral muscles. (From Leberer et al. 1986)

present at high concentrations in fast-twitch fibers of small mammals and hardly detectable in slow-twitch fibers (Celio and Heizmann 1982; Heizmann et al. 1982; Leberer and Pette 1986a). As shown by denervation and cross-innervation experiments, the expression of this protein is under neural control (Leberer and Pette 1986b; Leberer et al. 1987b; Müntener et al. 1987; Leberer and Pette 1990). Low-frequency stimulation suppresses the expression of parvalbumin in fast-twitch muscles of the rabbit (Klug et al. 1983a,b, 1988; Leberer and Pette 1986b; Leberer et al. 1987a) and rat (Bär et al. 1989; Simoneau et al. 1989). In the rabbit, its concentration starts to decrease 4 days after the onset of stimulation, is reduced to 50% by 11 days, and reaches the very low level characteristic of soleus muscle by 21 days (Fig. 18). The time course of its decay parallels that of the

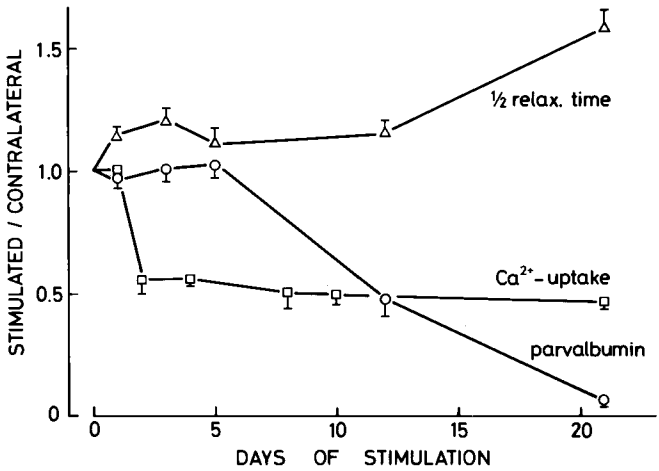

Fig. 19. Time course of changes in half-relaxation time (*½ relax. time*) parvalbumin content, and maximal Ca^{2+}-uptake capacity of the sarcoplasmic reticulum in low-frequency (10 Hz, 12 h daily) stimulated extensor digitorum longus and tibialis anterior muscles of the rabbit. Values are means ± SE (n = 3–8) and expressed as ratios of the values from stimulated versus unstimulated contralateral muscles. (Data are from Leberer et al. 1987a and from Klug et al. 1988)

decrease in type IIB/D fibers (Schmitt and Pette 1991). The decrease in parvalbumin protein is preceded by a reduction in the amount of the specific mRNA (Leberer et al. 1986). Low-frequency stimulated rat fast-twitch muscles also display a rapid decrease in parvalbumin, but this decrease is not as pronounced as in the rabbit (Simoneau et al. 1989). These data are consistent with the observation that even prolonged low-frequency stimulation in the rat induces only a moderate fast-to-slow transformation with the appearance of only some type I fibers (Termin et al. 1989b; M. Delp and D. Pette 1991, unpublished).

The functional consequences of the changes in parvalbumin content correlate with the increases in time to peak, half-relaxation time of the isometric twitch, and increases in the twitch to tetanus ratio observed soon after the onset of low-frequency stimulation (Fig. 19; Klug et al. 1988; Simoneau et al. 1989). All these changes are probably associated with a prolongation of the active state due to the reduced Ca^{2+}-buffering capacity of the cytosol.

2.6 Metabolic Changes

Increased contractile activity imposed upon fast-twitch glycolytic muscle fibers, which during normal locomotion are active only intermittently, causes an increased demand for enhanced energy supply.

Because fast-twitch glycolytic fibers are usually not exposed to sustained activity, this demand can only be met by a transition from anaerobic to aerobic energy metabolism. It is, therefore, not surprising that an important change which occurs in fast-twitch muscle subjected to chronic low-frequency stimulation consists of alterations in the activity and isozyme patterns of enzymes of energy supply.

2.6.1 Fuel Supply

Contractile activity of fast muscle leads to a well-known functional vasodilatation during which the blood flow increases approximately fivefold (Hilton et al. 1970). An additional change in the vascular bed is an increase in capillary density (see Sect. 2.2), which enables the working muscle to further increase perfusion and oxygen supply (Hudlická et al. 1977). An almost twofold increase in resting oxygen consumption has been found in 28-day low-frequency stimulated rabbit EDL, TA, and peroneal muscles. During contractile activity, higher than normal values for oxygen consumption have been found after only 14 days of stimulation and continue to increase thereafter (Hudlická et al. 1977, 1980). Two- to fourfold increases in blood flow and oxygen extraction in resting and contracting cat gracilis muscle were seen after 14–28-day low-frequency stimulation (Hoppeler et al. 1987). The elevated oxygen extraction may be aided by the higher myoglobin content found in chronically stimulated fast-twitch muscles of rabbit (Pette et al. 1973) and rat (Kaufmann et al. 1989). Consistent with this increase is a 15-fold augmentation of the myoglobin mRNA content in rabbit fast-twitch muscle (Underwood and Williams 1987).

In unstimulated rabbit fast-twitch muscle, there is a fourfold increase of glucose uptake during contractile activity imposed by short-term (10 min) low-frequency (4 Hz) stimulation. In muscles that had previously been subjected to chronic low-frequency (10 Hz, 28 days) stimulation, the glucose uptake at rest or during contractile activity is similar to that of unstimulated muscles (Hudlická et al. 1980). Conversely, in the same experiments a threefold increase in the consumption of free fatty acids was seen in contracting muscles that had previously been exposed for 28 days to chronic low-frequency stimulation (Hudlická et al. 1980). Increased fatty acid consumption may be facilitated by an improved transport capacity of fatty acids (Fig. 20). Indeed, chronic low-frequency stimulation leads to a 3.5-fold rise of the cytosolic fatty acid-binding protein in rat TA muscle within 21 days (Kaufmann et al. 1989). The expansion of the extracellular space, as indicated by a sixfold increase in the chloride

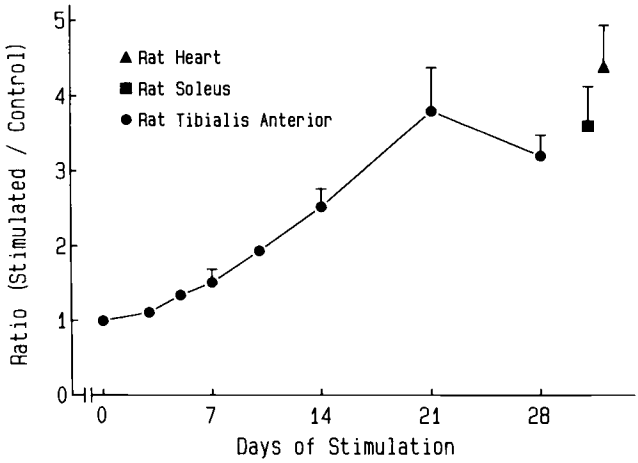

Fig. 20. Increase in fatty acid-binding protein of low-frequency stimulated (10 Hz, 10 h daily) rat tibialis anterior (TA) muscle. Values (means ± SE, n = 4–5) in the stimulated muscle, as well as in heart and soleus muscle, have been referred to the values in the unstimulated contralateral TA muscle. (Modified from Kaufmann et al. 1989)

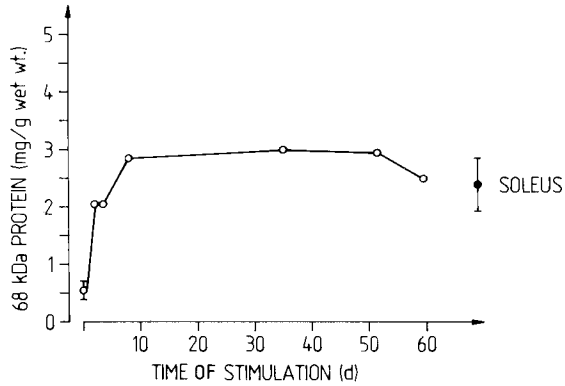

Fig. 21. Increase in albumin (68-kDa protein) content of low-frequency stimulated (10 Hz, 12 h daily) rabbit tibialis anterior muscle. Values are means from measurements on two animals per time point or means ± SD (zero time and soleus) from five animals. (From Heilig and Pette 1988)

space (Henriksson et al. 1986) and a five- to sixfold elevation of the albumin concentration (Heilig and Pette 1988) in chronically low-frequency stimulated rabbit EDL and TA muscles, may further facilitate substrate supply and metabolite exchange (Fig. 21).

2.6.2 Enzymes of Energy Metabolism

Chronic low-frequency stimulation induces a thorough rearrangement of the enzyme activity pattern of energy metabolism (Pette et al. 1972, 1973). The overall change consists of an enhanced

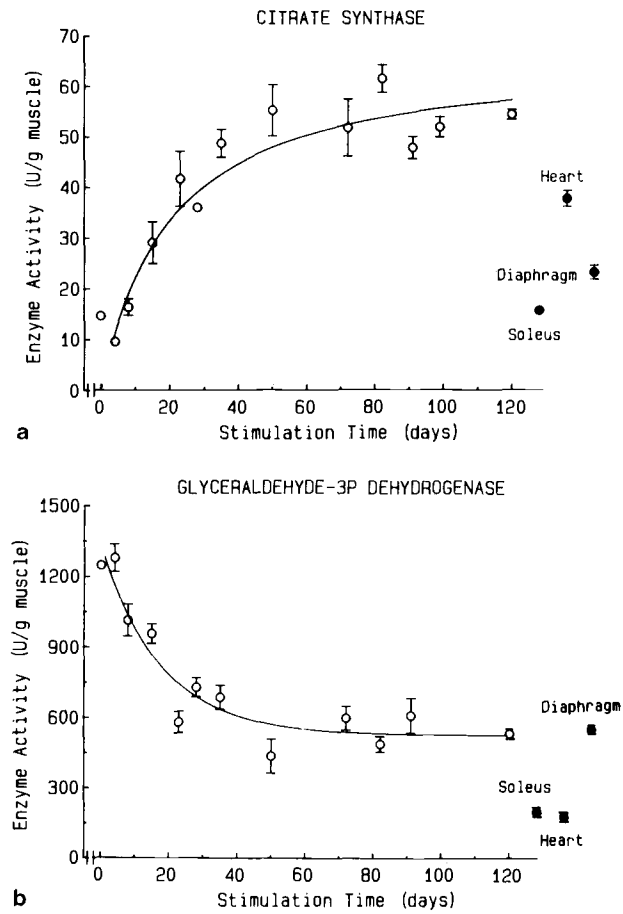

Fig. 22a,b. Time course of changes in the activity levels of two representative enzymes of aerobic (citrate synthase) and anaerobic (glyceraldehyde phosphate dehydrogenase) energy metabolism in rabbit tibialis anterior muscle as induced by chronic low-frequency stimulation (10 Hz, 12 h daily). For comparison, activities of the two enzymes were also determined in the diaphragm, soleus, and cardiac muscles. Values (means ± SE, n = 3–5) are from Hood and Pette (1989) and unpublished data (D. Pette 1990)

aerobic-oxidative capacity of the stimulated muscle due to severalfold increases in enzyme activities of aerobic-oxidative pathways (the citric acid cycle, fatty acid oxidation, ketone body utilization, respiratory chain) and concomitant decreases in enzyme activities of glycogenolysis and glycolysis, as well as of extramitochondrial transfer of energy-rich phosphates (adenylate kinase, MM creatine kinase). As shown in the rabbit, the stimulation-induced increases in enzymes of aerobic-oxidative pathways may reach values in the range or even above those found in cardiac muscle (Fig. 22).

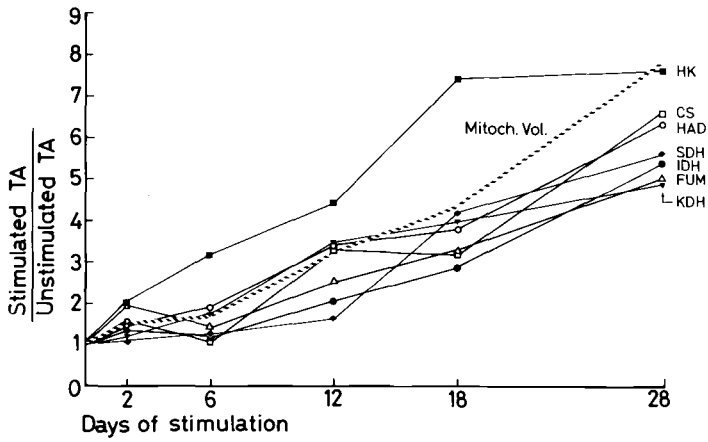

Fig. 23. Time course of changes in volume density of total mitochondria (*dashed line*) and in enzyme activities of the superficial portion of rabbit tibialis anterior (*TA*) muscle in response to chronic low-frequency stimulation (10 Hz, 12 h daily). Volume density of mitochondria and enzyme activities are given as ratios of stimulated versus unstimulated muscles. Abbreviations: CS, citrate synthase, FUM, fumarase HAD, 3-hydroxyacyl CoA dehydrogenase; HK, hexokinase; IDH, isocitrate dehydrogenase; KDH, ketoglutarate dehydrogenase; SDH, succinate-cytochrome *c* reductase. (Modified from Reichmann et al. 1985)

These findings have been confirmed and extended in more detailed studies (Pette et al. 1975, 1976; Heilig and Pette 1980; Klug et al. 1983b; Buchegger et al. 1984; Hudlická et al. 1984; Pette 1984; Reichmann et al. 1985, 1991; Schmitt and Pette 1985; Chi et al. 1986; Henriksson et al. 1986; U. Seedorf et al. 1986; R.S. Williams et al. 1986; Simoneau and Pette 1988a,b, 1989; Kaufmann et al. 1989; Hood and Pette 1989; Hood et al. 1989; Simoneau et al. 1990; Weber and Pette 1988, 1990a,b; Annex et al. 1991). A time course study has revealed that the activities of the enzymes of the citric acid cycle increase in parallel in low-frequency stimulated rabbit fast-twitch muscles (Fig. 23; Reichmann et al. 1985). This was also shown for enzymes involved in fatty acid transport and oxidation (palmitoyl-CoA transferase, 3-hydroxyacyl-CoA dehydrogenase, 3-ketoacyl-CoA thiolase) and enzyme activities representative of the respiratory chain complexes (NADH cytochrome *c* reductase, succinate-cytochrome *c* reductase, cytochrome *c* oxidase; Reichmann et al. 1991).

The extent of the stimulation-induced changes in the enzyme activity pattern of terminal substrate oxidation may be inversely related to the basal levels of these enzymes in different animal

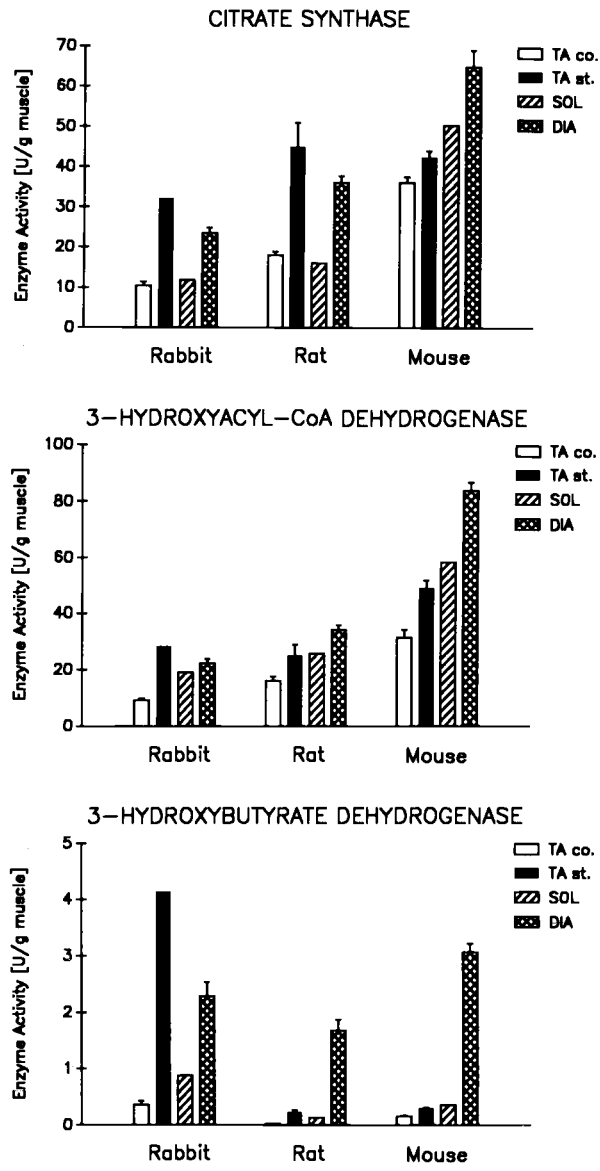

Fig. 24. Total activities (means ± SE) of citrate synthase, 3-hydroxyacyl-CoA dehydrogenase, and 3-hydroxybutyrate dehydrogenase in low-frequency stimulated (10 Hz, 10 h daily, 28 days) and control TA muscles of rabbit, rat and mouse. For comparison, data are given also for diaphragm (DIA) and soleus muscles of the same animals. (Data from Simoneau and Pette 1988a,b and D. Pete, unpublished results)

species. This is supported by results obtained from a comparative study which show that TA muscles of the mouse, rat, guinea pig, and rabbit respond differently to the same stimulation protocol (10 Hz, 10 h/day, for 28 days; Simoneau and Pette 1988a,b, 1989). Mouse TA muscle, which has the highest levels of these enzymes, changes the least (10%–50% increases), whereas rabbit TA muscle, with

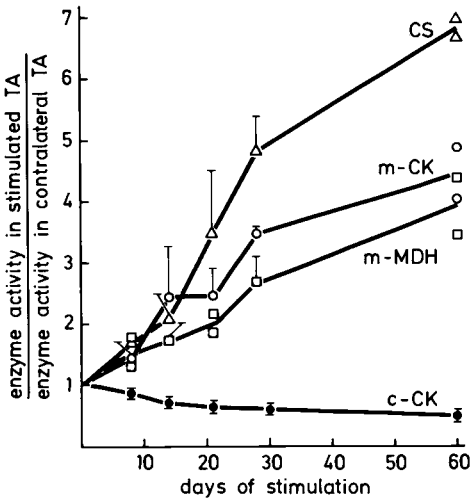

Fig. 25. Time course of changes in the activity levels of mitochondrial (*m-CK*) and cytosolic (*c-CK*) creatine kinase, mitochondrial citrate synthase (*CS*) and malate dehydrogenase (*m-MDH*) as induced by chronic low-frequency stimulation (10 Hz, 12 h daily) in rabbit tibialis anterior (*TA*) muscle. Enzyme activities (means ± SD, $n = 3$) are given as ratios of stimulated versus unstimulated muscles. (From Schmitt and Pette 1985)

the lowest initial levels, displays the greatest increases (more than threefold; Fig. 24). In mouse muscle, the stimulation-induced increases in these enzyme activities do not even reach the values found in soleus muscle or in the diaphragm, whereas in the rabbit much higher levels are attained in the stimulated TA muscle than in these normally "oxidative" muscles (Fig. 24). In larger animals with high basal activities of enzymes of aerobic-oxidative metabolism, i.e., the dog (Acker et al. 1987c; Ianuzzo et al. 1990a,b), sheep (U. Carraro and D. Pette 1990, unpublished), and calf (N. Guldner and D. Pette 1991, unpublished), chronic stimulation induces much smaller increases of these enzymes. Since these studies were performed on the latissimus dorsi muscle, a direct comparison with rabbit EDL and TA muscles may not be justified. Nevertheless, it appears that the initial activity levels of enzymes involved in aerobic-oxidative metabolism are related to the extent of the change that can be induced.

The increases in enzyme activities of the main pathways of substrate end-oxidation are also highest in the superficial portion of rabbit TA muscle, which is composed mainly of fast-twitch glycolytic fibers. In these fibers, the increase in enzyme activities of the citric acid cycle and fatty acid oxidation was six- to sevenfold (Fig. 23; Reichmann et al. 1985). The extent of this increase is so great that the oxidative capacity of the fast-twitch muscle transformed by chronic low-frequency stimulation by far exceeds that of a normal slow-twitch muscle. In the rabbit, chronic low-frequency stimulation thus induces a unique metabolic enzyme profile (Hood and Pette

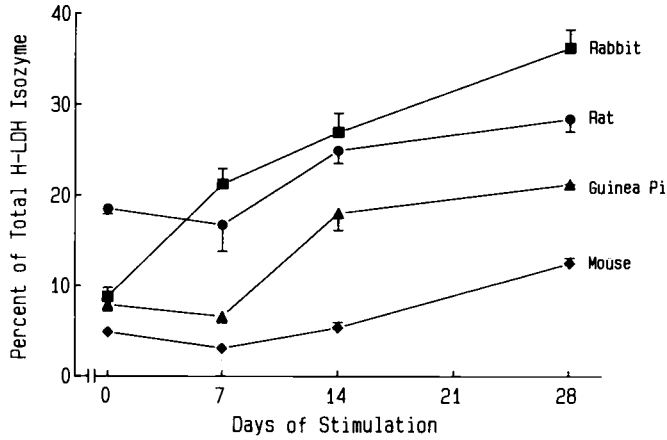

Fig. 26. Species-specific changes in the percentage of the H-subunit of lactate dehydrogenase (*H-LDH*) in low-frequency stimulated tibialis anterior (10 Hz, 10 daily) muscles of mouse, rat, guinea pig, and rabbit. Values are means ± SD (n = 3–4 animals). (From Simoneau and Pette 1989)

1989; see Fig. 22). These observations are consistent with the proposal that the extent of the induced changes in enzyme activities of aerobic-oxidative metabolism is inversely related to their initial levels before the onset of stimulation (Simoneau and Pette 1988a).

In parallel with these changes, there is an augmentation (six- to sevenfold) in mitochondrial volume density which may reach a value of 20% in the superficial portion of rabbit TA muscle (Fig. 23; Reichmann et al. 1985). The amount of total mitochondrial DNA increases five- to sevenfold in 21-day stimulated rabbit EDL and TA muscles (R.S. Williams et al. 1986). Not only does chronic low-frequency stimulation increase the mitochondrial volume density (Eisenberg and Salmons 1981; Reichmann et al. 1985; Hoppeler et al. 1987; Hudlická et al. 1987), but, as shown in rabbit muscle, it alters the enzymatic composition of the mitochondria. In contrast to a pronounced decrease in the cytosolic MM-creatine kinase, there is a severalfold increase in mitochondrial creatine kinase activity (Schmitt and Pette 1985), the key enzyme of the creatine phosphate shuttle (Fig. 25). Glycerol phosphate oxidase, a membrane-bound mitochondrial component of the glycerol phosphate cycle, decreases in parallel with the reduction of the extramitochondrial glycolytic enzyme activities (Pette et al. 1973, 1976; Heilig and Pette 1980; Reichmann et al. 1985). In addition, disproportionate increases are found for enzymes involved in ketone body utilization, e.g., the activity of 3-hydroxybutyrate dehydrogenase, a membrane-bound

mitochondrial enzyme, which increases up to 30-fold in the superficial rabbit TA muscle (Reichmann et al. 1985). The increase in this enzyme activity is most pronounced in the rabbit, smaller in rat, and does not occur in mouse. In view of the high activity levels of 3-hydroxybutyrate dehydrogenase in the diaphragms of these animals, the different effects of chronic low-frequency stimulation on the activity level of this enzyme in the TA muscles represent species-specific responses. It remains to be shown whether these changes reflect alterations within the existing population of mitochondria or whether low-frequency stimulation induces the formation of a mitochondrial population with a specific enzymatic composition.

Chronic low-frequency stimulation also induces changes in the isozyme pattern of metabolic enzymes. This has been demonstrated for two particular enzymes, phosphorylase kinase (Lawrence et al. 1986) and lactate dehydrogenase (Pette et al. 1973; Heilig and Pette 1980; Hudlická et al. 1984; U. Seedorf et al. 1986; Hood and Pette 1989; Simoneau and Pette 1989). In the case of phosphorylase kinase, the enzyme activity was reduced by 80% in 10-week stimulated rabbit TA muscle and the isozyme pattern shifted in the direction of a muscle with a high percentage of fast-twitch oxidative or slow-twitch oxidative fibers (Lawrence et al. 1986). The changes in lactate dehydrogenase (LDH) consist of increases in H-subunit-based isozymes, especially of LDH-1, LDH-2, and LDH-3, and decreases of the M-subunit-based isozymes, i.e., LDH-4 and LDH-5 (Pette et al. 1973; Hudlická et al. 1984; U. Seedorf et al. 1986; Hood and Pette 1989; Simoneau and Pette 1989). This shift in the LDH subunit composition is explained by increases in the protein amount of the H subunit and decreases in the protein amount of the M subunit (U. Seedorf et al. 1986). These alterations are preceded by decreases in the amount of mRNA encoding the M-LDH subunit and increases in the amount of mRNA encoding the H-LDH subunit (U. Seedorf et al. 1986). Comparative studies on several small mammals have shown that the stimulation-induced changes in the LDH isozyme pattern also occur in a species-specific manner (Fig. 26; Simoneau and Pette 1989). Rabbit TA muscle responds with a fourfold increase in the percentage of the H-LDH subunit, mouse TA shows only a twofold increase, and rat and guinea pig behave intermediately. Thus, the increase in H-LDH subunit is more pronounced in muscles which initially have a low than in muscles which initially have a high aerobic-oxidative capacity (Simoneau and Pette 1989).

Rearrangements of the enzyme pattern have been correlated in several cases with alterations of specific mRNAs. In chronically

stimulated rabbit EDL and TA muscles, the reductions in glycolytic enzyme activities, e.g., aldolase and glyceraldehyde phosphate dehydrogenase, are related to decreases in the amounts of their mRNAs (R.S. Williams et al. 1986, 1987; Hood et al. 1989). Conversely, increases in mitochondrial citrate synthase (U. Seedorf et al. 1986; R.S. Williams 1986; R.S. Williams et al. 1986; Annex et al. 1991) and mitochondrial cytochrome *b* (R.S. Williams et al. 1987) correspond to increases in these mRNAs. Increases in cytochrome *c* oxidase, an enzyme composed of nuclear-encoded and mitochondrial-encoded subunits, relate to elevations in both nuclear (R.S. Williams et al. 1987; Hood et al. 1989) and mitochondrial (Hood et al. 1989) mRNAs. The parallel increases in mRNAs of the mitochondrial-encoded subunit III and the nuclear-encoded subunit VIc suggest a coordinated expression of mitochondrial and nuclear genomes under these conditions (Fig. 27; Hood et al. 1989, 1992).

A time course study of the increase in citrate synthase showed a slight increase in enzyme activity which preceded the increase in its mRNA (U. Seedorf et al. 1986). Since the amount of cytosolic monosomes and polysomes was already elevated by this time, the early increase in citrate synthase could have resulted from enhanced translation of the preexisting messenger. The later and steeper increase in citrate synthase, which coincided with a steep rise in mRNA, was most likely caused by both enhanced transcription and translation (U. Seedorf et al. 1986).

One of the earliest changes in the enzyme pattern is a steep increase in hexokinase (HK) activity (Pette et al. 1972, 1973). This increase could indicate that glucose phosphorylation is a limiting step under the conditions of sustained contractile activity imposed on a fast-twitch muscle. The increase in HK is first noted after 2 days, and by 2 weeks HK is seven- to tenfold higher in low-frequency stimulated rabbit fast-twitch muscle than in control muscle (Reichmann et al. 1985; Chi et al. 1986; Henriksson et al. 1986). The elevation in total HK activity can be accounted for by an increase in HK isozyme II (Pette et al. 1973). An even higher increase (14-fold after 2 weeks) in total HK activity is induced by chronic low-frequency stimulation in rat TA muscle (Fig. 28). However, much smaller increases in HK activity than in rat and rabbit are observed in chronically stimulated TA muscles of mouse and guinea pig (Simoneau and Pette 1988a,b). The increase in HK activity can be fully accounted for by enhanced HK II synthesis which results in an increase in the amount of HK II protein (Weber and Pette 1988, 1990a,b; Fig. 28). Significant increases in the rate of HK II synthesis are detected as early as 2 h

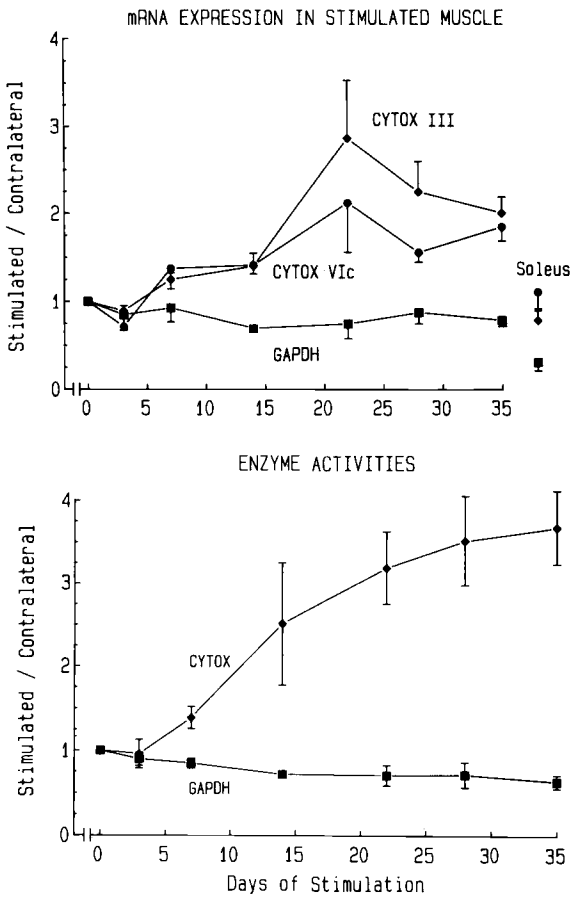

Fig. 27. Comparison of time courses of changes in specific mRNAs (**a**) with corresponding enzyme activities (**b**) as induced by chronic low-frequency stimulation (10 Hz, 10 h daily) in rat tibialis anterior muscle. Data (means ± SE, $n = 3–4$ for each time point) are given as ratios of stimulated muscles versus contralateral muscles. For comparison, values from soleus muscle have been included. Abbreviations: *CYTOX*, cytochrome c oxidase; *CYTOX III*, mitochondrial-encoded subunit; *CYTOX VIc*, nuclear-encoded subunit; *GAPDH*, glyceraldehyde phosphate dehydrogenase. (From Hood et al. 1989)

after the onset of stimulation (Pette et al. 1991; S. Hoffmann and D. Pette 1991, unpublished). In addition to the rise in HK II protein, chronic low-frequency stimulation induces an increase in the fraction of the mitochondrial-bound form of this enzyme, thus enhancing the coupling of glucose phosphorylation to the mitochondrial ATP-generating system (Weber and Pette 1990b). Low-frequency stimulation also enhances the synthesis of the GLUT-4 glucose transporter. In addition, it enhances its translocation into the sarcolemma membrane (S. Hofmann and D. Pette, 1992, unpublished).

The stimulation-induced increase in HK II is transient in both rabbit (Henriksson et al. 1986) and rat (Weber and Pette 1988, 1990b), for, after 3 weeks of stimulation, the enzyme activity declines (Fig. 28). This can be accounted for by reduced enzyme synthesis (Weber and Pette 1990a; S. Hoffmann and D. Pette 1991, unpublished). The rate of decline in HK II with ongoing low-frequency

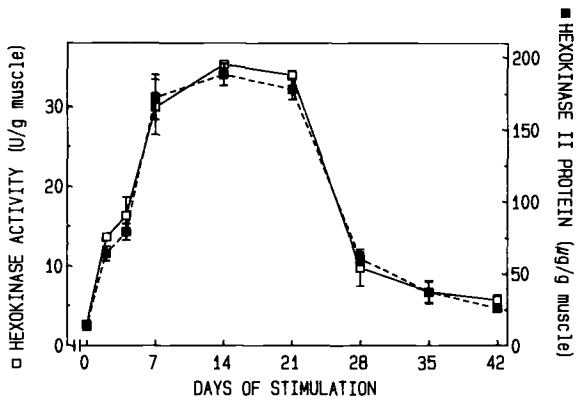

Fig. 28. Time course of stimulation-induced (10 Hz, 10 h daily) changes in total hexokinase activity (□) and immunochemically determined tissue contents of hexokinase isozyme II protein (■) in rat tibialis anterior muscle. Values represent means ± SE (n = 5). (From Weber and Pette 1990b)

stimulation (>3 weeks) is similar to that seen after cessation of stimulation (Weber and Pette 1990a,b). This indicates that the decay of HK II after longer periods of stimulation occurs as a result of an abrupt change in gene expression which returns the HK II synthesis to normal steady-state conditions. This may be related to the fact that energy metabolism, which is initially based upon glucose catabolism, eventually changes to fatty acid catabolism as a result of the meanwhile increased aerobic-oxidative potential in chronically stimulated muscle.

Finally, the literature contains information on an enzyme, carbonic anhydrase III (CAIII), the function of which in muscle is poorly understood (Gros and Dodgson 1988), but which may be implicated in excitation-contraction coupling by an effect on Ca^{2+} transients (Wetzel et al. 1990). Carbonic anhydrase III is present only in type I fibers (for review see Pette and Staron 1990). Pronounced increases (up to 15-fold) were observed in chronically stimulated rabbit EDL and TA muscles (Gros and Dodgson 1988). This increase occurred only after 3 weeks of stimulation, i.e., later than the increases in mitochondrial enzyme activities. The increase in CAIII activity correlated with that of its mRNA and its immunochemically determined protein in chronically stimulated rabbit EDL and TA muscles (Brownson et al. 1988). The observation that chronic low-frequency stimulation does not induce CAIII, neither at the mRNA nor at the protein level, in rat TA muscle is consistent with the lack of conversion to type I fibers in this species (Jeffery et al. 1990).

2.6.3 Metabolites

A time course study on changes in several metabolites of energy metabolism was performed in low-frequency stimulated rabbit TA muscle (Green et al. 1990, 1992). The changes induced by such increased contractile activity occur in three stages. First, within 15 min there is a marked reduction in ATP (50%–60%), phosphocreatine (60%), and glycogen (70%–80%), an approximately threefold increase in glucose, and a ten fold increase in lactate. Next, a period extending to 4 days of stimulation is characterized by a nearly complete recovery of ATP and phosphocreatine, low lactate, and an overshoot in glycogen content. The glycogen depletion, followed by an overshoot, had previously been noticed in low-frequency stimulated rabbit TA muscle by single fiber analysis (Maier and Pette 1987). During the succeeding phase, extending to 50 days, the metabolite profile approaches that of a slow-twitch muscle with moderate reductions in total adenine nucleotides, total creatine, ATP, phosphocreatine, and glycogen. Anaerobic glycolysis as indicated by the muscle lactate concentration, remains at low levels. These late changes are in agreement with data reported by Henriksson et al. (1988, 1990). Unfortunately, their study did not include the crucial early time points during which many of the most dramatic changes take place (Green et al. 1990, 1992). A similar study performed on low-frequency stimulated rat gastrocnemius–plantar muscles investigated in detail the changes in metabolite levels immediately after the onset (1 min) up to 180 min of stimulation (Hood and Parent 1991). In that study, similar changes were observed in the tissue contents of glycogen, lactate, phosphocreatine, ATP, adenosine diphosphate (ADP), and AMP as in the study on low-frequency stimulated rabbit TA (Green et al. 1990, 1992; Pette et al. 1991), i.e., rapid decreases in glycogen, phosphocreatine, and ATP concomitant with transient increases in lactate, free ADP (ADP_f), and AMP.

The time course of the changes during the first 2 days reveals an impressive capability of the muscle to recover from an initial, dramatic disturbance of energy metabolism (Green et al. 1990, 1992). Alterations in the metabolite profile occur almost immediately after the onset of stimulation, but only some of these changes persist with ongoing stimulation. These may be important in triggering long-lasting processes of metabolic and fiber-type transformation. In this context, the persistently depressed phosphorylation potential of the adenylic acid system, i.e., the reduced $ATP/(ADP_f \times Pi_f)$ ratio,

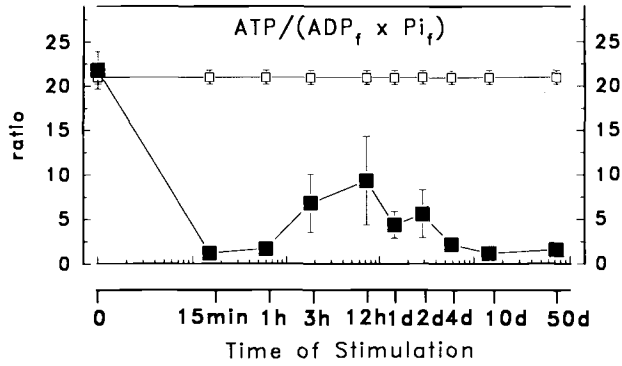

Fig. 29. Time course of changes in the ratio $ATP/(ADP_f \times Pi_f)$ in rabbit tibialis anterior muscle during continuous (24 h daily) 10 Hz stimulation ■, □, control. (Modified from Pette et al. 1991)

might be of special importance (ADP_f and Pi_f represent the concentrations of free ADP and free inorganic phosphate) (Fig. 29; Green et al. 1992; Pette et al. 1991).

Another interesting change, occurring soon after the onset of chronic low-frequency stimulation in rabbit fast-twitch muscle, is an increase in two important regulatory metabolites of carbohydrate metabolism (Green et al. 1991), glucose-1,6-bisphosphate (Glc-1,6-P_2) and fructose-2, 6-bisphosphate (Fru-2,6-P_2). Both of these effectors begin to increase 3 h after the onset of stimulation, reach maxima at 12–24 h (three fold for Glc-1,6-P_2, five fold for Fru-2,6-P_2), and decay after stimulation periods longer than 4 days. The fact that their increases coincide with the replenishment of glycogen after its intial depletion could indicate that Glc-1,6-P_2 and Fru-2,6-P_2 have, in addition to their regulatory effects in glycolysis and gluconeogenesis (for review see Beitner 1990), a role in glycogen metabolism (Green et al. 1991).

2.7 Time Course of Stimulation-Induced Changes

The stimulation-induced effects described so far have all been from experiments based on chronic low-frequency stimulation. Comparisons between various regimes of low-frequency stimulation, such as daily amount of treatment or frequency, are rare. It is likely that in the rabbit 8 h stimulation per day will produce different results than 24 h (Pette et al. 1976). Firstly, 8 h of stimulation cover only one

third of the 24 h stimulation period and, secondly, this protocol gives the muscle time to recover in between. The final outcome of changes using either method may, however, be ultimately similar after long-term periods of stimulation. The possibility exists that different time periods of stimulation are necessary to induce the same change in particular strains of rabbit. This makes comparisons of the results from different laboratories difficult. Even in animals from the same strain individual variations exist between the changes induced with identical stimulation protocols (e.g., Salmons and Vrbová 1969; Pette et al. 1973, 1976; Heilmann and Pette 1979; W.E. Brown et al. 1983; K. Seedorf et al. 1983; Staron et al. 1987; Maier et al. 1988; Termin et al. 1989b; see also Mabuchi et al. 1990). The reason for this variability is difficult to trace. It may be that the muscle characteristics of individual rabbits differ before stimulation commences so that they start from different basal levels. Other reasons may relate to the procedure of electrode implantation and changes associated with it. Even when great care is taken to place the electrodes at similar positions, small displacements, caused by movements of the conscious animal, as well as variable encapsulation of the electrodes by connective tissue, may cause individual variations in the efficiency of stimulation. Moreover, the activation of antagonists either by current spread or by intentional movements of the animal may alter the mechanical conditions of the limb during chronic stimulation. Some rabbits prefer to press the foot of the stimulated leg against the bottom of the cage, whereas others remain in a position that allows muscle shortening and movements of the paw. Such mechanical differences could have an impact on the degree of stimulation-induced changes. Several studies have shown that chronic low-frequency stimulation of rabbit fast-twitch muscle is more efficient when the stimulated muscles are kept in a stretched position (G. Goldspink 1985; Cotter and Phillips 1986; P. Williams et al. 1986). Therefore, in view of these variables it is not always easy to evaluate the exact time course of events in long-term stimulation experiments. Nevertheless, some time-linked patterns of change emerge.

Immediately after the onset of stimulation, there are dramatic changes in energy-rich phosphates and a pronounced depression of the energy charge (Fig. 29), as well as reductions of glycogen and other metabolites of energy metabolism (Maier and Pette 1987; Green et al. 1990, 1992; Hood and Parent 1991). Among the early changes are also those related to intracellular calcium. The decrease in Ca^{2+} uptake by the sarcoplasmic reticulum (Fig. 16), due to the partial inactivation of the sarcoplasmic reticulum Ca^{2+}-ATPase,

begins a few hours after the onset of stimulation (Dux et al. 1990). This may explain the severalfold increase in free [Ca^{2+}] observed by Sréter et al. (1987). These changes are followed by a reduction in parvalbumin content during the first week (Fig. 18; Klug et al. 1983a,b; Leberer et al. 1986; Simoneau et al. 1989).

The enhanced synthesis of HK II (Weber and Pette 1988, 1990a,b) occurs within the first hours. The elevated synthesis of this key enzyme for glucose phosphorylation in muscle may be causally related to the pronounced increase in glucose concentration of stimulated muscle (Green et al. 1990, 1992). Cessation of stimulation has an almost immediate effect on the rate of HK synthesis which decreases to normal values within 15 h (Weber and Pette 1990a).

Another early event in low-frequency stimulated fast-twitch muscle is an enhanced translational capacity and efficiency resulting from pronounced increases in monosomes and polysomes (Fig. 30; U. Seedorf et al. 1986). An approximately twofold increase in monosomes after 2 days of stimulation precedes the rise in both total RNA and poly(A^+)RNA (Pette 1984; U. Seedorf et al. 1986). Increases in total RNA and ribosome yield are detectable after 3–4 days and reach maxima (three- to fivefold increases) between 14 and 21 days (Fig. 30; Pette 1984; U. Seedorf et al. 1986). Interestingly, metabolites and enzymes of the polyamine pathway, including ornithine decarboxylase, are subject to pronounced transient increases in rabbit fast-twitch muscles during day 1–4 of low-frequency stimulation (Mastri et al. 1982). Ornithine decarboxylase, together with high amounts of polyamines, are thought to enhance ribosomal RNA synthesis (Russell 1983; Tabor and Tabor 1984).

An increase in perfusion capacity due to growth of new capillaries commences within the first 4 days (M.D. Brown et al. 1976; Hudlická et al. 1977, 1982b; Myrhage and Hudlická 1978). At the same time, activities and expression of enzymes involved in anaerobic metabolic pathways begin to decrease and those of aerobic-oxidative metabolism begin to increase.

The changes in myosin composition fall into two categories, i.e., the initial HCIIb → HCIId → HCIIa transitions and the ultimate fast-to-slow transition, i.e., the exchange of HCIIa with HCI. The time course of the rearrangement of the fast myosin HC isoform pattern has been elucidated for rat fast-twitch muscle (Termin et al. 1989b). However, the time course remains to be studied in more detail in the rabbit, especially in view of the HCIId → HCIIa transition (see Sect. 2.4.1). In our opinion, previous studies, including our own, have distinguished neither between type IIB and type IID

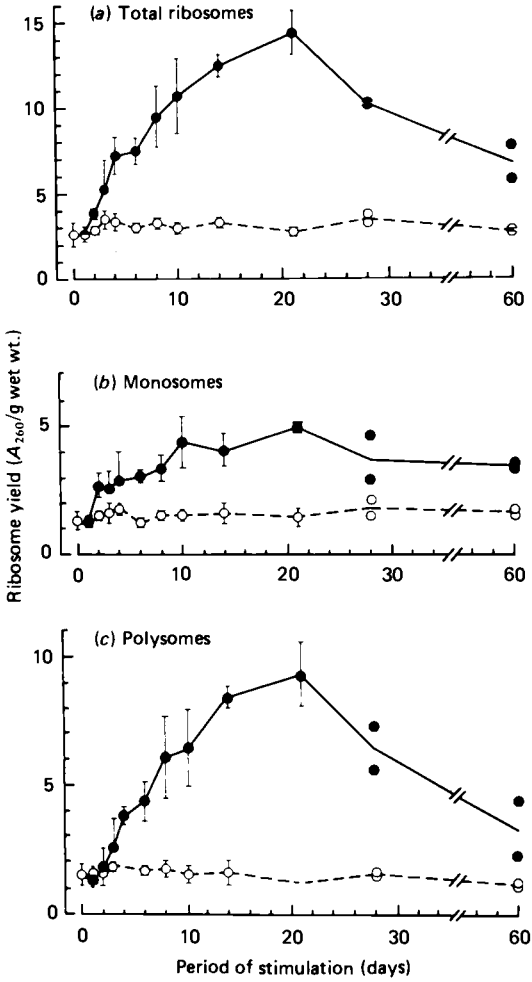

Fig. 30. Time course of changes in the yield of total ribosomes, monosomes, and polysomes from contralateral (○) and low-frequency (●; 10 Hz, 12 h daily) stimulated rabbit tibialis anterior muscles. (From U. Seedorf et al. 1986)

fibers nor between the MHC isoforms HCIIb and HCIId. The type IID fibers, which represent the major fraction in rabbit leg muscles may have erroneously been classified as type IIB fibers because it is difficult to distinguish fiber types IIB and IID by the conventional mATPase histochemistry. The electrophoretic separation of the MHC isoform HCIId has only recently been achieved (D. Pette et al. 1991, unpublished), and, therefore, previous electrophoretic studies have been unable to take this isoform into consideration. The expression of slow myosin in low-frequency stimulated rabbit EDL and TA muscles of rabbit begins only after stimulation periods longer than 3–4 weeks. Long stimulation periods lead to progressive in-

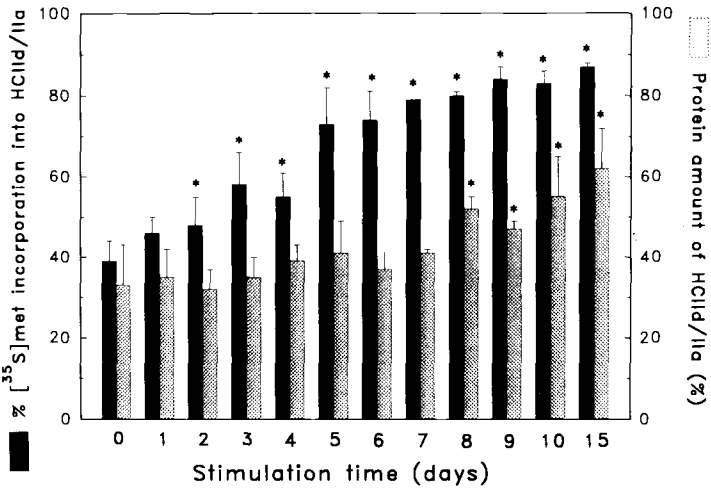

Fig. 31. Evaluation of relative protein amounts (*hatched columns*) and [^{35}S]methionine (*[^{35}S]met*) incorporation (*black columns*) into myosin HC isoforms *HCIId/IIa* in rat tibialis anterior muscle stimulated for different time periods. For both [^{35}S]methionine incorporation and protein data the sum of HCIIb + HCIId/IIa was set equal 100%. Values are means ± SD (n = 3–6 animals per time point). Changes with regard to zero time point were significant with $p < 0.05$ (marked by *asterisks*). (From Termin and Pette 1992)

creases in HCI. This isoform predominates after stimulation periods longer than 30 days of continuous (24 h/day) low-frequency stimulation (W.E. Brown et al. 1983; Staron et al. 1987; Franchi et al. 1990).

Detailed studies have elucidated the time course of the rearrangement of the fast-type MHC isoforms in rat fast-twitch muscles. Although the protein pattern of the MHC isoforms is unaltered during the first week of chronic low-frequency stimulation, changes in MHC isoform expression occur as early as 2 days after the onset of stimulation (see Fig. 10). Decreases in the amount of the mRNA encoding myosin HCIIb followed by increases in the amount of HCIIa mRNA are detectable at 2 days (Kirschbaum et al. 1989c, 1990b). These changes at the mRNA level coincide with a reduced HCIIb protein synthesis and an enhanced synthesis of HCIId/HCIIa (Fig. 31; Termin and Pette 1992). However, significant changes in the MHC composition of the muscle are first seen at day 8. This delay suggests that the newly synthesized heavy chain isoforms (HCIId and HCIIa) are rapidly turned over and are not inserted immediately into the thick filament. It is likely that the myosin HCIIb isoform, which is no longer synthesized, must be degraded before the newly formed isoforms HCIId and HCIIa can be inserted into the sarcomere. This

matches the half-life of HCIIb which is approximately 15 days (Termin and Pette 1992). Thus, protein degradation could be an important posttranslational regulatory step determining the remodeling of the thick filament (Termin and Pette 1992).

The time course of the rearrangement of the thin filament proteins in rabbit EDL and TA muscles differs between TnT on the one hand and TnI and TnC on the other hand. While the sequential exchange of the various fast TnT isoforms (TnT_{1f}, TnT_{2f}, TnT_{3f}, TnT_{4f}) appears to follow that of the various fast MHC isoforms (Schmitt and Pette 1990), the fast-to-slow transitions of TnT ($TnT_{3f} \rightarrow TnT_{1s}$, TnT_{2s}; Fig. 13), TnI ($TnI_f \rightarrow TnI_s$), and TnC ($TnC_f \rightarrow TnC_s$) occur later (Härtner and Pette 1990). It appears to coincide with the fast-to-slow transition of myosin, i.e., the appearance of the slow HCI after stimulation periods longer than 3–4 weeks. The expression of the slow Ca^{2+}-ATPase isoform, as well as the induction of phospholamban, also follows this time sequence (Figs. 14, 17; Leberer et al. 1989).

An unanswered question relates to the time course of transformation of different muscle fiber types. In view of the fact that a fast-twitch muscle is composed of various fast fiber subgroups (types IIB, IID, IIA), the stimulation-induced conversion could either occur as a one-step or as a sequential fast-to-slow transition. Thus, the possibility exists that the various fast fiber subgroups transform directly into type I fibers, or they pass from one fast phenotype to another before they ultimately reach the slow fiber state. The time course of changes in fiber type composition (Fig. 8) argues strongly against the first possibility. Thus, low-frequency stimulation of rabbit fast-twitch muscle initially leads to a steep decrease in type IIB/D fibers with subsequent and transitory increases in type IIA and C fibers. Pronounced increases in type I fibers occur only after long-term stimulation and represent the final fiber type conversion in rabbit muscle. An answer to this question can also be found in the changes of the MHC isoforms in chronically stimulated rat muscles. Rat EDL and TA muscles contain only a small percentage of type IIA fibers and are composed mainly of type IIB and type IID fibers. Electrophoretic analyses on low-frequency stimulated rat TA and EDL muscles reveal a progressive decrease in the amount of myosin HCIIb concomitant with transient increases in HCIId and HCIIa, the latter becoming ultimately the dominant isoform (Fig. 9; Termin et al. 1989b). An intermediate increase in HCIId could not be observed if the fiber type transition occurred in a single step, i.e., directly from type IIB to type IIA. Therefore,

the fast-to-slow conversion includes intermediate steps with the sequential expression of HCIIb → HCIId → HCIIa in the rat, and HCIIB → HCIId → HCIIa → HCI in the rabbit.

An additional question is whether the different fiber type transitions occur simultaneously or proceed in a sequential manner. Simultaneous fiber type transitions would lead to a progressive increase in type I fibers after the onset of stimulation. However, several independent studies have shown that noticeable increases in type I fibers are observed only after very long stimulation periods (Fig. 8; Staron et al. 1987; Maier et al. 1988; Aigner and Pette 1992; Pette 1992). Similar results have been obtained from studies on MHC isoform transitions at the mRNA level. Thus, the slow myosin HCI mRNA is expressed as the last isoform during the transformation process of chronically stimulated rabbit fast-twitch muscle (Kirschbaum et al. 1989a; Brownson et al. 1992). Similar results have been obtained in a study in which the appearance of HCI mRNA was followed at the cellular level by in situ hybridization (Aigner and Pette 1990, 1992). Only a few HCI mRNA-positive fibers can be detected in normal rabbit TA muscle. Their number increases markedly after stimulation periods longer than 30 days (Fig. 11; Aigner and Pette 1992), supporting the notion that the HCIIa → HCI transition represents the ultimate step of the fast-to-slow fiber type conversion. Because this conversion is essentially confined to long-term stimulation, it appears that the type IIA fibers do not transform in a synchronous manner. Taking into account that normal EDL and TA muscles of the rabbit contain only a small fraction of type IIA fibers, it is conceivable that only these fibers will initially perform the type IIA → type I transition. As the other fast fiber types reach the type IIA state, these newly formed IIA fibers become able to switch from myosin HCIIa to myosin HCI expression. The proposed model of sequential fiber type transitions implies that the genes coding for the different MHC isoforms respond to chronic low-frequency stimulation in a graded manner and are activated sequentially due to different thresholds.

2.8 Reversal of Stimulation-Induced Changes

Studies on the temporal pattern of the reversal of low-frequency stimulation-induced changes have been performed on the rabbit (Eisenberg et al. 1984; Sréter et al. 1987; J.M.C. Brown et al. 1989) and rat (Kirschbaum et al. 1988, 1990b; Weber and Pette 1990a,b).

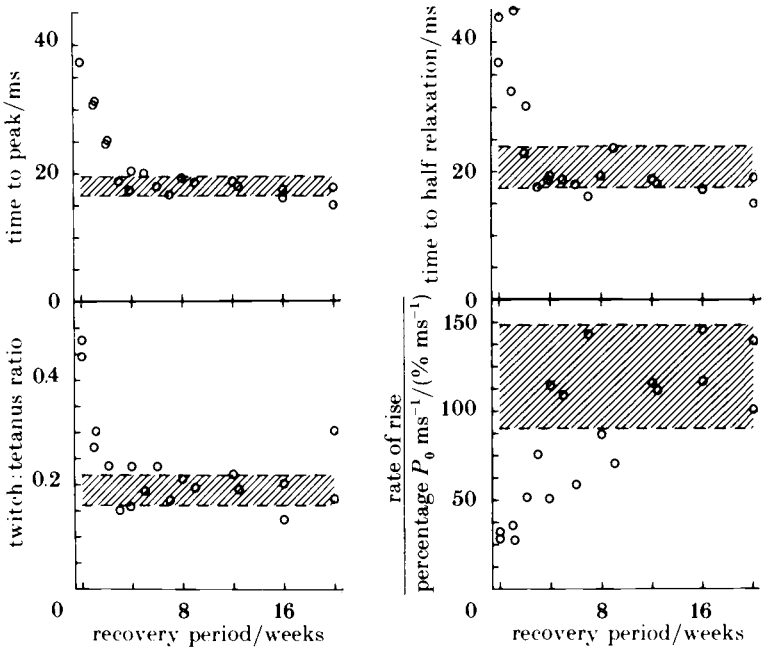

Fig. 32. Changes in physiological parameters measured in rabbit TA muscles that had been stimulated (10 Hz, 24 h daily) for 6 weeks and then allowed to recover for different periods. The time course of recovery is shown in relation to the pooled contralateral control muscles (*hatched band*, means ± SD; n = 20), P_0, maximum value of tetanic tension. (From J.M.C. Brown et al. 1989)

In the rabbit, the time course of complete reversion was such that the muscles had recovered their original fast properties by about 12 weeks after the cessation of stimulation (J.M.C. Brown et al. 1989). The contractile characteristics and post-tetanic potentiation typical of fast-twitch muscle return rapidly after 3–4 weeks (Figs. 32, 33; J.M.C. Brown et al. 1989). This coincides with a decline in histochemically defined type I fibers (Sréter et al. 1987; J.M.C. Brown et al. 1989) and electrophoretically determined slow isomyosin (Sréter et al. 1987). Changes in fatigue resistance, capillary density, and enzyme activity follow a more prolonged time course (Figs. 33, 34; J.M.C. Brown et al. 1989). The decline in enzyme activities of aerobic-oxidative metabolism corresponds closely to that established for the mitochondrial volume density (Eisenberg et al. 1984; J.M.C. Brown et al. 1989). Interestingly, the reversal of the morphological changes of the T-tubular system is faster. The T-tubules which are markedly reduced by chronic low-frequency stimulation (Eisenberg and Salmons 1981), increase to values characteristic of fast-twitch

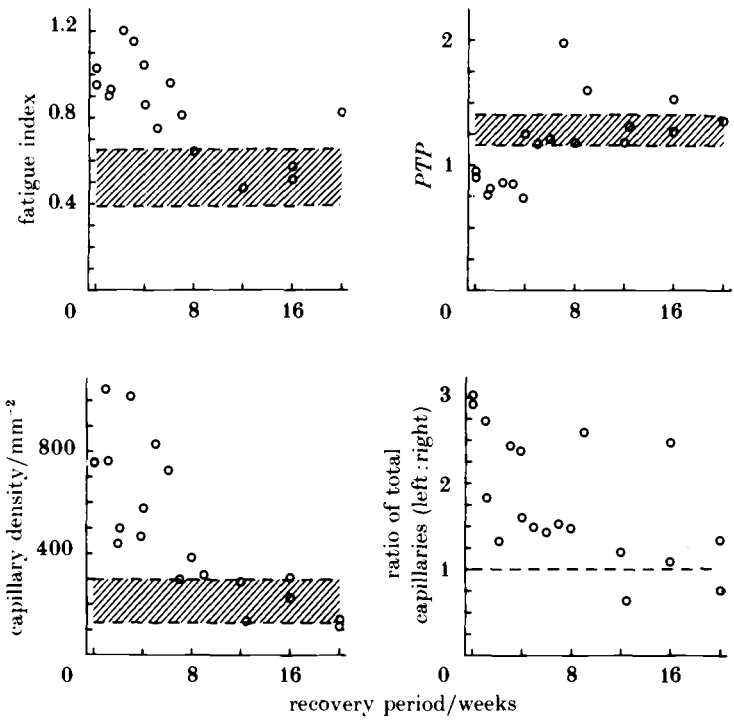

Fig. 33. Changes in fatigue behavior, post-tetanic potentiation (*PTP*), and capillary density in rabbit tibialis anterior muscles that had been stimulated for 6 weeks (10 Hz, 24 h daily) and then allowed to recover for different periods. The time course of recovery in three of the graphs is shown in relation to the pooled contralateral control muscles (*hatched band*, mean ± SD). In the graph at the *lower right*, a *broken line* at 1.0 denotes an identical (estimated) total number of capillaries in the muscles of the two limbs. (From J.M.C. Brown et al. 1989)

muscle 2–4 weeks after stimulation is discontinued (Eisenberg et al. 1984).

The reversal of the changes in proteins, cellular structures, and functional properties after cessation of stimulation is relatively slow. The corresponding changes at the mRNA level appear to occur much faster. To date, studies have only been performed on the reversal of changes in MHC mRNA isoforms. Indeed, HCIIb and HCIIa mRNAs are rapidly exchanged in rat TA muscle after cessation of stimulation (Kirschbaum and Pette 1988; Kirschbaum et al. 1989c, 1990b). Significant increases in the amount of HCIIb mRNA, which has been reduced in 15-day stimulated rat TA to 4% of its normal value, become detectable as early as 21 h after stimulation has been interrupted (Fig. 35). This reversal of the stimulation-induced

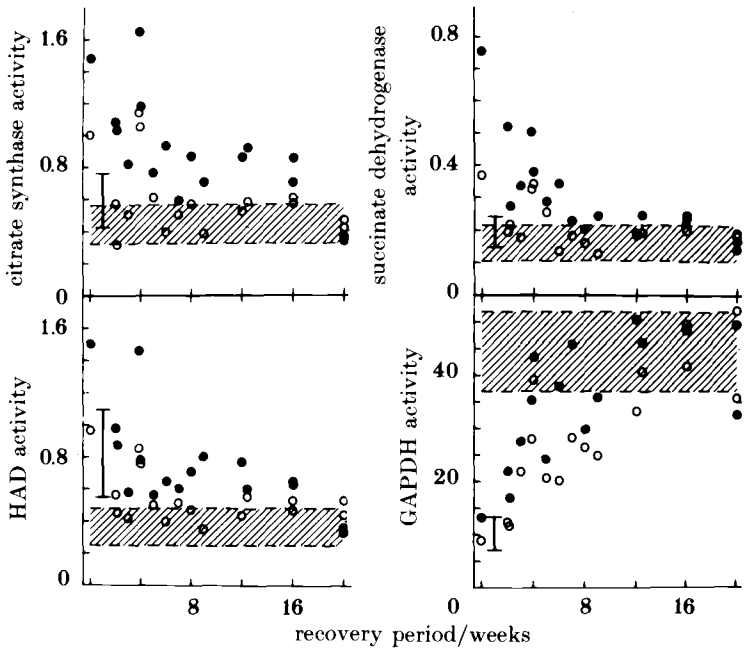

Fig. 34. Time course of changes in enzyme activities of energy metabolism in rabbit fast-twitch muscles during recovery after low-frequency stimulation (10 Hz, 24 h daily) for 6 weeks. Control ranges ± 95% confidence for fast-twitch muscles are indicated by *hatched areas*, those for slow-twitch muscle by *vertical bars*; *open circles*, EDL; *closed circles*, TA. *GAPDH*, glyceraldehyde phosphate dehydrogenase; *HAD*, 3-hydroxyacyl-CoA dehydrogenase. (From J.M.C. Brown et al. 1989)

changes, consisting of not only increases in HCIIb mRNA but also decreases in HCIIa mRNA, is progressive (Kirschbaum et al. 1990b). The reversal of the fast-to-slow transition has also been shown for fast and slow HC mRNAs in the rabbit. However, the reversal of the changes in the rabbit follows a slower time course than that of the rat. Thus, the reappearance of the fast MHC mRNA has been detected only 4 days after cessation of stimulation (Brownson et al. 1988, 1992).

2.9 Transformation and Replacement of Muscle Fibers

The numerous changes in molecular, structural, and functional properties of low-frequency stimulated fast-twitch muscles described so far raise the question as to the underlying processes associated with these alterations in phenotype. Do these changes reflect a fast-

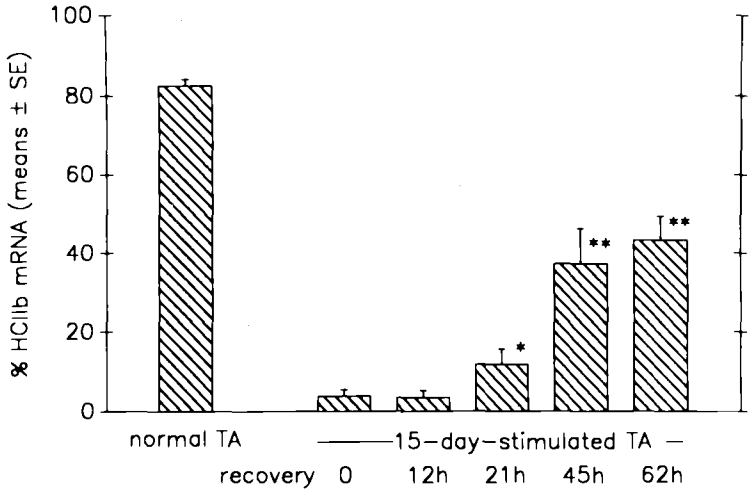

Fig. 35. Relative concentrations of myosin HCIIb mRNA in unstimulated and 15-day stimulated rat tibialis anterior (*TA*) muscles without and with recovery periods of increasing duration after cessation of stimulation. The data (means ± SE) were obtained by S1-nuclease mapping using a cDNA which yields, in addition to the fully protected HCIIa mRNA–DNA hybrid, a partially protected HCIIb mRNA–DNA hybrid. The densitometrically evaluated intensities of the two bands together were set equal to 100% and the percentage of HCIIb mRNA was calculated. Significance of changes with regard to the 15-day stimulated muscle is indicated: *, $p < 0.05$; **, $p < 0.001$. (Data from Kirschbaum et al. 1990b)

to-slow transformation of existing fibers or do they result from an exchange of fast-twitch fibers with newly formed slow-twitch fibers? Until recently it was believed that the fast-to-slow transitions were entirely due to a transformation of existing fast-twitch fibers. However, evidence is accumulating that, in addition to fiber transformation, some replacement of fast-twitch fibers may contribute to the overall changes (Maier et al. 1986, 1988; Maier and Pette 1987; Acker et al. 1987b; Aigner and Pette 1990, 1992; Pette 1992).

Histological and immunocytochemical analyses performed on rabbit EDL and TA muscles subjected to chronic low-frequency stimulation for different time periods, have found that 10%–20% of the total fiber population undergo degeneration a few days after the onset of stimulation. The deteriorating fibers, most of which are fast-twitch glycolytic, are replaced by newly formed fibers (Maier et al. 1986). The first signs of fiber degeneration (e.g., fiber swelling, acidophilia, increase in mononucleated cells) have been observed after 2 days. Most of these mononucleated cells are probably macrophages since their appearance is accompanied by a five- to sixfold

increase in the activity of β-galactosidase, a lysosomal marker (U. Seedorf and D. Pette 1986, unpublished). Increase in cell number is also indicated by an augmented DNA content of the stimulated muscle (Maier and Pette 1987). Phagocytosis of disrupted fibers is maximal between 6 and 10 days after the onset of stimulation. It is not known to what extent the transient elevations in metabolites and enzyme activities of the polyamine pathway observed during the first days in low-frequency stimulated rabbit muscle (Mastri et al. 1982) relate to the invasion of mononucleated cells and proliferative processes.

Incorporation of [^{3}H]thymidine into nuclei of putative satellite cells indicates their proliferation. Histological analyses suggest that satellite cells from fast-twitch oxidative fibers are also involved in the regenerative processes (Maier et al. 1986, 1988). Small myotubes expressing embryonic and neonatal myosins have been seen. In addition, a large fraction of the newly formed myotubes, which eventually develop into small fibers with a high oxidative potential, contains slow myosin in variable combinations with embryonic myosin (Maier et al. 1988). A significant increase in muscle fibers with central nuclei, as well as the appearance of the MB-hybrid of creatine kinase (Schmitt and Pette 1985), can be interpreted as additional signs of regenerative processes. Finally, in situ hybridization of the slow myosin HCI mRNA not only shows fibers with high concentrations of the message within and around their subsarcolemmic nuclei, but, in addition, reveals fibers displaying high amounts of HCI mRNA within and around centrally placed nuclei (Aigner and Pette 1990, 1992; Pette 1992).

Although fibers with centrally placed nuclei can be detected after prolonged stimulation, the acute phase of fiber degeneration and regeneration appears to be complete after 3–4 weeks of stimulation. Nuclear counts remained high, but most of the nuclei were closely associated with the periphery of the muscle fibers (Maier et al. 1986). Some of these might represent newly formed satellite cells as the fast-twitch muscle fibers undergo transformation or are substituted for by the newly formed fibers. The number of satellite cells in fast-twitch and slow-twitch muscles has been reported to be under neural control (Kelly 1978; Schultz 1984; Schultz and Darr 1990). Indeed, a three-fold increase in satellite cell yield was obtained from 15-day low-frequency stimulated rat TA muscle (Düsterhöft et al. 1991).

There appears to be a relationship between glycogen depletion and fiber degeneration (Maier and Pette 1987). Microphotometric evaluation of the histochemical staining for glycogen has shown

glycogen depletion of all fibers after the first 2 h of stimulation, which is in agreement with biochemical analyses on whole muscle (Green et al. 1990, 1992; Hood and Parent 1991). Thereafter, different responses are noted for different fiber types. Fast-twitch oxidative and slow-twitch oxidative fibers recover their glycogen stores. However, a high percentage of the fast-twitch glycolytic fibers do not recover and remain glycogen-depleted. Fiber degeneration is restricted to these fibers, suggesting that persistent exhaustion of the main fuel of this fiber type causes a collapse of energy metabolism and energy supply of the ionic pumps which could then initiate fiber deterioration (Maier and Pette 1987). It remains to be seen to what extent the early increases in total and free calcium detected during the first days of stimulation (Sréter et al. 1980, 1987) relate to such events. However, it is possible that other factors, e.g., mechanical disruption, as in exercise-induced muscular injury (for review see Armstrong 1990), also play a role in the initiation of fiber degeneration.

It is possible that degeneration–regeneration processes are contributing to different extents to the fast-to-slow conversion of chronically stimulated fast-twitch muscles in different animal species. The caged rabbit probably represents an extreme, with muscles rich in fast-twitch glycolytic fibers that are predisposed to exhaustion when exposed to persistently increased contractile activity. Fast-twitch fibers of other animal species may be more resistant to fiber deterioration because of their higher initial levels of enzymes representing aerobic-oxidative metabolic pathways. This would explain why Hoffman et al. (1985) were unable to observe signs of fiber degeneration or regeneration and were unable to detect embryonic myosin in dog diaphragm subjected to chronic low-frequency (10 Hz) stimulation. However, it must be kept in mind that the normal, unstimulated diaphragm is a muscle endowed for sustained contractile activity.

3 Slow-to-Fast Transitions

Although much less work has been carried out on this model, the first observations on the regulatory role of activity on the contractile properties were made on inactivated slow-twitch soleus muscle of the rabbit and cat (Vrbová 1963). Reducing the overall activity of this muscle by tenotomy leads to an increased speed of contraction

(Vrbová 1963; Buller and Lewis 1965). In the rabbit soleus, the slow time course of contraction, characteristic of this muscle, could be maintained by imposed continuous low-frequency, electrical but not by intermittent high-frequency stimulation (Vrbová 1966).

An additional model in which a slow-twitch muscle can be successfully transformed into a faster contracting muscle is the denervated soleus muscle of the rat, stimulated directly with a phasic high-frequency pattern (Lømo and Westgaard 1974; Lømo et al. 1980). On this model, the molecular changes underlying the altered contractile speed have been studied in detail (Eken and Gundersen 1988; Lømo 1989).

3.1 Phasic High-Frequency Stimulation of Slow-Twitch Muscle

Denervated rat soleus muscle, subjected to small amounts of phasic high-frequency stimulation (60 pulses at 100 Hz every 60 s or 25 pulses at 150 Hz every 15 s) during long time periods (>30 days) turns into a faster contracting muscle as judged from the time to peak twitch tension, half-relaxation time, and rate of tension development (Eken and Gundersen 1988; Gorza et al. 1988). Gundersen et al. (1988) found that the mATPase histochemistry of soleus fibers stimulated phasically at a high frequency (25 pulses at 150 Hz every 15 min) resembled that of type C fibers. This conclusion is consistent with the results from immunocytochemical studies showing a high proportion of fibers that strongly react with antibodies against fast myosin and weakly with antibodies against slow myosin (Gorza et al. 1988). The identity of the fibers positive for fast-type myosin was further elucidated and shown to be type 2x (Schiaffino et al. 1988, 1989; Ausoni et al. 1990).

In addition to the changes in fiber type and MHC composition, low-amount high-frequency stimulation (25 pulses at 150 Hz every 15 min) also affected several other biochemical properties of the stimulated soleus muscle (Leberer et al. 1987b; Gundersen et al. 1988). The immunochemically assessed total protein of the sarcoplasmic reticulum Ca^{2+}-ATPase increased to levels close to those found in rat fast-twitch EDL muscle (Fig. 36). Moreover, the extremely low parvalbumin content of normal soleus muscle was increased approximately 40-fold, although it did not reach the level characteristic of the EDL muscle. This may be due to the fact that the high-frequency stimulated soleus muscle is composed mainly of type 2x (type IID) fibers (Schiaffino et al. 1988, 1989; Ausoni et al. 1990) which, as compared to type IIB fibers, contain less parval-

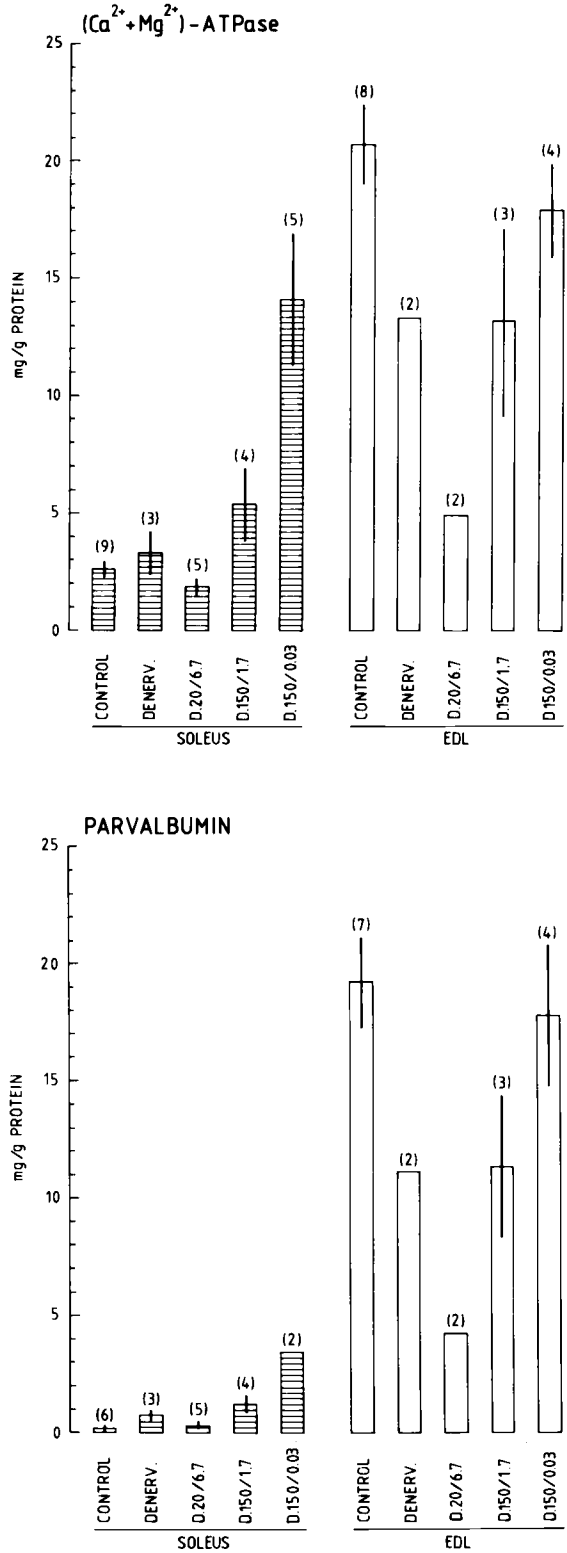

Fig. 36. Immunochemically determined tissue contents of sarcoplasmic reticulum (Ca^{2+} + Mg^{2+}-ATPase and cytosolic parvalbumin in normal (*control*), denervated (*denerv.*) and denervated stimulated soleus (*hatched columns*) and extensor digitorum longus (*open columns*) muscles of the rat. The indicated stimulation protocols were as follows: *D.20/6.7*, 20 Hz (10 s repeated every 30 s; mean frequency 6.7 Hz); *D.150/1.7*, 150 Hz (25 pulses at 150 Hz every 15 s; mean frequency 1.7 Hz); *D.150/0.03*, 150 Hz (25 pulses at 150 Hz every 15 min; mean frequency 0.03 Hz). Values (*n*) are given as means ± SD. (From Gundersen et al. 1988)

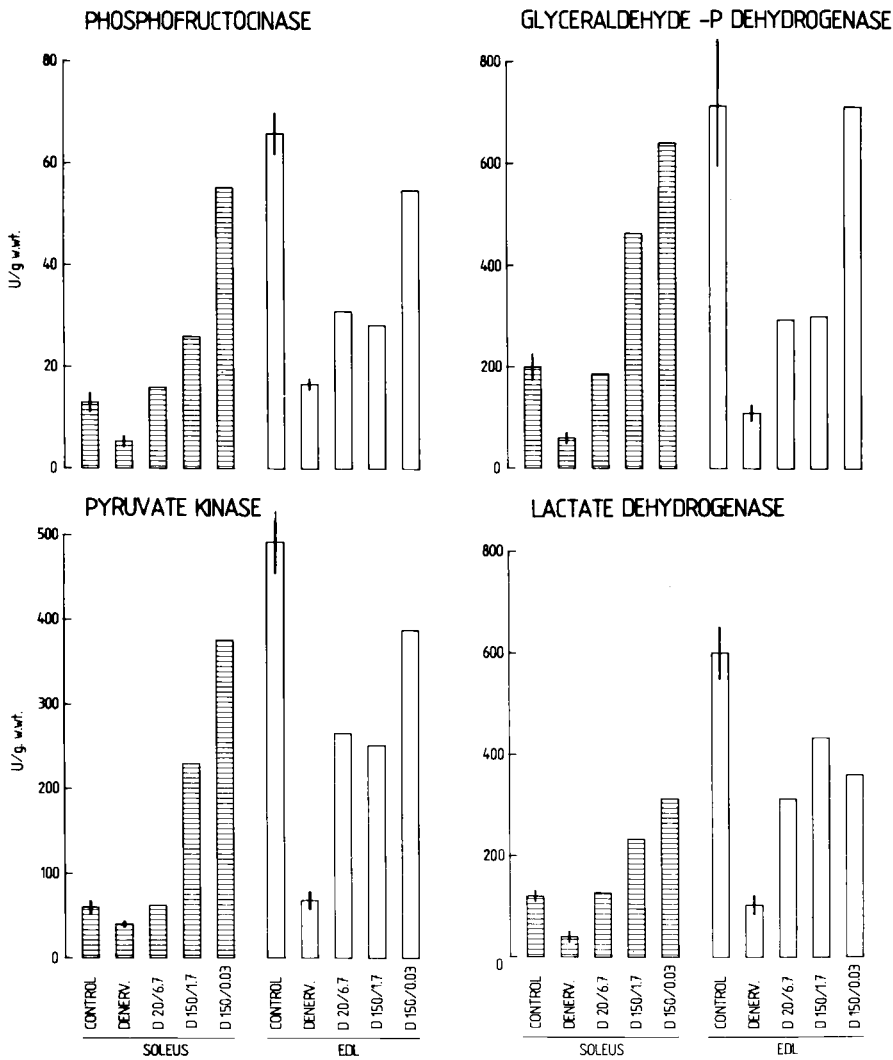

Fig. 37. Activities of glycolytic enzymes in normal (*control*), denervated (*denerv.*) and denervated stimulated soleus (*hatched columns*) and extensor digitorum longus (*open columns*) muscles of the rat. For explanation of the indicated stimulation protocols, see legend of Fig. 36. (From Gundersen et al. 1988)

bumin (Schmitt and Pette 1991). The same pattern of stimulation prevented the development of denervation-induced alterations, e.g., decreases in enzyme activities of aerobic-oxidative metabolism, as well as of glycogenolytic and glycolytic enzyme activities (Gundersen et al. 1988). The low-amount high-frequency stimulation induced increases in glycogenolytic and glycolytic enzymes, and also in

cytosolic creatine kinase, to levels similar to those found in normal fast-twitch EDL muscle (Fig. 37).

4 Modulation of Effects of Stimulation by Other Factors

Several observations support the notion that chronic stimulation-induced changes can be modulated by other factors. Among others, these include the mechanical condition of the stimulated muscle and the hormonal state of the organism.

Since the early studies on the impact of stretch on protein metabolism in muscle (Goldberg 1969; D.F. Goldspink 1977; Booth and Seider 1979; Vandenburgh and Kaufman 1980), a large body of literature has accumulated on changes of amino acid and protein metabolism related to alterations in load (for review see Booth 1988). Changes in muscle load have been shown to affect the composition of muscle fiber types, myofibrillar protein isoform patterns, and gene expression (e.g., Hoh and Chow 1983; G. Goldspink 1985; Gregory et al. 1986, 1990; Periasamy et al. 1989; Baldwin et al. 1990; Essig et al. 1991). In view of these observations, it is not surprising that stretch has a positive effect on the changes induced by low-frequency stimulation. The fast-to-slow fiber transition that occurs after low-frequency stimulation was found to be accelerated in rabbit TA when the muscle was immobilized in a neutral position (Cotter and Phillips 1986). Similar results were reported by P. Williams et al. (1986) who found greater stimulation-induced increases in type I and type IIA fibers when the muscle was immobilized in a stretched position. Finally, chronic low-frequency stimulation of rat EDL muscle combined with overload induces a slowing of the twitch contraction not seen with either overload or stimulation alone (Frischknecht and Vrbová 1991).

Influences of the hormonal state of the animal on the effects of chronic low-frequency stimulation have been elucidated for thyroid hormone. The regulatory role of thyroid hormone on muscle fiber composition (Ianuzzo et al. 1977; Nwoye and Mommaerts 1981) and myosin isoform expression is well established in fast-twitch and slow-twitch muscles of the rat (Gustafson et al. 1986; Izumo et al. 1986; Kucher et al. 1988; Kirschbaum et al. 1990a). The effects of thyroid hormone on rat fast-twitch muscle can be summarized as follows: Hypothyroidism slightly enhances the expression of myosin HCIIa and HCI, whereas normal and elevated levels of thyroid hormone

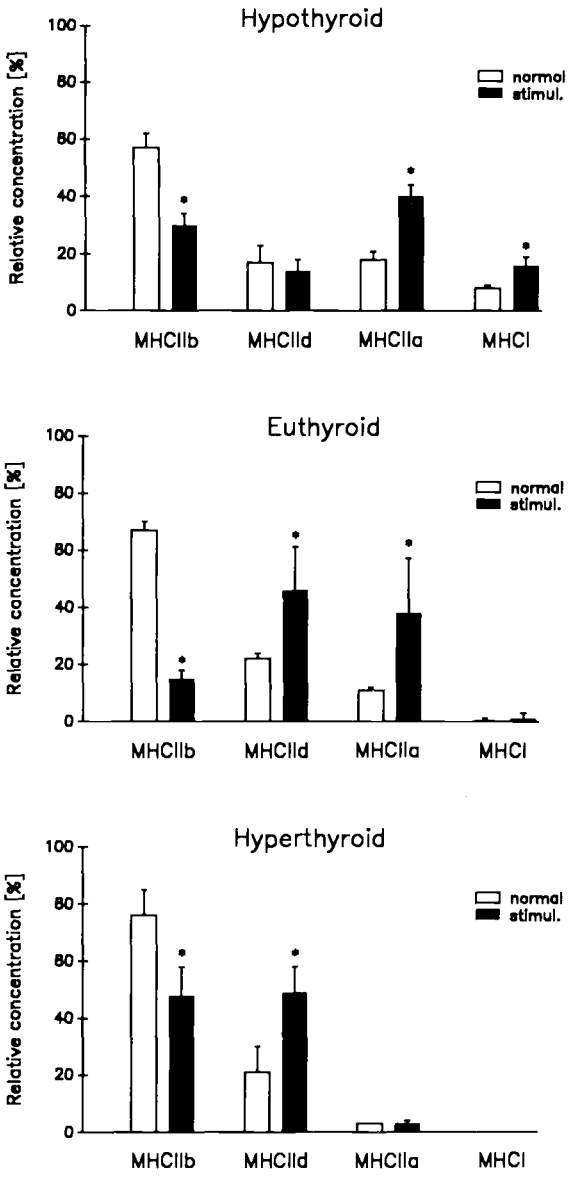

Fig. 38. Relative concentrations (means ± SD) of myosin HC isoforms in unstimulated and 35-day low-frequency stimulated (10 Hz, 10 h daily) tibialis anterior muscles of euthyroid, hypothyroid and hyperthyroid rats. (Data from Kirschbaum et al. 1990a)

reduce the expression of HCIIa and suppress that of HCI, leading to a shift towards HCIIb as the predominant MHC isoform.

Chronic low-frequency stimulation of rat fast-twitch EDL and TA muscles counteracts the slow-to-fast promoting effect of thyroid hormone in a graded manner (Kucher et al. 1988; Kirschbaum et al.

1990a). The antagonism between chronic low-frequency stimulation and thyroid hormone is conspicuous at both the mRNA and protein levels. Thus, after 35-day periods of low-frequency stimulation there is almost no detectable expression of HCI, but in the hypothyroid state the expression of the slow isoform is induced by low-frequency stimulation for 35 days at both the mRNA and protein level (Fig. 38). In addition, low-frequency stimulation markedly enhances the expression of HCIIa in the hypothyroid state. However, these stimulation-induced increases in HCI and HCIIa in the hypothyroid state, as well as that of HCIIa alone in the euthyroid state, are suppressed when the thyroid hormone level is increased (Fig. 38). Low-frequency stimulation in the hyperthyroid rat leads to a shift from HCIIb to HCIId, but no further progression to HCIIa takes place. A similar antagonism between the actions of thyroid hormone and neural activity has been observed in recent studies on the effect of thyroidectomy after cross-innervation. As judged from changes in contractile properties and fiber composition, the fast-to-slow transition induced in EDL muscle by cross-innervation with the slow soleus nerve was more pronounced in the hypothyroid than in the euthyroid rat (Tian and Feng 1990).

The antagonistic effects of thyroid hormone and chronic low-frequency stimulation may be relevant with regard to variations in the response between different animal species to similar stimulation regimes (Simoneau and Pette 1988a,b; Simoneau et al. 1990). Thus, it is possible that some of the differences described in the literature as variations in "adaptive ranges" (Gundersen et al. 1988; Westgaard and Lømo 1988; Ausoni et al. 1990) are due to differences in thyroid hormone levels or differences in the sensitivity to thyroid hormone between animal species. This may especially apply to the different responses of small mammals, such as mouse, rat, and rabbit (see Sects. 2.4.1 and 2.6.2).

5 Pattern of Activity versus Amount of Activity

5.1 Innervated Muscles

The question of whether the pattern, rather than the overall amount of activity, is the most important factor for the slow-to-fast transition or for the determination of the muscle phenotype has been addressed in several studies. The finding that a reduction in neuromuscular

activity of slow-twitch rabbit soleus muscle converts this muscle into a faster muscle (Vrbová 1963) was subsequently followed up by experiments in which this conversion was prevented by returning the slow type of activity to the muscle by chronic electrical stimulation. However, fast phasic activity was ineffective in maintaining the slow time course of contraction of the inactive soleus muscle (Vrbová 1966; Salmons and Vrbová 1969). The muscles stimulated at high frequencies had undergone severe degenerative changes and had lost many fibers (McMinn and Vrbová 1967). Therefore, these results must be interpreted with caution. Subsequent experiments have been carried out on several different experimental models on rats, rabbits, and cats.

Using the original model of the rabbit fast-twitch muscles converted to slow-twitch muscles by low-frequency electrical stimulation, the TA and EDL muscles were stimulated with trains of pulses at high frequencies (40–60 Hz). The regime of stimulation varied in different experiments. Hudlická et al. (1980, 1982a, 1984) used trains of 5 s duration 3 times a minute, while 40- to 60-Hz trains of 2.5 s duration delivered 6 times per minute were applied by Sréter et al. (1982) and Mabuchi et al. (1990). In both these experiments there were distinct signs of a fast-to-slow transition in the stimulated muscles. Increases in capillary density, fatigue resistance, and of the enzymes of aerobic-oxidative metabolism were observed. These changes differed only slightly from those seen after low-frequency stimulation (Hudlická and Tyler 1984; Hudlická et al. 1984). After 4 weeks of stimulation, the contractile properties and the myosin light chain pattern also changed so as to resemble more closely those in a slow-twitch muscle (Hudlická et al. 1982a; Sréter et al. 1982). Immunohistochemistry with monoclonal antibodies against HCIIb, HCIIa and HCI showed a fast-to-slow fiber conversion similar to that induced by chronic low-frequency stimulation (Mabuchi et al. 1990). Taken together, these results indicate that for the fast-to-slow transition of rabbit fast-twitch muscle, the total amount of activity may be more important than the exact pattern at which it is delivered. In all of these experiments, the sensory input from the stimulated limb was preserved, and this, in addition to the discomfort to the animal, may lead to uncontrolled reflex activity. To exclude these complications, Kernell and his colleagues worked on spinalized and deafferented cats using the peroneus longus muscle. No matter what pattern of activity was used (10 Hz, continuous, 20–40 Hz in trains, or 100 Hz in trains), if the muscles were activated for 5% of the total time per day, then the cat fast peroneus longus muscle became slower contracting, more fatigue resistant, contained a larger proportion of

oxidative fibers, and, as judged by the mATPase stain, contained more slow-twitch fibers (Eerbeek et al. 1984; Donselaar et al. 1987; Kernell and Eerbeek 1989). Although this set of results seems to support the previous findings (Sréter et al. 1982; Hudlická and Tyler 1984; Hudlická et al. 1982a, 1984; Mabuchi et al. 1990), the model of the spinalized and deafferented cat peroneus longus muscle has several drawbacks. The stimulation of this muscle began 14 days after the operation, and, at this time, the peroneus longus had probably become altered and more fatigable, as seen in patients with spinal cord injury (Lenman et al. 1989). This notion is supported by the inability of the experimental muscle to maintain force during a brief tetanus (Eerbeek et al. 1984). Thus, in this case the stimulation would have been applied to a highly abnormal muscle, and it is possible that any type of activity will have had a similar effect. One of the results of excess activation on such a muscle could be that many muscle fibers are selectively destroyed by excess activity. In support of this possibility are data presented by Eerbeek et al. (1984) and Donselaar et al. (1987). Their results show that the tension of the muscle decreases by 67% with low-frequency stimulation, but the fiber diameter decreases only by 40%, whereas with high-frequency stimulation the tension decrease is 51%, but the decrease in fiber diameters is very small (28%). Thus, in the case of high-frequency stimulation the decrease in tension can be explained partly by a decrease in fiber size. Provided that type IIB fibers were preferentially affected, this could account for the similar effect in both types of stimulation.

These carefully conducted studies on cats and rabbits highlight the difficulties inherent in the method of chronic stimulation, especially at higher frequencies. The major problem is to know what the contractile machinery does when stimulated at high frequencies, where the train lasts for seconds. Such a situation is most unusual during normal locomotor activity. Electromyograph (EMG) recordings during repeated high-frequency stimulation indicate that the muscle is unable to respond to each stimulus and, therefore, may be exposed to a different frequency than applied (Kaplove 1987; Pette and Vrbová 1985; Vrbová and Pette 1987).

5.2 Denervated Muscles

Stimulation of denervated muscles was undertaken for several reasons. One is to exclude any possible regulatory/trophic function the nervous system may exert. An additional reason may be an

attempt to reverse denervation-induced changes such as muscle wasting, and to maintain the muscle in good condition.

The majority of experiments pursuing the first aim were carried out on the soleus muscle of the rat. It was found by Lømo and his colleagues (Lømo and Westgaard 1974; Lømo et al. 1980) that the time course of contraction of the denervated soleus muscle can be altered according to the particular pattern of activity imposed upon the muscle. Rat soleus muscles stimulated at high frequencies became fast contracting, and those stimulated at low frequencies maintained their slow time course of contraction. However, denervation on its own causes soleus muscle to contract moderately faster and this change can be prevented by any frequency pattern, provided the contractions are maintained for a prolonged period of time (Al-Amood and Lewis 1987). This possibility is consistent with results of Gundersen et al. (1988), where the slow characteristics of denervated rat soleus muscle were preserved if the muscles were activated with a 20-Hz pattern for 20 s each minute; while using the high-amount phasic 150-Hz pattern (25 pulses at 150 Hz every 15 s) the muscles were active for only 667 ms in each minute. Thus, irrespective of the frequency, the total amount of time during which the muscle was contracting was very different in the two stimulation protocols. The long-lasting contraction protocol (20 Hz for 20 s each min) maintained the low parvalbumin content and the low Ca^{2+}-ATPase content of the sarcoplasmic reticulum characteristic of the slow-twitch soleus. The shorter-lasting activity delivered at high frequencies for only a fraction of a second in each minute induced the muscle to express the amounts of Ca^{2+}-ATPase and, to some extent, parvalbumin to the levels characteristic of a fast-twitch muscle (Fig. 36; Gundersen et al. 1988). The shift in the fiber type population is also consistent with this interpretation (Gundersen et al. 1988; Ausoni et al. 1990).

Several experiments on innervated muscle appear to argue against this interpretation. Hennig and Lømo (1987) stimulated innervated soleus muscles with intermittent trains of stimuli at high frequency, and induced some degree of transformation toward a fast-twitch muscle, as judged from the time course of contraction and fiber type composition. Trains delivered at a high frequency (100 Hz) may interfere with the muscle's excitability so that a burst of 100 Hz may be followed by a period of inactivity. Such a possibility may also explain the results of Westgaard and Lømo (1988) where rat soleus muscles were stimulated at 10 Hz and trains of 100 Hz were interspersed. If these trains were given infrequently, then the soleus remained slow. However, when the frequency at which these trains

were delivered increased, the soleus became fast-contracting, possibly because following a train at high frequency may have rendered the muscle refractory.

It is interesting that attempts to deliver complicated patterns of activity to the soleus muscle have not been checked at the level of the muscle by EMG recording. During normal activity, motor units are usually activated by patterns which the muscle fibers can follow. As such, there may be a limit as to what activity pattern a muscle fiber can respond to. Therefore, electrical stimulation may cause the activation of certain mechanisms to protect the muscle fibers from being driven in an inappropriate way.

Nevertheless, the capacity of the muscle to adapt to intermittent activity in a different way than to sustained activity is remarkable, regardless of whether it is frequency- or time-coded. Even in experiments where soleus was induced to become fast contracting, the conversion was incomplete (Gundersen et al. 1988). This inability of the muscle to become completely converted was considered to be due to a limited adaptive range of soleus muscle fibers. Although this may be the case, such a notion is difficult to prove, for it is always possible that a more complete conversion could be achieved using a more appropriate experimental protocol.

Regarding stimulation of the denervated rat EDL muscle, there are several reports as to the influence of various stimulation protocols. Carraro and colleagues (1986) showed marked increases in the amount of the slow myosin HCI in denervated rat EDL muscle after several weeks of direct low-frequency (10 Hz) stimulation. These results are in disagreement with the findings of Gundersen et al. (1988). Similar to the innervated EDL muscle of the rat (Termin et al. 1989b), chronic low-frequency stimulation of the denervated EDL or TA did not convert the muscle into a slow-twitch muscle. The majority of fibers were of the IIB type and there was only a moderate increase in type IIC fibers (Gundersen et al. 1988). These results led to the suggestion that, as in the soleus, only a partial transformation is possible in the EDL. However, taking into account the modulating effect of thyroid hormones, the partial transformations observed in both rat soleus and EDL muscles by electrical stimulation with heterologous frequency patterns may be influenced by the thyroid state of the animal (Kirschbaum et al. 1990a). In the rabbit, chronic low-frequency stimulation of the denervated TA muscle led to changes that were similar but not as extensive as those induced in the innervated muscle. The stimulation led to an increase in enzyme activities of aerobic-oxidative meta-

bolism, to a decrease in glycolytic enzyme activities, and to a shift in the LDH isozyme pattern toward that of a slow muscle (Reichmann and Nix 1985).

The effects of different patterns of electrical stimulation on the force output of denervated muscle is important, for it is this property of the muscle which may be of the ultimate importance in clinical practice. In the rat, according to Eken and Gundersen (1988), the most favorable regime that allows force to be maintained is the naturally occurring activity of a particular muscle. In soleus this would be a low-frequency continuous stimulation, and in the EDL intermittent, brief, high-frequency bursts.

In other species electrical stimulation of denervated skeletal muscles was used, not so much to study the effects of activity on muscle phenotype, but rather to evaluate the possible value of electrical stimulation for maintenance of muscle bulk and force. Experiments to evaluate whether or not electrical stimulation is beneficial have been attempted by many investigators since the beginning of this century (for brief review see Nix and Dahm 1987), but, as yet, no agreement has been reached as to the usefulness of this treatment. In a systematic study Gutmann and Guttmann (1944) demonstrated that electrical stimulation can retard atrophy of denervated rabbit muscle. This has also been shown for denervated rat muscles (Grodins et al. 1944). Fiber atrophy of denervated soleus muscle of guinea pig was shown to be suppressed by chronic low-frequency stimulation. In addition, stimulation of the denervated muscle maintained the histochemically assessed pattern of several enzymes related to aerobic-oxidative metabolism (Nemeth 1982). A recent study on rabbit fast-twitch muscle highlighted the importance of appropriate stimulation patterns (Nix and Dahm 1987). Denervated rabbit EDL muscles were stimulated under isometric conditions with 100 ms lasting bursts at 40 Hz every second, while in another group of animals the EDL muscles were stimulated at 1 Hz by pulses of long duration (7 ms). Both stimulation patterns were given for only 20 min each day. While the 40-Hz pattern using a short pulse width (0.2 ms) was reported to lead to degeneration of the muscle, the muscles stimulated at 1 Hz were less atrophic and produced more force than the unstimulated controls (Nix and Dahm 1987). In another study by Nix (1990), intermittent high-frequency stimulation resembling the normal motoneuron firing was applied to denervated rabbit EDL muscle and had no effect on contraction time, force output, fatigue resistance, fiber area, and muscle weight. These findings are in apparent contradiction to recently reported results obtained on long-term denervated soleus and EDL muscles of the rat, where stimula-

tion at high or low frequencies reduced the denervation-induced atrophic changes (Al-Amood et al. 1991; Schmalbruch et al. 1991).

A stimulation protocol that was able to maintain muscle force in chronically denervated rabbit leg muscles was developed by Mokrusch et al. (1990). Unusually long (20 ms) bidirectional impulses at a frequency of 25 Hz were used for stimulating the denervated rabbit hindlimb using large surface electrodes. As shown by morphometric analyses, two short-term (10 min) daily treatments were sufficient for maintaining nearly normal fiber size characteristics. Histochemical and biochemical analyses of metabolic enzyme activities showed a high percentage of fast-twitch oxidative fibers in the denervated stimulated muscles (Mokrusch et al. 1990, 1991). These results, together with those of Nix and Dahm (1987) indicate that long-duration pulses may be more appropriate for stimulation of denervated muscles of larger animals. Such a conclusion is consistent with findings on human denervated muscles.

Transcutaneous stimulation of denervated EDL and TA muscles was performed in patients with peripheral nerve lesions (Valencic et al. 1985, 1986). Stimuli of different pulse width and amplitude were tested. The optimal pulse width, which produced the largest response from the muscles, was of 20-ms duration. Monophasic stimuli of 20-ms duration and 25-Hz frequency were then used. This protocol of stimulation was carried out daily for 20 min on nine patients with peroneal nerve injury and led to an improvement of their dorsiflexion. It appears, thus, that stimuli of long pulse width are able to improve the force output of denervated muscle (Valencic et al. 1985, 1986).

6 Clinical Applications of Chronic Stimulation

Several clinical applications of chronic stimulation have been established. These include the treatment of denervated and immobilized skeletal muscle (see above), the use of transformed skeletal muscle for cardiac assist and repair, as well as the use of chronically stimulated skeletal muscle for sphincter assist.

The potential significance of the ability of a muscle to become fatigue resistant, or express a different phenotype as a result of activity has been recognized in many branches of clinical practice. Initially, it was necessary to establish that human muscle is also capable of changing its characteristics when subjected to chronic stimulation. This was shown for the TA muscle of normal adults, which became fatigue resistant after 6 weeks of low-frequency

stimulation (Scott et al. 1984, 1985). The effects of different patterns of activity have also been tested on human hand muscles. It has been demonstrated that low-frequency stimulation increases the fatigue resistance of these muscles, but leads to reduced force output. On the other hand, a mixed pattern of stimulation produces muscles that remain strong and become fatigue resistant (Rutherford and Jones 1988). In view of these encouraging results, chronic muscle stimulation can now be considered for application in medicine.

6.1 Prevention of Muscle Wasting, Loss of Strength, and Fatigability of Inactive and Diseased Muscles

It is well known that muscle wasting and weakness occur in many conditions associated with loss of function. These include, in addition to complete denervation, many neurological disorders and consequences of injury to the CNS which reduce or prevent the execution of voluntary movement. Not only muscle strength, but also fatigue resistance decreases in conditions such as spinal cord injury or multiple sclerosis (Lenman et al. 1989; Vrbová 1987). It is, therefore, reasonable to test whether returning the lost activity to the inactive muscles will restore some of their impaired function. Interestingly, the first attempts to do so were carried out before the properties of these diseased muscles were examined. Munsat et al. (1976) stimulated the quadriceps muscle of five patients with various neurological disorders for a total time of 4 h/day for 5–12 weeks by a phasic pattern of activity and carried out biopsies before commencement of stimulation and immediately afterwards. In patients whose muscles contracted isometrically the proportion of type I fibers increased. In one patient with tenotomy this increase did not occur; on the contrary, this patient had a higher proportion of type II fibers after stimulation. The size of type I fibers increased in all patients that were stimulated under isometric conditions. In addition, there was an increase in the proportion of fibers that had high levels of oxidative enzymes. In this series of experiments, the muscles were stimulated through implanted electrodes that were wrapped around the nerve so that some axonal damage could have occurred. Various other approaches were used to stimulate muscles of patients with spinal cord injury. In a group of quadriplegic patients Peckham et al. (1975) observed that stimulation could restore force and fatigue resistance to paretic forearm muscles. These authors also used invasive methods for muscle stimulation. More recently, noninvasive methods

have been used to stimulate paretic muscles with similarly satisfactory results (Vrbová et al. 1987; Gordon et al. 1990). Thus, it is possible to maintain the strength and fatigue resistance of muscles of patients with upper motoneuron lesions.

Another example where prolonged inactivity leads to muscle wasting is impairment of joint movements either caused by disease or injury and subsequent surgery. Surgery and subsequent immobilization of the knee joint leads to severe atrophy of the quadriceps muscle. This muscle wasting can be largely prevented by electrical stimulation of the quadriceps during the time of immobilization (Eriksson et al. 1981; Gould et al. 1982).

Chronic low-frequency stimulation has also been applied to the muscles of patients suffering from primary muscle disease such as Duchenne muscular dystrophy (DMD). It appears that low-frequency stimulation can slow the progress of the disease (Scott et al. 1986, 1990; Dubowitz 1988). Similar results have also been noted when the muscles of patients suffering from a variety of primary muscle diseases are subjected to electrical stimulation (Gregoric et al. 1988; Milner Brown and Miller 1988). Many questions regarding the method of administration of stimulation and the pattern and amount of activity are still waiting to be solved.

6.2 Assist of Anal Sphincter by Stimulated Skeletal Muscle

Chronic stimulation is also being used for treatment of anal incontinence by means of dynamic graciloplasty. In this case, the distal part of the gracilis muscle is wrapped around the anal canal and made fatigue resistant by chronic stimulation via an implanted stimulator. For defaecation, the stimulator can be switched off by a magnet (Baeten et al. 1988, 1991; Seccia et al. 1991; N.S. Williams et al. 1989, 1990).

6.3 Use of Chronically Stimulated Skeletal Muscle for Cardiac Assist

The stimulation-induced increase in fatigue resistance is an important prerequisite for the use of skeletal muscle to assist cardiac function. The use of skeletal muscle for cardiac assist was introduced by Carpentier and colleagues (Carpentier and Chachques 1985; Carpentier et al. 1985; Chachques et al. 1988) and Magovern and colleagues (Magovern et al. 1986, 1987, 1988). The principle of

this method, designated cardiomyoplasty, consists of wrapping the latissimus dorsi muscle around the heart and stimulating the muscle in synchrony with the heart contractions. For this purpose, a latissimus dorsi muscle flap, leaving its nerve and vascular pedicle intact, is transferred and sutured around the ventricles. The muscle flap is stimulated via its nerve by a burst-pulse generator which is triggered by a sensing electrode in the myocardium. After a few weeks of conditioning by increasing amounts of chronic stimulation, the muscle becomes fatigue resistant and is capable of contracting in synchrony with the heart.

Cardiomyoplasty has since been used by an increasing number of cardiosurgeons for the treatment of dilatative cardiomyopathy and cardiac aneurisms (for reviews see Chiu and Bourgeois 1990; Carpentier and Bourgeois 1991). Additional applications of skeletal muscle which has been conditioned by chronic stimulation are being developed for cardiac assist, in particular, auxiliary skeletal muscle ventricle pumps for counterpulsation during diastole (Acker et al. 1987a,b; Mannion et al. 1987, 1990).

7 Conclusions

The notion of the plasticity of muscle has opened new perspectives in muscle biology. It implies that skeletal muscle fibers are versatile entities, capable of changing their phenotype in response to altered functional demands. A large body of information in support of this has been derived from experiments using chronic electrostimulation. This experimental model is a suitable approach for studying both the ability and the extent of adaptive changes in skeletal muscle fibers under defined conditions. The most relevant experimental results stem from chronic low-frequency stimulation of fast-twitch muscle. It is well documented that this type of stimulation induces a fast-to-slow conversion of fast-twitch muscle fibers. The changes induced by chronic low-frequency stimulation affect all functional elements of the muscle fiber, i.e., the Ca^{2+}-handling system, energy metabolism, and the contractile apparatus. The replacement of fast-type myofibrillar protein isoforms by their specific slow-type counterparts, the induction of proteins normally not expressed in fast-twitch muscle, as well as quantitative changes in the profile of Ca^{2+}-sequestering proteins and metabolic enzymes are the major characteristics of the induced fiber type transformation. The time course of the changes of the various elements corresponds to a sequential and graded transition of fiber types in the order of type IIB $\rightarrow$ type

IID → type IIA → type I with the transient occurrence of intermediate fiber types. The degree of the transition induced by chronic low-frequency stimulation is different in various mammalian species. It has been shown to be modulated by additional factors, e.g., stretch and hormonal state. Chronic stimulation has also been used to induce a slow-to-fast transition in slow-twitch muscle, which is easiest achieved in the denervated state. The question as to the specificity of the pattern of stimulation as opposed to the overall change in the amount of contractile activity in chronic stimulation-induced transitions has as yet not been answered. Also, the molecular mechanisms underlying the stimulation-induced fiber type transitions have not been studied in sufficient detail. Thus, the question as to the primary signal which triggers the transformation process, as well as the processes involved in the signal transduction to the transcription level, is unanswered. In this regard, early and persistent changes in the ionic environment, alterations in the energy charge or of specific metabolites, the modification of transcription factors, as well as the possible role of known or as yet unidentified determination factors have to be considered.

The ability of skeletal muscle to alter its phenotype in response to chronic stimulation is now applied in clinical practice. In this context, the increase in fatigue resistance displayed by chronically stimulated muscles is of particular importance. Conditioned muscles can then be used to assist the function of impaired muscles, e.g., as a neosphincter or for cardiac assist.

References

Acker M, Anderson WA, Hammond RL, DiMeo F Jr, McCullum J, Staum M, Velchik M, Brown WE, Gale D, Salmons S, Stephenson LW (1987a) Oxygen consumption of chronically stimulated skeletal muscle. J Thorac Cardiovasc Surg 94:702–709

Acker MA, Hammond RL, Mannion JD, Salmons S, Stephenson LW (1987b) Skeletal muscle as the potential power source for a cardiovascular pump: assessment in vivo. Science 236:324–327

Acker MA, Mannion JD, Brown WE, Salmons S, Henriksson J, Bitto T, Gale DR, Hammond R, Stephenson LW (1987c) Canine diaphragm muscle after 1 yr of continuous electrical stimulation: its potential as a myocardial substitute. J Appl Physiol 62:1264–1270

Aigner S, Pette D (1990) In situ hybridization of slow myosin heavy chain mRNA in normal and transforming rabbit muscles with the use of a nonradioactively labeled cRNA. Histochemistry 95:11–18

Aigner S, Pette D (1992) Fast-to-slow transition in myosin heavy chain expression of rabbit muscle fibres induced by chronic low-frequency stimulation. In: El Haj AJ (ed) Molecular biology of muscle. Symp Soc Exp Biol 46 (in press)

Al-Amood WS, Lewis DM (1987) The role of frequency in the effects of long-term intermittent stimulation of denervated slow-twitch muscle in the rat. J Physiol (Lond) 392:377–395

Al-Amood WS, Buller AJ, Pope R (1973) Long-term stimulation of cat fast-twitch skeletal muscle. Nature 244:225–227

Al-Amood WS, Lewis DM, Schmalbruch H (1991) Effect of chronic electrical stimulation on contractile properties of long-term denervated rat skeletal muscle. J Physiol (Lond) 441:243–256

Annex BH, Kraus WE, Dohm GL, Williams RS (1991) Mitochondrial biogenesis in striated muscles: rapid induction of citrate synthase mRNA by nerve stimulation. Am J Physiol 260:C266–C270

Armstrong RB (1990) Initial events in exercise-induced muscular injury. Med Sci Sports Exerc 22:429–435

Ausoni S, Gorza L, Schiaffino S, Gundersen K, Lømo T (1990) Expression of myosin heavy chain isoforms in stimulated fast and slow rat muscles. J Neurosci 10:153–160

Baeten C, Spaans F, Fluks A (1988) An implanted neuromuscular stimulator for fecal incontinence following previously implanted gracilis muscle. Report of a case. Dis Colon Rectum 31:134–137

Baeten CGMI, Konsten J, Spaans F, Habets F, Soeters P (1991) Dynamic graciloplasty for fecal incontinence. In: Carraro U, Salmons S (eds) Basic and applied myology: perspectives for the 90's. Unipress, Padova, pp 293–300

Baldwin KM, Herrick RE, Ilyina-Kakueva E, Oganov VS (1990) Effects of zero gravity on myofibril content and isomyosin distribution in rodent skeletal muscle. FASEB J 4:79–83

Bär A, Pette D (1988) Three fast myosin heavy chains in adult rat skeletal muscle. FEBS Lett 235:153–155

Bär A, Simoneau J-A, Pette D (1989) Altered expression of myosin light chain isoforms in chronically stimulated fast-twitch muscle of the rat. Eur J Biochem 178:591–594

Bárány M (1967) ATPase activity of myosin correlated with speed of muscle shortening. J Gen Physiol 50:197–218

Bárány M, Close RI (1971) The transformation of myosin in cross-innervated rat muscles. J Physiol (Lond) 213:455–474

Barnard RJ, Edgerton VR, Furukawa T, Peter JB (1971) Histochemical, biochemical and contractile properties of red, white, and intermediate fibers. Am J Physiol 220:410–414

Beitner R (1990) Regulation of carbohydrate metabolism by glucose 1,6-bisphosphate in extrahepatic tissues; comparison with fructose 2,6-bisphosphate. Int J Biochem 22:553–557

Booth FW (1988) Perspectives on molecular and cellular exercise physiology. J Appl Physiol 65:1461–1471

Booth FW, Seider MJ (1979) Early change in skeletal muscle protein synthesis after limb immobilization of rats. J Appl Physiol 47:974–977

Breitbart RE, Nadal-Ginard B (1986) Complete nucleotide sequence of the fast skeletal troponin T gene. Alternatively spliced exons exhibit unusual interspecies divergence. J Mol Biol 188:313–324

Breitbart RE, Nadal-Ginard B (1987) Developmentally induced, muscle-specific trans factors control the differential splicing of alternative and constitutive troponin T exons. Cell 49:793–803

Briggs FN, Lee KF, Feher JJ, Wechsler AS, Ohlendieck K, Campbell, K (1990) Ca-ATPase isozyme expression in sarcoplasmic reticulum is altered by chronic stimulation of skeletal muscle. FEBS Lett 259:269–272

Briggs MM, Schachat F (1989) N-terminal amino acid sequences of three functionally different troponin T isoforms from rabbit fast skeletal muscle. J Mol Biol 206:245–249

Briggs MM, Lin JJ-C, Schachat FH (1987) The extent of amino-terminal heterogeneity in rabbit fast skeletal muscle troponin T. J Muscle Res Cell Motil 8:1–12

Brooke MH, Kaiser KK (1970) Three myosin adenosine triphosphatase systems: the nature of their pH lability and sulfhydryl dependence. J Histochem Cytochem 18:670–672

Brown J, Salmons S (1981) Percutaneous control of an implantable muscle stimulator via an optical link. J Biomed Eng 3:206–208

Brown JMC, Henriksson J, Salmons S (1989) Restoration of fast muscle characteristics following cessation of chronic stimulation: physiological, histochemical and metabolic changes during slow-to-fast transformation. Proc R Soc Lond [Biol] 235:321–346

Brown MD, Cotter M, Hudlická O, Smith ME, Vrbová G (1973) The effect of long-term stimulation of fast muscles on their ability to withstand fatigue. J Physiol (Lond) 238:47–48P

Brown MD, Cotter MA, Hudlická O, Vrbová G (1976) The effects of different patterns of muscle activity on capillary density, mechanical properties and structure of slow and fast rabbit muscles. Pflügers Arch 361:241–250

Brown WE, Salmons S, Whalen RG (1983) The sequential replacement of myosin subunit isoforms during muscle type transformation induced by long term electrical stimulation. J Biol Chem 258:14686–14692

Brown WE, Salmons S, Whalen RG (1985) Mechanisms underlying the asynchronous replacement of myosin light chain isoforms during stimulation-induced fibre-type transformation of skeletal muscle. FEBS Lett 192:235–238

Brownson C, Isenberg H, Brown W, Salmons S, Edwards Y (1988) Changes in skeletal muscle gene transcription induced by chronic stimulation. Muscle Nerve 11:1183–1189

Brownson C, Little P, Jarvis JC, Salmons S (1992) Reciprocal changes in myosin isoform mRNAs of rabbit skeletal muscle in response to the initiation and cessation of chronic electrical stimulation. Muscle Nerve 15:694–700

Buchegger A, Nemeth PM, Pette D, Reichmann H (1984) Effects of chronic stimulation on the metabolic heterogeneity of the fibre population in rabbit tibialis anterior muscle. J Physiol (Lond) 350:109–119

Buller AJ, Lewis DM (1965) Some observations on the effects of tenotomy in the rabbit. J Physiol (Lond) 178:326–342

Buller AJ, Pope R (1977) Plasticity in mammalian skeletal muscle. Philos Trans R Soc Lond [Biol] 278:295–305

Burke RE, Levine DN, Zajac FE (1971) Mammalian motor units: physiological-histochemical correlation in three types in cat gastrocnemius. Science 174:709–712

Burke RE, Levine DN, Tsairis P, Zajac FE (1973) Physiological types and histochemical profiles in motor units of the cat gastrocnemius. J Physiol (Lond) 234:723–748

Carpentier A, Bourgeois I (eds) (1991) Cardiomyoplasty. Futura, Mount Kisco

Carpentier A, Chachques J-C (1985) Myocardial substitution with a stimulated skeletal muscle: first successful clinical case. Lancet 1:1267

Carpentier A, Chachques J-C, Grandjean P, Perier P, Mitz V, Bourgeois I (1985) Transformation d'un muscle squelettique par stimulation séquentielle progressive en vue de son utilisation comme substitut myocardique. CR Acad Sci Paris 301:581–586

Carraro U, Catani C, Belluco S, Cantini M, Marchioro L (1986) Slow-like electrostimulation switches on slow myosin in denervated fast muscle. Exp Neurol 94:537–553

Carraro U, Catani C, Saggin L, Zrunek M, Szabolcs M, Gruber H, Streinzer W, Mayr W, Thoma H (1988) Isomyosin changes after functional electrostimulation of denervated sheep muscle. Muscle Nerve 11:1016–1028

Carraro U, Catani C, Rizzi C, Belluco S, DallaLibera L, Danieli-Betto D, Miracoli G, Arpesella G, Mikus P, Cirillo M, Parlapiano M, Seni M, Pierangeli A (1991) The use of transplanted skeletal muscle for cardiac assistance. In: Maréchal G, Carraro U (eds) Muscle and motility. Intercept, Andover, pp 157–164

Celio MR, Heizmann CW (1982) Calcium-binding protein parvalbumin is associated with fast contracting muscle fibres. Nature 297:504–506

Chachques JC, Grandjean P, Schwartz K, Mihaileanu S, Fardeau M, Swynghedauw B, Fontaliran F, Romero N, Wisnewsky C, Perier P, Chauvaud S, Bourgeois I, Carpentier A (1988) Effect of latissimus dorsi dynamic cardiomyoplasty on ventricular function. Circulation 78:III-203–III-216

Chi MM-Y, Hintz CS, Henriksson J, Salmons S, Hellendahl RP, Park JL, Nemeth PM, Lowry OH (1986) Chronic stimulation of mammalian muscle: enzyme changes in individual fibers. Am J Physiol 251:C633–C642

Chiu RC-J, Bourgeois I (eds) (1991) Transformed muscle for cardiac assist and repair. Futura, Mount Kisco

Ciesielski TE, Fukuda Y, Glenn WWL, Gorfien J, Jeffery K, Hogan JF (1983) Response of the diaphragm muscle to electrical stimulation of the phrenic nerve. J Neurosurg 58:92–100

Ciske PE, Faulkner JA (1985) Chronic electrical stimulation of nongrafted and grafted skeletal muscles in rats. J Appl Physiol 59:1434–1439

Clark BJ III, Acker MA, McCully K, Subramanian HV, Hammond RL, Salmons S, Chance B, Stephenson LW (1988) In vivo ^{31}P-NMR spectroscopy of chronically stimulated canine skeletal muscle. Am J Physiol 254:C258–C266

Cotter M, Hudlická O (1977) Effects of chronic stimulation on muscles in ageing rats. J Physiol (Lond) 266:102P–103P

Cotter M, Phillips P (1986) Rapid fast to slow fiber transformation in response to chronic stimulation of immobilized muscles of the rabbit. Exp Neurol 93:531–545

Cotter M, Hudlická O, Pette D, Staudte H, Vrbová G (1972) Changes of capillary density and enzyme pattern in fast rabbit muscles during long-term stimulation. J Physiol (Lond) 230:34P–35P

Cotter M, Hudlická O, Vrbová G (1973) Growth of capillaries during long-term activity in skeletal muscle. Bibl Anat 11:395–398

Cumming DV, O'Brien GA, Williamson HA, Dunn MJ, Pattison CW, Yacoub MH (1991) Analysis of gene expression at protein level in skeletal muscle used for cardiac assistance. In: Maréchal G, Carraro U (eds) Muscle and motility. Intercept, Andover, pp 165–168

Dawson JM, Hudlická O (1989) The effect of long-term activity on the microvasculature of rat glycolytic skeletal muscle. Int J Microcirc Clin Exp 8:53–69

Donselaar Y, Eerbeek O, Kernell D, Verhey BA (1987) Fibre sizes and histochemical staining characteristics in normal and chronically stimulated fast muscle of cat. J Physiol (Lond) 382:237–254

Dubowitz V (1988) Responses of diseased muscle to electrical and mechanical intervention. In: Plasticity of the neuromuscular System, Ciba Found Symp 138. Wiley, Chichester, pp 240–255

Düsterhöft S, Yablonka-Reuveni Z, Pette D (1991) Characterization of myosin isoforms in satellite cell cultures from adult rat diaphragm, soleus, and tibialis anterior muscles. Differentiation 45:185–191

Dux L, Green HJ, Pette D (1990) Chronic low-frequency stimulation of rabbit fast-twitch muscle induces partial inactivation of the sarcoplasmic reticulum Ca^{2+}-ATPase and changes in its tryptic cleavage. Eur J Biochem 192:95–100

Edwards RHT, Jones DA, Newham DJ (1982) Low-frequency stimulation and changes in human muscle contractile properties. J Physiol (Lond) 328:29P–30P

Eerbeek O, Kernell D, Verhey BA (1984) Effects of fast and slow patterns of tonic long-term stimulation on contractile properties of fast muscle in cat. J Physiol (Lond) 352:73–90

Eisenberg BR, Salmons S (1981) The reorganization of subcellular structure in muscle undergoing fast-to-slow type transformation. A stereological study. Cell Tissue Res 220:449–471

Eisenberg BR, Brown JMC, Salmons S (1984) Restoration of fast muscle characteristics following cessation of chronic stimulation. The ultrastructure of slow-to-fast transformation. Cell Tissue Res 238:221–230

Eken T, Gundersen K (1988) Chronic electrical stimulation resembling normal motor-unit activity: effects on denervated fast and slow rat muscles. J Physiol (Lond) 402:651–669

Eriksson E, Haggmark T, Kiessling TH, Karlsson J (1981) Effect of electrical stimulation on human skeletal muscle. Int J Sports Med 2:18–22

Essig DA, Devol DL, Bechtel PJ, Trannel TJ (1991) Expression of embryonic myosin heavy chain mRNA in stretched adult chicken skeletal muscle. Am J Physiol 260:C1325–C1331

Ferguson AS, Stone HE, Roessmann U, Burke M, Tisdale E, Mortimer JT (1989) Muscle plasticity: comparison of 30-Hz burst with 10-Hz continuous stimulation. J Appl Physiol 66:1143–1151

Fitzsimons RB, Hoh JFY (1983) Myosin isoenzymes in fast-twitch and slow-twitch muscles of normal and dystrophic mice. J Physiol (Lond) 343:539–550

Franchi LL, Murdoch A, Brown WE, Mayne CN, Elliott L, Salmons S (1990) Subcellular localization of newly incorporated myosin in rabbit fast skeletal muscle undergoing stimulation-induced type transformation. J Muscle Res Cell Motil 11:227–239

Frey M, Thoma H, Gruber H, Stöhr H, Huber L, Havel M, Steiner E (1984) The chronically stimulated muscle as an energy source for artificial organs. Preliminary results of a basic study in sheep. Eur Surg Res 16:232–237

Frey M, Thoma H, Gruber H, Stöhr H, Havel M (1986) The chronically stimulated psoas muscle as an energy source for artificial organs: an experimental study in sheep. In: Chiu R C-J (ed) Biomechanical cardiac assist: cardiomyplasty and muscle-powered devices. Futura, Mount Kisko, pp 179–191

Frischknecht R, Vrbová G (1991) Adaptation of rat extensor digitorum longus to overload and increased activity. Pflügers Arch 419:319–326

Gillis JM (1985) Relaxation of vertebrate skeletal muscle. A synthesis of the biochemical and physiological approaches. Biochim Biophys Acta 811:97–145

Goldberg AL (1969) Protein turnover in skeletal muscle: I. Protein catabolism during work-induced hypertrophy and growth induced with growth hormone. J Biol Chem 244:3217–3222

Goldspink DF (1977) The influence of immobilization and stretch on protein turnover of rat skeletal muscle. J Physiol (Lond) 264:267–282

Goldspink G (1985) Malleability of the motor system: a comparative approach. J Exp Biol 115:375–391

Gordon T, Stein RB, Martin T (1990) Physiological and histochemical changes in human muscle produced by electrical stimulation after spinal cord injury. J Neurol Sci 98 (suppl):141(Abstr553)

Gorza L (1990) Identification of a novel type 2 fiber population in mammalian skeletal muscle by combined use of histochemical myosin ATPase and anti-myosin monoclonal antibodies. J Histochem Cytochem 38:257–265

Gorza L, Gundersen K, Lømo T, Schiaffino S, Westgaard RH (1988) Slow-to-fast transformation of denervated soleus muscles by chronic high-frequency stimulation in the rat. J Physiol (Lond) 402:627–649

Gould N, Donnermeyer D, Pope M, Ashigaka I (1982) Transcutaneous muscle stimulation as a method to retard disuse atrophy. Clin Orthop 164:215–220

Grandjean PA, Bakels N, Berne E, Leinders R, Siekmeyer G, Urban R, Bourgeois IM (1990) Pulse generator for biomechanical cardiac assistance by counterpulsation technique. In: Chiu RC-J, Bourgeois I (eds) Transformed muscle for cardiac assist and repair. Futura, Mount Kisco, pp 281–290

Green HJ, Düsterhöft S, Dux L, Pette D (1990) Time dependent changes in metabolites of energy metabolism in low-frequency stimulated rabbit fast-twitch muscle. In: Pette D (ed) The dynamic state of muscle fibers. De Gruyter, Berlin, pp 617–628

Green HJ, Cadefau J, Pette D (1991) Altered glucose 1,6-bisphosphate and fructose 2,6-bisphosphate levels in low-frequency stimulated rabbit fast-twitch muscle. FEBS Lett 282:107–109

Green HJ, Düsterhöft S, Dux L, Pette D (1992) Metabolite patterns related to exhaustion, recovery, and transformation of chronically stimulated rabbit fast-twitch muscle. Pflügers Arch 420:359–366

Gregoric MV, Valencic V, Zupan A, Klemen A (1988) Effects of electrical stimulation on muscles of patients with progressive muscular disease. In: Wallinga WH, Boom BK, de Vries J (eds) Electrophysiological kinesiology. Proceedings of the 7th Congress of the International Society of Electrophysiological Kinesiology. Excerpta Medica, Amsterdam, pp 385–389

Gregory P, Low RB, Stirewalt WS (1986) Changes in skeletal-muscle myosin isoenzymes with hypertrophy and exercise. Biochem J 238:55–63

Gregory P, Gagnon J, Essig DA, Reid SK, Prior G, Zak R (1990) Differential regulation of actin and myosin isoenzyme synthesis in functionally overloaded skeletal muscle. Biochem J 265:525–532

Grodins F, Osborne S, Johnson F, Arano S, Ivy A (1944) The effect of appropriate electrical stimulation on atrophy of denervated skeletal muscle in the rat. Am J Physiol 142:221–230

Gros G, Dodgson SJ (1988) Velocity of CO_2 exchange in muscle and liver. Annu Rev Physiol 50:669–694

Gundersen K, Leberer E, Lømo T, Pette D, Staron RS (1988) Fibre types, calcium-sequestering proteins and metabolic enzymes in denervated and chronically stimulated muscles of the rat. J Physiol (Lond) 398:177–189

Gustafson TA, Markham BE, Morkin E (1986) Effects of thyroid hormone on α-actin and myosin heavy chain gene expression in cardiac and skeletal muscles of the rat: measurement of mRNA content using synthetic oligonucleotide probes. Circ Res 59:194–201

Guth L, Samaha FH (1969) Qualitative differences between actomyosin ATPase of slow and fast mammalian muscle. Exp Neurol 25:138–152

Gutmann E, Guttmann L (1944) The effect of galvanic exercise on denervated and reinnervated muscles in the rabbit. J Neurol Neurosurg Psychiatry 7:7–17

Härtner K-T, Pette D (1990) Effects of chronic low-frequency stimulation on troponin I and troponin C isoforms in rabbit fast-twitch muscle. Eur J Biochem 188:261–267

Härtner K-T, Kirschbaum BJ, Pette D (1989) The multiplicity of troponin T isoforms. Normal rabbit muscles and effects of chronic stimulation. Eur J Biochem 179:31–38

Havenith MG, van der Veen FH, Glatz JFC, Lucas C, Schrijvers-van Schendel JMC, Penn OCKM, Wellens HJJ (1990) Monitoring of muscle fiber type of canine latissimus dorsi muscle during chronic electric stimulation by enzyme- and immunohistochemistry. In: Chiu RC-J, Bourgois I (eds) Transformed muscle for cardiac assist and repair. Futura, Mount Kisco, pp 53–61

Heilig A, Pette D (1980) Changes induced in the enzyme activity pattern by electrical stimulation of fast-twitch muscle. In: Pette D (ed) Plasticity of muscle. De Gruyter, Berlin, pp 409–420

Heilig A, Pette D (1983) Changes in transcriptional activity of chronically stimulated fast twitch muscle. FEBS Lett 151:211–214

Heilig A, Pette D (1988) Albumin in rabbit skeletal muscle. Origin, distribution and regulation by contractile activity. Eur J Biochem 171:503–508

Heilig A, Seedorf K, Seedorf U, Pette D (1984) Transcriptional and translational control of myosin light chain expression in adult muscle. In: Eppenberger HM, Perriard J-C (eds) Developmental processes in normal and diseased muscle. Karger, Basel, pp 182–186 (Experimental biology and medicine, vol 9)

Heilmann C, Pette D (1979) Molecular transformations in sarcoplasmic reticulum of fast-twitch muscle by electro-stimulation. Eur J Biochem 93:437–446

Heilmann C, Pette D (1980) Molecular transformations of sarcoplasmic reticulum in chronically stimulated fast-twitch muscle In: Pette D (ed) Plasticity of muscle. De Gruyter, Berlin, pp 421–440

Heilmann C, Müller W, Pette D (1981) Correlation between ultrastructural and functional changes in sarcoplasmic reticulum during chronic stimulation of fast muscle. J Membr Biol 59:143–149

Heizmann CW, Berchtold MW, Rowlerson AM (1982) Correlation of parvalbumin concentration with relaxation speed in mammalian muscles. Proc Natl Acad Sci USA 79:7243–7247

Hennig R, Lømo T (1987) Effects of chronic stimulation on the size and speed of long-term denervated and innervated rat fast and slow skeletal muscles. Acta Physiol Scand 130:115–131

Henriksson J, Chi MM-Y, Hintz CS, Young DA, Kaiser KK, Salmons S, Lowry OH (1986) Chronic stimulation of mammalian muscle: changes in enzymes of six metabolic pathways. Am J Physiol 251:C614–C632

Henriksson J, Salmons S, Chi MM-Y, Hintz CS, Lowry OH (1988) Chronic stimulation of mammalian muscle: changes in metabolite concentrations in individual fibers. Am J Physiol 255:C543–C551

Henriksson J, Salmons S, Lowry OH (1990) Chronic stimulation of mammalian muscle: enzyme and metabolite changes in homogenates and individual fibers. In: Chiu RC-J, Bourgeois I (eds) Transformed muscle for cardiac assist and repair. Futura, Mount Kisco, pp 9–24

Hilton SM, Jeffries MG, Vrbová G (1970) Functional specialization of the vascular bed of the soleus muscle. J Physiol (Lond) 206:543–562

Hoffman RK, Gambke B, Stephenson LW, Rubinstein NA (1985) Myosin transitions in chronic stimulation do not involve embryonic isozymes. Muscle Nerve 8:796–805

Hoh JFY, Chow CJ (1983) The effect of the loss of weight-bearing function on the isomyosin profile and contractile properties of rat skeletal muscles. In: Kidman AD, Tomkins JK, Morris CA, Cooper NA (eds) Molecular pathology of nerve and muscle. Humana, Clifton, pp 371–384

Hood DA, Parent G (1991) Metabolic and contractile responses of rat fast-twitch muscle to 10-Hz stimulation. Am J Physiol 260:C832–C840

Hood DA, Pette D (1989) Chronic long-term stimulation creates a unique metabolic enzyme profile in rabbit fast-twitch muscle. FEBS Lett 247:471–474

Hood DA, Zak R, Pette D (1989) Chronic stimulation of rat skeletal muscle induces coordinate increases in mitochondrial and nuclear mRNAs of cytochrome c oxidase subunits. Eur J Biochem 179:275–280

Hoppeler H (1990) The range of mitochondrial adaptation in muscle fibers In: Pette D (ed) The dynamic state of muscle fibers. De Gruyter, Berlin, pp 567–586

Hoppeler H, Hudlická O, Uhlmann E (1987) Relationship between mitochondria and oxygen consumption in isolated cat muscles. J Physiol (Lond) 385:661–675

Hudlická O (1984) Development of microcirculation: capillary growth and adaptation. In: Renkin EM, Michel CC, Geiger SR (eds) Handbook of physiology, sect 2: the cardiovascular system. Williams and Wilkins, Baltimore MD, pp 165–216

Hudlická O, Price S (1990) The role of blood flow and/or muscle hypoxia in capillary growth in chronically stimulated fast muscles. Pflügers Arch 417:67–72

Hudlická O, Tyler KR (1984) The effect of long-term high-frequency stimulation on capillary density and fibre types in rabbit fast muscles. J Physiol (Lond) 353:435–445

Hudlická O, Brown M, Cotter M, Smith M, Vrbová G (1977) The effect of long-term stimulation of fast muscles on their blood flow, metabolism and ability to withstand fatigue. Pflügers Arch 369:141–149

Hudlická O, Tyler KR, Aitman T (1980) The effect of long-term electrical stimulation on fuel uptake and performance in fast skeletal muscles. In: Pette D (ed) Plasticity of muscle. De Gruyter, Berlin, pp 401–408

Hudlická O, Tyler KR, Srihari T, Heilig A, Pette D (1982a) The effect of different patterns of long-term stimulation on contractile properties and myosin light chains in rabbit fast muscles. Pflügers Arch 393:164–170

Hudlická O, Dodd L, Renkin EM, Gray SD (1982b) Early changes in fiber profile and capillary density in long-term stimulated muscles. Am J Physiol 243:H528–H535

Hudlická O, Aitman T, Heilig A, Leberer E, Tyler KR, Pette D (1984) Effects of different patterns of long-term stimulation on blood flow, fuel uptake and enzyme activities in rabbit fast skeletal muscle. Pflügers Arch 402:306–311

Hudlická O, Cotter MA, Cooper J (1986) The effect of long-term electrical stimulation on capillary supply and metabolism in fast skeletal muscle. In: Nix WA, Vrbová G (eds) Electrical stimulation and neuromuscular disorders. Springer, Berlin Heidelberg New York, pp 21–32

Hudlická O, Hoppeler H, Uhlmann E (1987) Relationship between the size of the capillary bed and oxidative capacity in various cat skeletal muscles. Pflügers Arch 410:369–375

Ianuzzo D, Patel P, Chen V, O'Brien P, Williams C (1977) Thyroidal trophic influence on skeletal muscle myosin. Nature 270:74–76

Ianuzzo CD, Hamilton N, O'Brien PJ, Desrosiers C, Chiu R (1990a) Biochemical transformation of canine skeletal muscle for use in cardiac-assist devices. J Appl Physiol 68:1481–1485

Ianuzzo CD, Hamilton N, O'Brien PJ, Dionisopoulos T, Salerno T, Chiu RC-J (1990b) Biochemical characteristics of cardiac and transformed canine skeletal muscle. In: Chiu RC-J, Bourgeois I (eds) Transformed muscle for cardiac assist and repair. Futura, Mount Kisco, pp 25–40

Izumo S, Nadal-Ginard B, Mahdavi V (1986) All members of the MHC multigene family respond to thyroid hormone in a highly tissue-specific manner. Science 231:597–600

Jeffery S, Kelly CD, Carter N, Kaufmann M, Termin A, Pette D (1990) Chronic stimulation-induced effects point to a coordinated expression of carbonic anhydrase III and slow myosin heavy chain in skeletal muscle. FEBS Lett 262:225–227

Jolesz F, Sréter FA (1981) Development, innervation, and activity-pattern induced changes in skeletal muscle. Annu Rev Physiol 43:531–552

Jorgensen AO, Jones LR (1986) Localization of phospholamban in slow but not fast canine skeletal muscle fibers. An immunocytochemical and biochemical study. J Biol Chem 261:3775–3781

Kaplove KA (1987) Reanalysis: impulse activity and fiber type transformation. Muscle Nerve 10:375–376

Kaufmann M, Simoneau J-A, Veerkamp JH, Pette D (1989) Electrostimulation-induced increases in fatty acid-binding protein and myoglobin in rat fast-twitch muscle and comparison with tissue levels in heart. FEBS Lett 245:181–184

Kelly AM (1978) Satellite cells and myofiber growth in the rat soleus and extensor digitorum muscles. Dev Biol 65:1–10

Kernell D, Eerbeek O (1989) Physiological effects of different patterns of chronic stimulation on muscle properties. In: Rose FC, Jones R (eds) Neuromuscular stimulation. Demos, New York, pp 193–200

Kernell D, Eerbeek O, Verhey BA, Donselaar Y (1987a) Effects of physiological amounts of high- and low-rate chronic stimulation on fast-twitch muscle of the cat hindlimb: I. Speed- and force-related properties. J Neurophysiol 58:598–613

Kernell D, Donselaar Y, Eerbeek O (1987b) Effects of physiological amounts of high- and low-rate chronic stimulation on fast-twitch muscle of the cat hindlimb: II. Endurance-related properties. J Neurophysiol 58:614–627

Kirschbaum BJ, Pette D (1988) Low-frequency stimulation of rat fast-twitch muscle induces rapid, reversible changes in myosin heavy chain expression. In: Carraro U (ed) Sarcomeric and non-sarcomeric muscles: basic and applied research prospects for the 90's. Unipress, Padova, pp 337–342

Kirschbaum BJ, Heilig A, Härtner K-T, Pette D (1989a) Electrostimulation-induced fast-to-slow transitions of myosin light and heavy chains in rabbit fast-twitch muscle at the mRNA level. FEBS Lett 243:123–126

Kirschbaum BJ, Simoneau J-A, Bär A, Barton PJR, Buckingham ME, Pette D (1989b) Chronic stimulation-induced changes of myosin light chains at the mRNA and protein levels in rat fast-twitch muscle. Eur J Biochem 179:23–29

Kirschbaum BJ, Simoneau J-A, Pette D (1989c) Dynamics of myosin expression during the induced transformation of adult rat fast-twitch muscle In: Stockdale F, Kedes L (eds) Cellular and molecular biology of muscle development. Liss, New York, pp 461–469 (UCLA symposia on molecular and cellular biology, new series, vol 93)

Kirschbaum BJ, Kucher H-B, Termin A, Kelly AM, Pette D (1990a) Antagonistic effects of chronic low frequency stimulation and thyroid hormone on myosin expression in rat fast-twitch muscle. J Biol Chem 265:13974–13980

Kirschbaum BJ, Schneider S, Izumo S, Mahdavi V, Nadal-Ginard B, Pette D (1990b) Rapid and reversible changes in myosin heavy chain expression in response to increased neuromuscular activity of rat fast-twitch muscle. FEBS Lett 268:75–78

Klug G, Reichmann H, Pette D (1983a) Rapid reduction in parvalbumin concentration during chronic stimulation of rabbit fast twitch muscle. FEBS Lett 152:180–182

Klug G, Wiehrer W, Reichmann H, Leberer E, Pette D (1983b) Relationships between early alterations in parvalbumin, sarcoplasmic reticulum and metabolic enzymes in chronically stimulated fast twitch muscle. Pflügers Arch 399:280–284

Klug GA, Houston ME, Stull JT, Pette D (1986) Decrease in myosin light chain kinase activity of rabbit fast muscle by chronic stimulation. FEBS Lett 200:352–354

Klug GA, Leberer E, Leisner E, Simoneau J-A, Pette D (1988) Relationship between parvalbumin content and the speed of relaxation in chronically stimulated rabbit fast-twitch muscle. Pflügers Arch 411:126–131

Kucher H-B, Kirschbaum BJ, Kelly AM, Pette D (1988) Modulation of thyroid hormone-induced effects on the expression of myosin heavy chain isoforms in rat fast-twitch muscle by chronic low-frequency nerve stimulation In: Carraro U (ed) Sarcomeric and non-sarcomeric muscles: basic and applied research prospects for the 90's. Unipress, Padova, pp 25–28

Kwong WH, Vrbová G (1981) Effects of low-frequency electrical stimulation on fast and slow muscles of the rat. Pflügers Arch 391:200–207

Laufer R, Changeux J-P (1989) Activity-dependent regulation of gene expression in muscle and neuronal cells. Mol Neurobiol 3:1–53

Lawrence JC Jr, Krsek JA, Salsgiver WJ, Hiken JF, Salmons S, Smith RL (1986) Phosphorylase kinase isozymes in normal and electrically stimulated skeletal muscles. Am J Physiol 250:C84–C89

Leberer E, Pette D (1986a) Immunochemical quantitation of sarcoplasmic reticulum Ca-ATPase, of calsequestrin and of parvalbumin in rabbit skeletal muscles of defined fiber composition. Eur J Biochem 156:489–496

Leberer E, Pette D (1986b) Neural regulation of parvalbumin expression in mammalian skeletal muscle. Biochem J 235:67–73

Leberer E, Pette D (1990) Influence of neuromuscular activity upon the expression of parvalbumin in mammalian skeletal muscle. In: Pette D (ed) The dynamic state of muscle fibers. De Gruyter, Berlin, pp 497–508

Leberer E, Seedorf U, Pette D (1986) Neural control of gene expression in skeletal muscle. Ca-sequestering proteins in developing and chronically stimulated rabbit skeletal muscles. Biochem J 239:295–300

Leberer E, Härtner K-T, Pette D (1987a) Reversible inhibition of sarcoplasmic reticulum Ca-ATPase by altered neuromuscular activity in rabbit fast-twitch muscle. Eur J Biochem 162:555–561

Leberer E, Staron RS, Gundersen K, Lømo T, Pette D (1987b) Control of parvalbumin expression in rat skeletal muscle by motor-unit specific activity patterns. In: Norman AW, Vanaman TC, Means AR (eds) Calcium binding proteins in health and disease. Academic, New York, pp 287–289

Leberer E, Härtner K-T, Brandl CJ, Fujii J, Tada M, MacLennan DH, Pette D (1989) Slow/cardiac sarcoplasmic reticulum Ca-ATPase and phospholamban mRNAs are expressed in chronically stimulated rabbit fast-twitch muscle. Eur J Biochem 185:51–54

Lenman AJR, Tulley FM, Vrbová G, Dimitrijevic MR, Towle JA (1989) Muscle fatigue in some neurological disorders. Muscle Nerve 12:938–942

Lieber RL (1986) Skeletal muscle adaptability: III. muscle properties following chronic electrical stimulation. Dev Med Child Neurol 28:662–670

Lømo T (1989) Long-term effects of altered activity on skeletal muscle. Biomed Biochim Acta 48:S432–S444

Lømo T, Westgaard RH (1974) Contractile properties of muscle: control by pattern of muscle activity in the rat. Proc R Soc Lond [Biol] 187:99–103

Lømo T, Westgaard RH, Engebretsen L (1980) Different stimulation patterns affect contractile properties of denervated rat soleus muscles. In: Pette D (ed) Plasticity of muscle. De Gruyter, Berlin, pp 297–309

Mabuchi K, Szvetko D, Pintér K, Sréter FA (1982) Type IIB to IIA fiber transformation in intermittently stimulated rabbit muscles. Am J Physiol 242:C373–C381

Mabuchi K, Sréter FA, Gergely J (1990) Myosin and sarcoplasmic reticulum Ca^{2+}-ATPase isoforms in electrically stimulated rabbit fast muscle. In: Pette D (ed) The dynamic state of muscle fibers. De Gruyter, Berlin, pp 445–462

Magovern GJ, Park SB, Magovern GJ Jr, Benckart DH, Tullis G, Rozar E, Kao R, Christlieb I (1986) Latissimus dorsi as a functioning synchronously paced muscle component in the repair of a left ventricular aneurism. Ann Thorac Surg 41:116

Magovern GJ, Heckler FR, Park SB, Christlieb IY, Magovern GJ Jr, Kao RL, Benckart DH, Tullis G, Rozar E, Liebler GA, Burkholder JA, Maher TD (1987) Paced latissimus dorsi used for dynamic cardiomyoplasty of left ventricular aneurysms. Ann Thorac Surg 44:379–388

Magovern GJ, Heckler FR, Park SB, Christlieb IY, Liebler GA, Burkholder JA, Maher TD, Benckart DH, Magovern GJ Jr, Kao RL (1988) Paced skeletal muscle for dynamic cardiomyoplasty. Ann Thorac Surg 45:614–619

Magovern GJ, Park SB, Christlieb IY, Magovern GJ Jr, Kao RL (1990) Paced conditioned latissimus dorsi for cardiac assist. In: Chiu R C-J, Bourgeois I (eds) Transformed muscle for cardiac assist and repair. Futura, Mount Kisco, pp 199–208

Maier A, Pette D (1987) The time course of glycogen depletion in single fibers of chronically stimulated rabbit fast-twitch muscle. Pflügers Arch 408:338–342

Maier A, Gambke B, Pette D (1986) Degeneration-regeneration as a mechanism contributing to the fast to slow conversion of chronically stimulated fast-twitch rabbit muscle. Cell Tissue Res 244:635–643

Maier A, Gorza L, Schiaffino S, Pette D (1988) A combined histochemical and immunohistochemical study on the dynamics of fast to slow fiber transformation in chronically stimulated rabbit muscle. Cell Tissue Res 254:59–68

Mannion JD, Bitto T, Hammond RL, Rubinstein NA, Stephenson LW (1986) Histochemical and fatigue characteristics of conditioned canine latissimus dorsi muscle. Circ Res 58:298–304

Mannion JD, Acker MA, Hammond RL, Faltemeyer W, Duckett S, Stephenson LW (1987) Power output of skeletal muscle ventricles in circulation: short-term studies. Circulation 76:155–162

Mannion JD, Shannon J, Chen W, Brown WE, Gale DR (1990) Skeletal muscle-powered assistance for the heart: assessment of a goat model. In: Chiu R C-J, Bourgeois I (eds) Transformed muscle for cardiac assist and repair. Futura, Mount Kisco, pp 117–127

Maréchal G, Biral D, Beckers-Bleukx G, Colson-van Schoor M (1989) Subunit composition of native myosin isoenzymes of some striated mammalian muscles. Biomed Biochim Acta 48:S417–S421

Marzocchi M, Brouillette RT, Klemka-Walden LM, Heller SL, Weese-Mayer DE, Brozanski BS, Caliendo J, Daood M, Ilbawi MN, Hunt CE (1990) Effects of continuous low-frequency pacing on immature canine diaphragm. J Appl Physiol 69:892–898

Mastri C, Salmons S, Thomas GH (1982) Early events in the response of fast skeletal muscle to chronic low-frequency stimulation. Polyamine biosynthesis and protein phosphorylation. Biochem J 206:211–219

Matsushita S, Pette D (1992) Inactivation of sarcoplasmic-reticulum Ca^{2+}-ATPase in low-frequency-stimulated muscle results from a modification of the active site. Biochem J 284: (in press)

Matsushita S, Dux L, Pette D (1991) Distribution of active and inactive (nonphosphorylating) sarcoplasmic reticulum Ca^{2+}-ATPase molecules in low-frequency stimulated rabbit fast-twitch muscle. FEBS Lett 294:203–206

McMinn RM, Vrbová G (1967) Motoneurone activity as a cause of degeneration in the soleus muscle of the rabbit. Q J Exp Physiol 52:411–415

Milner Brown HS, Miller RG (1988) Muscle strengthening through electrical stimulation combined with low resistance weights in patients with neuromuscular disorders. Arch Phys Med Rehabil 69:20–24

Mokrusch T, Engelhardt A, Eichhorn K-F, Prischenk G, Prischenk H, Sack G, Neundorfer B (1990) Effects of long-impulse electrical stimulation on atrophy and fibre type composition of chronically denervated fast rabbit muscle. J Neurol 237:29–34

Mokrusch T, Carraro U, Reichmann H, Engelhardt A, Neundorfer B (1991) Different reactions of denervated fast and slow rabbit muscles to a new type of electrical stimulation: a histochemical and biochemical study. In: Carraro U, Salmons S (eds) Basic and applied myology: perspectives for the 90's. Unipress, Padova, pp 173–182

Munsat TL, McNeal D, Waters R (1976) Effects of nerve stimulation on human muscle. Arch Neurol 33:608–617

Müntener M, Rowlerson AM, Berchtold MW, Heizmann CW (1987) Changes in concentration of the calcium-binding parvalbumin in cross-reinnervated rat muscles. Comparison of biochemical with physiological and histochemical parameters. J Biol Chem 262:465–469

Myrhage R, Hudlická O (1978) Capillary growth in chronically stimulated adult skeletal muscle as studied by intravital microscopy and histological methods in rabbits and rats. Microvasc Res 16:73–90

Nemeth PM (1982) Electrical stimulation of denervated muscle prevents decreases in oxidative enzymes. Muscle Nerve 5:134–139

Nix WA (1990) Effects of intermittent high frequency electrical stimulation on denervated EDL muscle of rabbit. Muscle Nerve 13:580–585

Nix WA, Dahm M (1987) The effect of isometric short-term electrical stimulation on denervated muscle. Muscle Nerve 10:136–143

Nix WA, Reichmann H, Schröder MJ (1985) Influence of direct low frequency stimulation on contractile properties of denervated fast-twitch rabbit muscle. Pflügers Arch 405:141–147

Nwoye L, Mommaerts WFHM (1981) The effects of thyroid status on some properties of rat fast-twitch muscle. J Muscle Res Cell Motil 2:307–320

Ohlendieck K, Briggs FN, Lee KF, Wechsler AW, Campbell KP (1991) Analysis of excitation-contraction-coupling components in chronically stimulated canine skeletal muscle. Eur J Biochem 202:739–747

Peckham PH, Mortimer JT, van der Meulen JP (1973) Physiologic and metabolic changes in white muscle of cat following induced exercise. Brain Res 50:424–429

Peckham PH, Mortimer JT, Marsolais EB (1975) Alteration in the force and fatiguability of skeletal muscle in quadriplegic humans following exercise induced by chronic electrical stimulation. Clin Orthop 114:326–334

Periasamy M, Gregory P, Martin BJ, Stirewalt WS (1989) Regulation of myosin heavy-chain gene expression during skeletal-muscle hypertrophy. Biochem J 257:691–698

Peter JB, Barnard RJ, Edgerton VR, Gillespie CA, Stempel KE (1972) Metabolic profiles of three fiber types of skeletal muscle in guinea pigs and rabbits. Biochemistry 11:2627–2633

Pette D (1984) Activity-induced fast to slow transitions in mammalian muscle. Med Sci Sports Exerc 16:517–528

Pette D (1985) Regulation of phenotype expression in skeletal muscle fibers by increased contractile activity. In: Saltin B (ed) Biochemistry of exercise VI. Human Kinetics, Champaign, pp 3–26 (International series on sport sciences, vol 16)

Pette D (1990) Dynamics of stimulation-induced fast-to-slow transitions in protein isoforms of the thick and thin filament. In: Pette D (ed) The dynamic state of muscle fibers. De Gruyter, Berlin, pp 415–428

Pette D (1991) Effects of chronic electrostimulation on muscle gene expression. Semin Thorac Cardiovasc Surg 3:101–105

Pette D (1992) Fiber transformation and fiber replacement in chronically stimulated muscle. J Heart Lung Transplant (in press)

Pette D, Düsterhöft S (1992) Altered gene expression in fast-twitch muscle induced by chronic low-frequency stimulation. Am J Physiol 262:R333–R338

Pette D, Heilmann C (1977) Transformation of morphological, functional and metabolic properties of fast-twitch muscle as induced by long-term electrical stimulation. Basic Res Cardiol 72:247–253

Pette D, Schnez U (1977) Coexistence of fast and slow type myosin light chains in single muscle fibres during transformation as induced by long term stimulation. FEBS Lett 83:128–130

Pette D, Simoneau J-A (1990) Chronic stimulation-induced alterations in phenotype expression and functional properties of skeletal muscle. In: Chiu R C-J, Bourgeois I (eds) Transformed muscle for cardiac assist and repair. Futura, Mount Kisco, pp 129–137

Pette D, Staron RS (1990) Cellular and molecular diversities of mammalian skeletal muscle fibers. Rev Physiol Biochem Pharmacol 116:1–76

Pette D, Tyler KR (1983) Response of succinate dehydrogenase activity in fibres of rabbit tibialis anterior muscle to chronic nerve stimulation. J Physiol (Lond) 338:1–9

Pette D, Vrbová G (1985) Invited review: neural control of phenotypic expression in mammalian muscle fibers. Muscle Nerve 8:676–689

Pette D, Staudte HW, Vrbová G (1972) Physiological and biochemical changes induced by long-term stimulation of fast muscle. Naturwissenschaften 59:469–470

Pette D, Smith ME, Staudte HW, Vrbová G (1973) Effects of long-term electrical stimulation on some contractile and metabolic characteristics of fast rabbit muscles. Pflügers Arch 338:257–272

Pette D, Ramirez BU, Müller W, Simon R, Exner GU, Hildebrand R (1975) Influence of intermittent long-term stimulation on contractile, histochemical and metabolic properties of fibre populations in fast and slow rabbit muscles. Pflügers Arch 361:1–7

Pette D, Müller W, Leisner E, Vrbová G (1976) Time dependent effects on contractile properties, fibre population, myosin light chains and enzymes of energy metabolism in intermittently and continuously stimulated fast twitch muscle of the rabbit. Pflügers Arch 364:103–112

Pette D, Düsterhöft S, Green HJ, Hofmann S (1991) Early metabolic events in chronic stimulation induced fast to slow transitions. In: Carraro U, Salmons S (eds) Basic and applied myology: perspectives for the 90's. Unipress, Padova, pp 55–62

Pluskal MG, Sréter FA (1983) Correlation between protein phenotype and gene expression in adult rabbit fast twitch muscles undergoing a fast to slow fiber transformation in response to electrical stimulation in vivo. Biochem Biophys Res Commun 113:325–331

Ramirez BU, Pette D (1974) Effects of long-term electrical stimulation on sarcoplasmic reticulum of fast rabbit muscle. FEBS Lett 49:188–190

Reichmann H, Nix A (1985) Changes of energy metabolism, myosin light chain composition, lactate dehydrogenase isozyme pattern and fibre type distribution of denervated fast-twitch muscle from rabbit after low frequency stimulation. Pflügers Arch 405:244–249

Reichmann H, Hoppeler H, Mathieu-Costello O, von Bergen F, Pette D (1985) Biochemical and ultrastructural changes of skeletal muscle mitochondria after chronic electrical stimulation in rabbits. Pflügers Arch 404:1–9

Reichmann H, Wasl R, Simoneau J-A, Pette D (1991) Enzyme activities of fatty acid oxidation and the respiratory chain in chronically stimulated fast-twitch muscle of the rabbit. Pflügers Arch 418:572–574

Riley DA, Allin EF (1973) The effects of inactivity, programmed stimulation, and denervation on the histochemistry of skeletal muscle fiber types. Exp Neurol 40:391–413

Romanul FCA, Sréter FA, Salmons S, Gergely J (1974) The effect of a changed pattern of activity on histochemical characteristics of muscle fibers. In:

Exploratory concepts in muscular dystrophy II. Excerpta Med Int Congr Ser 333:344–348
Roy RK, Mabuchi K, Sarkar S, Mis C, Sréter FA (1979) Changes in tropomyosin subunit pattern in chronic electrically stimulated rabbit fast muscles. Biochem Biophys Res Commun 89:181–187
Rubinstein N, Mabuchi K, Pepe F, Salmons S, Gergely J, Sréter F (1978) Use of type-specific antimyosins to demonstrate the transformation of individual fibers in chronically stimulated rabbit fast muscles. J Cell Biol 79:252–261
Russell DH (1983) Microinjection of purified ornithine decarboxylase into Xenopus oocytes selectively stimulates ribosomal RNA synthesis. Proc Natl Acad Sci USA 80:1318–1321
Rutherford OM, Jones DA (1988) Contractile properties and fatiguability of the human adductor pollicis muscle and first interosseus: a comparison of the effects of two chronic stimulation patterns. J Neurol Sci 85:319–331
Salmons S, Henriksson J (1981) The adaptive response of skeletal muscle to increased use. Muscle Nerve 4:94–105
Salmons S, Jarvis JC (1990) The working capacity of skeletal muscle transformed for use in a cardiac assist role. In: Chiu RC-J, Bourgeois I (eds) Transformed muscle for cardiac assist and repair. Futura, Mount Kisco, pp 89–104
Salmons S, Sréter FA (1976) Significance of impulse activity in the transformation of skeletal muscle type. Nature 263:30–34
Salmons S, Vrbová G (1969) The influence of activity on some contractile characteristics of mammalian fast and slow muscles. J Physiol (Lond) 201:535–549
Salmons S, Gale DR, Sréter FA (1978) Ultrastructural aspects of the transformation of muscle fibre type by long term stimulation: changes in Z discs and mitochondria. J Anat 127:17–31
Samaha FJ, Guth L, Albers RW (1970) Phenotypic differences between the actomyosin ATPase of the three fiber types of mammalian skeletal muscle. Exp Neurol 26:120–125
Sarzala MG, Szymanska G, Wiehrer W, Pette D (1982) Effects of chronic stimulation at low frequency on the lipid phase of sarcoplasmic reticulum in rabbit fast-twitch muscle. Eur J Biochem 123:241–245
Schachat FH, Williams RS, Schnurr CA (1988) Coordinate changes in fast thin filament and Z-line protein expression in the early response to chronic stimulation. J Biol Chem 263:13975–13978
Schachat F, Briggs MM, Williamson EK, McGinnis H (1990) Expression of fast thin filament proteins. Defining fiber archetypes in a molecular continuum. In: Pette D (ed) The dynamic state of muscle fibers. De Gruyter, Berlin, pp 279–291
Schiaffino S, Ausoni S, Gorza L, Saggin L, Gundersen K, Lømo T (1988) Myosin heavy chain isoforms and velocity of shortening of type 2 skeletal muscle fibres. Acta Physiol Scand 134:575–576
Schiaffino S, Gorza L, Sartore S, Saggin L, Ausoni S, Vianello M, Gundersen K, Lømo T (1989) Three myosin heavy chain isoforms in type 2 skeletal muscle fibres. J Muscle Res Cell Motil 10:197–205
Schiaffino S, Gorza L, Ausoni S, Bottinelli R, Reggiani C, Larson L, Edström L, Gundersen K, Lømo T (1990) Muscle fiber types expressing different myosin heavy chain isoforms. Their functional properties and adaptive capacity. In: Pette D (ed) The dynamic state of muscle fibers. De Gruyter, Berlin, pp 329–341
Schmalbruch H, Al-Amood WS, Lewis DM (1991) Morphology of long-term denervated rat soleus muscle and the effect of chronic electrical stimulation. J Physiol (Lond) 441:233–242
Schmitt T, Pette D (1985) Increased mitochondrial creatine kinase in chronically stimulated fast-twitch rabbit muscle. FEBS Lett 188:341–344

Schmitt TL, Pette D (1990) Correlations between troponin-T and myosin heavy chain isoforms in normal and transforming rabbit muscle fibers. In: Pette D (ed) The dynamic state of muscle fibers. De Gruyter, Berlin, pp 293–302

Schmitt TL, Pette D (1991) Fiber type-specific distribution of parvalbumin in rabbit skeletal muscle – a quantitative immunohistochemical and microbiochemical study. Histochemistry 96:459–465

Schultz E (1984) A quantitative study of satellite cells in regenerated soleus and extensor digitorum longus muscles. Anat Rec 208:501–506

Schultz E, Darr KC (1990) The role of satellite cells in adaptive or induced fiber transformations. In: Pette D (ed) The dynamic state of muscle fibers. De Gruyter, Berlin, pp 667–679

Schwarz G, Leisner E, Pette D (1983) Two telestimulation systems for chronic indirect muscle stimulation in caged rabbits and mice. Pflügers Arch 398:130–133

Scott OM, Vrbová G, Dubowitz V (1984) Effects of nerve stimulation on normal and diseased human muscle. In: Serratrice G, Gros D, Desnuelle C, Gastaut J-L, Peloissier J-F, Pouge J, Schiano A (eds) Neuromuscular diseases. Raven, New York, pp 583–587

Scott OM, Vrbová G, Hyde SA, Dubowitz V (1985) Effects of chronic low frequency electrical stimulation on normal human tibialis anterior muscle. J Neurol Neurosurg Psychiatry 48:774–781

Scott OM, Vrbová G, Hyde SA, Dubowitz V (1986) Responses of muscles of patients with Duchenne muscular dystrophy to chronic electrical stimulation. J Neurol Neurosurg Psychiatry 49:1427–1434

Scott OM, Hyde SA, Vrbová G, Dubowitz V (1990) Therapeutic possibilities of low frequency electrical stimulation in children with Duchenne muscular dystrophy. J Neurol Sci 95:171–182

Seccia M, Tortora A, Menconi C, Cavina E (1991) Electrostimulated neosphincter after abdominoperineal resection for rectal cancer: functional results in 41 cases. In: Carraro U, Salmons S (eds) Basic and applied myology: perspectives for the 90's. Unipress, Padova, pp 301–304

Seedorf K, Seedorf U, Pette D (1983) Coordinate expression of alkali and DTNB myosin light chains during transformation of rabbit fast muscle by chronic stimulation. FEBS Lett 158:321–324

Seedorf U, Leberer E, Kirschbaum BJ, Pette D (1986) Neural control of gene expression in skeletal muscle. Effects of chronic stimulation on lactate dehydrogenase isoenzymes and citrate synthase. Biochem J 239:115–120

Simoneau J-A, Pette D (1988a) Species-specific effects of chronic nerve stimulation upon tibialis anterior muscle in mouse, rat, guinea pig, and rabbit. Pflügers Arch 412:86–92

Simoneau J-A, Pette D (1988b) Specific effects of low-frequency stimulation upon energy metabolism in tibialis anterior muscles of mouse, rat, guinea pig and rabbit. Reprod Nutr Develop 28 (3 B):781–784

Simoneau J-A, Pette D (1989) Species-specific responses of muscle lactate dehydrogenase isozymes to increased contractile activity. Pflügers Arch 413: 679–681

Simoneau J-A, Kaufmann M, Härtner K-T, Pette D (1989) Relations between chronic stimulation-induced changes in contractile properties and the Ca^{2+}-sequestering system of rat and rabbit fast-twitch muscles. Pflügers Arch 414: 629–633

Simoneau J-A, Hood DA, Pette D (1990) Species-specific responses in enzyme activities of anaerobic and aerobic energy metabolism to increased contractile activity. In: Taylor AW, Gollnick PD, Green HJ, Ianuzzo CD, Noble EG, Metivier G, Sutton JR (eds) Biochemistry of exercise VII. Human

Kinetics Champaign, pp 95–103 (International series on sport sciences, vol 21)
Simoneau J-A, Kaufmann M, Pette D (1992) Asynchronous increases in oxidative capacity and resistance to fatigue of chronically stimulated muscles of rat and rabbit. J Physiol (Lond) (in press)
Sketelji J, Črne-Finderle N, Ribarič S, Brzin M (1991) Interactions between intrinsic regulation and neural modulation of acetylcholinesterase in fast and slow skeletal muscles. Cell Mol Neurobiol 11:35–54
Sréter FA, Gergely J, Salmons S, Romanul F (1973) Synthesis by fast muscle of myosin light chains characteristic of slow muscle in response to long-term stimulation. Nature New Biol 241:17–19
Sréter FA, Romanul FCA, Salmons S, Gergely J (1974) The effect of a changed pattern of activity on some biochemical characteristics of muscle. In: Exploratory concepts in muscular dystrophy II. Excerpta Med Int Congr Ser 333: 338–343
Sréter FA, Elzinga M, Mabuchi K (1975) The N-methylhistidine content of myosin in stimulated and cross-reinnervated skeletal muscles of the rabbit. FEBS Lett 57:107–111
Sréter FA, Mabuchi K, Köver A, Gesztelyi I, Nagy Z, Furka I (1980) Effect of chronic stimulation on cation distribution and membrane potential in fast-twitch muscles of rabbit. In: Pette D (ed) Plasticity of muscle. De Gruyter, Berlin, pp 441–451
Sréter FA, Pintér K, Jolesz F, Mabuchi K (1982) Fast to slow transformation of fast muscles in response to long-term phasic stimulation. Exp Neurol 75:95–102
Sréter FA, Lopez JR, Alamao L, Mabuchi K, Gergely J (1987) Changes in intracellular ionized Ca concentration associated with muscle fiber type transformation. Am J Physiol 253:C296–C300
Staron RS (1991) Correlation between myofibrillar ATPase activity and myosin heavy chain composition in single human muscle fibers. Histochemistry 96: 21–24
Staron RS, Pette D (1986) Correlation between myofibrillar ATPase activity and myosin heavy chain composition in rabbit muscle fibers. Histochemistry 86: 19–23
Staron RS, Pette D (1987a) Nonuniform myosin expression along single fibers of chronically stimulated and contralateral rabbit tibialis anterior muscles. Pflügers Arch 409:67–73
Staron RS, Pette D (1987b) The multiplicity of myosin light and heavy chain combinations in histochemically typed single fibres. Rabbit soleus muscle. Biochem J 243:687–693
Staron RS, Pette D (1987c) The multiplicity of myosin light and heavy chain combinations in histochemically typed single fibres. Rabbit tibialis anterior muscle. Biochem J 243:695–699
Staron RS, Gohlsch B, Pette D (1987) Myosin polymorphism in single fibers of chronically stimulated rabbit fast-twitch muscle. Pflügers Arch 408:444–450
Sweeney HL, Kushmerick MJ, Mabuchi K, Sréter FA, Gergely J (1988) Myosin alkali light chain and heavy chain variations correlate with altered shortening velocity of isolated skeletal muscle fibers. J Biol Chem 263:9034–9039
Tabor CW, Tabor H (1984) Polyoamines. Annu Rev Biochem 53:749–790
Tada M, Inui M (1983) Regulation of calcium transport by the ATPase-phospholamban system. J Mol Cell Cardiol 15:565–575
Termin A, Pette D (1990) Electrophoretic separation by an improved method of fast myosin HCIIb-, HCIId-, and HCIIa-based isomyosins with specific alkali light chain combinations. FEBS Lett 275:165–167

Termin A, Pette D (1991) Myosin heavy chain-based isomyosins in developing, adult fast-twitch and slow-twitch muscles. Eur J Biochem 195:577–584
Termin A, Pette D (1992) Changes in myosin heavy-chain isoform synthesis of chronically stimulated rat fast-twitch muscle. Eur J Biochem 204:569–573
Termin A, Staron RS, Pette D (1989a) Myosin heavy chain isoforms in histochemically defined fiber types of rat muscle. Histochemistry 92:453–457
Termin A, Staron RS, Pette D (1989b) Changes in myosin heavy chain isoforms during chronic low-frequency stimulation of rat fast hindlimb muscles – A single fiber study. Eur J Biochem 186:749–754
Thomason DB, Booth FW (1990) Atrophy of the soleus muscle by hindlimb unweighting. J Appl Physiol 68:1–12
Tian L-M, Feng D-P (1990) The interaction of thyroidectomy with spinal cord transection or cross-innervation in their effects on muscle phenotypic characteristics. Chin J Physiol Sci 6:1–12
Tyler KR, Wright AJA (1980) Light weight portable stimulators for stimulation of skeletal muscles at different frequencies and for cardiac pacing. J Physiol (Lond) 307:6P–7
Underwood LE, Williams RS (1987) Pretranslational regulation of myoglobin gene expression. Am J Physiol 252:C450–C453
Valenčič V, Vodovnik L, Štefančič M, Jelnikar M (1985) Functional electrical stimulation of denervated muscles. In: Carraro U, Angelini C (eds) Functional electrostimulation of neurones and muscles. CLEUP, Padova, pp 99–102
Velenčič V, Vodovnik L, Štefančič M, Jelnikar T (1986) Improved motor performance due to chronic stimulation of denervated tibialis anterior muscle. Muscle Nerve 9:612–617
Vandenburgh HH, Kaufman S (1980) In vitro skeletal muscle hypertrophy and Na pump activity. In: Pette D (ed) Plasticity of muscle. De Gruyter, Berlin, pp 491–506
Vrbová G (1963) The effect of motoneurone activity on the speed of contraction of striated muscle. J Physiol (Lond) 169:513–526
Vrbová G (1966) Factors determining the speed of contraction of striated muscle. J Physiol (Lond) 185:17P–18P
Vrbová G (1987) Modification of muscle properties induced by activity: possible applications for treatment. In: Rose C, Jones R (eds) Multiple Sclerosis: immunological and therapeutic aspects. Libbey, London, pp 149–153
Vrbová G, Pette D (1987) Reanalysis: impulse activity and fiber-type transformation: a reply. Muscle Nerve 10:569
Vrbová G, Dimitrijevic MM, Partridge M, Halter J, Verhagen-Metman L (1987) Reversal of increased muscle fatigue in paraplegic patients by electrical stimulation. 17th meeting of the Society of Neuroscience
Weber FE, Pette D (1988) Contractile activity enhances the synthesis of hexokinase II in rat skeletal muscle. FEBS Lett 238:71–73
Weber FE, Pette D (1990a) Rapid up- and down-regulation of hexokinase II in rat skeletal muscle in response to altered contractile activity. FEBS Lett 261:291–293
Weber FE, Pette D (1990b) Changes in free and bound forms and total amount of hexokinase isozyme II of rat muscle in response to contractile activity. Eur J Biochem 191:85–90
Westgaard RH, Lømo T (1988) Control of contractile properties within adaptive ranges by patterns of impulse activity in the rat. J Neurosci 8:4415–4426
Wetzel P, Liebner T, Gros G (1990) Carbonic anhydrase inhibition and calcium transients in soleus fibers. FEBS Lett 267:66–70

Wiehrer W, Pette D (1983) The ratio between intrinsic 115 kDa and 30 kDa peptides as a marker of fibre type-specific sarcoplasmic reticulum in mammalian muscles. FEBS Lett 158:317–320

Wilkinson JM, Grand RJA (1978a) Comparison of amino acid sequence of troponin I from different striated muscles. Nature 271:31–35

Wilkinson JM, Grand RJA (1978b) The amino-acid sequence of chicken fast-skeletal-muscle troponin I. Eur J Biochem 82:493–501

Williams NS, Hallan RI, Koeze TH, Watkins ES (1989) Construction of a neorectum and neoanal sphincter following previous proctocolectomy. Br J Surg 76:1191–1194

Williams NS, Hallan RI, Koeze T, Pilot M-A, Watkins ES (1990) Construction of neoanal sphincter by transposition of the gracilis muscle and prolonged neuromuscular stimulation for the treatment of faecal incontinence. Ann R Coll Surg Engl 72:108–113

Williams P, Watt P, Bicik V, Goldspink G (1986) Effect of stretch combined with electrical stimulation on the type of sarcomeres produced at the ends of muscle fibers. Exp Neurol 93:500–509

Williams RS (1986) Mitochondrial gene expression in mammalian striated muscle. J Biol Chem 261:12390–12394

Williams RS, Salmons S, Newsholme EA, Kaufman RE, Mellor J (1986) Regulation of nuclear and mitochondrial gene expression by contractile activity in skeletal muscle. J Biol Chem 261:376–380

Williams RS, Garcia-Moll M, Mellor J, Salmons S, Harlan W (1987) Adaptation of skeletal muscle to increased contractile activity. Expression of nuclear genes encoding mitochondrial proteins. J Biol Chem 262:2764–2767

Subject Index